THE UNIVERSITY
of EDINBURGH

Ca^{2+}/Calmodulin signalling during colony initiation in *Neurospora crassa*

Chia-Chen Chang

Ph.D. thesis
The University of Edinburgh
2015

Declaration

I hereby declare that I am the sole author of this thesis. The work, of which it is a record, has been carried out by myself. Results obtained through the collaboration with other individuals and institutions is appropriately indicated. All sources of information have been specifically acknowledged by means of referencing.

Chia-Chen Chang

January 2015

Acknowledgements

I would like to thank all the people who have contributed through their advice, discussion, encouragement, company, smiles, friendship and inspiration to support me in my life as a Ph.D. student. The invisible light you have brought to me made me strong to get through all the darkness and enlightened me to see this world in a different way.

First of all I would like to thank my supervisor Nick Read for giving me the opportunity to work in his brilliant team and always guiding me with the warmest encouragement. I would also like to thank him for giving me numerous opportunities to present my work at international meetings. In addition, I would like to thank Martin Barrios-Llerena and Thierry Le Bihan from the SynthSys Institute for the mass spectrometry analysis; my second supervisor Andrew Goryachev and Elaine Bignell for enriching my work with different aspects; André Fleißner, Rosa R. Mouriño Pérez and Michael Freitag for kindly helping out with strains and plasmids.

The best thing in my PhD life was to work with a group of talented and nice people. I would like to thank all members of the Read lab, past and present, especially Adokiye Beripiki, Alex Lichius, Alberto Muñoz and Meiling Chu for passing on their expertise in molecular cloning and experimental design. Thanks are also due to our Manchester Neurospora group, Patricia Hernandez Ortiz and Akira Alexander, for supporting me both with my lab work and through friendship. Also thanks to my worldwide companions, Adriana Contreras Valenzuela, Smija Mariam Kurian, Kathryn Lord, Jun-ya Shoji, Can Zhao, Pavlos Geranios, Sally Heywood for all your help. I have been very happy to work with you all. I would also like to thank all the MFIG members, especially Marcin Fraczek and Margherita Bertuzzi for sharing their scientific experience.

Extra special thanks for Constanze Seidel and Sergio Moreno Velasquez. You are not only my best colleagues and friends, you made me a home in Manchester. Many thanks for your generous encouragement and help. I could not get through those difficulties without you.

Thanks for the long-distance friendship support from Chih-Ying Lay, Hsiu-Hsin Hsieh, Blanca Ko, Shih-Chieh Liang, Tina Tsai, and Yi-chun Isabella Tsai. Sincerely thanks to my love, Jason, for the continuous support over the last four years. Finally, I would like to thank and embrace my family. My parents love me with their faultless support in everything I have chosen to do and their encouragement with all of my achievements.

All your love makes me free and makes my spirit to learn the wisdom in the world, to create ideas for the world, and to give my contribution to the world.

Abstract

The primary research aims of this thesis were to analyse the mechanism of Ca^{2+}/calmodulin (CaM) signalling during conidial germination and conidial anastomosis tube (CAT)-mediated fusion in *Neurospora crassa*. Ca^{2+} is an ubiquitous signalling molecule that regulates many important processes in filamentous fungi including spore germination, hyphal growth, mechanosensing, stress responses, circadian rhythms, and the virulence of pathogens. Transient increases in cytosolic free calcium ($[Ca^{2+}]_c$) act as intracellular signals. As the primary intracellular Ca^{2+} receptor, calmodulin (CaM) converts these Ca^{2+} signals into responses by regulating the activities of numerous target proteins. Ca^{2+}-free medium, antagonists of L-type Ca^{2+} channels, CaM and calcineurin were found to inhibit CAT fusion. In addition, my results showed that CAT chemotropism is dependent on extracellular Ca^{2+}.

65 genes were identified as likely components of the Ca^{2+} signalling machinery of *N. crassa* based on a comparative genomic analysis of *S. cerevisiae*, *A. fumigatus* and *C. albicans*. Deletion mutants of 29 of these genes were characterized in relation to their possible roles during colony initiation and development. Four of these mutants (Δ*cna-1*, Δ*cnb-1*, Δ*camk-1*, Δ*plc-2*, and Δ*rgs-1*), which were homokaryons, exhibited strong morphological phenotypes associated with CAT fusion.

To identify the protein machinery involved in Ca^{2+}/CaM signalling during colony initiation, proteins that directly or indirectly interacted with CaM were isolated from germlings by immunoprecipitation and analyzed by mass spectroscopy. A total of 286 putative Ca^{2+}/CaM-interacting proteins were identified in this way and 30 of these proteins contained CaM-binding motifs. This proteomics analysis provided evidence for Ca^{2+}/CaM signalling playing a role in regulating the activity of a wide range of proteins including MAP kinases in the cell integrity pathway, Ras/Rho signalling pathway, and microtubule and actin cytoskeletal proteins.

GFP labelled CaM localized as dynamic spots associated with the plasma membrane and cytoplasm in both germ tubes and CATs. Significant CaM accumulation was observed in the tips of CATs growing towards each other, around fusion pores at sites of CAT fusion, and at developing septa in germ tubes. CaM

localization was influenced by the actin and microtubule cytoskeleton during the colony initiation. Inhibition of F-actin polymerization with latrunculin-A suppressed the pronounced accumulation of CaM at growing germ tube and CAT tips. The movement of CaM associated with spindle pole bodies was prevented by treatment with the microtubule polymerization inhibitor benomyl. The absence of *myo-5* resulted in reduced CAT fusion and the lack recruitment of CaM at growing tips indicating a role for the motor protein, myosin-5, in these processes.

Finally, by expressing the genetically encoded Ca^{2+} sensor GCaMP6s under the control of *tef-1* promoter in *N. crassa*, I have been able to image $[Ca^{2+}]_c$ dynamics in this fungus for the first time. Using this I have been able to detect localized $[Ca^{2+}]_c$ spikes and waves in conidia, germ tubes and CATs. However, I obtained no clear evidence for localized $[Ca^{2+}]_c$ changes being associated with CAT chemotropism or fusion.

Table of content

Appendices

Abbreviations

°C	degrees Celsius
$[Ca^{2+}]_c$	cytosolic free Ca^{2+}
µg	microgram
µm	micrometer
A	(deoxy)adenosine
apoCaM	calcium-free CaM
ATP	adenosine triphosphate
bar	ignite resistance gene
BLASTp	basic local alignment search tool for proteins
bp	base pairs
BROAD	Broad Institute at MIT
C	(deoxy)cytidine
CaM	calmodulin
CaMK	Ca^{2+}/CaM dependent protein kinase
CAMZ	calmidazolium
cAMP	cyclic adenosin monophosphate
CAT	conidial anastomosis tube
cDNA	complementary DNA
CDRE	calcineurin-dependent response element
cm	centimeter
CnA	calcineurin catalytic subunit a
CnB	calcineurin catalytic subunit b
CSM	complete selection media
DAG	diacylglycerol
dH2O	distilled water
DIC	differential interference contrast
DMSO	dimethylsulfoxide
DNA	desoxyribonucleic acid
dNTP	desoxyribonucleotide triphosphate
EDTA	ethylenediaminetetraacetic acid
ER	endoplasmic reticulum
EtOH	ethanol
F-actin	filamentous actin
FGSC	Fungal Genetics Stock Center
Fig.	figure
FIGS	fructose-glucose-sorbose

FM4-64	Fei Mao dye 4-64 (N-(3-triethylammoniumpropyl)-4-(6-(4-diethylamino)phenyl)hexatrienyl pyridinium dibromide)
FP	fluorescent protein
G	(deoxy)guanosine
g	gram
gDNA	genomic DNA
GFP	green fluorescent protein
GPCR	G-protein-coupled receptor
GT	germ tube
GTPase	guanosine triphosphatase
h	hour
het	heterokaryon incompatibility gene
hph	hygromycin B resistance gene
HygB	hygromycin B
hygR	hygromycin resistance
InsP3	inositol 1,4,5-triphosphate
kb	kilo base pairs
kD	kilo Dalton
KI	knock-in
KO	knock-out
kV	kilo volts
l	liter
Lat A	latrunculin A
LB	Luria Bertani
LED	light-emitting diode
LTCCs	L-type voltage-gated calcium channels
M	molar
MAPK	mitogen-activated protein kinase
mat a	mating type locus a
mat A	mating type locus A
Mbp	mega base pairs
mg	milligram
min	minute
ml	millilitre
mm	millimetre
mM	millimolar
mRNA	messenger ribonucleic acid
NADP(H)	nicotinamide adenine dinucleotide phosphate

nat	nourseothricin resistance gene
NCBI	National Centre for Biotechnology Information
NCS	neuronal calcium sensor
N-free VM	nitrogen-free Vogel's medium
ng	nanogram
nm	nanometer
NTC	nourseothricin
OD600	optical density at 600 nm
ORF	open reading frame
PCR	polymerase chain reaction
pH	negative log of proton concentration
PIP_2	phosphatidylinositol 4,5-bisphosphate
PI-PLC	phosphoinositide-specific
PKC	protein kinase C
PLC	phospholipase C
RGS	regulator of G-protein signalling
RNA	ribonucleic acid
RNase	ribonuclease
ROCCs	receptor-operated Ca^{2+} channels
rpm	revolutions per minute
RT	room temperature
SCM	synthetic crossing medium
sec	second
sGFP	synthetic GFP = GFP(S65T)
SMART	simple modular architecture research tool
SOC	super optimal broth with catabolite repression
SOCCs	store-operated Ca^{2+} channels
SOD	superoxide dismutase
SPB	spindle pole body
Spk	Spitzenkörper
T	(deoxy)thymidine
TagRFP	red fluorescent protein RFP from the sea anemone *Entacmaea quadricolor*
TFP	trifluoperazine
Tm	melting temperature
U	unit
UV light	ultra-violet light
V	volt

v/v	volume per volume
VHF	vegetative hyphal fusion
VM	Vogel's medium
VOCCs	voltage-operated Ca^{2+} channels
vol.	volume
w/v	weight per volume
wt	wild type
WW domain	protein domain with two signature tryptophane (W) residues
YPD	yeast extract peptone dextrose
YRC	yeast recombinational cloning

Lists of figures

Lists of tables

Chapter 1
General introduction

Chapter 1 – General introduction

1.1. An overview of the model fungus *Neurospora crassa*

1.1.1. A well-established fungal model system

The orange bread mould *Neurospora crass* is a filamentous ascomycete fungus. It has been developed as a model organism for genetic and biochemical studies since the 1940s. Beadle and Tatum used it to establish the 'one gene-one enzyme' model to explore gene-regulated metabolic pathways. This benefited the understanding of inherited metabolic diseases in humans, and this earned them their Nobel Prizes (Perkins, 1992).

As a well characterized organism that has greatly contributed to agricultural, medical, and environmental studies for more than 70 years, *N. crassa* was the first filamentous fungus to have its genome sequenced and annotated. The whole 43 Mbp genome encodes more than 10,000 predicted genes with 54% GC content (Borkovich et al., 2004; Galagan et al., 2003; Turner et al., 2001). Its proteome with 10,082 predicted protein-coding sequences is approximately twice the size of the proteome of the fission yeast *Schizosacchromyces pombe* (~ 4940 protein coding genes) and the budding yeast *Sacchromyces cerevisiae* (~ 5400 protein coding genes)(Decottignies et al., 2003).

An analysis has shown that over 50% of the expressed *Neurospora* genes lack identifiable homologues in any organism and only about 33% have homologues in *S. cerevisiae* (Braun et al., 2000; Dunlap et al., 2007). Furthermore, *Neurospora* has little repeated DNA other than the ~150 copies of rDNA genes because of the epigenetic phenomenon of repeat-induced-point mutation (RIP) (Krumlauf and Marzluf, 1979; Krumlauf and Marzluf, 1980). RIP efficiently detects repeated DNA sequences and modifies both copies of the sequence duplication with numerous GC to AT mutations (Selker, 1990). This contributes to a genome defence system in *Neurospora* that inactivates transposons and resists genome redundancy (Kinsey et al., 1994).

The genome sequence is organized in seven linkage groups with genetic and physical maps which have been established in the bioinformatic database of the

Broad Institute (http://www.broadinstitute.org/annotation/genome/neurospora/MultiHome.html). As a result of the availability of a high-throughput gene knockout procedure for *N. crassa* (Colot et al., 2006), a comprehensive collection of deletion mutants for most of its genes is available from the Fungal Genetics Stock Centre (FGSC; http://www.fgsc.net) based at the University of Kansas, Missouri. Phenotypic characterization of these gene deletion strains is being carried out by the scientific community (Colot et al., 2006; Dunlap et al., 2007).

Key features of *N. crassa* that make it an excellent model organism and experimental system are as follows (Davis and Perkins, 2002):

- Easily cultured on defined media
- Fast growth rate (≥ 1 μm/sec) (Seiler and Plamann, 2003)
- Large hyphae (< 15 μm wide), which are useful for cytological studies
- Excellent genetics (predominately haploid)
- A collection of over 10,000 mutants is available (Dunlap et al., 2007)
- Numerous molecular and genomics tools have been established following from its completely sequenced genome (Galagan et al., 2003)
- Little gene redundancy facilitates functional analysis of genes
- Widely used as a biological model for filamentous fungi and other organisms

1.1.2. The life cycle of *N. crassa*

N. crassa is a morphologically complex organism with 28 morphologically distinct cell types and a complex interconnected network of hyphae (Bistis et al., 2003). The life cycle of *N. crassa* includes both asexual and sexual cycles (Fig. 1.1). During its asexual cycle, there are 3 different types of conidia produced from the vegetative colony: macroconidia, microconidia, and arthroconidia. The macroconidia, typically containing 2-6 haploid nuclei, are formed from macroconidiophores and develop an intense carotenoid pigment in the light. Uninucleate microconidia are produced from microconidiophores. Multinucleate arthrospores are formed directly from the individual cell compartment of vegetative hyphae. The germination of any asexual spore results in the formation of typically one germ tube that develops into the branched vegetative hyphae of the mycelium which then goes onto form more

asexual spores.

N. crassa is heterothallic and produces two mating types, mat A and mat a (Coppin et al., 1997). Sexual development in *N. crassa* is induced by nitrogen and carbon starvation. Fertilization normally involved a conidium (the male cell) of one mating type fusing with a trichogyne (female cell) formed by a protoperithecium of the opposite mating type. One or more male nucleus from the conidium migrate down the trichogyne into the protoperithecium where they pair up with nuclei of the opposite mating type and this event is thought to initiate the development of the perithecium. The nuclei fuse within an ascus mother cell to form a diploid nucleus which immediately undergoes meiosis. The four products of meiosis are followed by a further mitotic division to produce eight haploid nuclei enclosed within 8 ascospores. Release of the ascospores from the perithecium and the germination to form new colonies complete the life cycle (Metzenberg and Glass, 1990; Perkins and Davis, 2000).

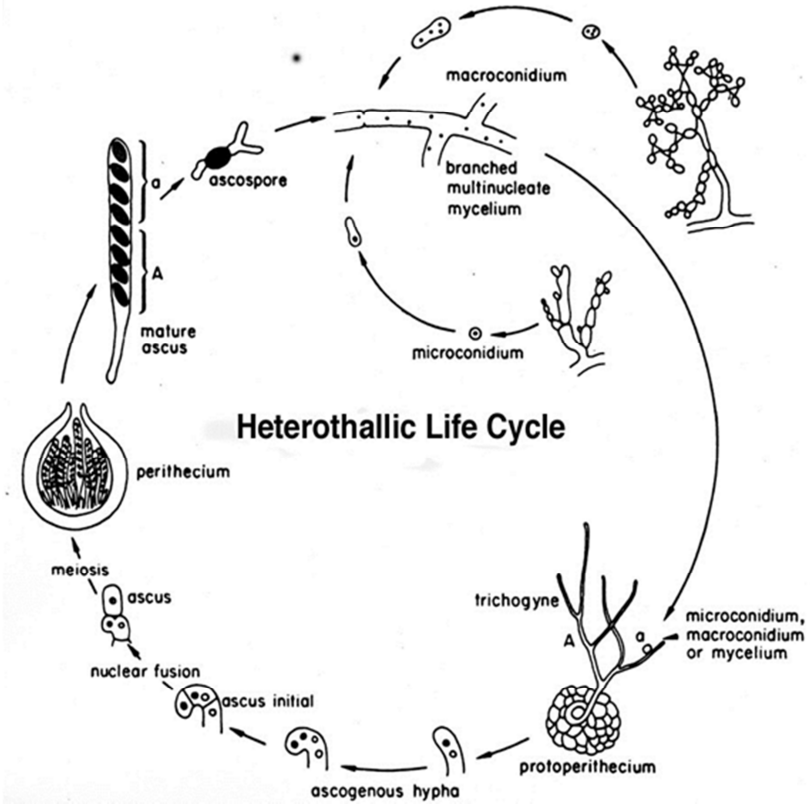

Figure 1.1 The life cycle of *N. crassa*

Image copied from (http://www.fgsc.net/neurospora/sectionb2.htm). The asexual cycle leads to the production of macroconidia, microconidia, and arthroconidia (not shown). The sexual cycle, in which the protoperithecium is fertilized by the fusion of

the female trichogyne with a male conidium of the opposite mating type and subsequent meiosis leads to the production of ascospores inside the perithecium (Davis, 2000).

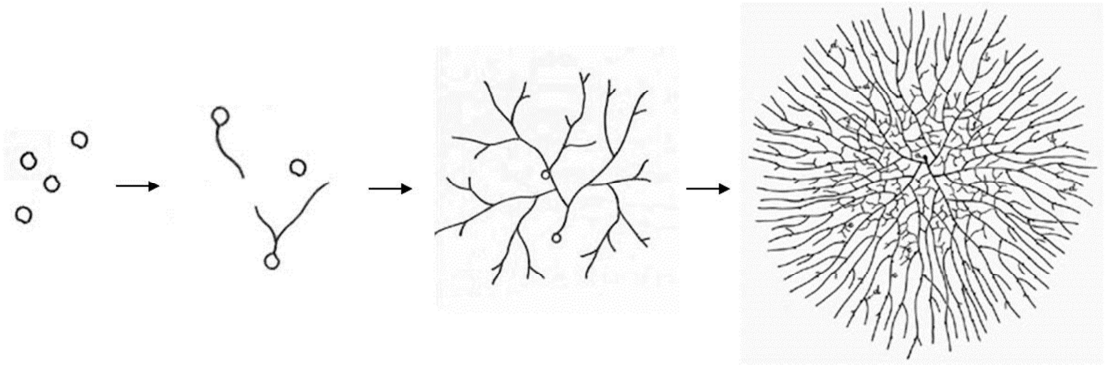

Figure 1.2 The development of a fungal colony
The colony is initiated by spores foming germ tubes. These branch fuse and differentiate into the vegetative hyphae of the mature colony.

1.2. Developmental pathways during colony initiation from conidia

Two developmental pathways from the conidium occur in *N. crassa*: germ tube (GT) formation involved in colony establishment; and conidial anastomoses tube (CAT) formation involved in generating interconnected networks of conidial germlings by cell fusion (Read et al., 2010; Roca et al., 2005a; Roca et al., 2005b).

1.2.1. Germ tube formation

Activation of the resting spore, isotropic growth, and polarized growth are the three main steps resulting in germ tube formation which is the first developmental stage in the life cycle of all filamentous fungi (d'Enfert, 1997). In *N. crassa*, the macroconidia initiate a complex cascade of biochemical and metabolic processes when triggered by environmental factors such as water, oxygen, and carbon dioxide (Griffin, 1994; Watkinson, 1994). Isotropic growth leads to the expansion of conidia before cell symmetry breaking and polarized cell outgrowth. These processes are associated with changes in gene and protein expression which accompany changes in cell wall synthesis (d'Enfert, 1997). Initially most of the organelles (e.g. nuclei and mitochondria) display a uniform distribution within growing GTs. After the GTs reach ~150 µm in length, the organelle organisation becomes polarized, and the Spitzenkörper, which is the vesicle organizing centre for hyphal growth and

morphogenesis forms at the hyphal tip when GTs differentiate into elongating and branching vegetative hyphae (Araujo-Palomares et al., 2007).

Various genes involved in the regulation of the cytoskeleton, signal transduction pathways, cell wall formation, membrane biosynthesis, and secretion are involved in regulating cell polarity during colony initiation (Seiler and Plamann, 2003).

1.2.2. Conidial anastomosis tube (CAT) mediated cell fusion and network formation

Cell fusion between conidia and conidial germlings is common and has been observed in over 73 ascomycete species (Roca et al., 2005b). Conidial anastomosis tubes, which are morphologically and physiologically different from germ tubes and under separate genetic control, are specialized hyphal protrusions that function in interconnecting networks of conidial germlings by cell fusion during colony initiation. CATs have been most characterised in *Colletotrichum lindemuthianum* and *N. crassa* (Fig.1.3). In terms of cell communication, CATs home towards each other whilst germ tubes avoid each other by means of positive and negative chemoattraction respectively (Lichius et al., 2014). CATs are unbranched and usually thinner and shorter than germ tubes. CATs can arise directly from conidia, germ tube tips or as subapical branches of germ tubes (Table 1.1; (Araujo-Palomares et al., 2007; Read et al., 2010; Read et al., 2012; Read et al., 2009; Roca et al., 2005a; Roca et al., 2005b).

The CAT-mediated cell fusion system in *N. crass*a provides an excellent experimental model for the study of the mechanistic basis of self-fusion between fungal spores, germlings, or hyphae (Read et al., 2012). The whole process of CAT fusion divides into a continuum of several distinct events: CAT induction, CAT chemotropism, cell-cell adhesion, cell wall remodelling/degradation, and plasma membrane merger (Fig. 1.4). The whole process can be analyzed within 4-6 h (Read et al., 2009).

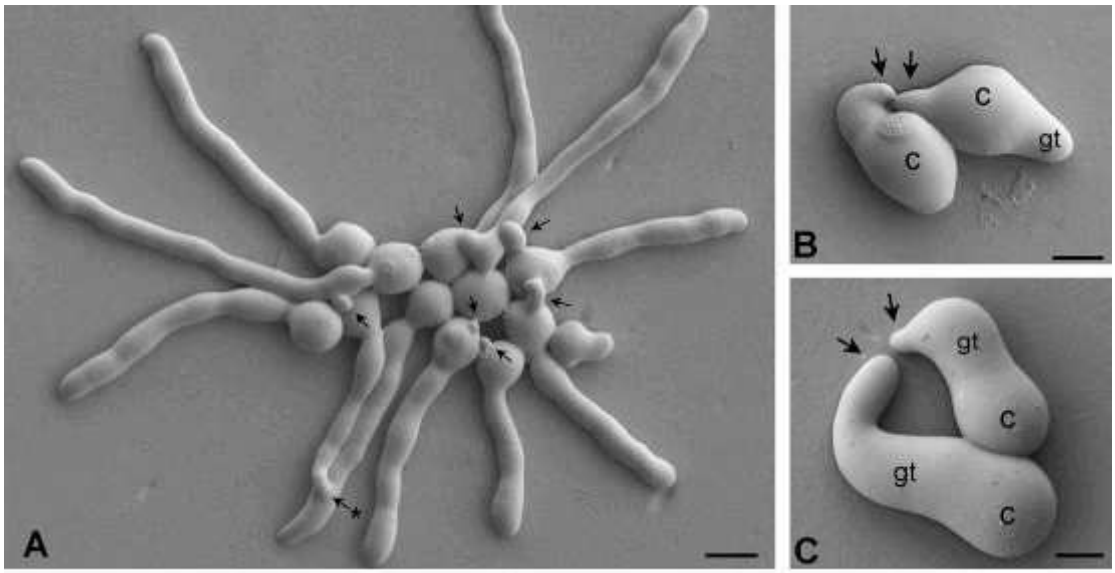

Figure 1.3 CAT fusion between conidia and conidial germlings in *N. crassa*.
Imaged by low-temperature scanning electron microscopy and reproduced from Roca et al., 2005a (A) Conidial germlings interconnected by CATs. CATs are formed directly from conidia (arrows) or from germ tubes (asterisk). Bar = 10 µm. (B, C) CATs (arrows) which are thinner and shorter than germ tubes and home towards each other. Abbreviation : gt (germ tube), c (conidium). Bar = 5 µm.

Table 1.1 The difference between CATs and germ tubes in *N. crassa*

Morphogenesis	Germ tubes	CATs
length	differentiate into longer vegetative hyphae	rarely extend longer than 10–12 µm
diameter	4-5 µm	2-2.5 µm
septate and branch	able to septate and branch	do not septate and branch
chemotropism	grow away from each other	chemotropically attracted to each other
fusion	generally unable to fuse directly	fuse to each other

1.2.3. Functional genes involved in cell-cell communication and fusion

There are three key stages during the process of CAT fusion: CAT induction, CAT chemotropism, and CAT fusion (Figure 1.4). CAT induction is dependent on conidial density about 10^6 conidia ml^{-1} in *N. crassa* and probably involves an extracellular CAT inducer produced by conidia which may present a form of quorum sensing (Read et al., 2010; Roca et al., 2005a). The unknown chemoattractant signal released from the tips of CATs induces the communication between two cells, and causes the cell cycle to arrest during the CAT chemoattraction phase (Roca et al., 2010). Orientation of CATs along this chemoattractant gradient results in them growing towards each other to establish cell-cell contact. When CATs adhere to each other, cell wall remodelling occurs around the contact site in order to prevent leakage during subsequent fusion pore formation. Cell wall degradation and reconstruction followed by the merging of plasma membranes completes the formation of the fusion pore. Upon establishment of cytoplasmic continuity, organelles including nuclei, become mixed between the fused germlings. CAT fusion has been shown to require F-actin but not microtubules (Roca et al., 2010), and the polarisome protein complex plays an important role in cell polarity regulation during different stages of the process (Fleissner and Glass, 2007; Lichius et al., 2012b; Read et al., 2010; Read et al., 2012; Read et al., 2009).

Recently, it has been known that more than 40 gene deletion mutants are compromised at different stages of CAT fusion (Table 1.2). These results provide clear evidence for the involvement of multiple proteins and signalling pathways in the whole processes of CAT fusion (Read et al., 2012). I summarized pathways which regulated by these genes into Fig. 1.5. It shows that STRIPAK complex, transcription factors and GPI anchor pathways are involved in CAT formation. Rho GTPase pathway and redox signalling are involved in both CAT formation and CAT chomotropism. MAPK pathway, F-action cytoskeletal regulation and polarisome complex are involved in the whole process of CAT fusion. Details of each pathway are discussed in the following sections.

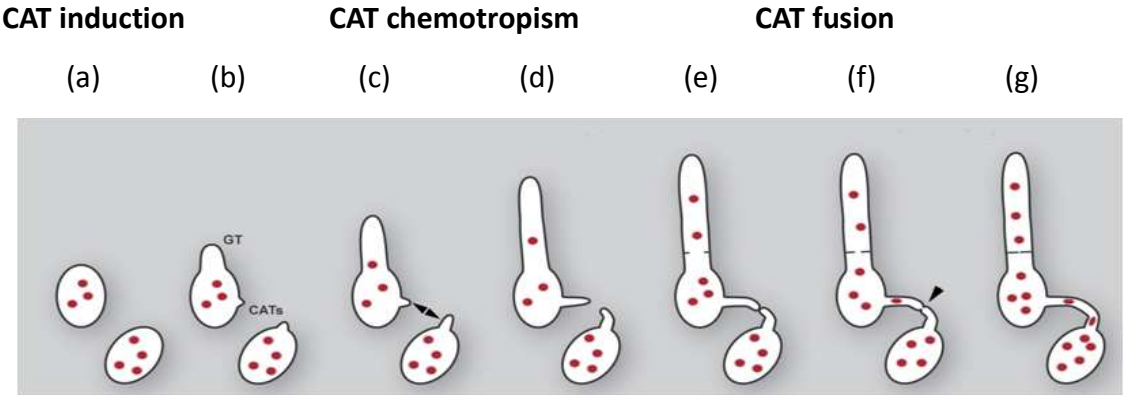

Figure 1.4 Summary of the continuum of developmental stages involved in CAT fusion and the signalling networks and proteins involved (from Read et al., 2012).
The three major stages of CAT-mediated cell-cell fusion are CAT induction, CAT chemotropism and CAT fusion. (a) Ungerminated macroconidia contain on average 2-6 nuclei (red dots) and initially grow exclusively by isotropic expansion. (b) Cell polarization leads to the outgrowth of germ tubes and CATs. (c) An unknown chemoattractant from both tips of CATs induce the communication between two genetically identical cells. (d) Orientation of CATs along this chemoattractant gradient results in them growing towards each other to establish cell-cell contact. (e) CATs adhere to each other and the cell wall becomes remodelled around the contact site in order to prevent leakage during subsequent pore formation. (f) Fusion pore formation (arrowhead) includes cell wall degradation and reconstruction and the merging of plasma membranes. (g) Upon establishment of cytoplasmic continuity, organelles including nuclei become mixed between fused germlings. The cell cycle is arrested during CAT chemotropism, and actin, but not microtubules, are required for CAT fusion to occur.

Table 1.2 Genes involved in different stages of CAT fusion in *N. crassa* as revealed from mutant analyses; updated from (Read et al., 2012)

Gene symbol	Gene loci	Translated protein	Protein functions	Developmental stage that mutant is defective
so (ham-1)	NCU02794	SOFT; WW domain protein	signalling pathway	CAT chemotropism (Fleissner and Glass, 2007; Fleissner et al., 2009b; Fleissner et al., 2005; Fu et al., 2011)
mak-2	NCU02393	MAP kinase	pheromone response pathway	CAT induction (Pandey et al., 2004; Roca et al., 2005a; Fu et al., 2011)
mak-1	NCU09842	MAP kinase	cell wall integrity pathway	CAT induction CAT chemotropism (Fu et al., 2011; Lichius, 2010)
mek-1	NCU06419	MAP kinase kinase	cell wall integrity pathway	CAT induction CAT chemotropism (Fu et al., 2011; Lichius, 2010)
mek-2	NCU04612	MAP kinase kinase	pheromone response pathway	CAT induction (Fu et al., 2011)
mik-1	NCU02234	MAP kinase kinase kinase	cell wall integrity pathway	CAT induction CAT chemotropism (Fu et al., 2011; Lichius, 2010)
nrc-1	NCU06182	MAP kinase kinase kinase	pheromone response pathway	CAT induction (Fu et al., 2011; Pandey et al., 2004; Roca et al., 2005b)
bem-1	NCU06593	MAP kinase activator	MAP kinase pathway	(Schurg et al., 2012)
hym-1	NCU03576	scaffold protein for the COT1 NDR kinase pathway	MAP kinase pathway	(Dettmann et al., 2012)
pp2A	NCU06563	catalytic subunit of protein phosphatase 2A	MAP kinase pathway	CAT induction (Fu et al., 2011)
amph-1	NCU01069	amphiphysin	vesicular trafficking, GTPase activator activity	CAT induction (Fu et al., 2011)
ham-10	NCU02833	C2 domain protein	vesicular trafficking, cell fusion protein complexes	CAT induction (Fu et al., 2011)
pkr-1	NCU00506	assembly factor for V-ATPase	vesicular trafficking	CAT induction (Fu et al., 2011)
cdc-24	NCU00957	guanine exchange factor	Rho GTPase pathway	CAT induction (Lichius, 2010)

Gene symbol	Gene loci	Translated protein	Protein functions	Developmental stage that mutant is defective
cdc-42	NCU06454	Rho GTPase	Rho GTPase pathway	CAT induction (Lichius et al., 2014)
rac-1	NCU02160	Rho GTPase	Rho GTPase pathway	CAT induction (Lichius et al., 2014; Fu et al., 2011)
rho-2	NCU08683	Rho2-GTPase	Rho GTPase signalling	reduced CAT fusion (Lichius, 2010)
rho-3	NCU00600	Rho3-GTPase	Rho GTPase signalling	reduced CAT fusion (Lichius, 2010)
rho-4	NCU03407	Rho protein	Rho GTPase signalling	reduced CAT fusion (Lichius, 2010)
rdi-1	NCU06561	Rho GDI alpha	Rho GTPase signalling	delayed CAT fusion (Lichius, 2010)
flbA	NCU08319	Rho GAP	Rho GTPase signalling	delayed CAT fusion (Lichius, 2010)
ham-2	NCU03727	striatin/phocein binder, trans-membrane protein	cell fusion proteins	CAT induction (Fu et al., 2011; Roca et al., 2005b; Xiang et al., 2002)
ham-3	NCU08741	striatin	cell fusion proteins	CAT induction (Fu et al., 2011; Simonin et al., 2010)
ham-4	NCU00528	coiled coil, trans-membrane protein	cell fusion proteins	not determined (Fu et al., 2011; Simonin et al., 2010)
ham-5	NCU01789	WD40 domain protein	cell fusion proteins	CAT induction (Aldabbous et al., 2010; Fu et al., 2011)
ham-6	NCU02767	small hydrophobic protein	cell fusion proteins	CAT induction (Fu et al., 2011)
ham-7	NCU00881	GPI anchor protein	cell fusion proteins	CAT induction (Fu et al., 2011)
ham-8	NCU02811	trans-membrane protein	cell fusion proteins	CAT induction (Fu et al., 2011)
ham-9	NCU07389	plekstrin domain protein	cell fusion proteins	CAT induction (Fu et al., 2011)
ham-11	NCU04732	hypothetical protein	cell fusion proteins	(Leeder et al., 2013)
lao-1	NCU05113	L-ascorbate oxidase-like protein	cell wall remodelling	CAT induction CAT chemotropism (Lichius, 2010)

Gene symbol	Gene loci	Translated protein	Protein functions	Developmental stage that mutant is defective
mob-3	NCU07674	Phocein	signalling pathway	CAT induction (Fu et al., 2011; Maerz et al., 2009; Maerz et al., 2010)
nor-1	NCU07850	NADPH oxidase regulator	signalling pathway	CAT induction CAT chemotropism (Lichius, 2010)
nox-1	NCU02110	NADPH oxidase	signalling pathway	CAT induction CAT chemotropism (Lichius, 2010)
prm-1	NCU09337	pheromone-regulated membrane protein 1-like	plasma membrane merger	CAT induction CAT chemotropism CAT fusion (Fleissner et al., 2009a; Palma-Guerrero et al., 2014)
rcm-1	NCU06842	regulator of conidiation and morphology-1	transcription factor	CAT induction (Aldabbous et al., 2010)
rco-1	NCU06205	regulator of conidiation-1	transcription factor	CAT induction (Aldabbous et al., 2010; Fu et al., 2011)
snf5	NCU00421	SWI-SNF complex subunit	transcription factor	CAT induction (Fu et al., 2011)
adv-1	NCU07392	arrested development-1	transcription factor	CAT induction (Fu et al., 2011)
ada-3	NCU02896	all development altered-3	transcription factor	CAT induction (Fu et al., 2011)
pp-1	NCU00340	protoperithecium-1	transcription factor	CAT induction (Li et al., 2005; Read et al., 2010)
gpig-1	NCU09757	GPI anchor protein	GPI anchor pathway	not determined (Bowman et al., 2006)
gpip-1	NCU06663	GPI anchor protein	GPI anchor pathway	not determined (Bowman et al., 2006)
gpip-2	NCU07999	GPI anchor protein	GPI anchor pathway	not determined (Bowman et al., 2006)
gpip-3	NCU06508	GPI anchor protein	GPI anchor pathway	not determined (Bowman et al., 2006)
gpit-1	NCU05644	GPI anchor protein	GPI anchor pathway	not determined (Bowman et al., 2006)
lfd-1	NCU09307	transmembrane protein, late fusion defect-1	membrane fusion	CAT fusion (Palma-Guerrero et al., 2014)
cot-1	NCU07296	colonial temperature sensitive-1	protein serine/threonine kinase activity	defective vegetative fusion (Maerz et al., 2008)
mss-4	NCU02295	phosphatidylinositol-4-phosphate 5-kinase	3-phosphoinositide biosynthesis	defective CAT fusion (Mahs et al., 2012)

Gene symbol	Gene loci	Translated protein	Protein functions	Developmental stage that mutant is defective
gdh-1	NCU00461	NAD-specific glutamate dehydrogenase 1	protein oxidation	defective CAT fusion (Lichius, 2010)
chm-1	NCU00406	p21-activated kinase	pheromone response	delayed CAT fusion (Lichius, 2010)
bud-6	NCU08468	actin-interacting protein	polarisome regulation	(Lichius et al., 2012b)
bni-1	NCU01431	cytokinesis protein SepA	polarisome regulation	(Lichius et al., 2012)
spa-2	NCU03115	the central polarisome scaffolding protein	polarisome regulation; pheromone response	reduced CAT fusion (Lichius, 2010; Lichius et al., 2012)
smco-7	NCU03616	Ras-2 protein	pheromone response	reduced CAT fusion (Lichius, 2010)
gna-3	NCU05206	G-alpha subunit 3	G-protein signalling	delayed CAT fusion (Lichius, 2010)

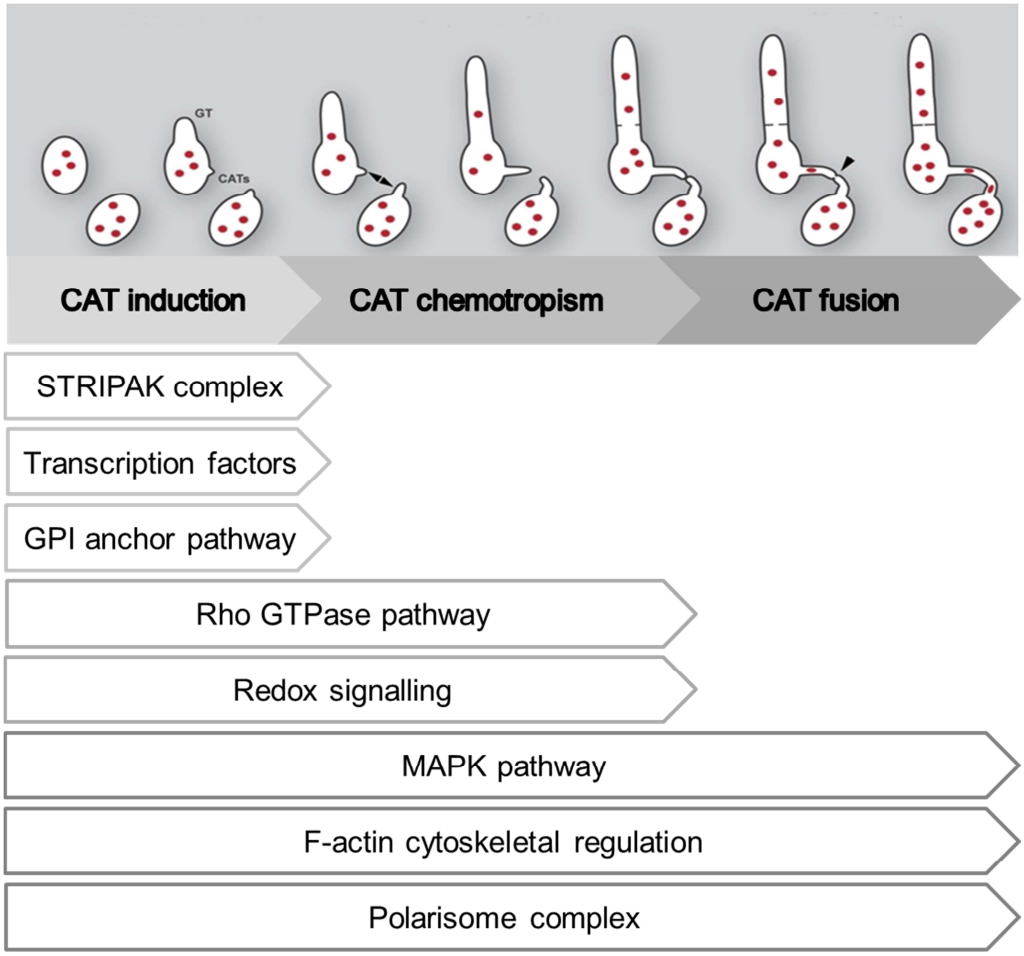

Figure 1.5 Time course of the involvement of different signalling protein complexes/pathways during CAT fusion

According to genes in Table 1.2, 6 paythways were summarized in different stages of CAT fusion. STRIPAK complex, transcription factors and GPI anchor pathways are involved in CAT formation. Rho GTPase pathway and redox signalling are involved in both CAT formation and CAT chomotropism. MAPK pathway, F-action cytoskeletal regulation and polarisome complex are involved in the whole process of CAT fusion.

1.2.3.1. The STRIPAK complex and the endocytosis

The striatin-interacting phosphatase and kinase (STRIPAK) complex is a group of proteins involved in signalling, cell cycle control, apoptosis, vesicular trafficking, Golgi assembly, and cell polarity regulation in mammalian cells (Hwang and Pallas, 2014; Kean et al., 2011). Deletion mutants of several genes of the STRIPAK complex homologues such as *ham-2* (NCU03727), *ham-3* (NCU08741), *ham-4* (NCU00528), *mob3* (NCU07674), and *pp2A* (NCU06563) are defective in CAT formation in *N. crassa*. HAM-2 is a homologue of PRO22 in *Sordaria macrospora* (Bloemendal et al., 2010), which is localized in the vacuolar network of vegetative hyphae. Genes encoding a striatin-like protein HAM-3 and a forkhead associated protein HAM-4 are required for hyphal fusion (Simonin et al., 2010). MOB-3 is a homologue of mammalian phocein that interacts with striatin as a scaffolding protein linking cell signalling and endocytosis (Benoist et al., 2006). PP2A is the catalytic subunit of protein phosphatase 2A that modulates many different signal transduction pathways, including the MAP kinase pathway, by dephosphorylation of the component kinases (Goudreault et al., 2009; Janssens and Goris, 2001).

Other CAT fusion proteins such as HAM-6 (NCU02767), HAM-7 (NCU00881), HAM-8 (NCU02833), and HAM-11 (NCU04732), have been identified to mediate the fusion between the plasma membranes at the tips of the fusion hyphae (Fu et al., 2011; Leeder et al., 2013). The *ham-9* gene (NCU07389) encodes a cytoplasmic protein with pleckstrin homology (PH) and sterile alpha motif (SAM) domains and is required for cell fusion. All of these genes are highly conserved in only the genomes of filamentous fungi. Three proteins AMPH-1 (NCU01069), HAM-10 (NCU02833), and PKR1 (NCU00506) are required for the exocytosis and endocytosis of vesicles at the growing tips of the fusion hyphae (Fu et al., 2011).

1.2.3.2. Transcription factors

Several transcription factors have been identified as being involved in CAT fusion (Read et al., 2012; Fu et al., 2011). RCM-1 and RCO-1 are the *N. crassa* homologues of the budding yeast Ssn6 and Tup1 proteins, which form a heterodimer that functions in regulating yeast cell growth (Aldabbous et al., 2010). PP-1 is the

homologue of the budding yeast Ste12p that is activated by the MAP kinases in the yeast pheromone response pathway (Qi and Elion, 2005). SNF-5 is homologous to the yeast Snf5p that coordinates the assembly and activity of the Snf/Swi complex in remodeling chromatin structure (Geng et al., 2001). ADV-1 is homologous to Pro1 which is a major transcription factor involved in regulating sexual development in *Sordaria macrospora* (Masloff et al., 1999). Transcriptional control of gene expression are believed to be involved during CAT induction and the final stages of CAT fusion.

1.2.3.3. Glycosylphosphatidylinositol (GPI) anchor pathway

In eukaryotic cells, a group of proteins are anchored to the outer leaflet of the plasma membrane via glycosylphosphatidylinositol (GPI) anchors. The presence of the GPI anchor is thought to play an important role in the trafficking of these proteins and providing them with attachment to the fungal plasma membrane (Mayor and Riezman, 2004) or cell wall (Frieman and Cormack, 2004). Mutants affected in the *gpig-1, gpip-1, gpip-2, gpip-3*, and *gpit-1* genes, which encode components of the *N. crassa* GPI anchor biosynthetic pathway, have been characterized and shown to have with deficient colonial morphologies, significantly reduced growth rates, altered hyphal growth patterns, and to exhibit considerable cell lysis. These results are consistent with the GPI anchor pathway being required for cell wall integrity that is associated with CAT fusion in *N. crassa* (Bowman et al., 2006).

1.2.3.4. Rho GTPase pathway

The small Rho-type GTPases Cdc42 and Rac1 are modulated through guanine nucleotide exchange factors (GEFs) (Schmidt and Hall, 2002) and GTPase-activating proteins (GAPs) (Bernards and Settleman, 2004) to switch between inactive GDP-bound and active GTP-bound states. These two proteins are key regulators of eukaryotic cell polarity by regulating cytoskeletal remodeling (Jaffe et al., 2005; Virag et al., 2007). In addition, they regulate the exocytosis of secretory granules by stimulation of IP_3 formation and Ca^{2+} mobilization upon antigen stimulation in mammalian cells (Hong-Geller and Cerione, 2000).

CDC-42 and RAC-1, and their Guanine Exchange Factor (GEF) CDC-24, have been

shown to be essential regulators for the establishment and maintenance of cell polarity in *N. crassa* (Araujo-Palomares et al., 2011). Recent studies identified an important role for CDC-42 showing that it is necessary and sufficient for normal germ tube growth, whereas RAC-1 is essential for CAT formation. Evidence has been obtained that CDC-42 regulates the negative chemotropisms of germ tubes and RAC-1 regulates the positive chemotropism of CATs (Lichius et al., 2014).

1.2.3.5. Redox signalling

Redox signalling is an electron-transfer process that plays a key messenger role in biological systems. NOX-1 (NADPH oxidase), NOR-1 (NOX regulator) and RAC-1 (Rho GTPase) are three key components of the NOX complex involved in redox signalling. Gene deletion mutants of these proteins are defective in CAT induction (Δrac-1) or CAT chemotropism (Δnox-1 and Δnor-1) in *N. crassa* (Lichius et al., 2014). In the plant pathogen *Botrytis cinerea*, mutants lacking the NADPH oxidase BcNoxA and its potential regulator BcNoxR were also shown to be inhibited in CAT fusion (Roca et al., 2012). The role of redox signalling during colony initiation is still unknown but results obtained with *N. crassa* suggest that it is important during CAT chemotropism (Lichius, 2010).

1.2.3.6. Mitogen-activated protein kinase (MAPK) pathway

Three MAPK cascade modules have been identified in *N. crassa* (Borkovich et al., 2004; Galagan et al., 2003), the pheromone response (PR) pathway, the cell wall integrity (CWI)/filamentous growth pathway, and the high osmolarity glycerol (HOG)/stress response pathway. Mutations in the genes encoding components of the PR pathway, including *nrc-1* (NCU06182), *mek-2* (NCU04612), *mak-2* (NCU02393), and the associated transcription factor *pp-1* (NCU00340), result in a defective phenotype of CAT fusion. MAK-2, that is involved in the ping-pong mechanism (Fleissner and Glass, 2007), is regulated by the *S. cerevisiae* BEM1 homologue in *N. crassa* (Schurg et al., 2012). It has also been demonstrated that a novel regulator, HYM-1, of the PR pathway, may coordinate nuclear Dbf2-related (NDR) and MAP kinase signalling during cell polarity regulation and intercellular communication

(Dettmann et al., 2012).

The CWI MAP kinase pathway (Qi and Elion, 2005) is believed to function in cell wall remodelling during CAT formation and CAT fusion. Three genes in the CWI pathway, including *mik-1* (NCU02234), *mek-1* (NCU06419), and *mak-1* (NCU11376), have previously been identified as necessary for cell fusion (Fleissner et al., 2008; Fu et al., 2011; Glass et al., 2000; Lichius, 2010; Read et al., 2010).

It has been revealed that the MAP kinase MAK-2 and the WW domain containing protein SO exhibit anti-phase oscillatory recruitment during CAT chemotropism. When CATs are less than 15 µm apart, SO can be repeatedly recruited to a CAT tip putatively acting as a signal sender, and MAK-2 is similarly transiently recruited to the opposite CAT tip that putatively acting as a signal receiver. The period of the oscillation is 6-12 min and it alternates back and forth for 4-6 times during chemotropic growth (Fleissner et al., 2009b; Goryachev et al., 2012; Read et al., 2012; Read et al., 2009). This pulsatile communication process, termed the ping-pong mechanism (Read et al., 2009), has been mathematically modelled using a generic activator inhibitor model of excitable behaviour (Fig. 1.6) (Goryachev et al., 2012). Although WW domains exist in many eukaryotic proteins, homologs of SO (e.g. PRO40 in *Sordaria macrospora*) are present only in filamentous ascomycetes (Engh et al., 2007a; Fleissner and Glass, 2007). Previous evidence had shown that a *mak-2* gene deletion mutant lacks CATs (Roca et al., 2005b) and a *so* gene deletion mutant produces CATs but they are unable to undergo chemotropism (Fleissner et al., 2005).

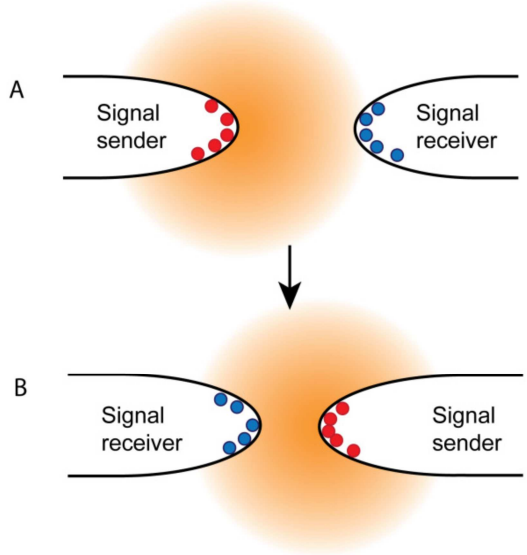

Figure 1.6 Ping-pong mechanism of self signalling during CAT chemoattraction
Image reproduced from Read et al., 2009. (A) SO (red) is believed to play a role in the CAT tip acting as the signal sender for releasing a chemoattractant signal (orange cloud), while MAK-2 (blue) is thought to act in the receiving signal transduction pathway in the opposite CAT tip to orientate tip growth towards the chemoattractant source. (B) In the second

half period the roles reverse: SO has been replaced by MAK-2 in the left tip to receive the signal from the right tip which releases the next chemoattractant pulse by the recruitment of SO. This sequence of pulsatile signalling repeats until both tips come into contact and fuse (Read et al., 2009).

1.2.3.7. The regulation of cytoskeleton and the polarisome

CAT fusion requires F-actin but not microtubules. Treatment with the microtubule depolymerising drug benomyl blocks the formation of elongated germ tubes but does not interfere with CAT-mediated cell fusion (Roca et al., 2010). F-actin patches that localize abundantly in CATs at different stages of CAT fusion are generally regarded as sites of endocytosis (Berepiki et al., 2011; Lichius, 2010). Another protein complex, the polarisome, which is involved in regulating the actin cytoskeleton and secretory machinery, is also required for polarized CAT growth and CAT fusion. Actin cables and BNI-1 (NCU01431), which functions as a formin involved in the nucleation of F-actin, accumulate at sites of CAT emergence prior to cell symmetry breaking. The polarisome complex including BNI-1, the actin interacting protein BUD-6 (NCU08468), and the central polarisome scaffolding protein SPA-2 (NCU03115) localize with an apical cap of F-actin at the chemotropically growing CAT tip. Upon CATs making contact with each other, these three polarisome proteins become concentrated at the site of fusion pore formation and disappear from the fusion site (Lichius et al., 2012). Some residual actin cables persist suggesting that they may be involved in a later stage of the fusion process (Berepiki et al., 2010; Roca et al., 2010; Lichius et al., 2011).

1.2.4. The prospective questions of the signal transduction in CAT fusion and colony initiation

In addition to the different signalling protein complexes/pathways indicated in Fig. 1.5 being involved in CAT fusion, preliminary data has been shown that the process is mediated by extracellular Ca^{2+}. The absence of extracellular Ca^{2+} inhibits CAT fusion but not CAT formation whilst Ca^{2+}-channel blockers inhibit CAT fusion (Chu, 2013a). These results have shown a possible role for Ca^{2+} signalling regulating these processes. Moreover, in mammalian systems, there are often links between the Ca^{2+}

signalling networks and other signal transduction pathways such as the MAPK pathway (Rosen et al., 1994) and redox signalling (Hidalgo and Zamora, 2007). Furthermore, Ca^{2+} signalling is also important in regulating the dynamic aggregation of the actin and microtubule cytoskeleton (Bennett and Weeds, 1986; Janmey, 1994; Keith et al., 1986; Stolz and Bereiter-Hahn, 1988).

1.3. Ca^{2+} signalling and homeostasis

About 130 years ago, Ringer started landmark experiments on Ca^{2+} signalling and opened up this comprehensive area of signalling research (Carafoli, 2002; Ringer, 1883). Knowledge of Ca^{2+} signalling has been applied in many fields including food and nutrition policy, disease control and drug development (Ross, 2011). Ca^{2+} is a ubiquitous and highly versatile intracellular signal responsible for regulating numerous cellular processes. It presents as a transient increase in the cytosolic free Ca^{2+} ($[Ca^{2+}]_c$) concentration. To achieve this versatility, the Ca^{2+} signalling system operates in many different ways to balance its sophisticated homeostatic mechanism. Fig. 1.7 is a model of Ca^{2+} signalling in mammalian cell. The level of $[Ca^{2+}]_c$ is determined by the regulation of a protein machinery. Ca^{2+} is locally introduced into the cytoplasm and binds to the effectors that are responsible for stimulating numerous Ca^{2+}-dependent processes. On the contrary, $[Ca^{2+}]_c$ is decreased by the combined action of buffers, pumps and exchangers (Berridge et al., 2003). Different machenisms will be introduced in the following sections.

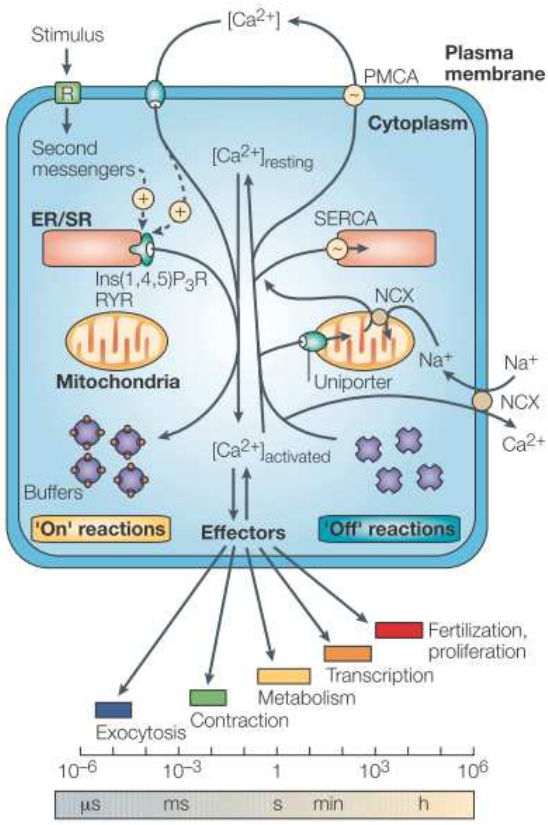

Figure 1.7 Ca^{2+}-signalling dynamics and homeostasis in mammalian cell
Image produced from Berridge et al., 2003. Abbreviations: PMCA, the plasma-membrane Ca^{2+}- ATPase; SERCA, sarco(endo)plasmic teticulum Ca^{2+}-ATPase; NCX, the Na^{+}/Ca^{2+} exchanger; Ins(1,4,5)P3R, inositol-1,4,5-trisphosphate receptor; RYR, ryanodine receptor.

1.3.1. Transport toolkit of Ca^{2+} signals

1.3.1.1. Ca^{2+} channels in the plasma membrane

In mammalian cells, $[Ca^{2+}]_c$ elevations are usually ascribed to Ca^{2+} influx through specific Ca^{2+}-selective channels, which are classified on the basis of their activation mechanisms (Berridge et al., 2000). (1) **Voltage-operated Ca^{2+} channels** (VOCCs), activated by depolarization of the plasma membrane (PM), are used largely by excitable cell types such as muscle and neuronal cells. (2) **Receptor-operated Ca^{2+} channels** (ROCCs), activated by the binding of an agonist to the extracellular domain of the channel, are mainly prevalent in secretory cells and at nerve terminals. (3) **Store-operated Ca^{2+} channels** (SOCCs), activated in response to depletion of the intracellular Ca^{2+} store (Bootman et al., 2000).

In contrast, Ca^{2+} channels are typically non-selective cation channels in the plasma membrane of plants (NSCCs) (Pei et al., 2000; Schroeder et al., 1990; Very and Davies, 2000). The three main groups of plant Ca^{2+}-permeable channels in the plant plasma membrane are classified as (1) the **depolarization-activated Ca^{2+} channels** (DACCs), (2) the **hyperpolarization-activated Ca^{2+} channels** (HACCs), and (3)

the **voltage-independent cation channels** (VICCs). The DACCs that are downregulated by the microtubule cytoskeleton and have been described in a number of cell types such as *Arabidopsis* root cells (Thion et al., 1998). The activation of the HACCs in hyperpolarized membrane potentials leads to an elevation of $[Ca^{2+}]_c$ in guard cells (Holda et al., 1998). The mechanism of VICCs is still unknown, but it is widely considered that the main physiological function is to catalyse the uptake of cations (Demidchik and Maathuis, 2007; Hetherington and Brownlee, 2004; Sanders et al., 2002). Besides these main cation channels, there are other different types of channels in plants including cyclic nucleotide-gated channels (CNGCs), amino acid-gated NSCCs, mechanosensitive ion channels, and vacuolar NSCCs. Meanwhile, It has recently been shown in tobacco and Arabidopsis that glutamate receptor-like channels (GLRs) facilitate Ca^{2+} influx across the plasma membrane, modulate the apical $[Ca^{2+}]$c gradient in pollen tubes, and consequently affect pollen tube growth and morphogenesis (Michard et al., 2011).

Three plasma membrane Ca^{2+} permeable channels have been identified in yeast (Fischer et al., 1997; Iida et al., 1994; Paidhungat and Garrett, 1997; Palmer et al., 2001). At least two independent Ca^{2+} influx systems contribute to the generation of Ca^{2+} signals in the yeast pheromone response including **high affinity Ca^{2+} influx system** (HACS) and **low affinity Ca^{2+} influx system** (LACS) (Iida et al., 1990). Cch1 and Mid1 have been defined as part of the high affinity Ca^{2+} influx system (HACS) that becomes activated very rapidly in response to alkaline stress (Viladevall et al., 2004) and slowly during prolonged exposure to mating pheromones (Iida et al., 1994). Cch1, localized only at the plasma membrane (Locke et al., 2000), is a homologue of the α1-subunit of L-type voltage-gated Ca^{2+} channels (Fischer et al., 1997; Iida et al., 1994; Muller et al., 2001). Mid1 is an integral N-glycosylated plasma protein localized at both the plasma membrane and ER (Yoshimura et al., 2004) with sequence homologs only found in fungi but with a secondary structure that is similar to regulatory α2/δ-subunits of animal voltage-gated Ca^{2+} channels (VGCCs) . Mid1 cooperates with Cch1 in mating pheromone-induced Ca^{2+} uptake (Paidhungat et al., 1997; Fischer et al., 1997; Muller et al., 2001) and the hyperosmotic stress-induced $[Ca^{2+}]_c$ transient (Iida et al., 1994; Fischer et al., 1997). Strains lacking either Cch1 or

Mid1, or lacking both Cch1 and Mid1, exhibit a biochemical defect in Ca^{2+} uptake activity and loss of viability after exposure to the mating pheromone α-factor. This suggests that these two proteins by working together can form a channel necessary for a general Ca^{2+} influx system (Fischer et al., 1997; Locke et al., 2000; Matsumoto et al., 2002; Palma-Guerrero et al., 2014). It has also been known that the HACS activity is much greater after calcineurin inactivation, suggesting the Cch1p-Mid1p mediated Ca^{2+} channel is subject to direct or indirect regulation by calcineurin (Muller et al., 2001). Since the HACS is inhibited by calcineurin in rich medium, LACS becomes essential for this response under these conditions (Groppi et al., 2011). Fig1, which is up-regulated in response to the mating pheromone, is the only characterized member of the LACS in fungi (Aguilar et al., 2007; Muller et al., 2003; Yang et al., 2011).

1.3.1.2. Ca^{2+} release from internal stores

The other principal source of $[Ca^{2+}]_c$ is from the release of Ca^{2+} from intracellular stores as endoplasmic reticulum (ER), mitochondria and vacuoles. The binding of certain hormones or growth factors to specific receptors on the plasma membrane of mammalian cells activate phospholipase C (PLC) which catalyses the hydrolysis of phosphatidylinositol 4,5-bisphosphate (PIP_2) to produce the intracellular messengers inositol 1,4,5-trisphosphate ($InsP_3$) and diacylglycerol (DAG). In mammalian cells, the highly mobile cytosolic second messenger $InsP_3$ interacts with and changes the conformation of its specific receptors ($InsP_3Rs$) on the ER or sarcoplasmic reticulum (SR) to release Ca^{2+} which usually then triggers the $[Ca^{2+}]_c$ oscillations. Another class of receptors, ryanodine receptors (RYRs), located on the ER/SR, are structurally and functionally analogous to the InsP3Rs. Both of the $InsP_3R$ and RYR receptors can be regulated by the Ca^{2+}-induced Ca^{2+} release (CICR) mechanism by being activated at low $[Ca^{2+}]_c$ ($InsP_3Rs$: 0.5–1 µM; RYRs : 1–10 µM) and inhibited at higher $[Ca^{2+}]_c$ ($InsP_3Rs$: >1 µM; RYRs : >10 µM). Cyclic ADP ribose (cADPR), Nicotinic acid adenine dinucleotide phosphate (NAADP), and Leukotriene B4 (LTB4) have also been shown to be intracellular messengers that regulates RYR activity (Bootman et al., 2001).

In plants, the intracellular Ca^{2+} stores include the ER, vacuoles, the nucleus,

chloroplasts, and mitochondria (McAinsh and Pittman, 2009; Sanders et al., 1999; Sanders et al., 2002; Xiong et al., 2006). Four different channels have been identified in the plant vacuolar membrane including $InsP_3$- and cADPR-gated channels, the vacuolar voltage-gated Ca^{2+} (VVCa) and slow-activating vacuolar (SV) channels (Hetherington and Brownlee, 2004; Pottosin and Schonknecht, 2007; Sanders et al., 2002). No homologues have been identified for animal InsP3Rs and RyRs in plants (Gilroy et al., 1990; MacRobbie, 2000; Schumaker and Sze, 1987; Wu et al., 1997).

In budding yeasts, Yvc1 localized in the vacuolar membrane is the homolog of the sole transient receptor potential (TRP) channel in mammalian cells (Denis and Cyert, 2002; Palmer et al., 2001; Zhou et al., 2003). Yvc1 can be activated by hyperosmotic shock to release Ca^{2+} into the cytoplasm (Denis and Cyert, 2002) and the released $[Ca^{2+}]_c$ further activates Yvc1 by Ca^{2+}-induced Ca^{2+} release (CICR) feedback (Zhou et al., 2003).

1.3.1.3. Ca^{2+} pumps and exchangers in the energized system

The “off” reaction, which includes various pumps and exchangers to remove Ca^{2+} from the cytoplasm, maintains the resting level of $[Ca^{2+}]_c$ at ~100 nM and ensures that the internal Ca^{2+} stores are kept loaded. In animal cells, four different pumping mechanisms are responsible for the Ca^{2+} efflux. In mammalian cells, plasma-membrane Ca^{2+}-ATPase (PMCA) and the Na^+/Ca^{2+} exchanger (NCX) localized at the plasma membrane extrude Ca^{2+} to the extracellular space. The sarcoendoplasmic reticulum Ca^{2+} transport ATPase (SERCA), stimulated by cADPR, pumps Ca^{2+} from the cytosol into the lumen of the ER. Mitochondria also have an active function during the recovery process in that they sequester Ca^{2+} rapidly through the mitochondrial Ca^{2+} uniporter (MCU). Recent studies have highlighted a family of Ca^{2+} pumps, known as secretory-pathway Ca^{2+}-ATPases (SPCAs), which might be responsible for Ca^{2+} sequestration into Golgi compartments (Berridge et al., 2003; Missiaen et al., 2007).

The mechanism of Ca^{2+} removal from the cytosol in plants involves different classes of proteins to those of mammalian cells. Vacuoles are the most prominent Ca^{2+} store in plant cells due to their large size and capacity for Ca^{2+} accumulation.

Unlike animals using opposing gradient in Na^+ as the driving force for Ca^{2+} transport, plants use H^+ almost exclusively for this purpose (Sze et al., 1999). A structurally related family of cation exchanger (CAX) genes, that encode H^+/Ca^{2+} exchangers, remove the $[Ca^{2+}]_c$ from the cytosol and restore the $[Ca^{2+}]_c$ to its resting level. These H^+/Ca^{2+} exchangers are present in the tonoplast and plasma membranes (Hirschi et al., 2001; White and Broadley, 2003). Six CAX genes plus five cation/Ca^{2+} exchanger (CCX) families similar to an animal Na^+/Ca^{2+} exchanger isoform have been found in *Arabidopsis* (Cai and Lytton, 2004; Kim et al., 2006).

Unlike mammalian cells, *S. cerevisiae* has not been found to have a Ca^{2+}-pumping ATPase in the plasma membrane or a SERCA-type ATPase in the ER (Eilam et al., 1985). More than 90% of the $[Ca^{2+}]_c$ is stored in yeast vacuole (Dunn et al., 1994) Vcx1, a protein that facilitates Ca^{2+}/H^+ exchange, and Pmc1, a Ca^{2+}-pumping ATPase, pump Ca^{2+} into the vacuole from the cytosol (Cunningham and Fink, 1994; Cunningham and Fink, 1996; Pozos et al., 1996). Pmr1, another Ca^{2+}-pumping ATPase, transports Ca^{2+} or Mn^{2+} into the Golgi (Antebi and Fink, 1992; Rudolph et al., 1989; Sorin et al., 1997).

1.3.2. Ca^{2+} binding proteins (CBPs)

How does the cell recognize and translate an elevation of $[Ca^{2+}]_c$ to a signal for downstream cellular pathways? Ca^{2+} binding proteins (CBPs) play primary roles of modulating the concentration of $[Ca^{2+}]_c$ and decoding the signals as Ca^{2+} sensors. Most CBPs selectively and reversibly bind Ca^{2+} in specific domains that results in a fast kinetics of this interaction (Yanez et al., 2012).

1.3.2.1. Intracellular CBPs with EF-Hand Domains

The classical EF-hand is a helix-loop-helix motif characterized by a sequence of residues flanked with two alpha helices. EF-hand motifs are divided into two major groups: (1) 12-residue canonical EF-hand loops that bind Ca^{2+} mainly via side chain carboxylates or carbonyls, and (2) pseudo 14-residue pseudo EF-hand loops that chelate Ca^{2+} primarily via backbone carbonyls (Zhou et al., 2006).

Calmodulin (CaM) is a Ca^{2+} modulated protein that is organized into 2 canonical

EF-hand pairs separated by a flexible helical linker. This predominant Ca^{2+} sensor exists in a Ca^{2+}-lacking form apocalmodulin and a Ca^{2+}-binding form Ca^{2+}/CaM (Jurado et al., 1999). Binding of Ca^{2+} is associated with a large conformational change and exposure of hydrophobic surfaces within each domain which triggers CaM's Ca^{2+} sensor activity that allows it to react with various target proteins. Moreover, the interaction of CaM with downstream target proteins also increases its Ca^{2+} binding affinity (Clapham, 2007; Clapham et al., 2001). The binding of Ca^{2+} to CaM exposes two hydrophobic surfaces in a methionine-rich crevice of each domain surrounded by negative charges, one in each globular domain. Ca^{2+}/CaM may then bind to its targets mainly by hydrophobic interactions with long hydrophobic side chains in the target sites (Chin and Means, 2000; Snedden and Fromm, 2001). The 3D structure of CaM is shown in Fig. 1.8.

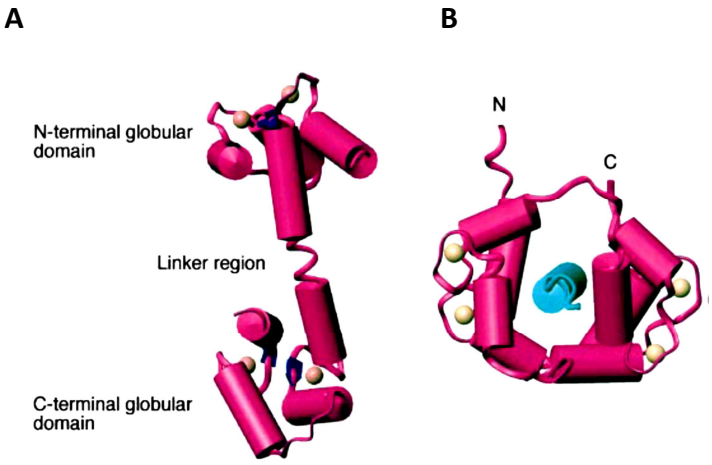

Figure 1.8 Three-dimensional structure of CaM (from Snedden and Fromm, 2001) (A) Crystal structure of Ca^{2+}/CaM. (B) Solution structure of Ca^{2+}/CaM-peptide complex. α-helices are shown as cylinders (pink in CaM, light blue in the target peptide); β-sheets are indicated as deep purple arrows, and Ca^{2+} ions as spheres in light brown. The structural images show only the backbones of CaM and the peptide without side chains.

Calcineurin, a CaM-dependent serine/threonine phosphatase, is a heterodimer protein consisting of a catalytic A subunit (CNA) and a regulatory B subunit (CNB). The CNB contains four EF-hand motifs and binds to CNA to regulate its phosphatase activity even in the absence of Ca^{2+} (Aramburu et al., 2000; Klee et al., 1998). At

resting $[Ca^{2+}]_c$ levels, CNA and CNB remain associated, but the enzyme is inactive due to an autoinhibitory domain at the C terminus of CNA. Upon elevation of $[Ca^{2+}]_c$, Ca^{2+}-bound CaM binds to CNA and displaces the autoinhibitory domain to activate its phosphatase activity (Klee et al., 1998). Calcineurin reacts to local or global $[Ca^{2+}]_c$ signals and controls immediate cellular responses to dephosphorylate serine residues of the transcription factor CRZ initiating a cascade of transcriptional events (Li et al., 2010).

Four types of protein kinases constitute the Ca^{2+} or Ca^{2+}/CaM dependent protein kinase or CaM-like domain protein kinase superfamily. They are distinguished by the different regulation from Ca^{2+}-binding (CDPKs), Ca^{2+}/CaM-binding (CaMKs), both Ca^{2+} and CaM-binding (CCaMKs), or CDPK-related protein kinases (CRKs). Calmodulin-dependent protein kinases (CaMKs) involved in many signalling cascades are serine/threonine-specific protein kinases that are regulated by CaM. Ca^{2+}-dependent protein kinases (CDPKs) are a unique family of kinases that contain three functional parts, catalytic, autoinhibitory and Ca^{2+} -binding domains. They are distinguished by a C-terminal calmodulin-like regulatory domain with four Ca^{2+}-binding EF hands (Harmon et al., 2000; Sanders et al., 1999). Genome sequence analyses indicate that CDPKs might only be present in plants and protozoans. More than 12 members of the CDPK superfamily have been identified in *Arabidopsis*. (Hrabak et al., 1996).

Neuronal Ca^{2+} Sensor (NCS) proteins consist of four EF-hand motifs but the first of these lacks Ca^{2+}-binding activity. Five classes of NCS proteins have been identified to have different roles in the regulation of neuronal function in neurons (Burgoyne, 2007). **Troponin C** is present in all striated muscle and is the trigger of myocyte contraction. One of its isoforms, fast skeletal muscle troponin C, is activated by Ca^{2+} binding to two low-affinity sites in its N-terminal domain. The other cardiac and slow skeletal muscle troponin C is activated by Ca^{2+} binding to a single affinity site (Gillis et al., 2007).

1.3.2.2. Intracellular CBPs without EF-Hand Domains

Calreticulin is involved in ER-dependent Ca^{2+} homeostasis and is the most

important CBP lacking EF-hand domains. It has been shown that calreticulin regulates Ca^{2+} uptake and release from the ER and mitochondria that act as intracellular Ca^{2+} reservoirs (Arnaudeau et al., 2002).

Annexins, also known as lipocortins, are a superfamily of Ca^{2+}-dependent phospholipid- and membrane-binding proteins, which are structurally related. They have a highly conserved C-terminal domain termed the annexin core and a variable N-terminal region. Annexins are located in the cytoplasm and are involved in various processes, including vesicle trafficking, membrane scaffolding and regulation (Rescher and Gerke, 2004). However, the existence of annexins in fungi are still unknown. There have been only 3 annexins genetically identified: ANX14 in *N. crassa* (Braun et al., 1998), ANXC3 and ANXC4 in *A. fumigatous* (Khalaj et al., 2004).

The C2 domain is a Ca^{2+}-binding motif originally identified in protein kinase C (PKC) (Naor et al., 1988). Amongst the best known proteins processing the C2 domain are PKC, synaptotagmins, phospholipase C (PLC) and phospholipase A (PLA). Besides Ca^{2+}, this domain has the ability to bind phospholipids, inositol polyphosphates and certain other intracellular proteins that mediate a wide range of intracellular processes, such as membrane trafficking, generation of lipid second messengers, activation of GTPases, and control of protein phosphorylation (Nalefski and Falke, 1996).

1.3.2.3. Extracellular CBPs (ECBPs)

Besides the intracellular Ca^{2+}, the extracellular Ca^{2+} is also important as a signal molecule for cell regulation and cell-cell communication (Sanders et al., 1999). The requirement for extracellular Ca^{2+} in the formation of intercellular adherens junctions has been shown and extensively studied (Chitaev and Troyanovsky, 1998; Green and Jucha, 1987; Volberg et al., 1986). Cadherin is a class of type-1 transmembrane proteins involved in cell-cell adhesion. It has been known that the cadherin-mediated cell-cell contact requires intracellular Ca^{2+} signalling (Ko et al., 2001).

Extracellular CBPs (ECBPs) have the potential to serve as important therapeutic targets because of the modulatory activities in numerous cellular functions such as blood-clotting, complement activation, cell-cell interactions, cell-matrix interactions,

receptor-ligand interactions, Ca^{2+} transport and Ca^{2+} homeostasis (Yáñez et al., 2012). The ECBPs have been classified in six groups according to the Ca^{2+} binding structure: (i) EF-hand domains; (ii) EGF-like domains; (iii) g -carboxyl glutamic acid (GLA)-rich domains; (iv) cadherin domains; (v) Ca^{2+} -dependent (C)-type lectin-like domains; and (vi) Ca^{2+}-binding pockets of family C G-protein-coupled receptors (Brown and MacLeod, 2001; Hofer and Brown, 2003; Yanez et al., 2012). The family C of the GPCR superfamily includes the extracellular Ca^{2+}-sensing receptor (CaR), metabotropic, glutamate receptors (mGluRs), GABA B receptors, taste receptors and putative pheromone receptors (Yáñez et al., 2012). In these diversely receptors, CaR is the remarkable and peculiar one expressed in varying amounts on the surface of many cell types and in diverse mammalian species (Hofer and Brown, 2003). The CaR is regulated directly by the phosphorylation of protein kinase C (PKC) that binds to the scaffolding protein filamin, which is linked to the ability of the CaR to signal through mitogen-activated protein kinase (MAPK) cascades (Awata et al., 2001; Hjalm et al., 2001).

1.3.3. Ca^{2+} waves and the mysterious language

The equilibrium between the 'on' and 'off' reactions yields a low $[Ca^{2+}]_c$ concentration of ~100 nM when the cells are at rest. However, stimulation of cells causes a transient increase in $[Ca^{2+}]_c$ up to 1 μM or more (Bootman et al., 2001). These continuous and repetitive intracellular Ca^{2+} spikes are commonly patterned in Ca^{2+} oscillations and waves (Jaffe, 2010). A Ca^{2+} wave involves a localized increase in $[Ca^{2+}]_c$ that is followed by a succession of similar $[Ca^{2+}]_c$ increases in immediately adjacent region in a cell. Since Ca^{2+} channels have very short open-times, they only introduce brief pulses of Ca^{2+} that remain localized close to the site of Ca^{2+} channels (Bootman et al., 2001). The local control of various physiological functions is responsible for generating global Ca^{2+} signals (Bootman et al., 2001).

Ca^{2+} waves were first reported in 1978 as the Ca^{2+} "tsunami" that crosses the egg of medaka fish during fertilization (Gilkey et al., 1978). The information contained in the Ca^{2+} waves is still not clear, but it has been shown, for example, that the kinase activity of CaMKII is sensitive to Ca^{2+} oscillations (De Koninck and

Schulman, 1998).

The lower occurrence of Ca^{2+} waves reported in higher plant cells may be due to the domination of plant cells by a large central vacuole. In both *Fucus* rhizoid and pollen tubes, Ca^{2+} waves propagate through regions that contain ER but no large vacuole (Price et al., 1994). In tobacco and Arabidopsis, glutamate receptor–like channels (GLRs) that facilitate Ca^{2+} influx across the plasma membrane modulate the apical $[Ca^{2+}]_c$ gradient and consequently affect pollen tube growth and morphogenesis (Michard et al., 2011).

Compared with animals and plants, relatively little is known about Ca^{2+} signalling in fungi. Due to several technical difficulties or low signal, the utility of fluorescent dyes and the protein-based Ca^{2+} sensor aequorin expressed in fungi has been limited (Knight et al., 1991; Nair et al., 2011a; Nelson et al., 2004; Rogers et al., 2007; Shaw et al., 2001; Silverman-Gavrila and Lew, 2003). Three unique Ca^{2+} signatures have been found to be associated with mechanical perturbation, hypo-osmotic shock, and high external Ca^{2+} in cell population of Aspergillus expressing recombinant aequorin (Nelson et al., 2004). The first successful expression of a FRET-based Ca^{2+} sensor (Cameleon YC3.60; Nagai et al., 2004) has recently been reported in the three plant pathogens, *Magnaporthe oryzae*, *Fusarium oxysporum*, and *Fusarium graminearum*. Different pulsatile Ca^{2+} signatures were observed in different organisms under hyphal growth, development, pathogenesis, and in response to environmental stimuli (Kim et al., 2012).

1.4. Ca^{2+} signalling in filamentous fungi

1.4.1. Fungal cellular function with Ca^{2+} signalling

Many different biological processes have been known to be involved in Ca^{2+} signalling including sporulation, spore germination, cell cycle and hyphal tip growth (Brand and Gow, 2009; Brand et al., 2009; Brand et al., 2007; Cui et al., 2009; Shaw et al., 2001). Ca^{2+} signalling studies in different fungi are listed in Table 1.3.

Table 1.3 Processes involving Ca^{2+} signalling in fungi

Stress or process	Yeast	Filamentous fungi	References
Alkaline stress	*S. cerevisiae*	—	Serrano et al., 2002; Viladevall et al., 2004; Arino, 2010
Antifungal treatment	*S. cerevisiae*	—	Edlind et al., 2002; Courchesne and Ozturk, 2003; Gupta et al., 2003; Courchesne et al., 2009; Ouedraogo et al., 2011; Martin et al., 2011
Appressorium formation	—	*Zoophthora radicans,* *Colletotrichum trifolii* *Colletotrichum gloeosporioides*	Kim et al., 1998; Magalhaes et al., 1991; Warwar and Dickman, 1996
Cell cycle	*S. cerevisiae*	*Aspergillus nidulans*	Rasmussen et al., 1990; 1994
Circadian rhythm	—	*Neurospora crassa*	Techel et al., 1990
Cold shock	*S. cerevisiae*	—	Batiza et al., 1996; Peiter et al., 2005
ER stress	*S. cerevisiae;* *C. neoformans*	—	Hong et al., 2010
Germination	—	*Colletotrichum trifolii* *Neurospora crassa*	Rao et al., 1997; Warwar and Dickman, 1996
Glucose-induced Ca^{2+} elevation	*S. cerevisiae*	—	Batiza et al., 1996; Coccetti et al., 1998; Tisi et al., 2002; Tokes-Fuzesi et al., 2002; Aiello et al., 2004; Kellermayer et al. 2004; Tropia et al., 2006
High external Ca^{2+}	*S. cerevisiae*	—	Miseta et al., 1999a; Miseta et al., 1999b; Forster and Kane, 2000
Hyper-osmotic shock	*S. cerevisiae*	—	Matsumoto et al., 2002; Denis et al., 2002; Zhou et al., 2003
Hyphal branching	—	*Aspergillus niger,* *Fusarium graminearum* *Neurospora crassa*	Reissig and Kinney, 1983; Meyer et al., 2009; Robson et al., 1991a; 1991b
Hyphal tip growth	—	*Saprolegnia ferax* *Candida albicans* *Cryptococcus neoformans* *Fusarium graminearum* *Zoophthora radicans* *Neurospora crassa*	Takeuchi et al., 1988; Hyde and Heath, 1995; Brand et al., 2007; Cruz et al., 2001; Fox and Heitman, 2005; Robson et al., 1991 a; 1991b; Magalhaes et al., 1991
Hypo-osmotic shock	*S. cerevisiae*	—	Batiza et al., 1996; Loukin et al., 2007; Loukin et al., 2008
Iron toxicity	*S. cerevisiae*	—	Peiter et al., 2005

Processes	Yeast	Filamentous fungi	References
Ion stress and salt tolerance	*S. cerevisiae*	—	Mendoza et al., 1996; Matheos et al., 1997; Matsumoto et al., 2002
Mating	*S. cerevisiae; Cryptococcus neoformans*	—	Cruz et al., 2001; Fox and Heitman, 2005
Mechanosensing	—	*Aspergillus awamori, Aspergillus niger, Candida albicans*	Nelson et al., 2004; Bencina et al., 2005; Brand et al., 2007
Microtubule stability	*Ustilago maydis*	—	Adamikova et al., 2004
Oxidative stress	—	*Aspergillus nidulans*	Greene et al., 2002
Programmed cell death	—	*N. crassa*	Gonçalves and Videira, 2014
Salicylic acid	*S. cerevisiae*	—	Mori et al., 1998
Virulence	—	*Cryptococcus neoformans* *Botrytis cinerea* *Magnaporthe oryzae* *Candida albicans* *Aspergillus fumigatus* *Histoplasma capsulatum* *Colletotrichum lagenarium* *Ophiostoma ulmi* *Histoplasma capsulatum*	Sebghati et al., 2000; Odom et al., 1997; Kraus et al., 2003 and 2005; Kmetzsch et al.,2010; Schumacher et al., 2008; Choi et al., 2009; Bader et al., 2003; Blankenship et al., 2003; Sanglard et al., 2003; Steinbach et al., 2006; immermann et al., 1997; Sakaguchi et al., 2008; GADD and BRUNTON, 1992; Sebghati et al., 2000

1.4.2. Ca^{2+} signalling machinery in filamentous fungi

Ca^{2+} signalling in fungi has been most studied in the yeast model *S. cerevisiae* (Fig. 1.9) and similar studies on filamentous fungi (Fig. 1.10) are still limited (Nguyen et al., 2008). Comparative genomic analyses of the Ca^{2+} signalling machinery have been previously executed in *N. crassa*, *M. grisea*, *M. oryzae*, *Aspergillus* spp and *Fusarium* spp (Bencina et al., 2009; Zelter et al., 2004). Some essential proteins (e.g. Cch1) have been identified in fourteen different human fungal pathogens and has been analyzed as possible drug targets (Prole and Taylor, 2012). Some Ca^{2+}-signalling proteins that have been studied by systematic functional analysis are listed in Table 1.4.

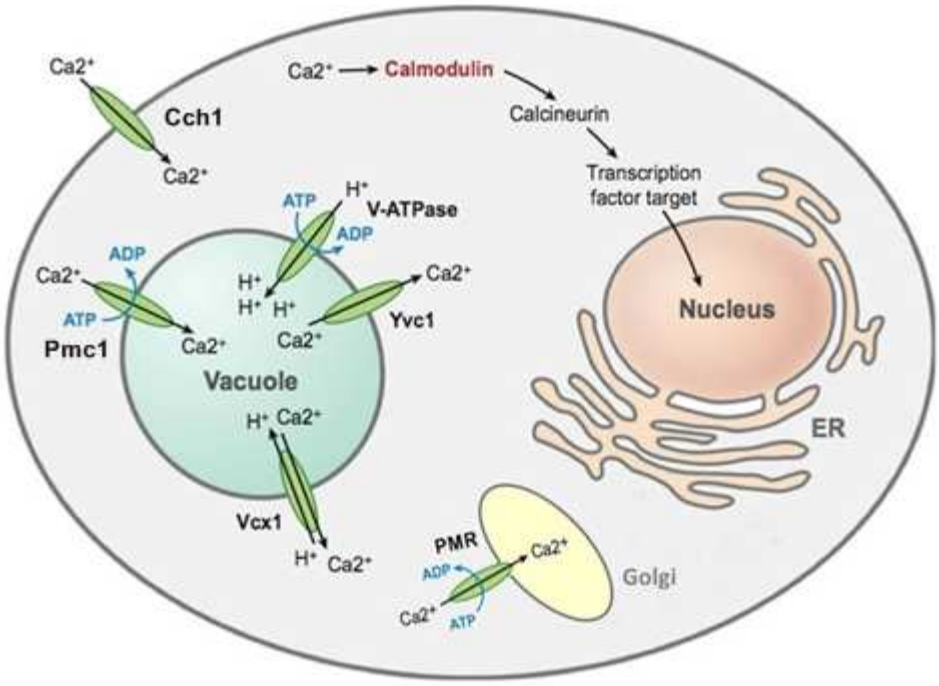

Figure 1.9 Key components fo Ca^{2+} signalling and homeostasis in yeast (adapted from Dolinski and Botstein, 2007; Chu, 2013).

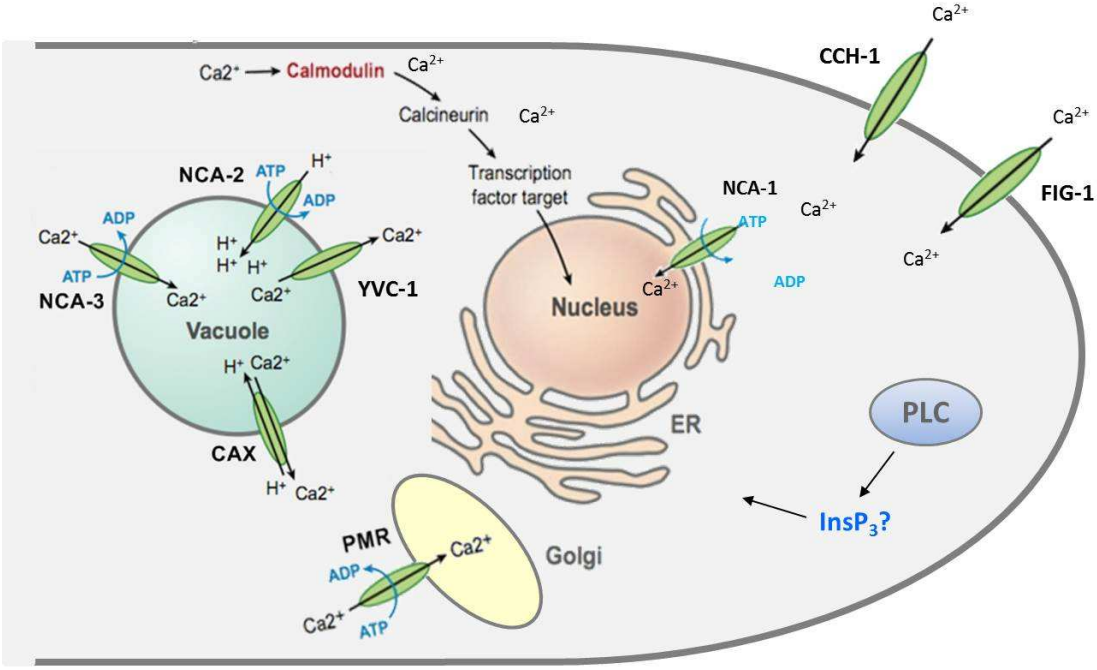

Figure 1.10 Ca^{2+} signalling and homeostasis in *N. crassa* (adapted from Dolinski and Botstein, 2007; Chu, 2013).

Table 1.4 Ca^{2+} signalling machinery in filamentous fungi

Protein	Organism	Protein; topic studies	References
Ca^{2+} permeable channels	*N. crassa*	MID-1; vegetative growth	Lew et al., 2008
	G. zeae	Cch1/Mid1; ascospore discharge	Cavinder et al., 2011
	B. cinerea	Cch1/Mid1; vegetative growth	Harren and Tudzynski, 2013
	C. albicans	Cch1/Mid1; stress response, virulence	Reedy et al., 2009
	C. albicans	Yvc1; stress response	Yu et al., 2013
	A. nidulans	FigA; cell development	Zhang et al., 2014
Ca^{2+} pumps	*N. crassa*	NCA-1, NCA-2, NCA-3, and CAX; $[Ca^{2+}]c$	Bowman et al., 2011
	N. crassa	PMR; $[Ca^{2+}]c$ and cell development	Bowman et al., 2012
	A. fumigatus	PMR1-like; genetic identification	Soriani et al., 2005
	A. fumigatus	PmrA; fungal infection	Dinamarco et al., 2012
	C. neoformans	ENA1; virulence	Idnurm et al., 2009
	C. neoformans	Eca1; virulence, stress tolerance	Fan et al., 2007
Ca^{2+} exchangers	*N. crassa*	CAX; electrical phenotypes	Hamam and Lew, 2012
Phosopholipase C	*N. crassa*	PLC; genetic characterization	Jung et al., 1997
	B. fuckeliana	PLC; genetic characterization	Jung et al., 1997
	A. nidulans	PLC; genetic characterization	Jung et al., 1997
	M. oryzae	MoPLC1; pathogenicity	Rho et al., 2009
	C. neoformans	CnPLC1; virulence	Lev et al., 2013
Calmodulin	*N. crassa*	CaM; Circadian conidiation	Nakashima, 1986
	H. capsulatum	CaM; genetic characterization	El-Rady and Shearer, 1996
	P. brasiliensis	CaM; genetic characterization	Carvalho et al., 2003
	C. albicans	CaM; hyphal formation	Sato et al., 2004
	M. grisea	MoCaM; appressorium formation	Lee and Lee., 1998
Calcineurin	*N. crassa*	CNB-1; vegetative growth	Kothe and Free, 1998
	S. sclerotiorum	Cna1; sclerotial formation	Harel et al., 2006
	C. neoformans	Cna1/CnB1; mating and haploid fruiting	Odom et al., 1997
	A. fumigatus	CnaA; hyphae growth	da Silva Ferreira., 2007
	C. albicans	Cna1/CnB1; hyphae growth	Sanglard et al., 2003
	C. albicans	Rcn1; stress response, virulence	Reedy et al., 2009
	C. glabrata	CnB1; cell wall integrity	Miyazaki et al., 2010
	U. maydis	Ucn1; virulence	Egan et al., 2009
CRZ	*A. fumigatus*	CrzA; regulation of *pmc* genes	Cramer et al., 2008
	C. albicans	Crz1; hyphal growth	Onyewu et al., 2004
	C. glabrata	Crz1; cell wall integrity	Miyazaki et al., 2010
	M. oryzae	Crz1; appressorium formation	Dinamarco et al., 2012
	M. grisea	Crz1; Ca^{2+} homeostasis	Choi et al., 2009
	B. cinerea	Crz1; sclerotial formation, conidiation	Zhang et al., 2009
	C. neoformans	Crz1; cell wall integrity	Lev et al., 2012

Ca^{2+} and/or CaM binding proteins	*N. crassa* *N. crassa* *N. crassa* *S. schenckii* *M. oryzae* *C. neoformans*	CAMK-1; phosphorylation of FRQ NCS-1; Ca^{2+} stress tolerance CaM-PrP; genetic characterization SSCMK1; genetic characterization MoCMK1; appressorial formation Cts1; high-temperature stress	Yang et al., 2001 Deka et al., 2011 Higuch et al., 1990 Liz Valle-Aviles et al., 2007 Liu et al., 2009 Aboobakar et al., 2011
Calcipressin	*A. fumigatus* *C. neoformans*	CbpA; Ca^{2+} homeostasis, hyphal growth Cbp1; hyphal elongation	Pinchai et al., 2009 Gorlach et al., 2000

Abbreviations used for strains : *Aspergillus nidulans, Aspergillus fumigatus, Botrytis cinerea, Botryotinia fuckeliana, Candida albicans, Candida glabrata, Cryptococcus neoformans, Gibberella zeae, Histoplasma capsulatum, Magnaporthe oryzae, Neurospora crassa, Paracoccidioides brasiliensis, Sclerotinia sclerotiorum, Sporothrix schenckii, Ustilago maydis*

1.5. Key questions and the research aim of this thesis

The overall objective of this thesis was to investigate the role of Ca^{2+} signalling during colony initiation using a combination of genetic molecular biology, proteomics analysis, and live-cell imaging techniques.

The primary research aims were:

<u>Chapter 3</u>: A pharmacological analysis of Ca^{2+} signalling during colony initiation

- To determine the influence of extracellular Ca^{2+} on different stages of CAT fusion
- To determine the influence of CaM and calcineurin antagonists on CAT fusion
- To test the effects of a antifungal drug, caspofungin, on CAT fusion

<u>Chapter 4</u>: Comparative genomics and gene deletion mutant analysis of Ca^{2+}/CaM signalling during colony initiation

- To provide a more comprehensive identification of genes involved in the Ca^{2+} signalling machinery of *N. crassa*
- To provide a comparative genomic analysis of 65 proteins involved in the Ca^{2+} signalling machinery in *N. crassa* with two human pathogen *A. fumigatus* and *C. albicans*
- To analyse the morphological phenotypes of 40 gene deletion mutants of the Ca^{2+} signalling/homeostasis machinery to identify possible roles for Ca^{2+} signalling during colony initiation and development

<u>Chapter 5</u>: Proteomics analysis of CaM-binding proteins and protein complexes

- To align CaM protein sequences and it's Ca^{2+}-binding sites in different fungi
- To identify the CaM-interacting proteome using immuno-precipitation and mass spectrometry
- To analyze the potential biological processes regulated by Ca^{2+}/CaM signalling during colony initiation from this proteomic analysis

<u>Chapter 6</u>: Live-cell imaging of proteins involved in Ca^{2+} signalling machinery

- To label proteins (CaM, CNA-1, CNB-1 and CaMK-1) involved in Ca^{2+} signalling with fluorescent proteins and localize their subcellular distribution in conidial germlings
- To analyse CaM dynamics in germlings and mature hyphal tips and determine the influence of extracellular Ca^{2+} on this localization
- To image CaM-GFP in the absence of target genes which are involved in CAT fusion
- To co-localize CaM-GFP with F-actin during colony initiation

<u>Chapter 7</u>: Live-cell imaging of intracellular Ca^{2+} using the protein-based GCaMP Ca^{2+} sensors

- To obtain GCaMPs expressing strains in *N. crassa* and establish a routine screening method for the selection of GCaMP expressing strains.
- To image $[Ca^{2+}]_c$ in living cells of *N. crassa* at different developmental stages by wide-field fluorescence microscopy
- To analysis the Ca^{2+} signatures in germlings and determine whether they play a role on Ca^{2+} signalling at different stages if CAT fusion
- To determine the influence of Ca^{2+} modulating pharmacological agents on these Ca^{2+} sgnatures

Chapter 2
Materials and Methods

Chapter 2–Materials and Methods

2.1 Organisms and strains

2.1.1 *E. coli* strains

The *E. coli* strain used in this study for plasmid DNA (pDNA) selection and amplification was DH5α (#18265-017, Invitrogen).

2.1.2 yeast strains

The yeast strain used in this study for yeast recombinational cloning was FY834 (Winston et al., 1995).

2.1.3 *N. crassa* strains

N. crassa wild type and gene deletion strains were obtained from the Fungal Genetics Stock Center (FGSC, School of Biological Sciences, University of Missouri, Kansas City, USA). Wild type strains FGSC 2489 (*mat A,* 74-OR23-1VA) and FGSC 4200 (*mat a,* ORS-SL6a) were used as controls. The *N. crassa* strains generated during this study were derived from FGSC 9717 (*mat A his-3 mus-51::bar*$^{+}$), FGSC 9718 (*mat a mus-51::bar*$^{+}$), FGSC 9719 (*mat a mus-52::bar*$^{+}$), or 9720 (*mat A his-3 mus-51::bar*$^{+}$). A total of 65 *N. crassa* strains, including 29 gene deletion homokariotic mutants (Table 2.1), were screened and 19 transformants were created in this study (Table 2.2).

Table 2.1 Gene deletion *N. crassa* strains from FGSC used in this study

No.	strain	KO locus	genotype	Mating type	strain type
1	FGSC4200	-	ORS-SL6a	a	homokaryon
2	FGSC2489	-	74-OR23-1VA	A	homokaryon
3	FGSC6103	-	his-3 (Y234M723)	A	homokaryon
4	FGSC9716	-	his-3 (1-234-723)	a	homokaryon
5	FGSC9717	-	Δmus-51::bar+; his^{-3}	A	homokaryon
6	FGSC9718	-	Δmus-51::bar^{+}	a	homokaryon
7	FGSC9719	-	Δmus-52::bar^{+}	a	homokaryon
8	FGSC9720	-	Δmus-52::bar^{+}; his^{-3}	A	homokaryon
9	FGSC11887	NCU04421	*Δanx-14::hph*	a	homokaryon
10	FGSC12548	NCU09123	*Δcamk-1::hph*	a	homokaryon
11	FGSC12448	NCU02283	*Δcamk-2::hph*	a	homokaryon
12	FGSC11536	NCU06177	*Δcamk-3::hph*	A	homokaryon
13	FGSC11545	NCU09212	*Δcamk-4::hph*	a	homokaryon
14	FGSC11531	NCU03750	*Δncu03750:hph*	a	homokaryon
15	FGSC13072	NCU00914	*Δstk-16::hph*	a	homokaryon
16	FGSC15898	NCU01564	*Δncu01564::hph*	a	homokaryon
17	FGSC13049	NCU02115	*Δncu02115::hph*	a	homokaryon
18	FGSC15890	NCU02738	*Δpef-1::hph*	a	homokaryon
19	FGSC11169	NCU02814	*Δchk-2::hph*	a	homokaryon
20	FGSC11403	NCU04379	*Δncs-1:hph*	a	homokaryon
21	FGSC11405	NCU05225	*Δnde-1:hph*	a	homokaryon
22	FGSC11246	NCU06650	*Δncu06650::hph*	a	homokaryon
23	FGSC11541	NCU06948	*Δncu06948::hph*	a	homokaryon
24	FGSC11299	NCU08741	*Δham-3::hph*	a	homokaryon
25	FGSC21396	NCU02833	*Δham-10::hph*	a	homokaryon
26	FGSC12022	NCU01266	*Δplc::hph*	a	homokaryon
27	FGSC12023	NCU02175	*Δplc::hph*	a	homokaryon
28	FGSC11411	NCU06245	*Δplc::hph*	a	homokaryon
29	FGSC11618	NCU04120	*Δcmd-1::hph*	a	heterokaryon
30	FGSC17929	NCU03804	*Δcna-1::hph*	a	heterokaryon
31	FGSC12512	NCU03833	*Δcnb-1::hph*	a	heterokaryon
32	FGSC11494	NCU07952	*Δcrz-1::hph*	a	heterokaryon
33	FGSC11613	NCU01241	*Δagc-1::hph*	a	heterokaryon
34	FGSC15488	NCU04265	*Δinv::hph*	a	heterokaryon
35	FGSC11502	NCU06347	*Δend-3::hph*	a	heterokaryon
36	FGSC11503	NCU06617	*Δcdc-4::hph*	a	heterokaryon
37	FGSC11504	NCU09871	*Δnde-2::hph*	a	heterokaryon

Table 2.2 Protein-labelling *N. crassa* strains used in this study

No.	strain	Original host strain	Protein expressed	genotype	strain type
1	NCCC001	FGSC9718	CaM-GFP	*Pcmd-1::cmd-1-sgfp::hph*$^+$*,Δmus-51::bar*$^+$	heterokaryon
2	NCCC002	FGSC9718	CaM-GFP	*Pcmd-1::cmd-1-sgfp::hph*$^+$	homokaryon
3	NCCC003	FGSC9718	CaM-GFP	*Pcmd-1::cmd-1-sgfp::nat*$^+$*,Δmus-51::bar*$^+$	heterokaryon
4	NCCC004	FGSC9718	CaM-GFP	*Pcmd-1::cmd-1-sgfp::nat*$^+$	homokaryon
5	NCCC005	FGSC9718	CaM-mCherry	*Pcmd-1::cmd-1-mcherry::nat*$^+$*,Δmus-51::bar*$^+$	heterokaryon
6	NCCC006	FGSC9717	CaM-GFP	*his-3*$^+$*::Pccg-1-cmd-1-sgfp::bar*$^+$*,Δmus-51::bar*$^+$	heterokaryon
7	NCCC007	FGSC9717	GFP-CaM	*his-3*$^+$*::Pccg-1- sgfp- cmd-1::bar*$^+$*,Δmus-51::bar*$^+$	heterokaryon
8	NCCC008	FGSC9718	CaM-V5	*Pcmd-1::cmd-1-v5-hat::nat*$^+$*,Δmus-51::bar*$^+$	homokaryon
9	NCCC009	FGSC9718	CNA-GFP	*Pcna-1::cna-1-sgfp::hph*$^+$*,Δmus-51::bar*$^+$	heterokaryon
10	NCCC010	FGSC9718	CNA-GFP	*Pcna-1::cna-1-sgfp::hph*$^+$	homokaryon
11	NCCC011	FGSC9717	CNA-GFP	*his-3*$^+$*::Pccg-1-cna-1-sgfp::bar*$^+$*,Δmus-51::bar*$^+$	heterokaryon
12	NCCC012	FGSC9718	CNB-GFP	*Pcnb-1::cnb-1-sgfp::hph*$^+$*,Δmus-51::bar*$^+$	heterokaryon
13	NCCC013	FGSC9718	CNB-GFP	*Pcnb-1::cnb-1-sgfp::hph*$^+$	homokaryon
14	NCCC014	FGSC9717	CNB-GFP	*his-3*$^+$*::Pccg-1-cnb-1-sgfp::bar*$^+$*,Δmus-51::bar*$^+$	heterokaryon
15	NCCC015	FGSC9718	CaMK-1-GFP	*Pcamk-1::camk-1-sgfp::hph*$^+$*,Δmus-51::bar*$^+$	heterokaryon
16	NCCC016	FGSC9718	CaMK-1-GFP	*Pcamk-1::camk-1-sgfp::hph*$^+$*,Δmus-51::bar*$^+$	homokaryon
17	NCCC017	FGSC9718	NCS-1-GFP	*Pncs-1::ncs-1-sgfp::hph*$^+$*,Δmus-51::bar*$^+$	heterokaryon
18	NCCC018	FGSC9718	NCS-1-GFP	*Pncs-1::ncs-1-sgfp::hph*$^+$*,Δmus-51::bar*$^+$	homokaryon
19	NCCC019	FGSC9717	GCaMP3	*his-3+::Pccg-1- gcamp3::bar*$^+$*,Δmus-51::bar*$^+$	heterokaryon
20	NCCC020	FGSC9717	GCaMP3	*his-3+::Ptef-1- gcamp3::bar*$^+$*,Δmus-51::bar*$^+$	heterokaryon
21	NCCC021	FGSC9717	GCaMP5	*his-3+::Pccg-1- gcamp5::bar*$^+$*,Δmus-51::bar*$^+$	heterokaryon
22	NCCC022	FGSC9717	GCaMP5	*his-3+::Ptef-1- gcamp5::bar*$^+$*,Δmus-51::bar*$^+$	heterokaryon
23	NCCC023	FGSC2489	GCaMP5	*Pccg-1- gcamp5::bar*$^+$	heterokaryon
24	NCCC024	FGSC9717	GCaMP6s	*his-3+::Pccg-1- gcamp6s::bar*$^+$*,Δmus-51::bar*$^+$	heterokaryon
25	NCCC025	FGSC6103	GCaMP6s	*his-3+::Pccg-1- gcamp6s::bar*$^+$*,Δmus-51::bar*$^+$	heterokaryon
26	NCCC026	FGSC9717	GCaMP6s	*his-3+::Ptef-1- gcamp6s::bar*$^+$*,Δmus-51::bar*$^+$	heterokaryon
27	NCCC027	FGSC9717	GCaMP6s	*his-3+::Ptef-1- gcamp6s::bar*$^+$*,Δmus-51::bar*$^+$	homokaryon
28	NCCC028	FGSC6103	GCaMP6s	*his-3+::Ptef-1- gcamp6s::bar*$^+$*,Δmus-51::bar*$^+$	heterokaryon
29	NCCC029	FGSC6103	GCaMP6s	*his-3+::Ptef-1- gcamp6s::bar*$^+$*,Δmus-51::bar*$^+$	homokaryon
30	NCCC030	FGSC2489	GCaMP6s	*Pccg-1- gcamp6s::bar*$^+$	heterokaryon
31	NCCC031	FGSC4200	GCaMP6s	*Pccg-1- gcamp6s::bar*$^+$	heterokaryon
32	NCCC032	NCCC003 NCAL005	CaM-GFP lifeact-TagRFP	*Pcmd-1::cmd-1-sgfp::nat*$^+$*,Δmus-51::bar*$^+$ *Pccg-1::lifeact-tagrfp::bar*$^+$	homokaryon
33	NCCC033	NCCC026 FGSC11442	CaM-GFP lifeact-TagRFP Δ*myo-5*	*Pcmd-1::cmd-1-sgfp::nat*$^+$*,Δmus-51::bar*$^+$ *Pccg-1::lifeact-tagrfp::bar*$^+$ *Δmyo-5::hph*$^+$	homokaryon

2.2 Culture media and growth conditions

2.2.1 Culture media for *E. coli*

E. coli strains were grown in Luria Bertani (LB) medium (Table 2.3) at 37^{o}C. Media for transformants with a selection marker were supplemented with 100 μg/ml ampicillin or 10 μg/ml phleomycin.

Table 2.3 Media for *E. coli*

Media	Full name	Component (w/v)
LB	Luria Bertani medium broth	tryptone 1%, yeast extract 0.5 %, NaCl 1%
LA	Luria Bertani medium agar	tryptone 1%, yeast extract 0.5 %, NaCl 1%, Agar 1.5%
SOC	Super Optimal broth	tryptone 1%, yeast extract 0.5 %, NaCl 1%, KCl 2.5 μM, $MgCl_2$ 5 μM

2.2.2 Culture media for Yeast

Yeast strains were grown in yeast extract peptone dextrose (YPD) medium at 30^{o}C. Transformants were selected on SC-Ura plates (Table 2.4).

Table 2.4 Media for Yeast

Media	Full name	Component (w/v)
YPD	Yeast Extract Peptone Dextrose	yeast extract 1%, peptone 2%, dextrose 2%
YPDA	Yeast Extract Peptone Dextrose agar	yeast extract 1%, peptone 2%, dextrose 2%, agar 1.5%
SC-Ura	Synthetic complete without uracil	dropout base (Yeast Nitrogen Base 1.71 g/L, ammonium sulfate 5 g/L and dextrose 20 g/L) with glucose 2.67%, dropout base synthetic minus uracil 2%, agar 1.5%

2.2.3 Culture media for *N. crassa*

N. crassa cultures for experiments were grown on standard Vogel's medium (VM; Table 2.5 and Table 2.6) in Petri dishes or on slants at 35^{o}C in dark for 3 days and moved to 25^{o}C with light for 2 days to promote conidiation. Stock cultures were preserved on slants at -20 ^{o}C or at -80 ^{o}C. Media for mutants with selection marker were supplemented with the antibiotics listed in Table 2.7.

Table 2.5 Media for *N. crassa*

Media	Full name	Component (w/v)
VM	Standard Vogel's minimal media	1X Vogel's salts 50x stock solution, 2 % sucrose, 1.5 % agar
VM + his	Standard Vogel's minimal media + histidine	1X Vogel's salts 50x stock solution, 2 % sucrose, 1.5 % agar, 100 µg/ml histidine
LNVM + Ign	Low nitrogen Vogel's minimal media + Ignite	1X Nitrogen free Vogel's salts 50x stock solution, 0.5% L-Proline, 2% sucrose, 1.5% agar, 80 µg/ml Ignite
SCM	Synthetic crossing medium	1X Synthetic crossing medium 50x stock solution, 2% sucrose, 1.5% agar
MC	MC medium	0.1X Synthetic crossing medium 50x stock solution, 0.5% sucrose, 1.5% agar
CSM	Complete selection media	1X Vogel's salts 50x stock solution, 1M Sorbitol, 1.5% agar; add 1X FIGS after autoclaved
LNCSM + Ign	Low nitrogen complete selection media + Ignite	1X Nitrogen free Vogel's salts 50x stock solution, 0.5% L-proline, 1.5% agar; add 1X FIGS and 100 µg/ml Ignite after autoclaved

Table 2.6 Salts stock solutions for *N. crassa*

Composition of Vogel's biotin stock solution (stored at 4°C)

Component	Quantity
d-Biotin	5 g
dH_2O	Add 1 l

10X FIGS solution (autoclaved)

Component	Quantity
sorbose	200 g
fructose	5 g
glucose	5 g
dH_2O	Add 1 l

Composition of Vogel's trace elements solution (stored at 4°C)

Component	Quantity
Citric acid-$1H_2O$	5 g
$ZnSO_4$-$7H_2O$	5 g
$Fe(NH_2)_4\ SO_4$-$7H_2O$	1 g
$CuSO_4$-$5H_2O$	0.25 g
$MnSO_4$-$1H_2O$	0.05 g
$H_2\ BO_4$	0.05 g
Na_2MoO_4-$2H_2O$	0.05 g
dH_2O	Add 1 l

Composition of Vogel's salts 50x stock solution (stored at 4°C)

Component	Quantity
Na_3Citrate-$2H_2O$	126.7 g
KH_2PO_4	250 g
NH_4NO_3 (eliminated for nitrogen free Vogel's salts)	100 g
$MgSO_4$-$7H_2O$	10 g
$CaCl_2$-$2H_2O$	5 g
Vogel's trace elements solution	5 ml
Biotin solution	5 ml
dH_2O	Add 1 l

Composition of synthetic crossing medium 50x stock solution (stored at 4°C)

Component	Quantity
KNO_3 (eliminated for nitrogen free Vogel's salts)	50 g
K_2HPO_4	35 g
KH_2PO_4	25 g
$MgSO_4$-$7H_2O$	25 g
NaCl	5 g
$CaCl_2$-$2H_2O$	5 g
Vogel's trace elements solution	5 ml
Biotin solution	2.5 ml
dH_2O	Add 1 l

Table 2.7 Selection markers for *N. crassa* used in this study.

Antibiotics	Final concentration
Hygromycin B (Calbiochem)	200 μg/ml
Nourseothricin (Werner BioAgents)	25 μg/ml
Ignite (Basta; glufosinate ammonium; phosphinothricin, #77182-82-2, Sigma-Aldrich)	100 μg/ml

2.3 Plasmid DNA

Plasmids used and engineered in this study are listed in Table 2.8.

Table 2.8 Plasmids used in this study.

Plasmid	Vector backbone	Genotype	Source/Reference
pCC001	pRS426	*cmd-1-5f-v5hat-hph-cmd-1-3f*	This study
pCC002	pRS426	*cmd-1-5f-sgfp-hph-cmd-1-3f*	This study
pCC003	pRS426	*cmd-1-5f-sgfp-nat-cmd-1-3f*	This study
pCC004	pCCG::C-Gly::GFP	*his-3-Pccg-1- cmd-1-sgfp*	This study
pCC005	pCCG::C-Gly::GFP	*his-3-Pccg-1-sgfp-cmd-1*	This study
pCC006	pRS426	*cna-1-5f-sgfp-hph-cna-1-3f*	This study
pCC007	pRS426	*cnb-1-5f-sgfp-hph-cnb-1-3f*	This study
pCC009	pCCG::C-Gly::GFP	*his-3-Pccg-1- crz-1-sgfp*	This study
pCC010	pRS426	*camk-1-5f-sgfp-hph-camk-1-3f*	This study
pCC011	pRS426	*ncs-1-5f-sgfp-hph-ncs-1-3f*	This study
pCC012	pRS426	*plc-1-5f-sgfp-hph-plc-1-3f*	This study
pCC013	pRS426	*rgs-1-5f-sgfp-hph-rgs-1-3f*	This study
pCC018	pCCG::C-Gly::GFP	*his-3-Pccg-1- gcamp3*	This study
pCC019	pCCG::C-Gly::GFP	*his-3-Ptef-1- gcamp3*	This study
pCC018	pCCG::C-Gly::GFP	*his-3-Pccg-1- gcamp5*	This study
pCC019	pCCG::C-Gly::GFP	*his-3-Ptef-1- gcamp5*	This study
pCC021	pBABRAR	*Pccg-1- gcamp5-bar*	This study
pCC018	pCCG::C-Gly::GFP	*his-3-Pccg-1- gcamp6s*	This study
pCC019	pCCG::C-Gly::GFP	*his-3-Ptef-1- gcamp6s*	This study
pCC021	pBABRAR	*Pccg-1- gcamp6s-bar*	This study

2.4 Comparative genomic analysis

Potential hypothetical protein orthologs from *N. crassa* (reciprocally blasted and cross-compared with the *S. cerevisiae* genome) were identified based on: E-values, % identities and number of positives, as well as conserved protein domains.

The following genome and proteome online tools were used to compare and re-probe gene and protein sequences, and validate predicted functional domains:

(1) Genome database at the BROAD institute of MIT and Cambridge website
http://www.broadinstitute.org/
Neurospora crassa
http://www.broad.mit.edu/annotation/genome/neurospora/
Saccharomyces cerevisiae
http://www.broad.mit.edu/annotation/genome/saccharomyces_cerevisiae/

(2) Saccharomyces genome database
http://www.yeastgenome.org/

(3) Aspergillus genome database
http://www.aspgd.org/

(4) Candida genome database
http://www.candidagenome.org/

(5) GenBank at NCBI
http://www.ncbi.nlm.nih.gov/genbank/index.html

(6) SMART
http://smart.embl-heidelberg.de/

(7) Functional Domains
http://www.ebi.ac.uk/InterProScan/

2.5 Gene deletion mutant screening assays

2.5.1. Colony phenotypic analysis

To observe 16 h young colony and 5 d mature colony morphology, each strain was inoculated in the centre of an agar plate. Petri dishes were routinely incubated at 35°C for 16 h in the dark. Images were taken at 16 h for young colonies. Cultures used for observations on 5 d mature colony were incubated at 35°C for 3 days and moved to 25^{o}C with light for 2 days to promote conidiation. The colony extension rate, colony morphology and conidiation were analysed for 29 homokaryotic mutant.

2.5.2. CAT fusion assays

A cell suspension was prepared by harvesting the conidia from the plate cultures in liquid Vogel's medium, and was incubated at a final concentration of 1 x 10^6 spores/ml in 8-well slide culture chambers (Nalg Nunc, Rochester, NY, USA) at 35°C. Measurements were made at 4 h or 5 h. CAT fusion was quantified according to the method described by Roca et al. (2010). Germination was defined as the number of conidia with any protrusion emerging from the main spore body and cell fusion defined as the number of germlings that had fused with other germlings. The error bars indicate standard deviations.

2.5.3. Vegetative hyphal fusion assays

A Petri dish containing Vogel's medium was inoculated in its centre and cultures incubated at 35°C for 16 h. A 3 cm^3 block of agar medium from the colony periphery was cut out from the Petri dish and placed on a 48 x 64 mm cover slip. Differential interference contrast microscopy (DIC) and fluorescence microscopy were used to observe the presence of vegetative hyphal fusion (Hickey et al., 2002b).

2.6 Biochemical agents and inhibitors

A spore suspension was prepared by harvesting conidia from the plate cultures of the wild type *N. crassa* FGSC 2489 strain in liquid medium containing biochemical inhibitors (Table 2.9) at different concentrations. These conidial suspensions, at a final concentration of 1 x 10^6 conidia/ml, were incubated in 8-well slide culture chambers (Nalg Nunc) at 35°C. Measurements were made after 4 h. CAT fusion and conidial germination were quantified according to the method described by Roca et al. (2010). For live-cell imaging, pharmacological inhibitors were added to the fungi growing in the 8-well slide culture chambers during time course sequences.

Table 2.9 Biochemical agents used in this study.

Antibiotics	Function	Stock conc.
Calmidazolium (#57265-65-3, Sigma-Aldrich)	CaM antagonist	100 mM
Trifluoperazine (#440-17-5, Sigma-Aldrich)	CaM antagonist	100 mM
FK506 (#109581-93-3, Sigma-Aldrich)	Calcineurin inhibitor	10 mM
Cyclosporin A (#59865-13-3, Sigma-Aldrich)	Calcineurin inhibitor	10 mM
Caspofungin diacetate (#179463-17-3, Sigma-Aldrich)	Antifungal drug	10 mM
Benomyl (#17804-35-2, Sigma-Aldrich)	microtubule depolymerzer	3 mg/ml
Latrunculin A (#76343-93-6, Sigma-Aldrich)	F-actin polymerization inhibitor	1 mM

2.7 Molecular cloning techniques

2.7.1. Genomic database

All information of genes is from the *N. crassa* genome database at the BROAD institute. (http://www.broadinstitute.org/annotation/genome/neurospora/MultiHome.html)

2.7.2. Primer design

Primers used in this study were supplied by Invitrogen (Invitrogen Ltd., Paisley, UK) or Eurofins (Eurofins MWG Operon) and are listed in Supplementary Table A.1. Genes and primers were analysed by the DNADynamo sequence analysis and Oligos software. Primer details were also analysed using Oligos 6.0 Primer Analysis Software and the Finnzyme Tm calculator online tool (https://www.finnzymes.fi/tm_determination.html).

2.7.3. Expression system

A gene knock-in expression and tagging strategies were performed in order that the fusion protein was under control of the labeled gene's native promoter and expressed from its endogenous locus (Larrondo et al., 2009). Since the genome of *N. crassa* has been completely sequenced, a library of DNA flanks has been generated as a part of the *N. crassa* knockout project (Colot et al., 2006). High-throughput expression approaches were developed including using yeast recombinational cloning (YRC) (Oldenburg et al., 1997) and recipient strains exhibiting high homologous recombination frequency (Ninomiya et al., 2004). In order to prevent

the tagged genes inserting into other gene loci, the knock-in strategy was used to create strains expressing different GFP fusion proteins for live-cell imaging.

2.7.4. Extraction of genomic DNA from *N. crassa*

The desired strain was grown in 9 cm petri dish with 25 ml liquid VM at 35°C overnight. The mycelium was carefully dried with sterile Miracloth (#475855, Calbiochem, Merk KGaA, Darmstadt, Germany), and was shocked-frozen in liquid nitrogen. The thawed sample was placed into a 2 ml Eppendorf tube which contained ~ 50 µl glass beads (G9268-250G, 425-600 µm, Sigma) and 1 ml extraction buffer (Tris 100 mM, NaCl 1.4 M, EDTA 10 mM, CTAB 2%, pH 8) was mixed by vigorous vortexing at maximum speed for 5-10 minutes and then shaking by Fastprep-24 instrument (MPBio) for 60 s at 4 m/sec. The mixture was incubated at 60-65°C for 10 min and subsequently centrifuged (13400rpm for 2 min). RNase (#19101, Qiagen; 10 ng/µl final concentration) was added to ~ 700 µl of supernatant in a new tube and incubated at 37°C for 15-30 min. To extract genomic DNA (gDNA), a 700 µl chloroform:isoamyl alcohol (25:1) mixture was sequentially added. Phase separation was achieved by centrifugation at 4°C with 12,000 g for 10 min. The upper gDNA fraction (~ 600 µl) was transferred into a fresh 1.5 ml Eppendorf tube containing a 600 µl chloroform/isoamylalcohol 49:1 mixture and the separation steps repeated. The final upper aqueous layer was transferred to a fresh 1.5 ml Eppendorf tube containing 600 µl pre-chilled (-20°C) isopropanol, and was incubated at -20°C for more than 30 min. The precipitated gDNA was pelleted by centrifugation at 14,000 g for 15 min at 4°C, and washed once in 800 µl 75% EtOH. The final gDNA product was dried as much as possible at room temperature for 10 min, and then resuspended in 50-100 µl of 10 mM Tris-HCl at 65°C.

2.7.5. Polymerase chain reaction (PCR)

For molecular cloning, PCR was used to amplify specific DNA sequences from DNA templates. Phusion® High-Fidelity DNA Polymerase (M0530S, NEB) was used in this study. Initial denaturation and melting temperatures were 98 ^{O}C. The PCR parameters were set by the Piko® Thermal Cycler (Finnzymes Instruction Oy, Espoo,

Finland) according to the different T_m of each primer set and the different lengths of DNA.

2.7.6. Fusion PCR

To knock-out specific genes in *N. crassa*, fusion PCR was used to generate the DNA fragments for transformation. Hot Start Taq DNA Polymerase (M0495S, NEB) was used to create fusion DNA fragments by parameters:

Cycles	Temperature	Time
1	98°C	2 min
10	98°C	10 s
	58°C	5 s
	72°C	1 min/kb + 20 s increments per cycle
15	98°C	10 s
	61°C	5 s
	72°C	1 min/kb+ 20 s increments per cycle
1	72°C	2 min + 1 min/kb

2.7.7. DNA electrophoresis

Agarose was added to 1 x TAE buffer and heated to dissolve it and prepare 1% agarose gel. 5 µl of ethidium bromide was added to the cooled gel and poured into a gel tray. The appropriate number of combs were placed in the gel tray. The gels were allowed to cool for 15-30 min at room temperature. Solidified gels were placed in the electrophoresis chamber and covered with 1 x TAE buffer. Samples with loading buffer were loaded onto the different wells. The parameters used for electrophoresis were 130 V for 45 min. A UV lightbox was used to visualize the DNA bands.

2.7.8. Ethanol precipitation of DNA

Ethanol precipitation was used to concentrate or purify the DNA. 1/10 volume 3 M sodium acetate (pH 5.2) was added to the DNA solution in an Eppendorf tube. 3 volumes of chilled (-20°C) 95-100% EtOH were mixed with the DNA solution and precipitated for 30 min at 4 °C . The mix was centrifuged at 14,000 rpm and 4 °C for 15 min. After removing the supernatant, the DNA pellet was washed in 500 µl 70% chilled (-20°C) EtOH and centrifuged at 14,000 rpm at 4 °C for 5 min. The pellet was

dried for 10 min at RT and resuspended in water or Tris-HCl (pH 8.5) buffer.

2.7.9. Yeast recombinational cloning

2.7.9.1. Yeast transformation

The *Saccharomyces cerevisiae* strain FY834 (*MATα, ura3-52, leu2Δ1, trp1Δ 63, his3Δ200, lys2Δ202*) was used for yeast recombinational cloning. A cell culture was grown in 3 ml of YPD in a glass tube at 30 ^{o}C with shaking at 180 rpm for 24 h, and 1 ml of overnight cell culture was inoculated into 50 ml YPD in a 250 ml flask and incubated under the same conditions. When the O.D. 600 reached 1, the cell suspension was centrifuged at 14,000 g for 10 min. The pellet was washed with 25 ml sterile water once and with 1 ml 100 mM lithium acetate once. The final cell pellet was re-suspended in 400 µl 100 mM lithium acetate.

50 µl of competent yeast cell suspension was transferred into a sterile Eppendorf tube, and was quickly spun for 15 sec to discard the supernatant. A PEG transformation mix was prepared according to the formula in Table 2.10. and completely mixed with the cell pellet. The transformation solution was incubated at 30 ^{o}C for 30 min, and then 42 ^{o}C for 30 min. After washing with 1 ml sterile water once, the cell pellet was resuspended in 150 µl sterile water and spread onto a SC-Ura plate. Plates were incubated at 30 ^{o}C for 3 days.

Table 2.10 PEG transformation mix

Component	Quantity
50% PEG	240 µl
1 M lithium acetate	36 µl
Sheared salmon sperm DNA (2 mg/mL)	50 µl
dH_2O	32 µl
DNA fragment	2 µl

2.7.9.2. Yeast genomic DNA extraction

2 ml of YPD was added to the transformation plate, and colonies were scraped off with the end of a microscope slide. The cell suspension was spun quickly for 15

sec, and the supernatant was removed. The pellet was re-suspended in 100 µl STET (8% sucrose, 50 mM Tris pH 8, 50 mM EDTA, 5% Triton X-100) and 0.2 g 0.45 mm glass beads were added before vortexing vigorously for 5 min. Following addition of another 100 µl of STET, the tube was vortexed briefly and placed in a boiling water bath for 3 min, and then cooled on ice. After spinning at 4 ^{o}C at 14,000 g for 10 min, the 100 µl supernatant was transferred to a fresh Eppendorf tube containing 50 µl of 7.5 M ammonium acetate, and incubated at -20 ^{o}C for 1 h. Finally, 100 µl of supernatant was removed for DNA EtOH precipitation to purify the yeast gDNA.

2.7.10. In-Fusion^{TM} cloning

In-FusionTM Advantage PCR Cloning Kit (#63961, Clontech Laboatories, Takara Bio Europe, Saint-Germainen-Laye, France) was used for DNA ligation. (http://www.clontech.com)

2.7.11. *E. coli* transformation

2.7.11.1. Electroporation

The *Escherichia coli* strain DH5α was used for molecular cloning. A cell culture was grown in 5 ml LB medium in a tube at 37 ^{o}C with shaking at 250 rpm for 16 h and then 1 ml of overnight cell culture was inoculated into 100 ml LB medium in a 500 ml flask and incubated under the same conditions. When the O.D.600 reached 0.4, the cell suspension was rapidly cooled in a ice-water bath for 20 min and then centrifuged at 1,000 g for 15 min at 4 ^{o}C. The pellet was washed with 500 ml of ice-cold sterile water once, 250 ml of ice-cold 10% glycerol once, and 10 ml of ice-cold 10% glycerol once. The final cell pellet was re-suspended in ice-cold GYT medium to a final cell concentration of 2.5 X 10^{10} cells/ml. 40 µl/tube aliquots were made for immediate use or they were stocked at -80 ^{o}C.

40 µl of competent cell suspension and 10 pg to 25 ng DNA were mixed in a sterile Eppendorf tube and incubated on ice for 5 min. The conidia/DNA mix was transferred to a pre-chilled (-20^{o}C) 0.2 cm gapped electroporation cuvette (#Z706086-50EA, Sigma-Aldrich). Electroporation was performed in a BioRad Gene PulserTM (BioRad Laboratories Ltd., Herts, UK) using the following parameters:

voltage 2.5 kV/cm, capacitance 25 µF and resistance 200 ohms. After electroporation, cells were immediately recovered by adding 1 ml of SOC medium at room temperature and transferred to a sterile Eppendorf tube. Samples were incubated at 37 ^{o}C with 250 rpm shaking for 1 h. Different volumes of the electroporated cells were plated onto LA medium containing 100 µg/ml ampicillin. The plates were finally inverted and incubated at 30 ^{o}C for 16 h.

2.7.11.2. Heat-shock transformation

A 25-50 µl aliquot of competent cells was incubated with 10 ng DNA for 5 min. After a 45 sec heat shock at 42 °C in a water bath, the cells were left on wet ice for 5 min, then recovered with 900 µl of pre-warmed (42 °C) SOC medium and incubated for 45-60 min at 37 °C and 250 rpm. Cells were pelleted and resuspended in 200 µl of fresh SOC. 50 and 150 µl were plated onto LB agar supplemented with the appropriate antibiotic and incubated at 37 °C overnight.

2.7.12. Colony PCR

The colonies of *E. coli* transformants were picked into microtubes containing 5 µl dH_2O for PCR templates, and they were transferred to LA plates (100 µg/ml ampicillin) at the same time. Specific primer sets were used for colony PCR. The colonies were amplified with a specific PCR product were picked to inoculate in LB for plasmid extraction.

2.7.13. Plasmid extraction

Plasmid minipreps were performed using ZyppyTM Plasmid Miniprep Kit (D4020, Zymo Research, U.S.A.) according to the manufacturer's instructions.

2.7.14. Sequencing

DNA sequencing PCRs were performed by BigDye® Terminator v3.1 Cycle Sequencing kit (#4337455, Applied Biosystems, Warrinton, UK), and analysed by The GenePool Sequencing Service, Ashworth Laboratories University of Edinburgh, Edinburgh, UK. Sequences were analysed by FinchTV version 1.4.0 software from

Geospiza Inc., Seattle, USA, and blasted by DNADynamo sequence analysis software.

2.7.15. Restriction enzyme digestion

DNA fragments for *N. crassa* transformation were prepared by restriction digestion. There are two NcoI sites in this plasmid system. Restriction enzymes were purchased from New England Biolabs (New England Biolabs Ltd., Hitchin, UK) or Promega (Promega Bioscience, Inc., Southampton, UK). Restriction digests were performed according to the manufacturer's instructions.

2.8 Transgenic *N. crassa* strains

2.8.1. Transformation of *N. crassa*

2.8.1.1. Competent cell preparation

For obtaining a fresh stock of conidia from *N. crassa*, the desired strain was incubated in a 250 ml flask with 50 ml of Vogel's medium at 25 ^{o}C under constant light. Conidia were collected after 2-3 weeks of growth by adding 50 ml of sterile water. The suspension of conidia was filtered through a sterile Miracloth (#475855, Calbiochem, Merk KGaA, Darmstadt, Germany) to separate out hyphal fragments and larger arthroconidia. The conidial suspension were washed three times with 20 ml ice-cold 1 M sorbitol by centrifugation at 560 g for 10 min. Depending on the pellet quantity, the conidia were resuspended in ice-cold 1 M sorbitol to produce a conidial concentration that was adjusted to 2.5 x 10^9 cells/ml, and 50 µl aliquots of the conidial suspension were dispensed into 1.5 ml Eppendorf tubes. Competent cell could be used immediately or stored at -80 ^{o}C.

2.8.1.2. Electroporation

40 µl of conidia (2.5 x 10^9 cells/mL) and 1-5 µg of linearised DNA were mixed in a sterile Eppendorf tube and were incubated together on ice for 5 min. The conidia/DNA mix was transferred to a pre-chilled (-20 ^{o}C) 0.2 cm gapped electroporation cuvette (#Z706086-50EA, Sigma-Aldrich). Electroporation was performed in a BioRad Gene Pulser^{TM} (BioRad Laboratories Ltd., Herts, UK) using the following parameters: voltage 1.5 kV/cm, capacitance 25 µF and resistance 600 ohms.

After electroporation, cells were immediately recovered by adding 1 ml of ice-cold 1 M sorbitol, gently mixed by inversion. 500 µl of cell suspension with 9.5 ml YPD were transferred to a 50 ml Falcon tube and incubated at 30^{o}C with 180 rpm shaking for 4 h. The cell suspension was concentrated to 500 µl by centrifugation at 1000 g for 10 min, and were plated on CSM (containing 200 µM hygromycin B) plates. The plates were incubated at 30 ^{o}C for 4-10 days.

2.8.1.3. Transformant screening

The visible colonies were picked and transferred to Vogel's agar medium containing 200 µM hygromycin B for vegetative growth and homokaryon purification. The transformants were routinely compared with the untransformed wild type with respect to their colony extension rate, colony morphology and cell morphology under the light microscope.

2.8.1.4. Homokaryon purification

Cultures in MC media were incubated at 25°C for 7-10 days. Microconidia were harvested from cultures by adding 10 ml of sterile water to tubes followed by rigorous vortex mixing for 30-60 sec. The conidial suspensions were passed into 10 ml YPD through 5 µm Millex Durapore filter units (Millipore catalog number SLSV025LS) using sterile conditions, and were incubated at 35°C with shaking (180 rpm) for 3-4 h. The cell suspension was concentrated to 500 µl by centrifugation at 1000 g for 10 min, and then vortexed to resuspend and inoculated onto CSM plate with appropriate antibiotic and incubated for 3-5 days at 35 °C.

2.8.2. Creation of *N. crassa* mutants by sexual crosses

To induce the sexual cycle in Neurospora, strains of opposite mating types were grown under nitrogen and carbon-limiting conditions on solid synthetic crossing medium (SCM) and were incubated in the dark for 2-3 weeks at 25°C. Upon successful fertilization, mature perithecia were formed that eventually shot out the meiotic progeny, the ascospores. The ascospores were collected from the Petri dish lid by flooding it with dH_2O and heat shocked at 60°C for 30 min in a water bath. The

cell suspension was plated onto CSM with the appropriate antibiotic for selection and incubated for 3-5 days at 35 °C.

2.9 PCR-based genotyping

To verify the transformants generated in this study, multiplex PCR was employed. A diagram showing the general positions of primers used for genotyping is shown in Fig. 2.1. Genotyping primers are listed in Supplimentary Table A.1. Primers sets were chosen to confirm the presence of the deletion or epitope cassette as G-F + 3'-R,and H-F + 3'-R, or to check the integration of 5' egfp-tagged cassette as primer sets of H-F + 3'-R. Genomic DNA was isolated for PCR-based genotyping as described previously (Irelan et al.,1993).

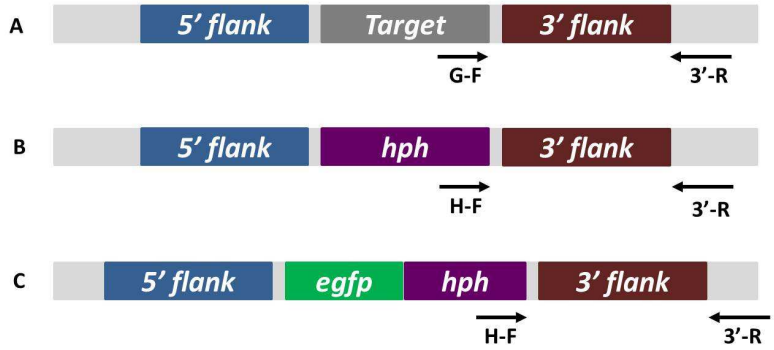

Figure 2.1 Schematic representation of genotyping
The primer set of G-F and 3'-R were used to amplify the gene cassette from the wild-type for control. (B) The primer set of H-F and 3'-R were used to amplify the gene cassette from the gene deletion mutants. (C) The primer set of H-F and 3'-R were used to amplify the gene cassette from the GFP-targeted protein mutants.

2.10 Proteomics analysis

2.10.1. Immunoprecipitation

A cell suspension, prepared by harvesting the conidia from plate cultures of *N. crassa* strain expressing CaM-V5-HAT protein, was inoculated in 2 l flasks containing 500 ml of liquid Vogel's medium to a final concentration of 1 x 10^6 spores/ml and then incubated at 35°C with shaking at 150 rpm for 4 h. The germlings were collected by centrifugation for 5000 x g at 4°C for 10 min and washed once with 250 ml ddH_2O. The collected germlings (~ 10 g) were then frozen in liquid nitrogen and ground into a

fine powder with a pre-cooled pestle and mortar. Ice-cold HG extraction buffer (50 mM HEPES [pH 7.4], 137 mM NaCl, 10% glycerol freshly supplemented with a protease inhibitor cocktail [complete, EDTA-free tablet, Roche] and 1 mM PMSF) was added to the frozen grindate (5 ml of buffer/g of grindate) which was resuspended by vortexing for three 20 s pulses, inverted once every minute for 5 min and then centrifuged for 2370 x g at 4°C for 10 min. The supernatant was carefully removed and used immediately for affinity purification.

For affinity purification, anti-V5 monoclonal antibody (Invitrogen) was coupled to M-270 epoxy Dynabeads (Invitrogen) at a concentration of 10 mg/ml according to the manufacturer's instructions. The Dynabeads were washed three times in HG extraction buffer before adding to the supernatants. 4 ml of cell extract was added to 250 µl anti-V5 Dynabeads and incubated on a roller at 4°C for 1 h. Anti-V5 Dynabeads Beads were collected with a Dynal magnet and washed twice in antibody-Dynabead wash buffer (ADWB; 50 mM HEPES pH 7.4, 150 mM NaCl, 0.02% Tween-20), once in ADWB minus Tween-20 and the proteins eluted twice in 20 µl 100 mM glycine-HCl (pH 2.5).

Purified protein samples were mixed with one-quarter volume of 4x sample buffer (0.2 M Tris-HCl, pH 6.8, 8% (w/v) SDS, 40% glycerol, 10% β-mercaptoethanol, 0.025% bromophenol blue) for SDS–PAGE. Samples were boiled for 5 min, and then separated by 10% SDS–PAGE. Gels were stained with either SYPRO Ruby (Invitrogen) or Safe blue (Invitrogen). For immunoblots, equal amounts of protein (100 µg) were separated by 10% SDS-PAGE, transferred to an Amersham Hybond nylon membrane in CAPS transfer buffer (10 mM CAPS [pH 11], 10% methanol) for 80 min at 80 V and the membrane was then blocked in PBS, 2% skimmed milk, 0.2% Tween-20. V5-HAT-tagged proteins were probed using mouse monoclonal anti-V5 antibody (Invitrogen; diluted to 1:10,000) and goat antimouse IgG- IRDye 800CW conjugate (LiCOR; diluted to 1:20,000) in PBS, 2% skimmed milk, 0.02% Tween-20. Membranes were washed for 30 min in PBS then imaged using a LiCOR Odyssey scanner.

2.10.2. Mass spectrometry

Destained SDS-PAGE gel bands were digested with sequencing grade modified porcine trypsin (Promega, ~ 5-10 ng/µl) solutions in 50 mM ammonium bicarbonate, and evaporated to dryness by vacuum centrifugation. Micro-HPLC/MS/MS analyses were performed using an online system consisting of a micro-pump Agilent 1200 binary HPLC system (Agilent) coupled to a hybrid LTQ Orbitrap XL instrument (Thermo-Fisher). The LTQ was controlled through Xcalibur 2.0.7 and LTQ Orbitrap XL MS2.4SPI. Capillary Picotip columns (10 cm long, 360 mm outer diameter, 75 mm inner diameter) with a 15 mm tip opening and fitted with a borosilicate frit were obtained from New Objective (Presearch). Fused-silica tubing 59 was from Composite Metal (UK). Samples were analysed on a 2 h gradient for data dependent analysis. MS/MS data were searched using Mascot version 2.2 (Matrix Science Ltd.), against the Neurospora genome and annotations database (http://www.broad.mit.edu/annotation/fungi, accessed August 2013).

2.10.3. Computational proteomics analysis

The proteomics data from mass spectrometry was analized against the Neurospora genome and annotations database (http://www.broad.mit.edu/annotation/fungi).

The protein sequence was blasted with

CaM-binding site database (http://calcium.uhnres.utoronto.ca/ctdb/ctdb/).

Geneontology (http://www.geneontology.org/).

DAVID Bioinformatics Resources 6.7 (http://david.abcc.ncifcrf.gov/home.jsp).

STRING (http://string-db.org/).

Osprey (http://biodata.mshri.on.ca/osprey/servlet/Index)

2.11 Microscopy

Microscopes and software used in this study are listed in Table 2.11. Images were analysed using ImageJ software.

Table 2.11 Microscopes used in this study

Microscope	Details	Purpose
Brightfield light microscopy	Nikon Eclipse TE 2000E inverted microscope	To count cell numbers
Fluorescence stereo microscopy	Leica MZ 16F stereomicroscope	To screen fluorescent transformants
Differential interference contrast microscopy	Nikon Eclipse TE 2000E inverted microscope	To analyse CAT fusion and hyphal fusion phenotypes
Widefield fluorescence microscopy	Nikon Eclipse TE 2000E inverted microscope. Light source: Till Photonics Polychrom IV monochromator or CooLED. Software: MetaMorph® Microscopy Automation and Image Analysis Software	To image fluorescent protein-tagged transformants
Confocal laser scanning microscopy	Nikon Eclipse TE 2000U inverted microscope coupled to a Bio-Rad Radiance 2100 system Software: Lasersharp 2000	To image fluorescent protein-tagged transformants

Chapter 3

A pharmacological analysis of Ca^{2+} signalling during colony initiation

Chapter 3 – A pharmacological analysis of Ca^{2+} signalling during colony initiation

3.1. Introduction

A number of previous studies have analyzed the effect of various pharmacological agents on the growth and branching of mature vegetative hyphae of *N. crassa*. The presumed elevation of $[Ca^{2+}]_c$ by Ca^{2+}-selective ionophores has been found to induce apical branching (Reissig and Kinney, 1983). Extracellular Ca^{2+} has also been shown to be required for hyphal tip extension and morphogenesis (Takeuchi et al., 1988), and the addition of Ca^{2+} to hyphae has been reported to alter branching morphology (Kawano and Said, 2002). However, there have been a limited number of other pharmacological studies on the role of Ca^{2+} signalling/homeostasis during colony initiation and development in *N. crassa*. Nevertheless, a previous study has demonstrated that the removal of extracellular Ca^{2+} caused the inhibition of CAT fusion but not CAT induction implying that CAT chemotropism was blocked (Chu, 2013).

In this chapter, 5 drugs were used to investigate the potencial mechanisms in Ca^{2+} signalling that regulate different stages of colony initiation. Many $[Ca^{2+}]_c$ signals are mediated by the ubiquitous Ca^{2+} binding protein, calmodulin (CaM), which functions as a Ca^{2+}-dependent regulator of various downstream pathways, including G protein mediated signalling (Kawano et al., 1997), cytoskeletal function, cyclic nucleotide metabolism, ion transport, protein phosphorylation, dephosphorylation cascades, and cell proliferation (Bkaily and Sperelakis, 1986; Crivici and Ikura, 1995; Gnegy, 1993). Two antagonists of CaM that are commonly used in pharmacological studies on the role of CaM are calmidazolium (CMZ) and trifluoperazine (TFP). Calmidazolium has been widely used as a chemical tool for investigating the Ca^{2+}/CaM-dependent regulation of various cellular processes. Trifluoperazine (TFP) is another strong inhibitor of CaM, which inactivates Ca^{2+}/CaM by directly binding to cause a major tertiary-structural alteration in Ca^{2+}/CaM. This conformational change inhibits the interaction of Ca^{2+}/CaM and its target enzymes (Vandonselaar et al., 1994).

Calcineurin, a serine/threonine phosphatase, is one of the Ca^{2+}-binding proteins that can be activated by Ca^{2+}/CaM. The inhibitors, FK506 (tacrolimus) and cyclosporin A (CsA), have a similar mechanism in blocking the function of calcineurin.

The structures of these CaM and calcineurin inhibitors are showed in Fig. 3.1.

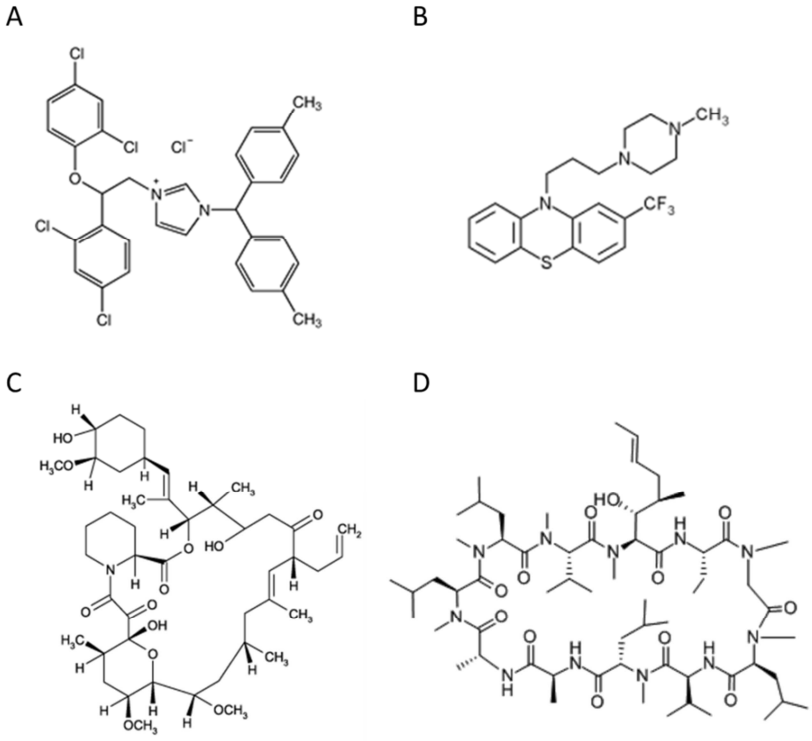

Figure 3.1 The chemical structure of CaM and calcineurin antagonists
(A) Calmodazolium (CMZ; calmidazolium chloride; 1-[bis-(4-chlorophenyl)methyl]-3-[2-(2,4-dichlorophenyl)-ethyl]-1H-imidazolium chloride). (B) Trifluoperazine (TFP; 2-trifluoromethyl-10-[3-(4-methyl-1-piperazinyl)propyl]phenothazine) (C) FK506 (Tacrolimus) (D) Cyclosporin A (CsA)

Caspofungin (Fig. 3.2) is a noncompetitive inhibitor of fungal β-1,3 glucan synthase (Fig. 3.3). It belongs to the echinocandin class of antifungal agents and is a water-soluble amphipathic lipopeptide (Deresinski and Stevens, 2003; Groll and Walsh, 2001). Caspofungin has received US Food and Drug Administration (FDA) approval for the treatment of invasive aspergillosis in patients who are refractory to or intolerant of other therapies (Deresinski and Stevens, 2003). Mutants defective in this Ca^{2+}-signalling machinery have been shown to be associated with hypersensitivity to echinocandins (Parent et al., 1993). Caspofungin activity is also

enhanced by calcineurin/TOR inhibitors for all Aspergillus isolates studied (Kontoyiannis et al., 2003). These results indicate that the mechanism of caspofungin may be involved in Ca^{2+} signalling/homeostasis in filamentous fungi.

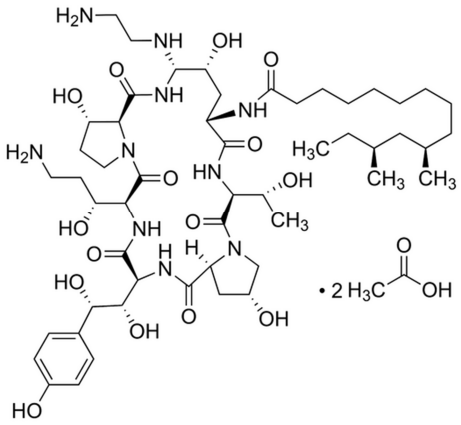

Figure 3.2 The chemical structure of caspofungin

Synonym:1-[(4R,5S)-5-[(2-Aminoethyl)amino]-N2-(10,12-dimethyl-1-oxotetradecyl)-4-hydroxy-L-ornithine]-5-[(3R)-3-hydroxy-L-ornithine]-pneumocandin (Sigma 179463-17-3)

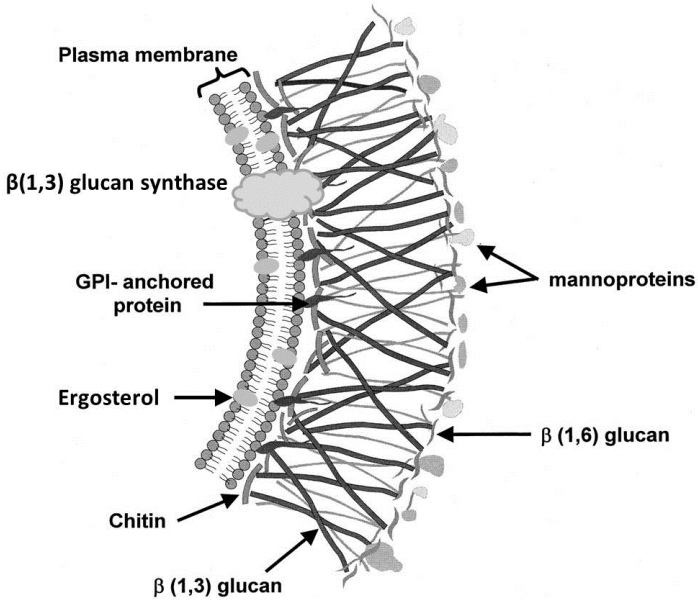

Figure 3.3 The location of β-1,3 glucan synthase **in the structure of fungal cell wall**

β-1,3 glucan is one of the main structures in the fungal cell wall. The target of caspofungin, β-1,3 glucan synthase, which is localized to the plasma membrane, is an enzyme with the two subunits, Fksp and Rho1p. (Garcia-Effron et al., 2009)

The aims of the research described in this chapter were:

- To determine the influence of extracellular Ca^{2+} on different stages of CAT fusion
- To investigate the existence of chemoattractants between two homing CATs
- To investigate whether extracellular Ca^{2+} acts as a chemoattractant or not
- To determine the influence of CaM and calcineurin antagonists on CAT fusion
- To test the effects of caspofungin on CAT fusion

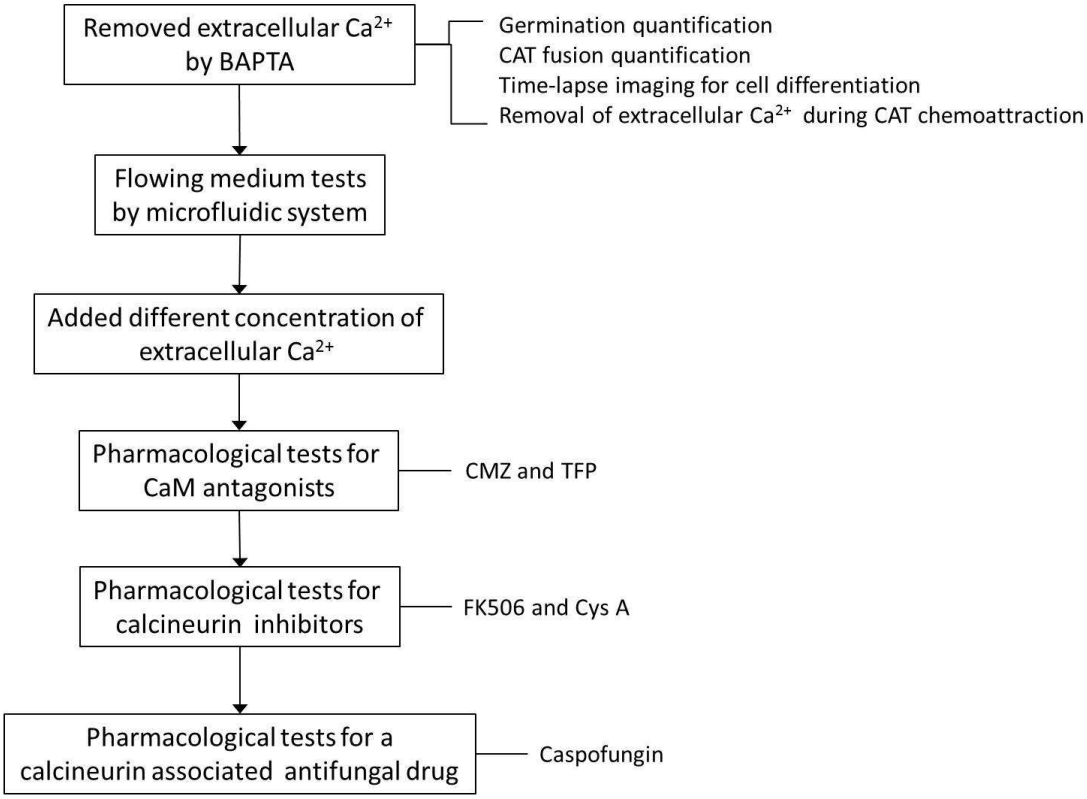

Figure 3.4 Flowchart of the pharmacological tests of extracellular Ca^{2+} and inhibitors of Ca^{2+}-signalling associated proteins

The aims of this chapter were to understand the roles of extracellular Ca^{2+}, CaM and calcineurin during colony initiation. Different concentration of extracellular Ca^{2+} and drugs were used in different cell stages to verify their influence.

3.2. Results

3.2.1. CAT fusion is Ca^{2+}-dependent

A previous PhD student (Dr. Meiling Chu) in Prof. Nick Read's lab had shown that the omission of extracellular Ca^{2+} from Vogel's medium or the addition of 5 mM BAPTA (a Ca^{2+} chelator) to Vogel's medium caused the inhibition of CAT fusion in *N. crassa* (Chu, 2013). I repeated the experiments and obtained the same results (Figs. 3.5 A, B and C). In the absence of extracellular Ca^{2+}, CATs were formed as short and thin protrusions but they did not grow towards each other and fuse (Fig 3.5 B). The addition of 680 µM $CaCl_2$ back to the 5 h-incubated Ca^{2+}-free cell sample (Fig 3.5 B), however, induced CAT chemotropism (Fig 3.5 C). CAT fusion started to appear after 2 h incubated at 35^{o}C (8 ± 1%), and the amount of CAT fusion increased with time (Fig 3.5 D).

3.2.2. The extension rate of germ tubes is Ca^{2+}-dependent

Previous results have shown that low extracellular Ca^{2+} inhibits the growth and conidiation of the mature colony of the wild type (Chu, 2013). In my study, I measured the extension rates of germ tubes during colony initiation by live-cell imaging under DIC microscopy. Conidia were incubated for 5 h at 35^{o}C and recorded for 10 min at room temperature and the lengths of individual germ tubes were analyzed in time courses by ImageJ. Germ tubes growing in the Ca^{2+}-free medium possessed an extension rate of 0.08 ± 0.03 µm/min which was approximately one third of the rate of germ tubes growing in normal Vogel's medium (0.23 ± 0.08 µm/min).

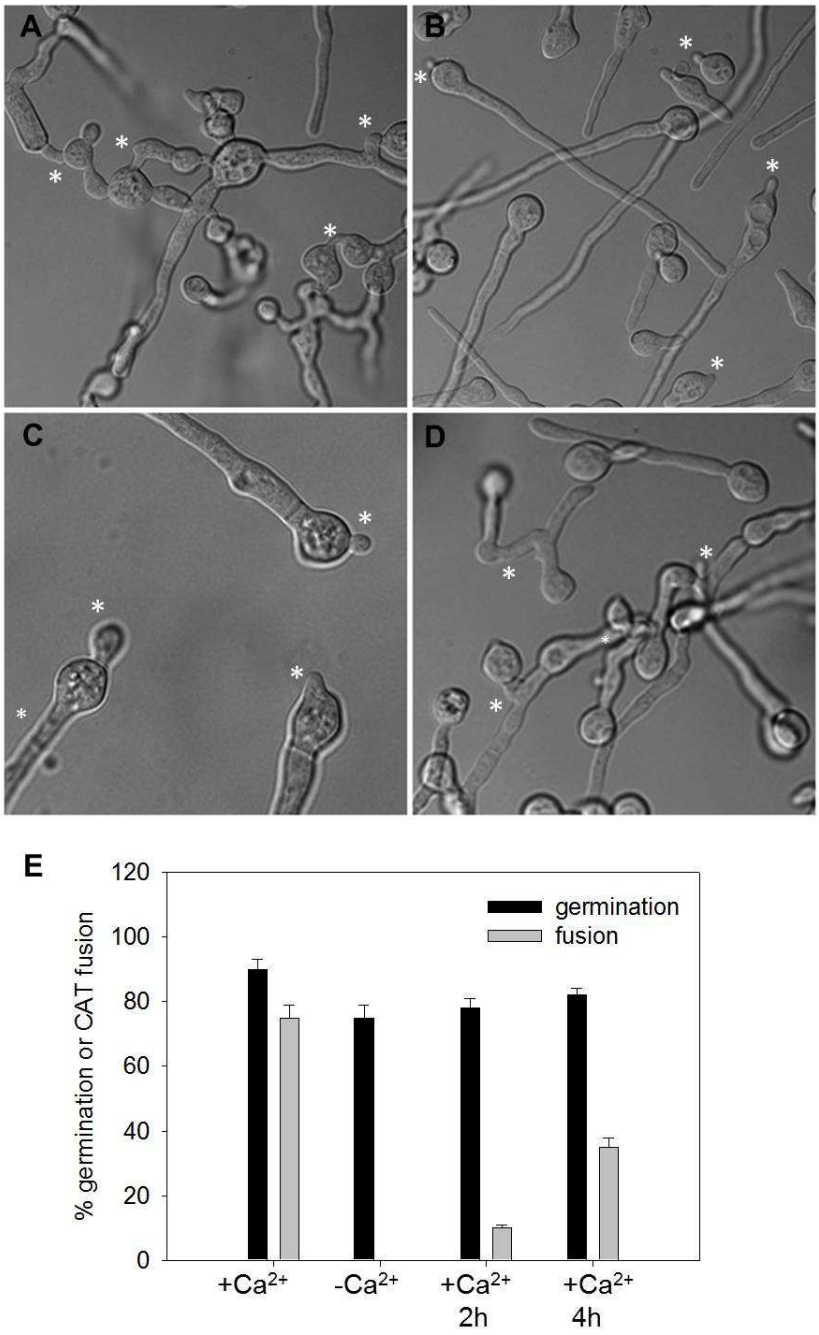

Figure 3.5 Extracellular Ca^{2+} is required for CAT fusion

Conidial germination and CAT fusion visualized by DIC microscopy. Note: short conidial protrusions (*) that resemble CATs or are CAT fusion sites. Conidia were incubated with the inhibitor for 5 h at 35°C in different media: (A) Standard liquid Vogel's medium which contains ~ 680 µM $CaCl_2$ (B and C) Conidia were incubated in Ca^{2+}-free Vogel's medium. CATs were produced but no chemotropism was observed. (D) A final concentration ~ 680 µM $CaCl_2$ was added to the 5 h-incubated Ca^{2+}-free sample (B) and incubated for a further 2 hours at 35°C. CAT fusion appeared after 2 h. (E) Quantification of the effects of removing and adding extracellular Ca^{2+} on germination and CAT fusion (n=100). The error bars indicate standard deviations.

3.2.3. Extracellular Ca^{2+} is required for CAT commitment

To analyse the time-dependent influence of extracellular Ca^{2+} on CATs, conidia were incubated for 4 h at 35 ^{o}C and then subsequently imaged for > 9 h at room temperature using DIC microscopy. As the time lapse images in Fig. 3.6 show (Supplementary movie 1), the CATs formed did not undergo chemotropism in the Ca^{2+}-free medium at the beginning. The CATs remained short and thin cell protrusions and ceased growing for at least 6 h, then started to swell and elongate after 8 h. The CATs then differentiated into germ tubes. Instead of homing towards each other, these newly differentiated and long germ tubes tended to avoid each in contrast to CATs, which grow towards each other.

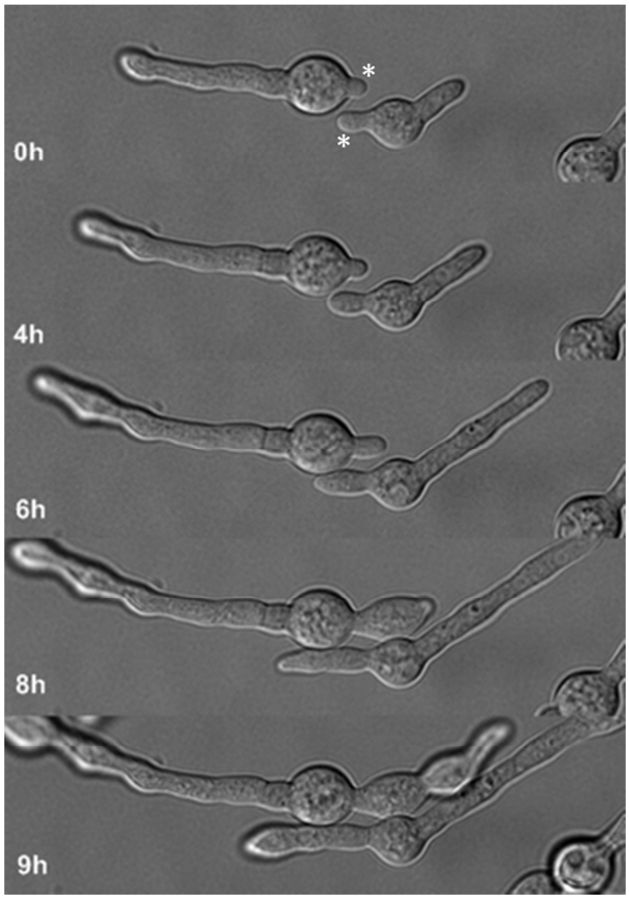

Figure 3.6 Extracellular Ca^{2+} is required for CAT commitment
Conidia were incubated in 5 µM BAPTA for 4 h at 35^{o}C. Time lapse images were then captured between the 4 h and 9 h points at room temperature using DIC microscopy. CATs differentiated into germ tubes in the absence of Ca^{2+} at the 6 h time point (10 h in total). Note: short conidial protrusions (*) are CATs.

3.2.4. Extracellular Ca^{2+} is required for CAT chemotropism , CAT fusion, and the 'ping-pong' recruitment of MAK-2

To analyse the possible roles of extracellular Ca^{2+} during CAT chemotropism and CAT fusion, BAPTA (final conc. 5 mM) was added to remove the extracellular Ca^{2+} whilst two CATs were homing toward each other. Conidia were incubated in Vogel's medium with BAPTA for 4 h at 35^{o}C. Time lapse images were captured at 1 min intervals at room temperature using DIC microscopy (Fig. 3.7). Two CATs grew towards each other and fused in the general Vogel's medium containing 680 µM Ca^{2+} (Fig. 3.7 A; supplementary movie 2). However, the removal of extracellular Ca^{2+} by adding BAPTA while CATs were exhibiting chemotropic growth towards each other seemed to cause the two CATs to lose the ability to recognize each other and the CAT fusion process was halted (Fig. 3.7 B and C; supplementary movie 3 and 4). The 'CATs' then grew very slowly, became fatter and seemed to differentiate into germ tubes in the absence of extracellular Ca^{2+}, as described in the previous section. In addition, the removal of extracellular Ca^{2+} also prevented the cell protrusions from attaching to each other when their tips made contact. After making contact, they started to swell and elongate at the 6 h time point and took on the morphology and behavior of germ tubes (Fig. 3.7 D; supplementary movie 5).

The "ping-pong" mechanism, involving the imaging of the oscillatory recruitment of fluorescent protein labelled MAK-2 and SO, provides reporters of CAT chemotropism (Fleißner et al., 2009; Read et al., 2009). Conidia were incubated in the CellASIC microfluidic system (CellASIC® ONIX Microfluidic Platform; Millipore) with a flow rate 20 µm/sec of vogel's medium for 3.5 h at 35^{o}C. Time lapse images were captured at 1 min intervals at room temperature by wide-field fluorescence microscopy (Fig. 3.8). The fluorescent signal of MAK-2 MAP kinase labeled with GFP localized at the tips of cell protrusions and showed the oscillation with about a period of 5 min (Fig 3.8 A), as reported previously (Fleißner et al., 2009). BAPTA (final conc. 5 mM) was added to remove the extracellular Ca^{2+} while two CATs showing the "ping-pong" recruitment of MAK-2 were growing towards each other (Fig 3.8 B). The oscillatory accumulation of MAK-2 at oppositing CATs tips disappeared after a few minutes, and this coincided with the two CATs ceasing growth. Interestingly, after

BAPTA treatment, one of the conidial germlings developed a second elongated germ tube and another cell protrusion which may have been either a CAT or a germ tube initial.

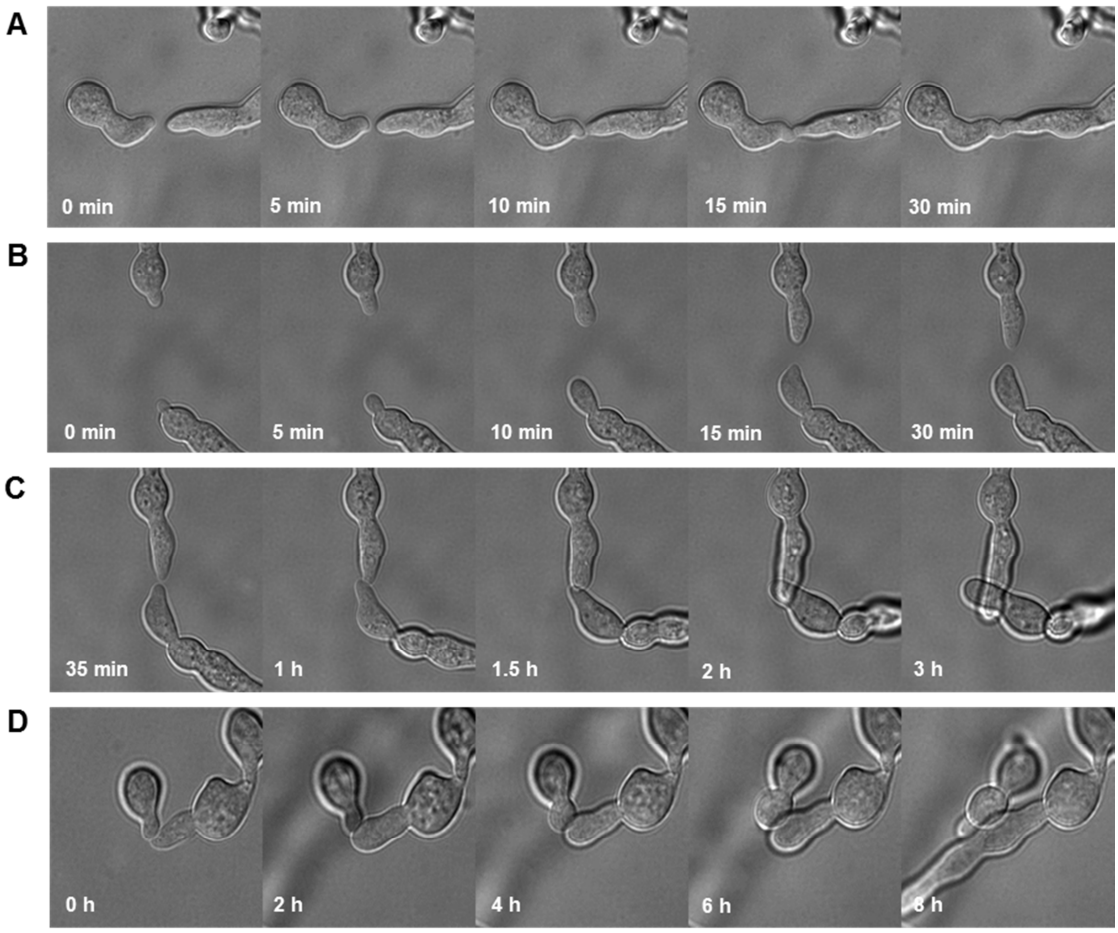

Figure 3.7 Extracellular Ca^{2+} is required for CAT chemotropism and CAT fusion
Conidia were incubated in Vogel's medium with the Ca^{2+} chelator, BAPTA, for 4 h at 35^{o}C. Time lapse images were captured at 1 min intervals at room temperature using DIC microscopy. (A) CAT fusion between two germlings (control). Two CATs grew towards each other and fused. (B) CAT chemotropism between two germlings. Two CATs were homing towards each other to a point just before they made contact. (C) 5 µM BAPTA was added at the 30 min time point in (B). The extension rate of the two CATs was immediately greatly reduced. After making contact, these cell protrusions did not attach, became fatter and seemed to differentiate into germ tubes. (D) 5 µM BAPTA was added after two CATs had made contact with each other at the 0 h time point. The CAT fusion process stopped and two CATs started to swell and elongate after 6 h, and differentiated into elongated germ tubes.

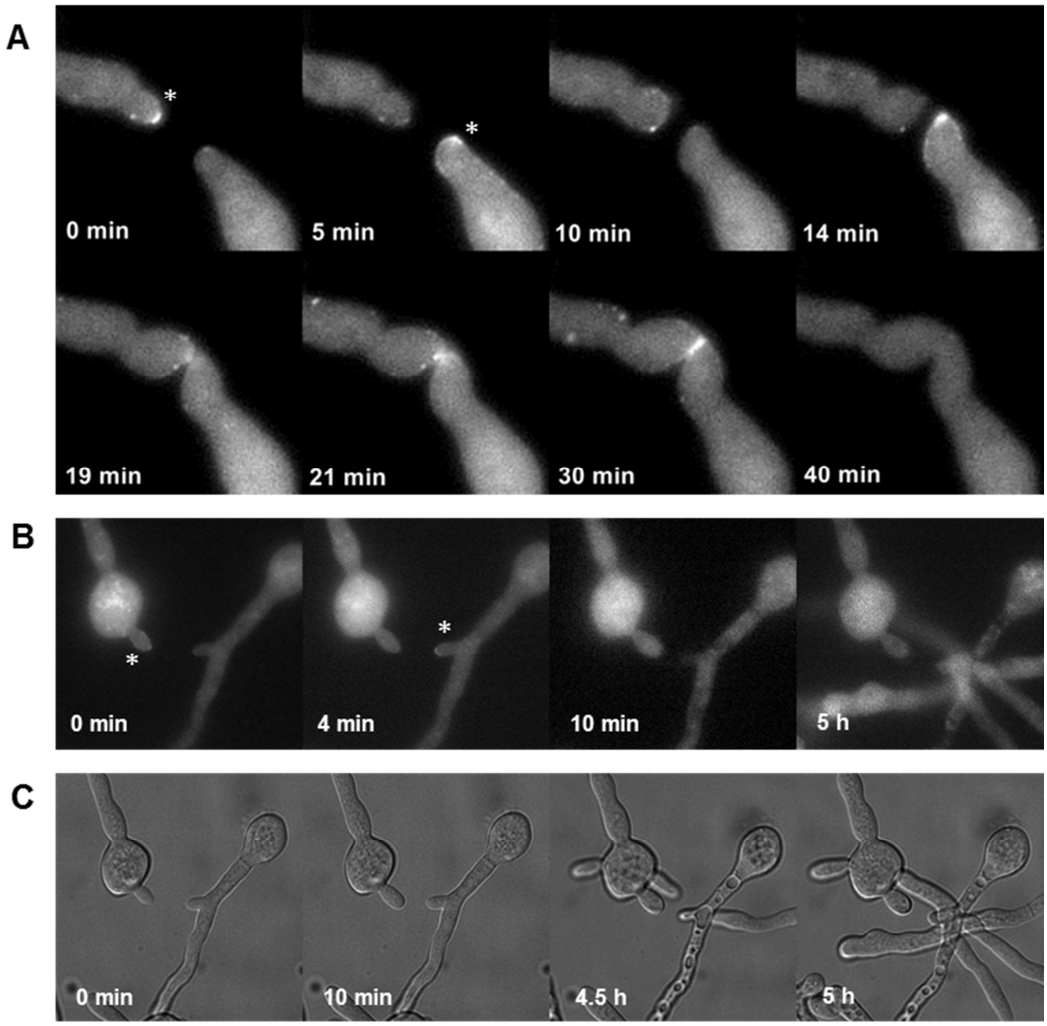

Figure 3.8 Extracellular Ca^{2+} is required for the ping-pong ocillatory recruitment of MAK-2. Conidia were incubated in a microfluidic chamber with Vogel's medium with a flow rate of 20 µm/sec for 4 h at 35^{o}C. Time lapse images were captured at 1 min intervals at room temperature using fluorescence microscopy and DIC microscopy. (A) The ping-pong recruitment exhibited by MAK-2-GFP in two CATs that are growing chemotropically towards each other. MAK-2-GFP accumulation (*) appeared successively in each CAT tip. (B) The removal of extracellular Ca^{2+} stopped the oscillatory recruitment of MAK-2-GFP in the two CATs homing towards each other. MAK-2-GFP accumulation appeared alternatively in the two CAT tips (weak fluorescence at the tips asterisked in the images). MAK-2-GFP accumulated at tips disappeared after adding 5 µM BAPTA between the 5 and 10 min time points. (C) DIC images of the same cells in (B) but with no 4 min time point and with an extra 4.5 h time point shown. When extracellular Ca^{2+} was removed by adding 5 mM BAPTA at the 10 min time point, the two CATs homing towards each other stopped their chemotropism and their extension rate was greatly slowed down. In this example, a germ tube and another cell protrusion appeared after the 4.5 h time point following the BAPTA treatment.

3.2.5. CAT chemotropism is oriented by intercellular chemoattractants

Since the extracellular Ca^{2+} was known to be an essencial factor during CAT chemoattraction from section 3.2.1 to 3.2.4, two questions were raised subsequently: (1) Is there any chemoattractant secreted from both CAT tips during CAT chemoattraction? (2) What is the role of extracellular Ca^{2+} in these chemoattractants?

To provide evidence for the release of diffusible chemoattractants being involved in CAT chemotropism, the CellASIC microfluidic system was used with different flow rates of the Vogel's growth medium. The microfluidic system traps cells in a monolayer in the culture chambers of the microfluidic device. Each culture chamber occupied a 3.0 x 3.0 mm in area and had 3-stepped heights of 5, 6, and 7 µm. Conidia were incubated in the microfluidic chamber at 35^{o}C for 3 h. The germination rates were similar with both 210 and 20 µm/sec flow rates, but the amount of CAT fusion decreased from 82% to 5% with the higher flow rate (Fig. 3.9 F). After 3 h of incubation with a flow rate of 210 µm/sec (Fig. 3.9 A), the cells were incubated for one more hour at 20 µm/sec (Fig. 3.9 B). Cells started to undergo chemotropism at the lower flow rate which was particularly evident 4 h after switching to the lower flow rate (Fig. 3.9 C). The flow velocity was increased to 210 µm/sec after 3 h incubation with a flow rate of 20 µm/sec (Fig. 3.9 D). Two homing cells did not undergo fusion after switching the flow rate (Fig. 3.9 E and F). These results provided direct evidence for two CAT tips homing towards each other being orientated by diffusible chemoattractants released from the CAT tips. The higher flow rate flushed away the chemoattractant signal between the two CATs and thus prevented the CAT chemotropism.

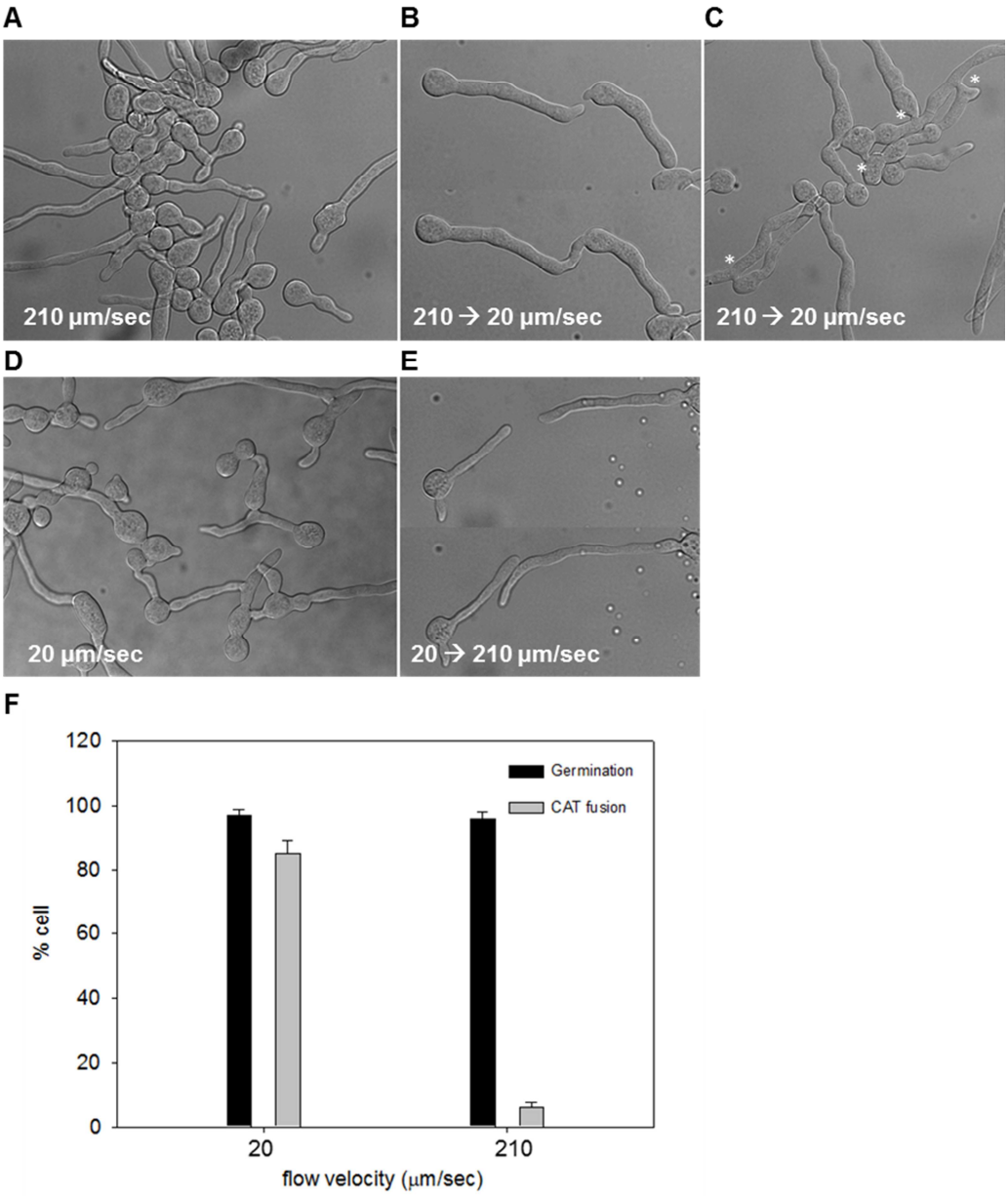

Figure 3.9 CAT chemotropism is oriented by intercellular chemoattractants

Conidia were incubated in the CellASIC microfluidic chamber at 35°C and images were captured using DIC microscopy. (A) Cells incubated with a medium flow rate of 210 µm/sec for 3 h. Only 5% CAT fusion was observed. (B and C) The flow rate was decreased to 20 µm/sec for a further hour after 3 h incubation with a flow rate of 210 µm/sec. CATs started to home towards each other and fuse at the lower flow rate. (D) Conidia were incubated in the CellASIC microfluidic system chamber at 35°C for 3 h with a flow rate of 20 µm/sec. CATs were formed and CAT fusion (*) was initiated with this slow flow rate. (E) The flow rate was increased to 210 µm/sec after 3 h incubation with a flow rate of 20 µm/sec. The CAT fusion was stopped at the higher flow rate. (F) Cells involved in germination and CAT fusion with different growth medium flow rates (n=100). The error bars indicate standard deviations.

3.2.6. Extracellular Ca^{2+} does not directly act as a chemoattractant

According to the results in section 3.2.5, it indicated a clear evidence that the CAT chemotropism is driven by chemoattractant between cells. Thus, I hypothesized 5 mechanisms as to how Ca^{2+} may regulate CAT chemotropism: (1) Ca^{2+} acts as a chemoattractant; (2) Ca^{2+} acts as an activator of the chemoattractant; (3) Ca^{2+} is required to activate the chemoattractant receptor which is most likely at the plasma membrane surface; (4) Ca^{2+} is required for the chemoattractant to interact with the receptor; (5) Ca^{2+} is taken up by Ca^{2+} channels located in the plasma membrane of CAT tips within which it plays a role as an intracellular signal in regulating the CAT chemotropic machinery.

To investigate whether extracellular Ca^{2+} acts as a chemoattractant or not, three different concentrations of extracellular Ca^{2+} (0 µM, 680 µM and 0.2 M) were applied in medium during colony initiation. If extracellular Ca^{2+} acts as a chemoattractant, the elimination of Ca^{2+} gradient between two CATs by a ~300 fold high concentration (0.2 M) of extracellular Ca^{2+} would disturb the CAT chemotropism. However, results showed that the germination and CAT fusion rates were similar in both cultures incubated with 680 µM and 0.2 M extracellular Ca^{2+}. In addition, there is a dose-response relationship between concentration of extracellular Ca^{2+} (75 µM to 1000 µM) and percentage of CAT fusion (data from Dr. Patricia Hernández-Ortiz). Taken all together, it indicates that the extracellular Ca^{2+} is required for CAT chemotropism but does not act as a chemoattractant.

Evidences for other hypotheses are more fully evaluated in chapter 8 in the link of results reported in chapters 4-7.

3.2.7. CAT fusion is more sensitive to CaM antagonists than germination

To investigate the importance of CaM during colony initiation, two common CaM antagonists calmidazolium (CMZ) and trifluoperazine (TFP) were applied. The IC50 value of CMZ for conidial germination and CAT fusion were 1-2 µM (Fig. 3.10 B). The IC50 value of TFP for conidial germination and CAT fusion were ~ 60 µM and ~ 40 µM respectively (Fig. 3.11 B). CAT fusion was slightly more sensitive than germination to both CaM antagonists and particularly to TFP. The inhibition of germination by both

antagonists at high concentration was associated with both the shrinkage of conidia and the formation of granules within the cytoplasm of conidia (Figs. 3.10 A and 3.11 A).

3.2.8. CAT fusion is much more sensitive than germination to calcineurin inhibitors

The calcineurin antagonists FK506 and cyclosporin A (CysA) were applied to investigate the role of calcineurin in conidial germination and CAT fusion. The IC50 value of FK506 for CAT fusion was ~ 3.5 µg/ml (Fig. 3.12 B). The IC50 value of CysA for CAT fusion was ~ 1.5 µg/ml (Fig. 3.13 B). CAT fusion was much more sensitive than conidial germination. Following treatment with these two inhibitors, CATs were still formed but did not undergo chemotropism (Fig. 3.12 A and Fig. 3.13 A).

3.2.9. Caspofungin caused a remarkable inhibition of CAT fusion

The antifungal drug caspofungin was tested for its effects on colony initiation. It is a β-1,3 glucan synthase inhibitor and it has been previously reported that its mode-of-action may involve Ca^{2+} signalling. The IC50 value of caspofungin for conidial germination and CAT fusion were about 12.5 µg/ml and 0.34 µg/ml respectively (Fig. 3.14 B) indicating that CAT fusion is highly selectively inhibited by the drug. Following treatment with 5 µg/ml caspofungin (a concentration which completely inhibits CAT fusion), CATs were still formed but did not undergo chemotropism..

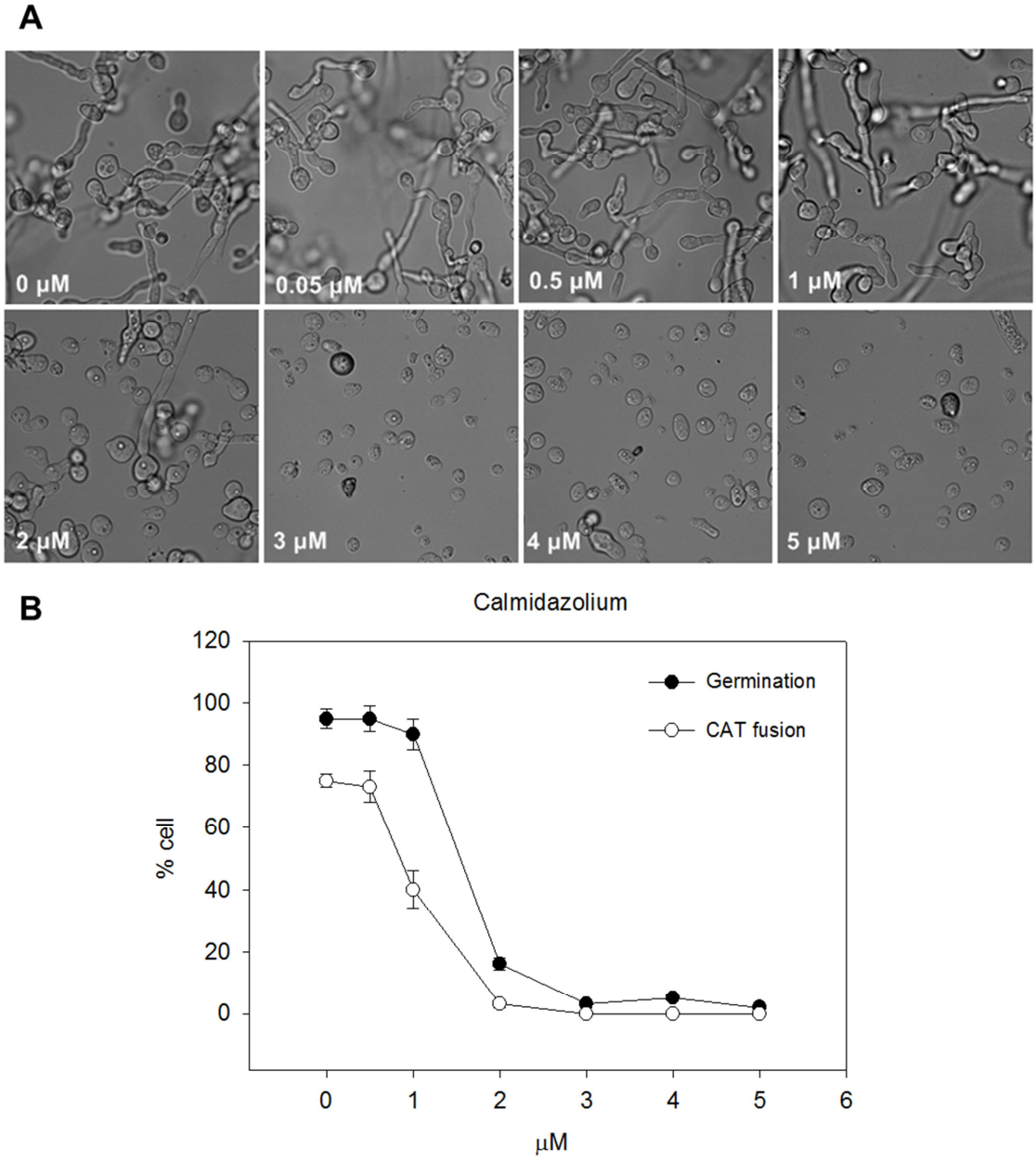

Figure 3.10 CMZ inhibited CAT fusion slightly more selectively than germination

(A) Images of conidial germination and CAT fusion after treatment with different concentrations of CMZ. Conidia were incubated in liquid medium with the inhibitor for 5 h at 35^{o}C and imaged by DIC. (B) Quantification of cells involved in germination and CAT fusion (n=100). The error bars indicate standard deviations.

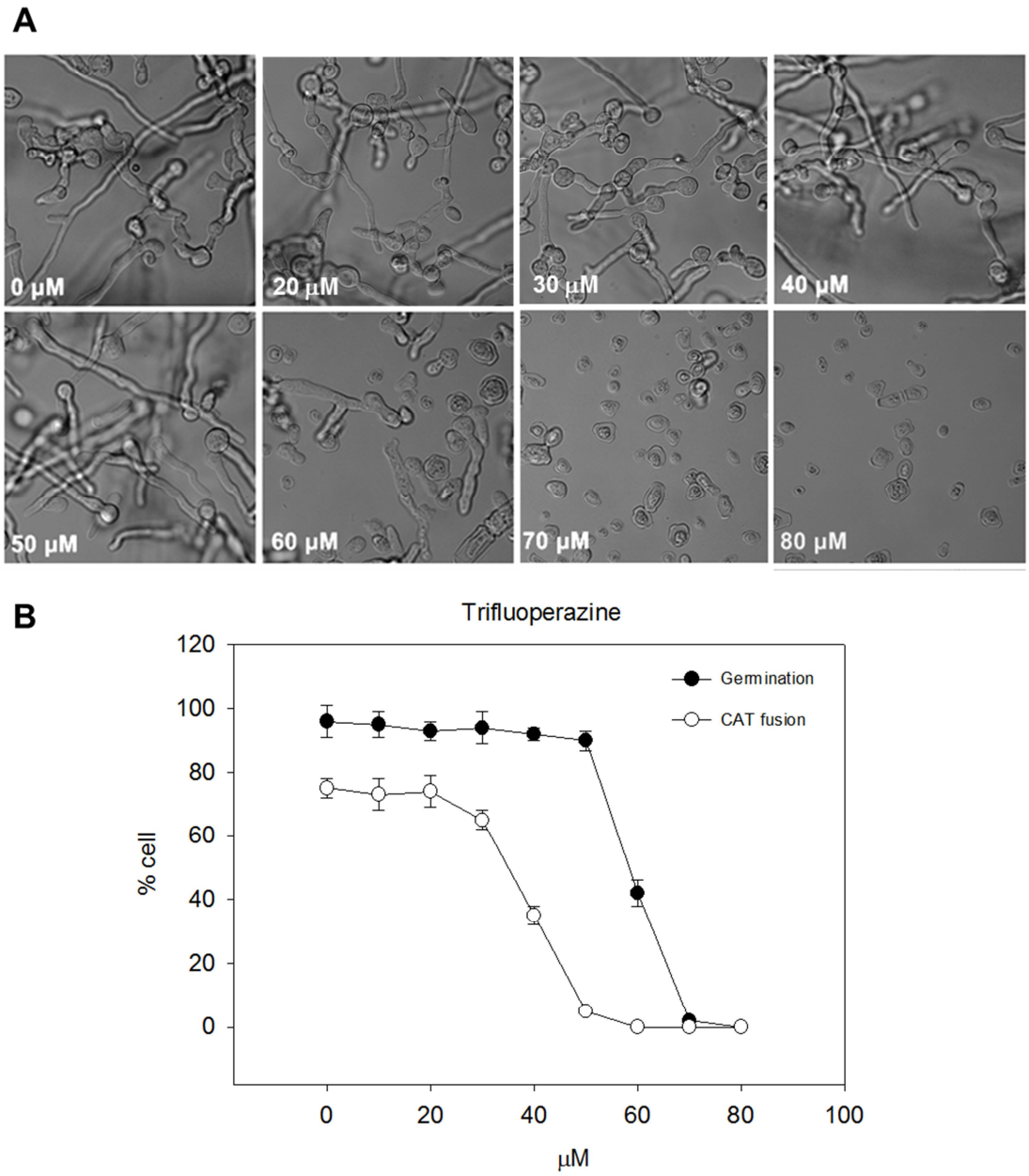

Figure 3.11 CAT fusion was significant and more sensitive than germination to TFP
(A) Images of conidial germination and CAT fusion after treatment with different concentrations of TFP. Conidia were incubated in liquid medium with the inhibitor for 5 h at 35^{o}C and imaged by DIC. (B) Quantification of cells involved in germination and CAT fusion (n=100). The error bars indicate standard deviations.

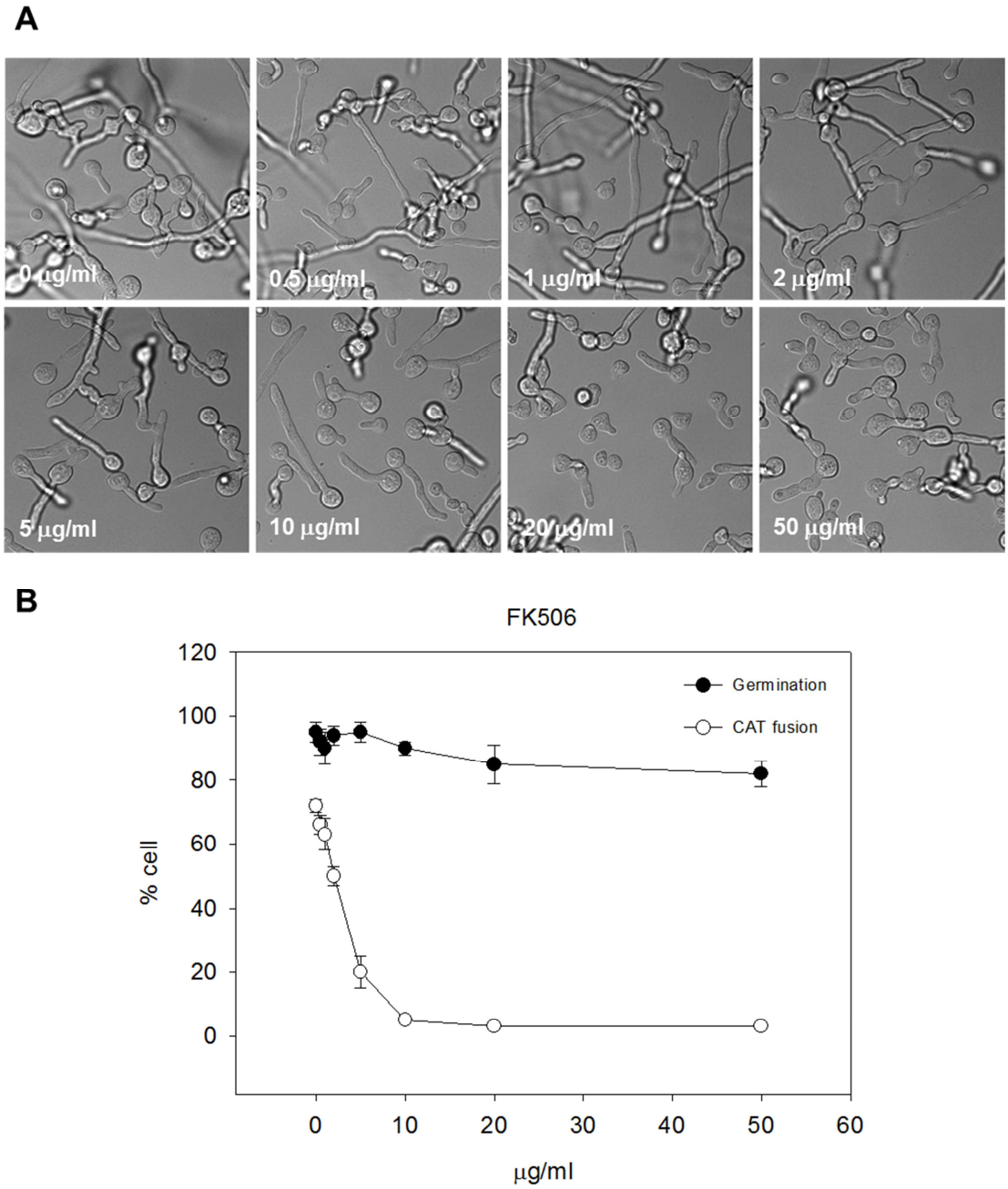

Figure 3.12 FK506 significantly inhibited CAT fusion

(A) Images of conidial germination and CAT fusion after treatment with different concentrations of FK506. Conidia were incubated in liquid medium with the inhibitor for 5 h at 35^{o}C and imaged by DIC. (B) Quantification of cells involved in germination and CAT fusion (n=100). The error bars indicate standard deviations.

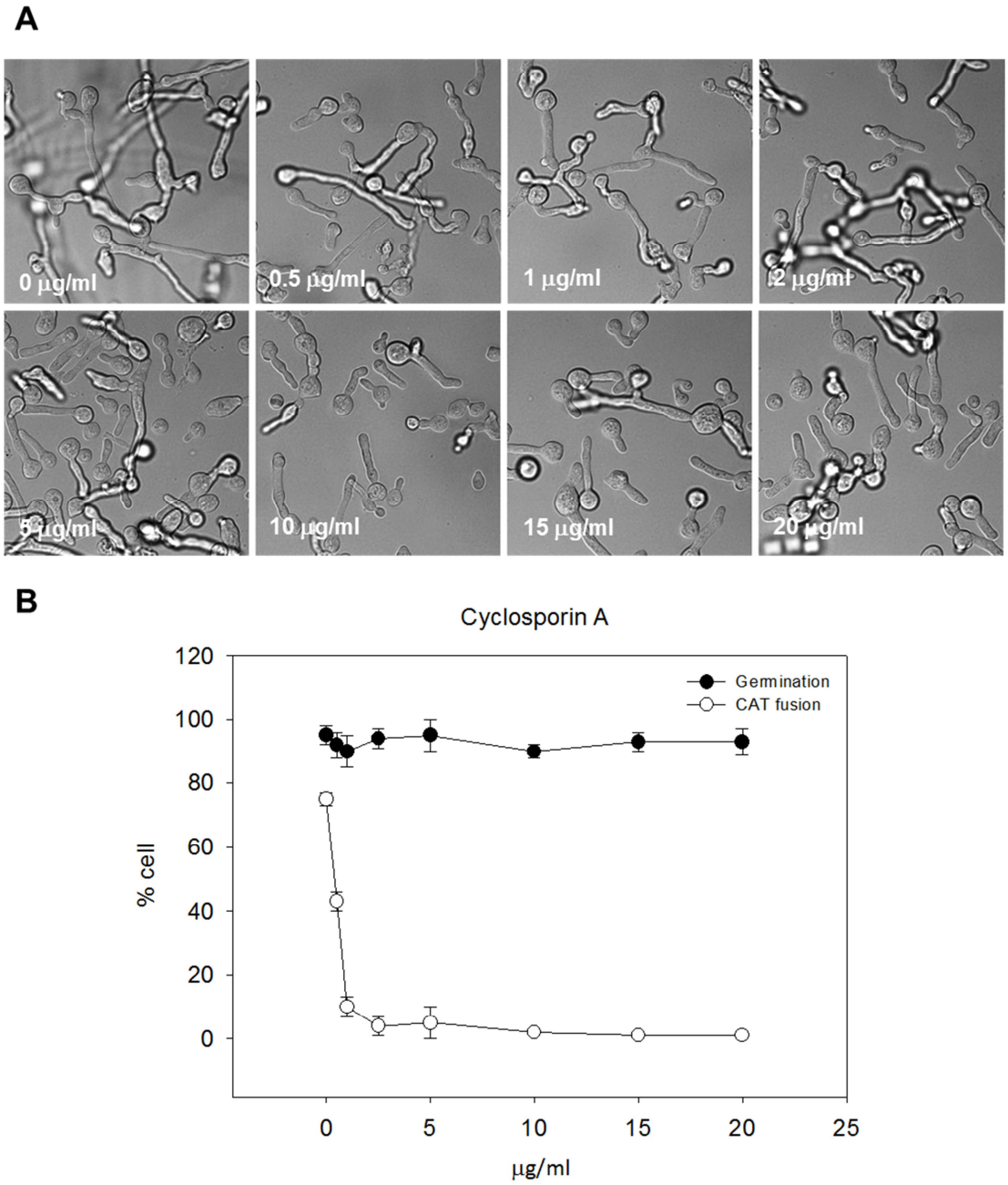

Figure 3.13 CsA significantly inhibited CAT fusion

(A) Images of conidial germination and CAT fusion after treatment with different concentrations of CsA. Conidia were incubated in liquid medium with the inhibitor for 5 h at 35^{o}C and imaged by DIC. (B) Quantification of cells involved in germination and CAT fusion (n=100). The error bars indicate standard deviations.

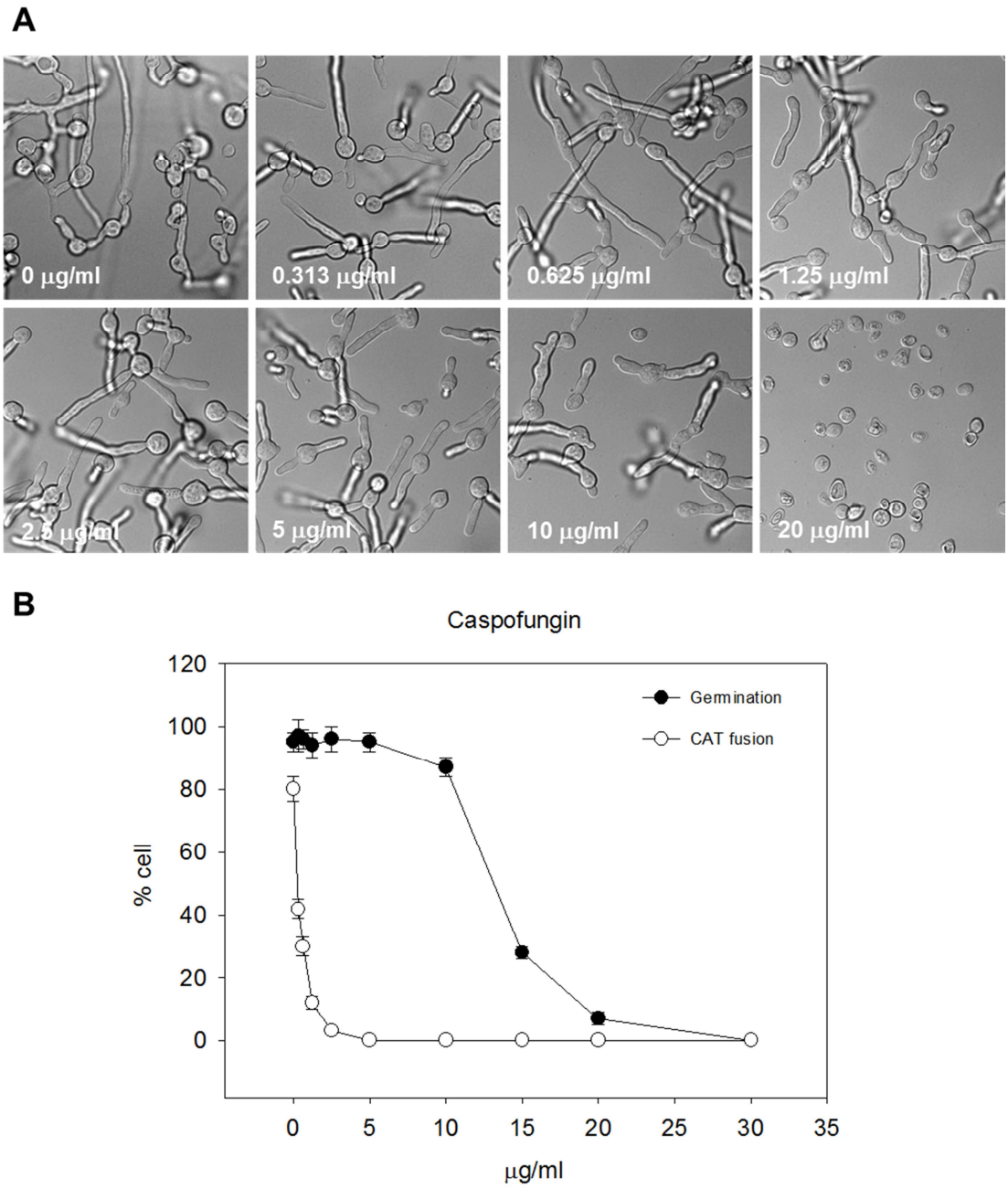

Figure 3.14 The antifungal drug, caspofungin significantly inhibited CAT fusion (A) Images of conidial germination and CAT fusion after treatment with different concentrations of caspofungin. Conidia were incubated in liquid medium with the inhibitor for 5 h at 35^{o}C and imaged by DIC. (B) Quantification of cells involved in germination and CAT fusion (n=100). The error bars indicate standard deviations.

3.3. Discussion

3.3.1. Extracellular Ca^{2+} is not necessary for conidial germination

It has been reported that Ca^{2+} and CaM modulate spore germination and are important in the early cell development on the host surface of several plant pathogens including *Fusarium udum*, *F. oxysporum* f. sp. *ciceri* , *Curvularia lunata*, *Alternaria alternata*, *Curvularia lunata*, *A. brassicicola*, *Colletotrichum capsici* and *C. trifolii* (Prithiviraj et al., 1998; Warwar and Dickman, 1997). Ca^{2+} has a stimulatory effect on germination in the human fungal pathogen, *Sporothrix schenckii* (Rivera-Rodriguez and Rodriguez-del Valle, 1992). In *Neurospora*, my results indicate that conidial germination is independent of extracellular Ca^{2+}. Conidia germinated in Ca^{2+}-depleted environment and also produced CATs during colony initiation, confirming previous results (Chu, 2013). Assuming Ca^{2+} is also required for conidial germination in *Neurospora*, the internal Ca^{2+} or Ca^{2+} stored in the cell wall may play a role resulting in spore germination in this fungus.

3.3.2. Extracellular Ca^{2+} is involved in germ tube growth and CAT commitment during colony initiation

Germ tubes grew readily in Ca^{2+}-free medium but with a slower extension rate than in normal Vogel's medium containing 680 µM Ca^{2+}. This demonstrates that the germ tube extension rate is dependent on extracellular Ca^{2+}.

When germlings remained in Ca^{2+}-depleted environment for an extended time (~ 6 h), CATs differentiated into germ tubes (Fig. 3.6). This was further supported by the results of an experiment in which Ca^{2+} was removed from two CATs homing towards each other (Fig. 3.7 B). These two CATs once in Ca^{2+}-free medium lost the ability to recognize each other and finally developed into germ tubes that grew past each other without attaching to each other (Fig 3.7 C). This is the first report that CATs can differentiate into germ tubes. Although the mechanism is unknown, my results indicate that the extracellular Ca^{2+} is essential for CAT chemotropism and for long term CAT commitment. The pause of several hours before CATs that had stopped growing differentiate into germ tubes may be due to a change in the transcriptional regulation of gene expression. I am not aware of any study demonstrating that

Ca^{2+}-signalling can be involved in regulation in cell differentiation in fungi. In the oomycete *Phytophthora palmivora*, the differentiation of zoospores is extremely sensitive to external Ca^{2+} concentration, which cannot be substituted by other ions (Griffith and Schulman, 1988). In mouse epidermal cells, the modification of the Ca^{2+} concentration in the culture medium markedly alters the pattern of proliferation and differentiation (Hennings et al., 1980). Ca^{2+} in stem cells and progenitor cells also drives the differentiation towards the great diversity of specialized neuronal cells and glial cells (Tonelli et al., 2012).

3.3.3. Potential role for extracellular Ca^{2+} in CAT attachment

In general, cell-cell fusion involves recognition and adhesion between two fusing cells. I found that two CATs homing towards each other lost the ability to attach to each other shortly after the removal of Ca^{2+} from the external medium (Fig 3.7 C). Whether this was due to the cell protrusions differentiating into germ tubes that do not naturally adhere to other germ tubes or whether Ca^{2+} is directly required for the attachment of CATs as a prelude to CAT fusion is not clear at this stage. There is evidence for extracellular Ca^{2+} being required for cell adhesion molecules (CAMs) to function in cell attachment in other systems (Hirano et al., 1987; Kemler et al., 1989). With regard to fungi, the binding of *Sporothrix schenckii* yeast cells to the extracellular protein fibronectin (Fn) in human cells was found to be increased in the presence of Ca^{2+}, and this effect was reversed when the chelating agents EDTA and EGTA were added (Lima et al., 2001).

3.3.4. Pharmaceutical drugs that target Ca^{2+} signalling selectively inhibit CAT fusion

Drugs that target two main Ca^{2+} signalling proteins, CaM and calcineurin, were found to significantly inhibit both germination and CAT fusion. Germination and CAT fusion were both inhibited by CaM antagonists (CMD and TFP) but CAT fusion was more sensitive than germination in these two chemical treatments. In the slime mould *Dictyostelium discoideum*, CaM mediates gamete fusion (Lydan and O'Day, 1993) and in chicken skeletal myoblasts, TFP was found to inhibit myoblast fusion

(Bar-Sagi and Prives, 1983). However, CMZ exerts its inhibitory effect not only via its binding to CaM but may also interfere directly with the CaM-targetted enzymes (Gietzen et al., 1982). CMZ has been reported to also inhibit Ca^{2+} influx through voltage-gated Ca^{2+} channels (Klockner and Isenberg, 1987; Nakazawa et al., 1993), the CaM-induced activation of phosphodiesterase (PDE) and Ca^{2+}-transport ATPase (Gietzen et al., 1982). Because the non-specific side-effect, the results of CMZ and TFP can not directly present the influence of CaM during colony initiation. It only briefly showed that CaM and Ca^{2+} homeostasis play important roles during these stages.

In contrast to germination, CAT fusion was significantly inhibited by calcineurin inhibitors (FK506 and Cyclosporin A). These drugs did not greatly inhibit CAT formation, however, indicating that calcineurin is important in regulating CAT chemotropism as a prelude to CAT fusion. Calcineurin is activated through binding of Ca^{2+}/CaM and dephosphorylates the cytosolic forms of transcription factors such as CrzA, which are recruited to nucleus in which they regulate the expression of specific genes. CrzA has been known to regulate conidial germination, hyphal growth, and pathogenesis of *A. fumigatus*. (Cramer et al., 2008).

Previous results suggest that the mode-of-action of the antifungal agent, caspofungin, may be regulated by Ca^{2+} signalling (Parent et al., 1993). Thus, caspofungin was used to test its possible effects on CAT fusion during colony initiation. Caspofungin was found to significantly inhibited CAT chemotropism in *N. crassa* (Fig. 3.13) further supporting a link between its mode-of-action and Ca^{2+} signalling

Two L-type Ca^{2+} channel blockers, verapamil and diltiazem, have been previously shown to selectively inhibit CAT fusion in a dose dependent manner (Chu, 2013). Taken together with my results using BAPTA, CaM antagonists and calcineurin inhibitors (Figs. 3.10–3.13), I have summarized the results with different Ca^{2+} modulators and how they may influence colony initiation in *N. crassa* (Figs. 8.1 and 8.2).

3.4. Summary

- Conidial germination is Ca^{2+}-independent but the extension rate of germ tubes is Ca^{2+}-dependent.
- Extracellular Ca^{2+} is required for CAT commitment, CAT chemotropism, possibly CAT attachment, and the ping-pong recruitment of MAK-2.
- Ca^{2+} /CaM regulated signalling plays an important role during colony initiation.
- Calcineurin regulated signalling is associated with CAT chemotropism.
- Calcineurin associated antifungal drug, caspofungin, highly selectively inhibited CAT fusion.
- CAT chemotropism is oriented by diffusible intercellular chemoattractants.

Chapter 4

Comparative genomics of Ca^{2+}/CaM signalling machinery and phenotypic analysis of mutant strains during colony initiation

Chapter 4 – Comparative genomics of Ca^{2+}/CaM signalling machinery and phenotypic analysis of mutant strains during colony initiation

4.1. Introduction

The sequencing of the genome in *N. crassa* has provided many novel insights into the biology of this fungus and other filamentous fungi (Borkovich et al., 2004; Galagan et al., 2003). The follow-on Neurospora functional genomics project in Fungal Genetics Stock Center (FGSC; http://www.fgsc.net/) has provided gene deletion mutants for nearly all of the ~ 10,000 genes of *N. crassa*, which has greatly speeded up the functional analysis of genes in this model organism.

Forty-eight putative Ca^{2+} signalling proteins and genes have been previously identified and characterized in *N. crassa* (Borkovich et al., 2004; Zelter et al., 2004) and a comparative genomic analysis of the Ca^{2+} signalling machinery in *N. crassa, S. cerevisiae* and the rice blast fungus *M. grisea* has been made (Zelter et al., 2004). However, little functional analysis of the Ca^{2+} signalling machinery and its mechanistic basis in filamentous fungi have made. In this chapter, 4 fungal organisms were chosen for the comparative genomic analysis according to their morphology and pathogenicity. Two of them were yeast (*S. cerevisiae* and *C. albicans*) and the other two were filamentous fungi (*N. crassa* and *A. fumigatus*).

The aims of the research described in this chapter were:

- To provide a more comprehensive identification of genes involved in the Ca^{2+} signalling machinery of *N. crassa*
- To provide a comparative genomic analysis of 65 proteins involved in the Ca^{2+} signalling machinery in *N. crassa* with *S. cerevisiae* and the two human pathogen *A. fumigatus* and *C. albicans*
- To analyse the morphological phenotypes of 40 gene deletion mutants of the Ca^{2+} signalling/homeostasis machinery to identify possible roles for Ca^{2+} signalling during colony initiation and development

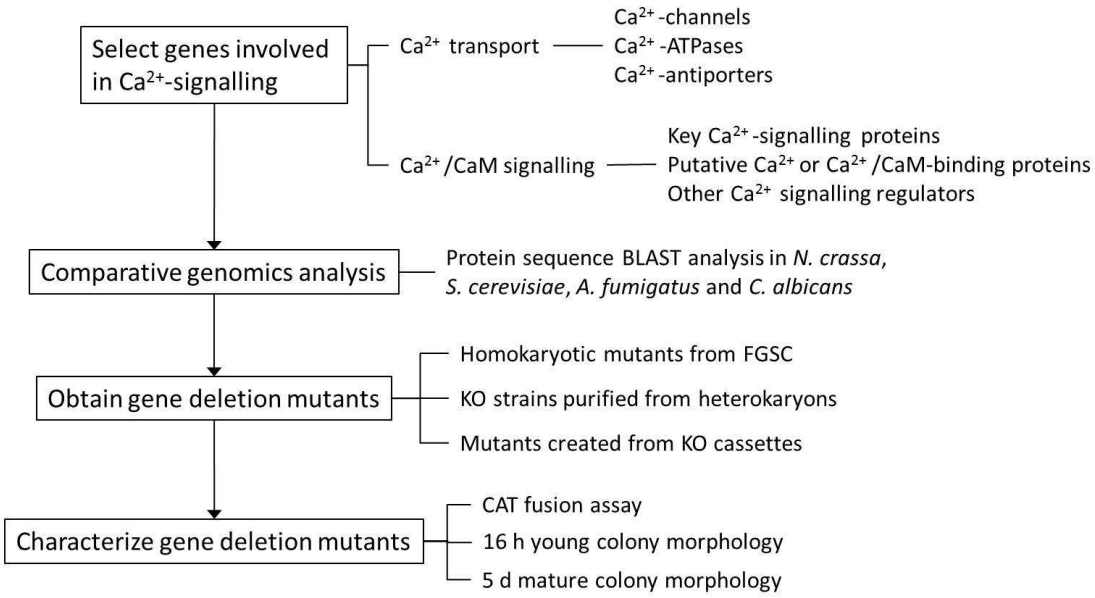

Figure 4.1 Flowchart of the screening process for the genomics and phenomics analysis. The flowchart summarizes the stages taken to identify genes that are components of the Ca^{2+}-signalling machinery, how mutants of these genes were analyzed, and how the gene deletion mutants phenotypes were characterized.

4.2. Results

4.2.1. Comparative genomics analysis

Predicted proteins in *N. crassa* related with Ca^{2+} signalling machenisms were selected from previous studies (Borkovich et al., 2004; Zelter et al., 2004) and protein clusters in different organisms were selected from their genomic database as listed belowed. It is known that more Ca^{2+} signalling proteins are present in *N. crassa* than in *S. cerevisiae* (Zelter et al., 2004). Thus, in this chapter, protein sequences of *N. crassa* were taken as the template to BLAST against with *S. cerevisiae* (RM11-1a), *A. fumigatus* (Af293) and *C. albicans* (SC5314 Assembly 22) genome. Potential hypothetical protein homologs from the four organisms were identified based on E values, % identities and gaps, and conserved domains present. Six databases and online tools were used to analyze the genome sequence and homologs:

(1) Neurospora crassa Database
https://www.broadinstitute.org/annotation/genome/neurospora/MultiHome.html

(2) Saccharomyces cerevisiae RM11-1a Database

http://www.broadinstitute.org/annotation/genome/saccharomyces_cerevisiae

(3) Saccharomyces Genome Database (SGD) http://www.yeastgenome.org/

(4) Candida Genome Database (CGD) http://www.candidagenome.org/

(5) Aspergillus Genome Database (AspGD) http://www.aspgd.org/

(6) NCBI PSI BLAST

http://www.ncbi.nlm.nih.gov/blast/Blast.cgi?CMD=Web&PAGE=Proteins&PROGRAM=blastp&RUN_PSIBLAST=on

These target proteins were classified into 6 groups: Ca^{2+}-channels, Ca^{2+}-ATPases, Ca^{2+}-transporters, key Ca^{2+}-signalling or Ca^{2+}/CaM-binding proteins, putative Ca^{2+} or Ca^{2+}/CaM-binding proteins, and other Ca^{2+}/CaM signalling regulators.

The first cluster (Table 4.1) includes components associated with Ca^{2+} transport to and from the extracellular environment, the cytoplasm, and the internal organelles (Chu, 2013b). Three groups of proteins (Ca^{2+}-channels, Ca^{2+}-ATPases and Ca^{2+}-transporters) were involved in this cluster. Ten Ca^{2+}-ATPases were identified in *N. crassa*, of which one was new (ENA-1; NCU05046.7). Meanwhile, NCU10143.7 has had its gene locus changed from NCU01437.1 from the previous publication (Borkovich et al., 2004). Nine Ca^{2+} transporters were recognized in *N. crassa*, of which one was new as the homolog of the mitochondrial Ca^{2+} uniporter (MCU) from Homo sapiens (NCU08166).

Table 4.1 Ca^{2+}-permeable channels, Ca^{2+}- pumps and Ca^{2+}-transporters in *N. crassa*, *S. cerevisiae*, *A. fumigatus*, and *C. albicans*

Protein	Gene locus	Closest homologs in:		
	N. crassa	*S. cerevisiae*	*A. fumigatus*	*C. albicans*
Ca^{2+} channels				
Ca^{2+}-channel pore-forming subunit (CCH-1)	NCU02762	SCRG_00804 (Cch1p)	Afu1g11110	orf19.3298 (CCH1)
Ca^{2+}-channel protein (MID-1)	NCU06703	SCRG_03417 (Mid1p)	Afu5g05840	orf19.3212 (MID1)
Ca^{2+}-channel protein (YVC-1)	NCU07605	SCRG_01486 (Yyc1p)	Afu3g13490	orf19.2209 (YVC1)
Ca^{2+}-channel protein (FIG-1)	NCU02219	SCRG_02926 (Fig1p)	Afu3g09060	orf19.138 (FIG1)

Putative transient receptor potential Ca^{2+} channel family protein	NCU08283	SCRG_01486 (Yvc1p)	Afu6g11300 (TRP-2)	-
hypothetical protein	NCU06601	SCRG_01486 (Yvc1p)	Afu6g11180	orf19.2209 (YVC1)
Ca^{2+} ATPases				
Ca^{2+}-ATPase (NCA-1)	NCU03305	SCRG_01158 (Pmr1p)	Afu6g06740	orf19.2552
Ca^{2+}-ATPase (NCA-2)	NCU04736	SCRG_01013 (Pmc1p)	Afu1g10880	orf19.1727 (PMC1)
Ca^{2+}-ATPase (NCA-3)	NCU05154	SCRG_01013 (Pmc1p)	Afu1g10880	-
Ca^{2+}-ATPase (PMR-1)	NCU03292	SCRG_01158 (Pmr1p)	Afu2g05860	orf19.2553 orf19.7089 (PMR1)
Ca^{2+}-ATPase (PH-7)	NCU08147	SCRG_00473 (Ena5p)	Afu2g01320	orf19.5170 (ENA21) orf19.6070 (ENA2)
Ca^{2+}-ATPase	NCU04898	SCRG_04438 (Spf1p)	Afu3g13790	orf19.30 (SPF1)
Ca^{2+}-ATPase	NCU03818	SCRG_05226 (Neo1p)	Afu6g03950	orf19.783
Ca^{2+}-transporting ATPase 3	NCU07966	SCRG_00473 (Ena5p)	Afu4g09440	orf19.5170 (ENA21) orf19.6070 (ENA2)
ATPase type 13A2	NCU10143	SCRG_01671	Afu5g05520	orf19.1573
Ca^{2+}-transporting ATPase 3 (ENA-1)	NCU05046	SCRG_00473 (Ena5p)	Afu4g09440	orf19.5170 (ENA21) orf19.6070 (ENA2)
Ca^{2+} transporters				
Membrane bound cation transporter (CAX)	NCU07075	SCRG_00622 (Vcx1p)	Afu1g04270 (VcxA)	orf19.405 (VCX1)
Membrane bound cation transporter	NCU00916	SCRG_00622 (Vcx1p)	Afu4g03320	orf19.405 (VCX1)
Membrane bound cation transporter	NCU00795	SCRG_00622 (Vcx1p)	Afu4g03320	orf19.405 (VCX1)

Ca^{2+}/H^{+}-antiporter	NCU06366	SCRG_00622 (Vcx1p)	Afu2g07630	orf19.405 (VCX1)
Vacuolar Ca^{2+} transporter/ H^{+} -exchanger	NCU07711	SCRG_00622 (Vcx1p)	Afu2g05325	orf19.405 (VCX1)
Ca^{2+}-permease	NCU05360	SCRG_03444	Afu4g04670	orf19.7670
Ca^{2+}/H^{+}-exchanger	NCU02826	SCRG_00696	Afu7g03880	-
Ca^{2+}/Na^{+}-exchanger	NCU08490	-	Afu4g03320	-
Homolog of mitochondrial Ca^{2+} uniporter (MCU) from *Homo sapiens*	NCU08166	-	Afu4g10310	-

The second cluster (Table 4.2) includes key Ca^{2+}-signalling or Ca^{2+}/CaM-binding proteins, putative Ca^{2+} or Ca^{2+}/CaM-binding proteins and other Ca^{2+} signalling regulators. A total of 41 proteins were identified in *N. crassa* in this cluster, of which 5 were novel to that identified in previous analyses (Borkovich et al., 2004; Zelter et al., 2004). Four essential proteins were listed in the group of key Ca^{2+}-signalling or Ca^{2+}/CaM-binding proteins: calmodulin (CaM), calcineurin (CN), the calcineurin-responsive transcription factor (CRZ) and Ca^{2+}/CaM-dependent protein kinase (CaMK). CaM, the calcineurin catalytic subunit (CNA), calcineurin regulatory subunit (CNB), and CRZ are present as single proteins in these different fungi except for *S. cerevisiae* which has 2 types of CNA (Cna1p and Cna2p; (Cyert et al., 1991). There are 4 homologs of Ca^{2+}/CaM-dependent protein kinases in *N. crassa*, 2 in *S. cerevisiae*, 2 in *C. albicans*, and 4 in *A. fumigatus*.

Putative Ca^{2+} or Ca^{2+}/CaM-binding proteins were identified by the presence of sequence-based Ca^{2+} or CaM binding sites. Ca^{2+}-binding proteins usually contain EF hands or C2 domains. The C2 domain is a Ca^{2+}-binding motif of approximately 130 residues in length originally identified in the Ca^{2+}-dependent isoforms of protein kinase C (Nalefski and Falke, 1996). It has been shown that Ca^{2+}/CaM can target a range of different types of proteins, such as kinases, phosphatases, various signalling proteins, cytoskeletal and muscle proteins in mammalian cells. The IQ CaM-binding motif, which has the following sequence, has also been identified:

[FILV]Qxxx[RK]Gxxx[RK]xx[FILVWY]. Besides, three classes of recognition motifs exist for many of the known CaM binding proteins. One motif is related to Ca^{2+}-independent binding and the other two related motifs are for Ca^{2+}-dependent binding. The latter are termed 1-14 and 1-5-10 based on the position of conserved hydrophobic residues (Rhoads and Friedberg, 1997).

The annexins are a group of proteins that are capable of binding negatively charged phospholipids in a Ca^{2+}-dependent manner. They contain a 70 amino acid repeat sequence called an annexin repeat (Geisow, 1986). Annexins have been shown to be involved in the trafficking and organization of vesicles, exocytosis, endocytosis and can also be involved in Ca^{2+}-channel formation (Gerke et al., 2005). The first fungal annexin ANX14 was identified in *N. crassa* (Braun et al., 1998). ANXC3 and ANXC4 were identified in *A. fumigatous* (Khalaj et al., 2004). In Table 4.2, These two putative annexins were compared between *N. crassa* and *A. fumigatus*, and homologs of these proteins were absent in *S. cerevisiae* and *C. albicans.*

HAM-3, a homolog of PRO11 in *Sordaria macrospora*, also shows homology to several vertebrate WD40 proteins, such as striatin and zinedin, which seem to be involved in Ca^{2+}-dependent signalling in cells of the central nervous system and are believed to function as scaffolding proteins linking signalling and eukaryotic endocytosis (Poggeler and Kuck, 2004). HAM-10 possesses a putative C2 domain and its activity is thought to be regulated by $[Ca^{2+}]_c$ levels (Fu et al., 2011). RGS-1 is a homolog of the human regulator of G protein signalling 4 (RGS4), which regulates the G protein-mediated PLC pathway that releases Ca^{2+} from intracellular stores. However, when the local concentration of $[Ca^{2+}]_c$ is elevated, the binding of Ca^{2+}/CaM displaces PIP_3 to restore the GAP activity of RGS4. This feedback regulation of RGS GAP Activity by Ca^{2+}/CaM and PIP_3 provides a fine-tuning mechanism for Ca^{2+} homeostasis in mammalian cells (Popov et al., 2000).

The last group of proteins within the second cluster shown in Table 4.2 is composed of other Ca^{2+} signalling regulators including 9 proteins, of which 5 had not been previously described as part of the Ca^{2+}-signalling machinery in *N. crassa*. Four PLCs are present in *N. crassa*. According to the protein BLAST analysis, 4 PLC homologs have been described in *N. crassa,* 2 PLCs in *S. cerevisiae*, 3 PLCs in *C.*

albicans, and 2 in *A. fumigatus*. In addition, 1 predicted calcineurin-binding protein, that is a homolog of calcipressin, and 4 calcineurin inhibitors-binding proteins, were also included in this group (Table 4.2).

Table 4.2 Key Ca^{2+}-signalling or Ca^{2+}/CaM binding proteins and other Ca^{2+}-signalling regulators in *N. crassa*, *S. cerevisiae*, *A. fumigatus*, and *C. albicans*

Protein	Gene locus	Closest homologs in:		
	N. crassa	*S. cerevisiae*	*A. fumigatus*	*C. albicans*
Key Ca^{2+} signalling proteins				
Calmodulin (CaM)	NCU04120	SCRG_02857 (Cmd1p)	Afu1g02930	orf19.4413 (CMD1)
Calcineurin catalytic subunit a (CNA-1)	NCU03804	SCRG_04371 (Cna1p)	Afu5g09360 (CnaA)	orf19.6033 (CMP1)
Calcineurin regulatory subunit b (CNB-1)	NCU03833	SCRG_03838 (Cnb1p)	Afu6g04540 (CnBA)	orf19.4009 (CNB1)
Calcineurin-responsive transcription factor (CRZ)	NCU07952	SCRG_03162 (Crz1p)	Afu1g06900 (CrzA)	orf19.7359 (CRZ1)
Ca^{2+}/CaM-dependent protein kinase-1 (CaMK-1)	NCU09123	SCRG_01386 (Cmk2p)	Afu2g13680	orf19.1754 (CMK2)
Ca^{2+}/CaM-dependent protein kinase-2 (CaMK-2)	NCU02283	SCRG_01386 (Cmk2p)	Afu3g09550	orf19.5911 (CMK1)
Ca^{2+}/CaM-dependent protein kinase-3 (CaMK-3)	NCU06177	SCRG_01169 (Tos3p)	Afu5g05980	orf19.5376
Ca^{2+}/CaM-dependent protein kinase-4 (CaMK-4)	NCU09212	SCRG_04201 (Rck2p)	Afu2g03490	orf19.2268 (RCK2)
Putative Ca^{2+} or Ca^{2+}/CaM binding proteins				
Calreticulin	NCU09265	SCRG_05691 (Cne1p)	Afu4g12850 (ClxA)	orf19.5300 (Calnexin)
Ca^{2+}/CaM binding protein	NCU03750	SCRG_02857 (Cmd1p)	Afu5g13630	orf19.4413 (CMD1)
Aspartate-glutamate transporter (AGC1)	NCU01241	SCRG_02511 (Agc1p)	Afu7g05220	orf19.4966 (AGC1)
Ca^{2+} dependent mitochondrial carrier protein	NCU01564	SCRG_03219 (Sal1p)	Afu2g15780	orf19.1403
hypothetical protein	NCU02115	-	Afu6g07310	-

Homolog of spindle-pole body protein Pcp1 in Aspergillus flavus	NCU02411	-	Afu3g09370	-
Peflin-1 (PEF-1)	NCU02738	SCRG_00956	Afu3g08540	orf19.2180
Serine/threonine-protein kinase (CHK-2)	NCU02814	SCRG_02343 (Rad53p)	Afu7g03750	orf19.4002 (DUN1)
Invertase (INV)	NCU04265	SCRG_05335 (Suc2p)	Afu2g01240 (InvB)	-
Neuronal Ca^{2+} sensor 1 (NCS-1)	NCU04379	SCRG_00160 (NCS-1)	Afu6g14240 (NcsA)	orf19.4726
Mitochondrial NADH dehydrogenase (NDE-1)	NCU05225	SCRG_00581 (Nde2p)	Afu2g05450	orf19.339 (NDE1)
Actin cytoskeleton-regulatory complex protein (END-3)	NCU06347	SCRG_03220 (End3p)	Afu1g13020	orf19.1711 (END3)
Myosin regulatory light chain cdc4	NCU06617	SCRG_01103 (Mlc1p)	Afu7g05950	orf19.2416.1 (MLC1)
Secretory phospholipase A2 (PLA-2)	NCU06650	-	-	-
EF hand domain-containing protein	NCU06948	SCRG_02857 (Cmd1p)	Afu4g10050 (CmdA)	orf19.4413 (CMD1)
Centrin 3	NCU09871	SCRG_01640 (Cdc31p)	Afu4g11160	-
Alternative NADH-dehydrogenase (NDE-2)	NCU08980	SCRG_02036 (Nde1p)	Afu1g11960	orf19.339 (NDE1)
Serine/threonine protein kinase-16 (STK-16)	NCU00914	SCRG_01619 (Kin4p)	Afu1g14810	orf19.3751 orf19.846
Annexin XIV (ANX-14)	NCU04421	-	Afu2g13890 (Anxc3.2)	-
Annexin (ANX-4)	NCU02139	-	Afu3g07020 (Anxc4)	-
Hyphal anastomosis-3 (HAM-3)	NCU08741	SCRG_05461 (Pro11p;Rsa4p)	Afu5g01780	-
Hyphal anastomosis-10 (HAM-10)	NCU02833	SCRG_01826	Afu7g02350	orf19.6012
Regulator of G protein signalling; Developmental regulator flbA	NCU08319	SCRG_04389.1 (SST2)	Afu2g11180 (FlbA)	orf19.4222 (SST2)

Other Ca^{2+}/CaM signalling regulators				
Phospholipase C (PLC-1)	NCU06245.2	SCRG_02233.1 (PLC1)	Afu3g07940	orf19.5506 (PLC1)
Phospholipase C (PLC-2)	NCU01266.2	SCRG_02233.1 (PLC1)	Afu1g13250	orf19.5797 (PLC2)
Phospholipase C (PLC-3)	NCU11415	SCRG_02233.1 (PLC1)	Afu1g13250	orf19.1586 (PLC3)
Phospholipase C (PLC-4)	NCU02175.2	SCRG_02233.1 (PLC1)	Afu3g07940	orf19.5506 (PLC1)
Calcineurin binding protein	NCU01504	-	Afu2g13060 (CbpA)	-
FK506 resistant-2 (FKR-2)	NCU04140.7	SCRG_00024.1 (FPR2)	Afu6g12170 (Fkbp1)	orf19.4952.1
FK506-resistant-3 (FKR-3)	NCU04371	SCRG_03269.1 (FPR1) SCRG_04386.1 (FPR4)	Afu4g04020 (Fkbp2)	orf19.6452
FK506-resistant-4 (FKR-4)	NCU03241	SCRG_01824.1 (FPR3)	Afu6g08580 (Fkbp4)	orf19.1030
Cyclosporin-resistant-1 (CSR-1)	NCU00726	SCRG_00367.1 (CPR1)	Afu2g03720 (Cyp4)	orf19.6472 (CYP1)
Peptidyl-prolyl cis-trans isomerase (binds to calcineurin inhibitor cyclosporin A)	NCU03853	SCRG_04173.1 (CPR6)	Afu2g02050 (Cyp7)	orf19.7654 (CPR6)

4.2.2. Morphological phenotypes analysis of gene deletion mutants

Morphological phenotypes of 29 homokaryotic mutant strains in genes encoding key Ca^{2+}-signalling or Ca^{2+}/CaM-binding proteins and other Ca^{2+} signalling regulators listed in Table 4.2, were analyzed. Other Ca^{2+}-channel, Ca^{2+}-ATPase, and Ca^{2+}-transporters have been analyzed in a previous study (Chu, 2013). Most of the mutants used in this study were obtained from FGSC except Δ*cna-1*, Δ*cnb-1,* Δ*crz-1* and Δ*end-3*. Homokaryons were purified from some of the mutant strains that were only available as heterokaryons from the FGSC (FGSC17929, Δ*cna-1*; FGSC11494, Δ*crz-1*; and FGSC11502, Δ*end-3*) using the microconidiation method described in section 2.8.1.4. The Δ*cnb-1* mutant was generated with the knock-out cassette, which was constructed by fusion PCR (section 2.7.6). The results in this section mainly describe the morphological phenotypes of each mutant in relation to conidial

germination and CAT fusion. All strains were inoculated on Vogel's medium plates and were incubated at 35^{o}C in dark for 3 days following by 25^{o}C with light for 2 days. Conidia were collected and diluted to a concentration of 1 X 10^{6} cells/ml and incubated at 35^{o}C in dark for 4 h within the 8-well chambers. Images were obtained by DIC microscopy. The information for every strain is listed in Table A.2.

4.2.2.1 Key Ca^{2+}-signalling proteins

Seven homokaryons were analysed in this group, except Δ*cmd-1* which could not be purified from the heterokaryon. *Cmd-1* encodes CaM which is the main intracellular Ca^{2+} sensor/receptor regulating many important cellular pathways and thus, not unexpectedly is an essential gene. Homokaryons of Δ*cmd-1* were unable to survive.

4.2.2.1.1 The calcineurin catalytic subunit a (CNA-1) deletion mutant showed a delayed CAT fusion phenotype

Conidia were incubated at 35^{o}C in dark. A delayed CAT fusion phenotype was shown in this mutant. Only ~ 10% CAT fusion was observed at the 4 h time point but increased to ~ 30% at the 8 h time point (Fig. 4.3 and 4.6). To distinguish CATs from germ tubes, and thus determine where CAT formation had been detected, the microtubule polymerization inhibitor, benomyl, was used because it has been shown that CAT formation is microtubule independent whilst the formation of long germ tubes is microtubule dependent (Roca et al., 2010). Following benomyl treatment, Δ*cna-1* produced CATs but had a lower CAT fusion rate than the wild type (Fig. 4.6). The colony extension rate (~ 1.41 mm/h) was also slower than the wild-type (~ 4.75 mm/h).

4.2.2.1.2 Calcineurin regulatory subunit b (CNB-1) deletion mutant had a similar but not identical phenotype to the Δcna-1 mutant

The knock-out cassette of Δ*cnb-1* was created by fusion PCR. The primer set CNB-KO-P1F and CNB-KO-P2R were used to amplify the 5' flank. Primer set HPH-CC-F and HPH-DD-R were used to amplify the *hph* fragment. The primer set CNB-KI-P3 and

CNB-KI-P4 were used to amplify the 3' flank. Three PCR products and the primer set CNB1-KO-P1fF and CNB1-KO-P4fR were applied for the final fusion PCR (Fig 4.2). The whole cassette (3494 bp) was transformed into *N. crassa* (FGSC9718) to produce the gene deletion mutant (Fig. 4.2).

Eight homokaryons were purified from one of the heterokaryotic transformants (section 2.8.1.4) and screened using the CAT fusion assay (section 2.5.2). Conidia were incubated at 35^{o}C in dark. Delayed germination and CAT fusion phenotypes were shown in this mutant (Fig. 4.3 and 4.6). No CAT fusion was observed at 4 h but increased to ~ 60% at 7 h (Fig. 4.6). This mutant produced CATs but had lower CAT fusion rate than the wild type and its germlings had a different morphology to the wild type (Fig. 4.6). The colony extension rate (~ 1.39 mm/h) was also slower than the wild-type (~ 4.75 mm/h).

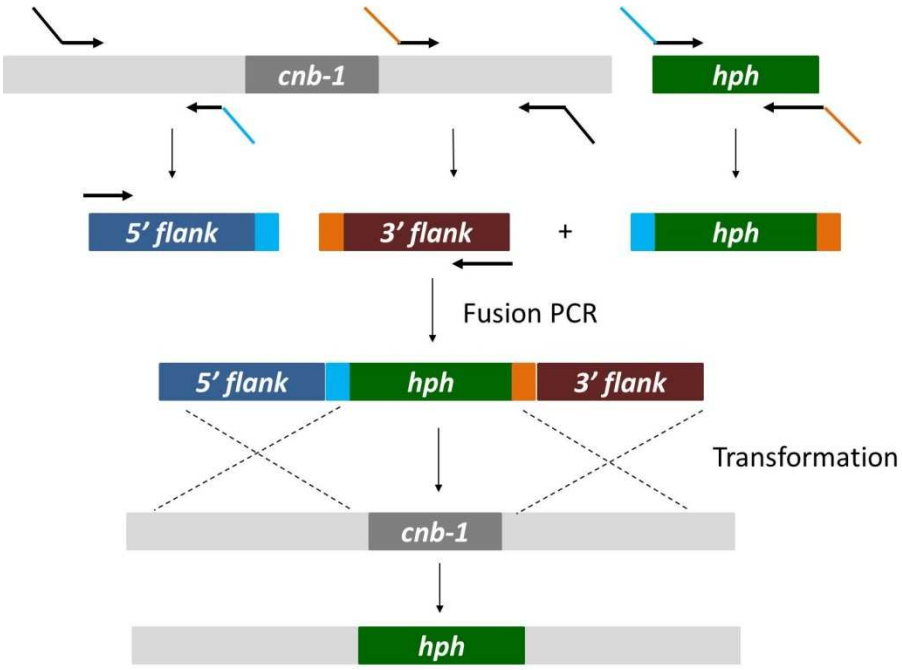

Figure 4.2 Schematic representation of fusion PCR strategy

Location of primer binding sites used to amplify fragments from the genomic DNA or plasmid template. Primers were used in the following combinations: CNB-KO-P1F and CNB-KO-P2R for the 5' flank , CNB-KI-P3 and CNB-KI-P4 for the 3' flank, and HPH-CC-F and HPH-DD-R for the *hph* fragment with the *trpC* promoter. Three PCR products and the primer set CNB1-KO-P1fF and CNB1-KO-P4fR were applied for the final fusion PCR to generate the whole cassette. After the electroporation

transformation, the *hph* cassette replaced the original *cnb-1* gene by homologous recombination.

4.2.2.1.3 The calcineurin regulated transcription factor (CRZ-1) deletion mutant showed a slower colony extension but no obvious changes in germination or CAT fusion

A homokaryon of Δ*crz-1* was purified from the heterokaryon FGSC11494 by the microconidiation method. Conidia were incubated at 35^{o}C in dark for 4 h. No obvious changes in their germination and CAT fusion phenotypes were observed in the Δ*crz-1* deletion mutant compared to the wild-type (Fig. 4.3). The extension rate of its 16 h colony (~ 0.5 mm/h) was much slower than that of the wild-type (~ 4.75 mm/h).

4.2.2.1.4 The Ca^{2+}/CaM-dependent kinase-1 (CaMK-1) plays an important role in conidial germination and CAT fusion

Four CaMKs have been identified in *N. crassa* as CaMK-1 (NCU09123), CaMK-2 (NCU02283), CaMK-3 (NCU06177), and CaMK-4 (NCU09212). Only FGSC12548, the homokaryon of the NCU09123 (*camk-1*) deletion mutant, exhibited a significantly different phenotype in the form of slower colony extension (~ 0.13 mm/h), reduced conidiation, reduced germination, and defective CAT fusion (Fig 4.4). This mutant produced CATs but showed no CAT fusion at the 4 h time point which increased to ~ 10% CAT fusion at the 8 h time point (Fig. 4.6). The conidia of this mutant had a variable morphology, and the mutant produced more microconidia than the wild type (Fig. 4.6). These phenotypes were transient and disappeared after successive subculturing. The second subculture was inoculated from the first culture plate, and the third one was inoculated from the second one. The colony extension rates, conidial germination and CAT fusion were increased with successive subculturing (Fig. 4.7). In addition, the extension rate of 16 h colonies of FGSC12448 (Δ*camk-2*) were slightly faster (~ 5.31 mm/h) than the wild-type (~ 4.75 mm/h).

4.2.2.2 Putative Ca^{2+} or Ca^{2+}/CaM binding proteins

4.2.2.2.1 The RGS-1 protein plays an important role in the CAT fusion process

NCU08319 (*rgs*-1) encodes a regulator of G-protein signalling (RGS) protein and is a homolog of the human RGS4, which regulates G protein-mediated PLC signalling that is involved in IP_3-mediated Ca^{2+} released from intracellular stores. According to the BLAST analysis, it is also a homolog of FlbA in *A. nidulans*. The KO mutant produced straighter germ tubes than the wild type and it exhibited markedly reduced CAT fusion during colony initiation. Longer CATs were observed with the benomyl treatment but no obvious CAT chemotropism was shown between these CATs (Fig. 4.6). Furthermore, its mature colony had a more fluffy appearance than the wild type (Fig. 4.3).

4.2.2.3 Other Ca^{2+}/CaM signalling regulators

4.2.2.3.1 Phospholipase C-2 (PLC-2) is involved in conidial germination

Four PLCs have been identified in *N. crassa* as PLC-1 (NCU06245), PLC-2 (NCU01266), PLC-3 (NCU11415), and PLC-4 (NCU02175). Only FGSC12022, the homokaryon of the NCU01266 (*plc-2*) deletion mutant, exhibited a significantly altered phenotype with slower colony extension (~1.88 mm/h), reduced germination and reduced CAT fusion during colony initiation (Fig 4.5). This mutant produced CATs but showed very low CAT fusion (Fig. 4.6). This may be caused by the defective conidial germination.

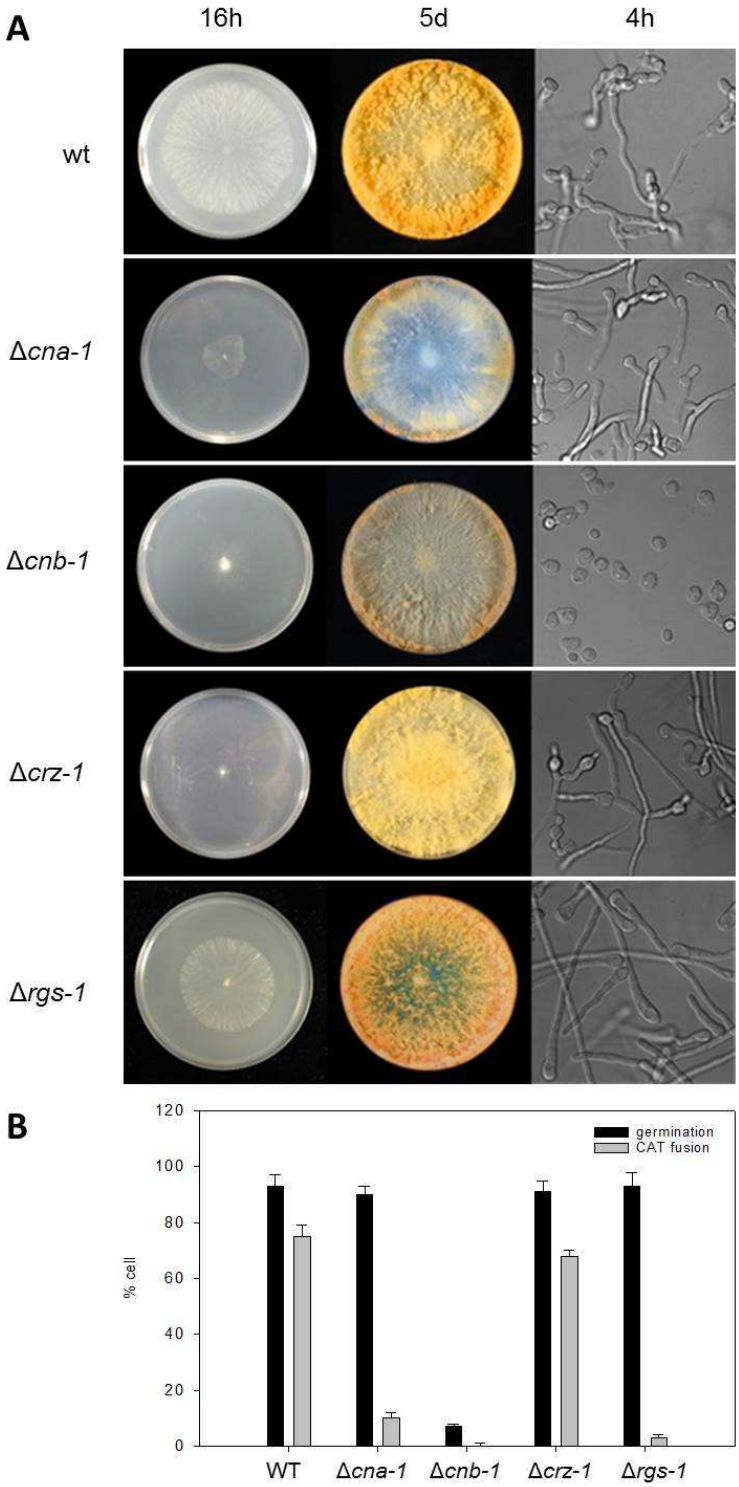

Figure 4.3 Colony morphology, growth, germination and cell fusion of Δ*cna-1*, Δ*cnb-1*, Δ*crz-1*, and Δ*rgs-1* mutants. (A) Images of young colonies were captured at the 16 h time point with incubation for 16 h at 35 °C in dark. Images of mature colonies were captured at the 5 d time point with incubation for 3 d at 35 °C in dark and 2 d at 25 °C with light. Images of germlings incubated for 4 h at 35 °C in dark were captured using DIC microscopy. (B) Germination and cell fusion of germlings at the 4 h time point were quantified (*n* = 100). The error bars indicate standard deviations.

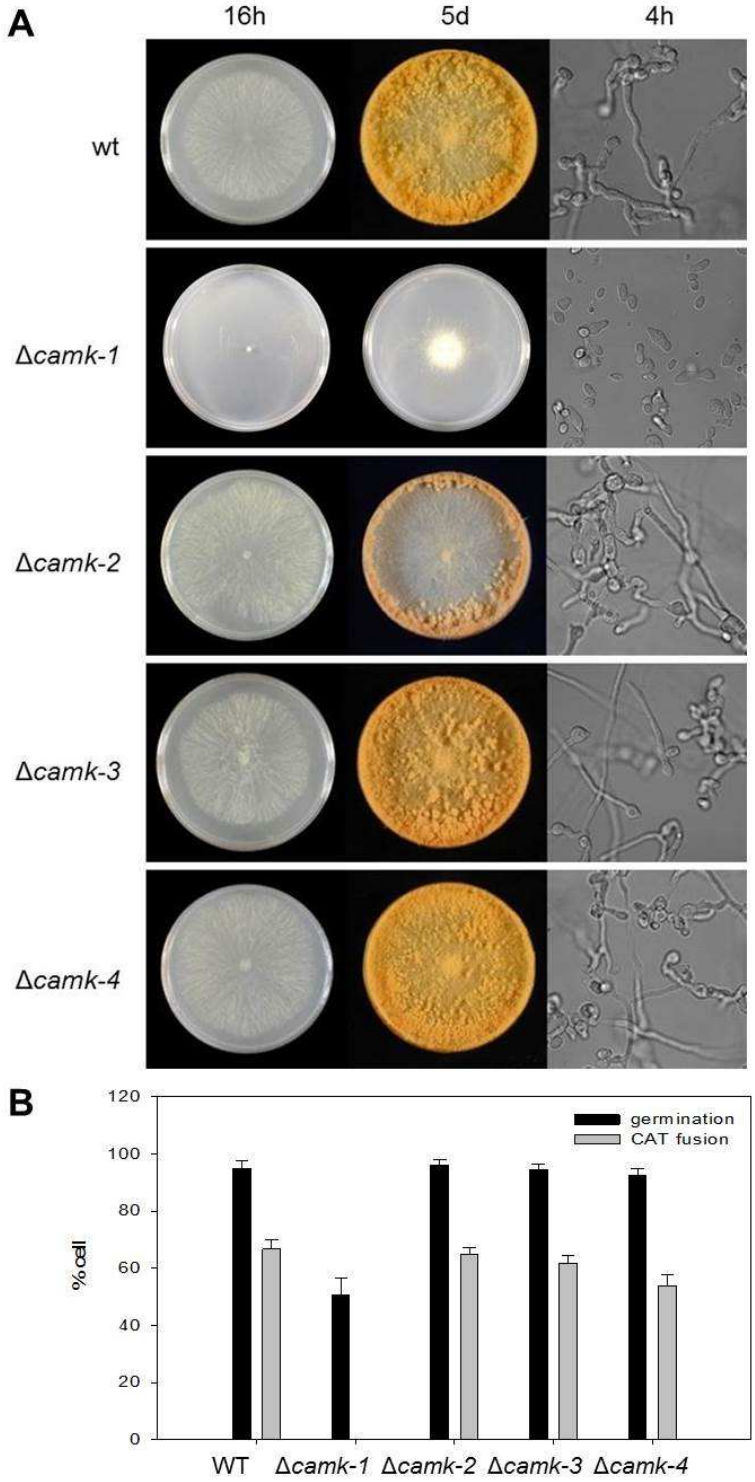

Figure 4.4 Ca^{2+}/CaM-dependent kinase-1 (CaMK-1) plays an important role for conidial germination (A) Images of young colonies were captured at the 16 h time point with incubation for 16 h at 35 °C in dark. Images of mature colonies were captured at the 5 d time point with incubation for 3 d at 35 °C in dark and 2 d at 25 °C with light. Images of germlings incubated for 4 h at 35 °C in dark were captured using DIC microscopy. (B) Germination and cell fusion of germlings at the 4 h time point were quantified (*n* = 100). The error bars indicate standard deviations.

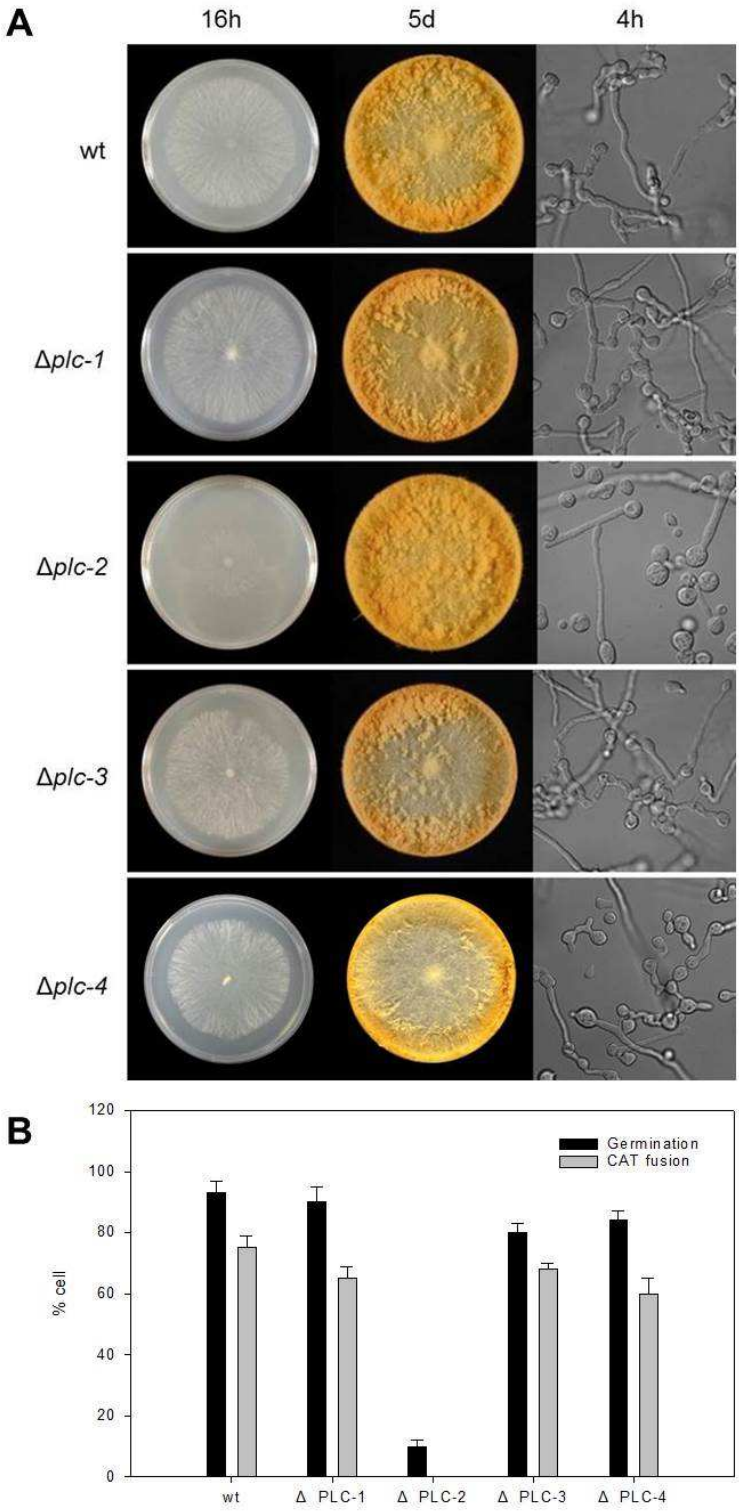

Figure 4.5 Phospholipase C-2 (PLC-2) is essential for conidial germination. (A) Images of young colonies were captured at the 16 h time point with incubation for 16 h at 35 °C in dark. Images of mature colonies were captured at the 5 d time point with incubation for 3 d at 35 °C in dark and 2 d at 25 °C with light. Images of germlings incubated for 4 h at 35 °C in dark were captured using DIC microscopy. (B) Germination and cell fusion of germlings at the 4 h time point were quantified (*n* = 100). The error bars indicate standard deviations.

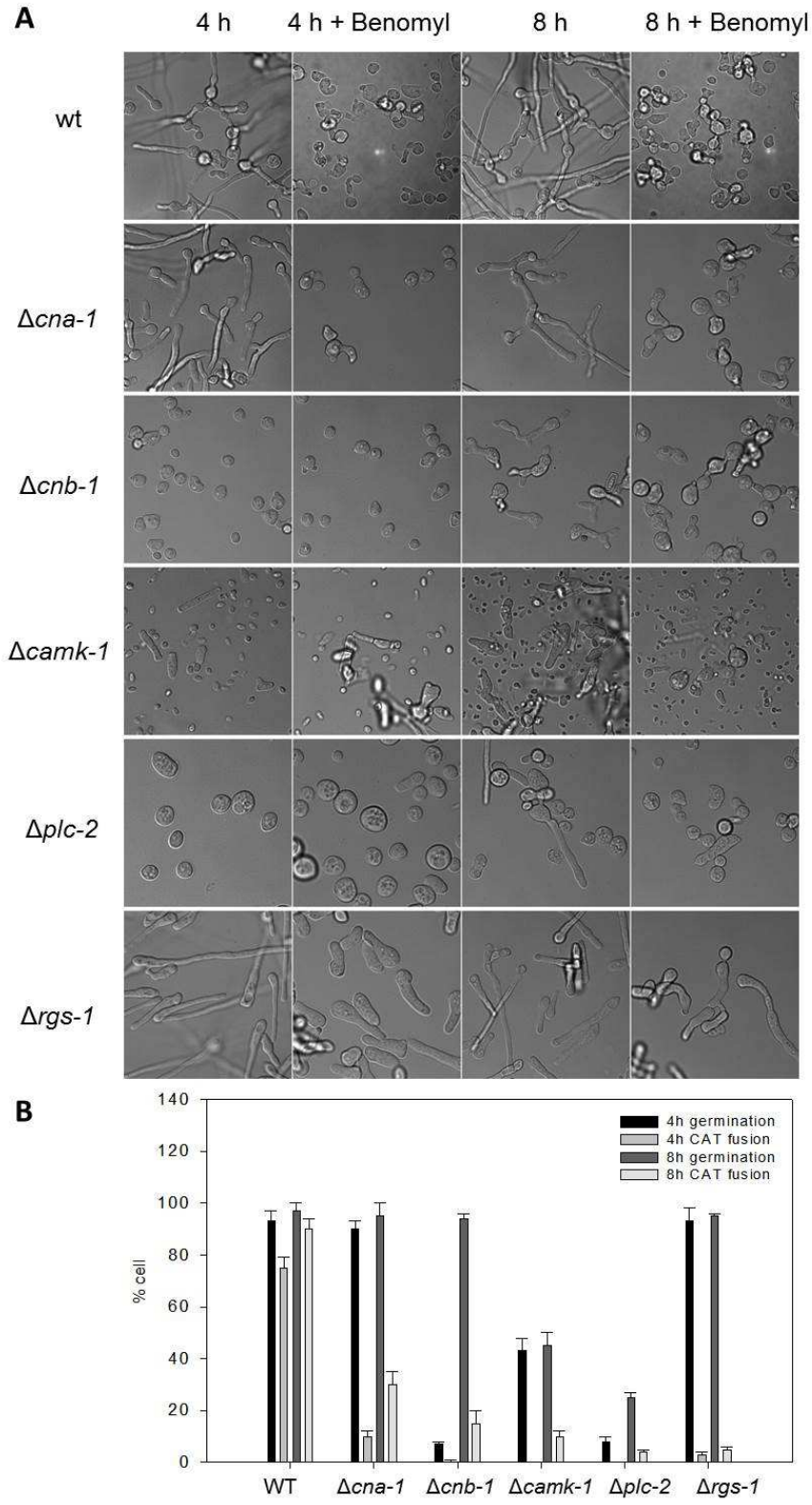

Figure 4.6 Germination and cell fusion with longer incubation time and benomyl treatment in *cna-1*, *cnb-1*, *camk-1, plc-2, camk-1,* and *rgs-1* null mutants. (A) Conidia were incubated in liquid VM or treated with 5 µM benomyl at 35^{o}C in dark to determine the CAT formation. Images were captured at the 4 h and 8 h time points to determine whether no CAT fusion or delayed CAT fusion. (B) Germination and cell fusion of germlings at the 4 h and 8 h time point were quantified (*n* = 100). The error bars indicate standard deviations.

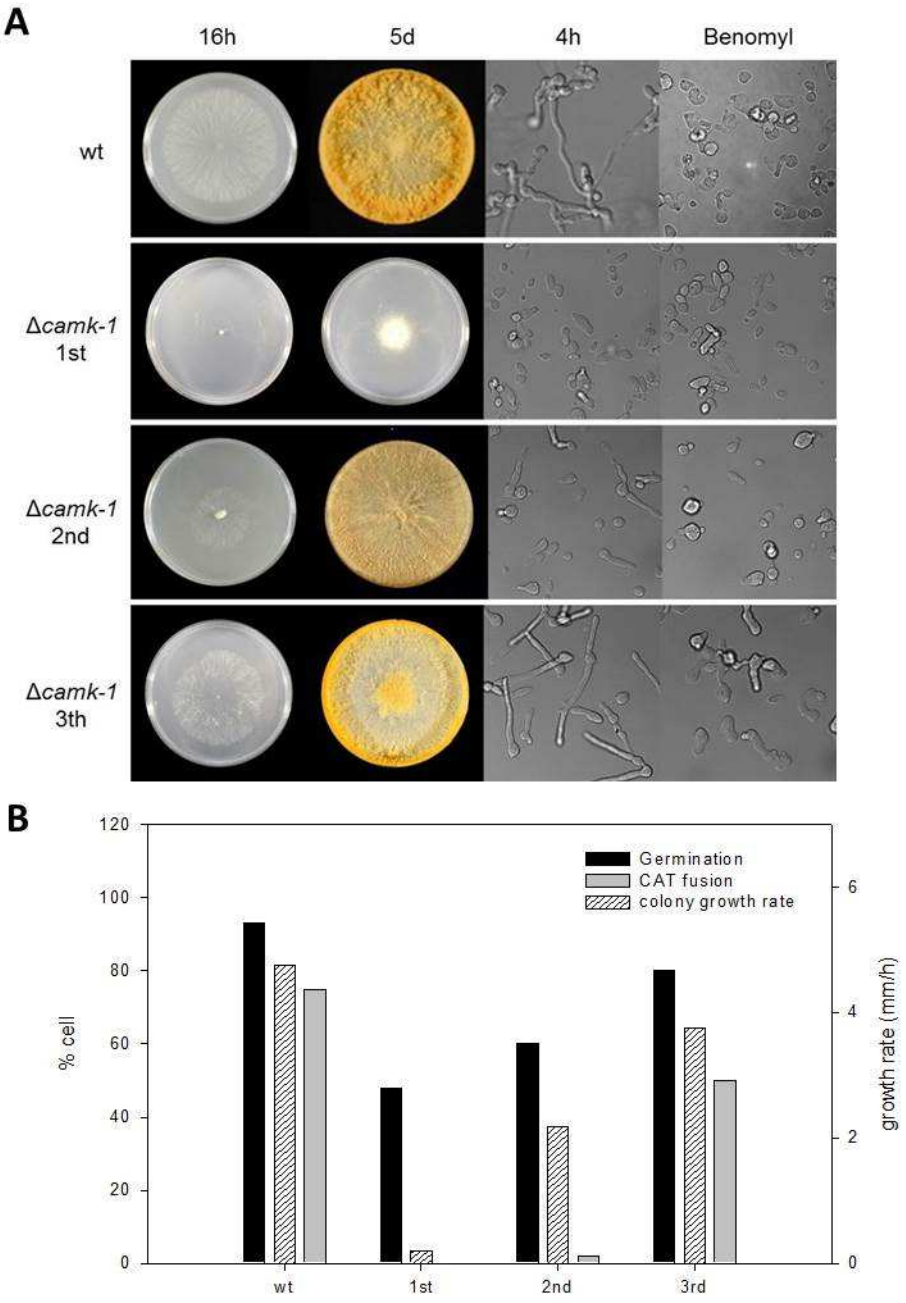

Figure 4.7 The transient phenotypes of Δ*camk-1* over 3 generations. The Δ*camk-1* mutant was subcultured twice to obtain the second and third generations mutants. The wild-type phenotypes were recovered more and more by the subcultures. (A) Images of young colonies were captured at the 16 h time point with incubation for 16 h at 35 °C in the dark. Images of mature colonies were captured at the 5 d time point with incubation for 3 d at 35 °C in dark and 2 d at 25 °C with light. Images of germlings incubated for 4 h at 35 °C in dark were captured using DIC microscopy. (B) Germination and cell fusion of germlings at the 4 h time point were quantified (*n* = 100). The colony extension rate was measured between the 16 h and 24 h time point with incubation at 35 °C in dark. The error bars indicate standard deviations.

4.3. Discussion

The budding yeast, *S. cerevisiae*, has a much simpler Ca^{2+}-signalling apparatus then filamentous fungi. In the budding yeast, Ca^{2+}-signalling has been reported to regulate the cell cycle, mating, sensing of glucose and glucose starvation, resistance to salt stress and cell survival (Cyert and Thorner, 1992; Fischer et al., 1997; Matheos et al., 1997; Nakajima-Shimada et al., 1991; Tisi et al., 2004). Compared to the single-cell yeast system, filamentous fungi undergo much more complex growth patterns and development. In filamentous fungi, there is evidence for the involvement of Ca^{2+} in far more physiological processes, including the cell cycle, sporulation, spore germination, hyphal tip growth, hyphal orientation, hyphal branching, and circadian rhythms (Karamushka and Gadd, 1994; Shaw et al., 2001).

One of the limitations of a sequence-based comparative analysis of the Ca^{2+}-signalling machinery is the difficulty of identifying proteins with defined functions simply based on their sequence similarity to their known counterparts in other organisms. This is further complicated by results from BLAST analyses that have shown that certain key components of animal and plant Ca^{2+}-signalling machineries (Berridge et al., 2003; Sanders et al., 2002), such as IP_3 R and ryanodine receptors, are not identifiable in fungi even where there is evidence from physiological and phamacological studies that proteins of these types are present. The research described in this chapter concentrated on known and the identification of other likely candidates of components of the Ca^{2+}-signalling machinery in *N. crassa*, and the characterization of the phenotypes of gene deletion mutants of these components, particularly in relation to colony initiation (conidial germination and CAT fusion).

Table 4.3 Genes and mutants screened in this study

Gene group	No. of genes	lethal genes	homokaryons	with different phenotypes during colony initiation
Ca^{2+}-channels	6	0	6	**Δ*cch-1*** (reduced CAT chemotropism) **Δ*cch-1*Δ*mid-1*** (reduced CAT chemotropism and colony extension rate)
Ca^{2+}-ATPases	10	1	9	-
Ca^{2+} transporters	9	0	7	-
Key Ca^{2+}-signalling proteins	8	1	7	**Δ*cna-1*** (delayed CAT fusion) **Δ*cnb-1*** (delayed germination and CAT fusion, altered germlings morphology) **Δ*crz-1*** (reduced colony extension rate) **Δ*camk-1*** (reduced conidial germination, CAT fusion, colony extension rate and conidiation)
Putative Ca^{2+} or Ca^{2+}/CaM binding proteins	23	5	15	**Δ*rgs-1*** (reduced CAT fusion, fluffy colony morphology)
Other Ca^{2+}/CaM signalling regulators	9	0	9	**Δ*plc-2*** (reduced conidial germination and CAT fusion)

A total of 65 genes associated with Ca^{2+} signalling have now been analysed in *N. crassa*. Forty of these genes have been classfied as Ca^{2+} or Ca^{2+}/CaM-binding proteins and regulators, and 25 genes have been classfied as Ca^{2+}-transporters (Table 4.1). The Ca^{2+}-transporters part were studied previously (Chu, 2013). I mainly focused on the Ca^{2+} or Ca^{2+}/CaM signalling components of these 40 genes, of which 6 genes were unable to generate homokaryons, including *cmd-1* (NCU04120), *agc-1* (NCU01241), *nuf-1* (NCU02411), NCU04265, *cdc-4* (NCU06617) and *cdc-31* (NCU09871). With the exception of mutants that I generated for 2 genes, the rest of the gene deletion mutants were obtained from the FGSC. Of 32 homokaryotic mutants analysed, 5 mutants showed defective phenotypes in conidial germination and CAT fusion. These mutants were Δ*cna-1* (NCU03804), Δ*cnb-1* (NCU03833), Δ*camk-1* (NCU09123), Δ*rgs-1* (NCU08319) and Δ*plc-1* (NCU01266). There were various phenotypes observed in these mutants. I only focused on germination rate, CAT formation and CAT fusion rate. I determined the defective phenotypes in CAT chemotropism when CATs were formed but CAT fusion rate was decreased. A specific marker or a check point of CAT fusion in *N. crassa* has not been established yet. Therefore, it was diffcult to verify defective phenotypes in the fusion step.

4.3.1. CaM-dependent protein kinase-1 (CaMK-1) is involved in conidial germination.

Ca^{2+}/CaM-dependent protein kinases (CaMKs) are serine/threonine-specific protein kinases regulated directly by the Ca^{2+}/CaM complex. CaMKs undergo rapid autophosphorylation in the presence of activated CaM, have a broad range of substrates and regulate many cellular functions in eukaryotic organisms (Braun and Schulman, 1995; Soderling et al., 2001). There are three CaM kinases in *A. nidulans*, which are CmkA, CmkB and CmkC. Evidence has been obtained which indicates that the multifunctional CmkA may be involved in nuclear division and hyphal growth and is required for cell viability (Dayton and Means, 1996; Dayton et al., 1997; Kornstein et al., 1992). Four CaMKs have been identified in *N. crassa*, of which CaMK-1 is involved in the circadian clock by regulating the phosphorylation of FRQ. The Δ*camk-1* strain showed slower vegetative growth, lower amounts of aerial hyphae, and reduced conidiation than the wild-type (Yang et al., 2001). It also exhibited decreased conidial germination and no CAT fusion at the 4 h time point compared to the wild type. indicating that these processes may be regulated by CaMK-1.

4.3.2. Phospholipase C-2 (PLC-2) is important for conidial germination

Phospholipase C (PLC) cleaves phosphatidylinositol 4,5-bisphosphate (PIP_2) to inositol 1,4,5-triphosphate ($InsP_3$) and diacylglycerol (DAG) (Kinnunen and Holopainen, 2000). IP_3 has been reported to release Ca^{2+} from vesicles which act as intracellular Ca^{2+} stores in order to maintain a high $[Ca^{2+}]_c$ in the hyphal tip (Silverman-Gavrila and Lew, 2002). The Ca^{2+} released by IP_3 may work with DAG to activate protein kinase C (PKC) that induces the CWI MAPK pathway (Nishizuka, 1986). This IP_3-induced mechanism in animal cells also causes Ca^{2+}-induced Ca^{2+} release (CICR) to generate Ca^{2+} waves in the cytoplasm (Barbara, 2002). Previous studies had provided evidence that deletion of the gene of fungal phosphoinositide-specific PLC (PI-PLC) in *Magnaporthe oryzae* (MoPLC1) suppressed an increase in $[Ca^{2+}]_c$, resulting in defective phenotypes, including suppressed appressorium formation and pathogenicity (Rho et al., 2009). Deletion of PLC1 in yeast resulted in a pleiotropic phenotype, with defects in growth, carbon source utilization, and increased

sensitivity to osmotic stress and high temperature (Flick and Thorner, 1993; Payne and Fitzgerald-Hayes, 1993). *S. cerevisiae* has only one PLC gene, but *N. crassa* has four (Galagan et al., 2003; Zelter et al., 2004).

Only the Δ*plc-2* exhibited a significantly altered phenotypes with slower colony extension, and greatly reduced germination and CAT fusion in *N. crassa* (Fig. 4.6 and 4.7). This result suggests that PLC-2 may play a role in regulating conidial germination and CAT fusion.

4.3.3. Calcineurin plays an important role during CAT chemotropism and young colony establishment.

The *cna-1* and *cnb-1* deletion mutants showed a delayed CAT fusion phenotype (Fig. 4.3). Germlings of Δ*cna-1* and Δ*cnb-1* had a similar morphology to those treated with calcineurin inhibitors (Fig. 3.12 and 3.12). Conidia produced CATs but there was no obvious chemotropism between these cells. This indicates that calcineurin-regulated signalling is probably involved in CAT chemotropism mechanism. Calcineurin is a Ca^{2+}/CaM-dependent serine/threonine protein phosphatase that controls morphogenesis and stress responses in eukaryotes (Chen et al., 2010b; Klee et al., 1979). The catalytic A and regulatory B subunits of calcineurin need to form a complex to stabilize the protein conformation. My results showed the CNB-1 influenced the morphology more than CNA-1 during colony initiation in *N. crassa* (Fig. 4.3 and 4.6). This may be caused by the activation of CNA from CNB.

In response to Ca^{2+} stimuli from extracellular or intracellular sources, calcineurin stimulates phosphatase activity and converts signals to various outputs by dephosphorylating relevant substrates. The transcription factor CRZ in fungi, or nuclear factor of activated T cells (NFAT) in mammals, are recruited to the nucleus to regulate gene expression by being dephosphorylated by activated calcineurin (Chen et al., 2010b; Liu et al., 2006b; Reedy et al., 2010). In addition to CRZ, The leucine-zipper-type Yap1 transcription factors, phosphoinositide PIP_2 binding proteins Slm1 and Slm2, and endoplasmic reticulum (ER) transmembrane protein Hph1 have also been described as substrates of calcineurin phosphatase activity in *S.*

cerevisiae (Heath et al., 2004; Stie and Fox, 2008; Szlufcik et al., 2006; Yokoyama et al., 2006). In addition, the Ca^{2+} channels, Cch1 and Mid1, have been shown to be the upstream elements of the calcineurin pathway in *S. cerevisiae* (Muller et al., 2001), and these Ca^{2+}-channel proteins have been demonstrated to work in concert with calcineurin to control growth during stress in *C. albicans* and *Cryptococcus neoformans* (Liu et al., 2006a; Reedy et al., 2010). The gene deletion mutants of CCH-1/MID-1 have also been shown defective phenotypes in CAT chemotropism (Chu, 2013).

4.3.4. CAT chemotropism may be regulated through the calcineurin-mediated CWI pathway

Calcineurin may play a role in regulating CAT chemotropism in *N. crassa* by crosslinking with other signalling pathways. The rapamycin-insensitive Tor complex 2 (TORC2) kinase pathway, which interacts with several components associated with actin polarization, secretion, endocytosis, and cell wall biosynthesis, has been shown to crosstalk with calcineurin through the PH domain-containing subunits Slm1 and Slm2 (Audhya et al., 2004; Cybulski and Hall, 2009; Fadri et al., 2005). The TORC2 complex activates P21-activated protein kinase (PAK), which is an essential activator (MAPKKKK) of the MAPK cascade required for cell wall integrity (CWI) signalling (Chen and Thorner, 2007; Roelants et al., 2002; Sanchez-Mir et al., 2014a; Sanchez-Mir et al., 2014b). In addition, MAPK signalling pathways have been demonstrated to interact with calcineurin in *C. neoformans* and *U. maydis* (Egan et al., 2009; Kraus et al., 2003). Interestingly, two of the three different MAPK pathways in *N. crassa* have been demonstrated to be involved in different stages of the CAT fusion process (Poggeler and Kuck, 2004). The deletion mutants of 3 genes in the pheromone-response (PR) and CWI pathway were all shown to be defective in CAT fusion (Fleissner et al., 2009b; Galagan et al., 2003; Pandey et al., 2004). Furthermore, use of an inhibitable variant of MAK-1 and MAK-2 showed that these MAP kinase pathways are involved in CAT chemotropism (Fleissner et al., 2009b; Galagan et al., 2003). This suggests that CAT chemotropism might be regulated by calcineurin interacting with the CWI or PR MAPK pathway. No evidence was shown for the high

osmolarity glycerol (HOG) MAP kinase pathway being involved in CAT fusion (Lichius, 2010b).

4.3.5. G protein via RGS-1 may be involved in CAT fusion process

Regulators of G protein signalling (RGS proteins) are a large family of highly diverse and multifunctional signalling proteins, which share a conserved signature domain (RGS domain) that binds directly to activated Gα subunits to participate as negative regulators or effectors in G protein pathways (Diverse-Pierluissi et al., 1999; Hepler, 1999). The G protein signalling pathway is also involved in intracellular Ca^{2+} regulation. G protein-coupled receptors (GPCRs) play a critical role in negative feedback to modulate the activity of the CaV2 subfamily of the voltage-operated Ca^{2+} channels (VOCCs) in human cells. The intracellular N terminus of CaV2α1 subunits provides essential determinants for G-protein modulation (Dolphin, 2003). It has been shown that RGS4 in human cells binds alternatively with PIP_3 and the Ca^{2+}/CaM complex as a GTPase activating protein which blocks IP_3/Ca^{2+} signalling. This study demonstrated that RGS is a modulator for fine-tuning the frequency of Ca^{2+} oscillations (Soderling et al., 2001). More than 20 mammalian RGS proteins have been identified to date (Hepler, 1999). However, only one homolog was found in *N. crassa*. The gene NCU08319 encodes a RGS superfamily domain protein, and has identified from BLAST analysis as the homolog of *flbA* in *A. nidulans* and *Saccharomyces cerevisiae* SST2 (Borkovich et al., 2004). Loss of the *flbA* gene function in *A. nidulans* leads to the formation of fluffy colonies with long, twisted, interwoven aerial hyphae (Lee and Adams, 1994).

The *N. crassa* deletion mutant of *rgs*-1 (FGSC12372; NCU08319) had a similar phenotype to that of *A. nidulans*. In addition to the fluffy colonies, it produced straighter germ tubes than the wild type and it exhibited significantly reduced CAT fusion during colony initiation. Interestingly, longer CATs were observed with the benomyl treatment but no obvious CAT chemotropism was shown between these CATs (Fig. 4.6). The human RGS4 has been known to be involved in the regulation of $[Ca^{2+}]_c$ homeostasis. Thus, I presume that these CATs may develop into germ tubes based on the results in Chapter 3 (Fig. 3.6). This result is the first evidence that

G-protein signalling may play a role in regulating CAT fusion in *N. crassa.*

4.4. Summary

- A total of 65 genes associated with Ca^{2+} signalling have been identified by BLAST analysis, of which 40 genes were classfied as Ca^{2+} or Ca^{2+}/CaM binding proteins and other regulators, and 25 genes were classfied as Ca^{2+} transport components.
- The calcineurin catalytic subunit a (CNA-1) and regulatory subunit b (CNB-1) deletion mutants showed a delayed CAT fusion phenotype that may be caused by the inhibition of CAT chemotropism.
- The calcineurin regulated transcription factor (CRZ-1) deletion mutant showed a slower colony extension rate but no inhibition of conidial germination or CAT fusion.
- The Ca^{2+}/CaM-dependent kinase-1 (CaMK-1) plays an important role in conidial germination.
- Phospholipase C-2 (PLC-2) is essential for conidial germination.
- Regulator of G protein signalling-1 (RGS-1) is involved in the CAT fusion process.

Chapter 5

Proteomics analysis of CaM-binding interacting proteins and protein complexes

Chapter 5 – Proteomics analysis of CaM-interacting proteins and protein complexes

5.1. Introduction

Calmodulin (CaM) is a highly conserved, soluble, signalling protein that has both Ca^{2+}-dependent and Ca^{2+}-independent binding partners (section 1.3.2.1). It acts as the main intracellular Ca^{2+} sensor or receptor by binding Ca^{2+} ions via four EF hands. EF hand contains a Ca^{2+}-binding loop conservatively starting with an aspartate (Asp, D) and ending in a glutamate (Glu, E) residue (Babu et al., 1988). Many proteins involved in Ca^{2+} signal transduction alter their activity in response to changes in $[Ca^{2+}]_c$ levels, but are themselves not able to bind Ca^{2+} ions. Some of these proteins utilize CaM as a mediator of the initial elevated Ca^{2+} signal to alter their activity and to regulate multiple cellular functions (Vetter and Leclerc, 2003).

Proteomics analysis is a powerful technique that facilitates the association and comparison of complex mixtures of proteins. Large-scale proteomic methods are valuable for studying the dynamics of proteins and their posttranslational modification in living cells (Gingras et al., 2007). Recently, mass spectrometry (MS), in contrast to nuclear magnetic resonance and X-ray crystallography, has been used to provide a large amount of information on individual proteins involved in specific biological responses (Matthiesen, 2007).

To date, more and more different fungal species are having their genomes sequenced and annotated. A genetic analysis of the Ca^{2+} signalling components and the phenotypes of their gene deletion mutants in *N. crassa* were shown in Chapter 4. Previously, no proteomics analyses focused on of Ca^{2+}/CaM signalling in fungi have been performed (Kim et al., 2007). Thus, the aims of the research described in this chapter were:

- To align CaM protein sequences and it's Ca^{2+}-binding sites in different fungi
- To identify the CaM-interacting proteome using immuno-precipitation and mass spectrometry
- To analyze the potential biological processes regulated by Ca^{2+}/CaM signalling during colony initiation from this proteomic analysis

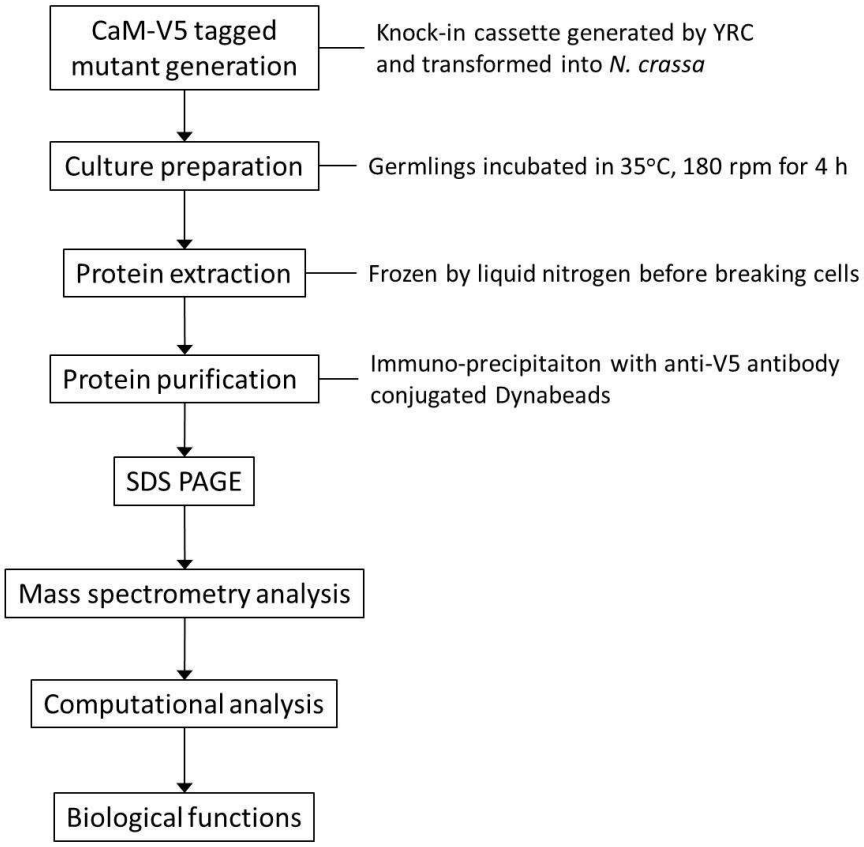

Figure 5.1 Flowchart of the proteomic analysis in this chapter

The cmd-1 gene was tagged with V5 epitope and transformed into *N. crassa*. 4 h-old germlings were used to prepare the protein extraction sample. Total protein extraction was purified using the anti-V5 antibody conjugated Dynabeads. The protein elution was separated by SDS PAGE and followed by mass spectrometry analysis. Computational analysis of the raw data combined with protein classification provided an indication of the biological functions that the CaM interacting proteins might be involved in.

5.2. Results

5.2.1. Identification and Characterization of CaMs from different fungi

CaM protein sequences were obtained from the National Center for Biotechnology Information (NCBI) protein database and the alignment of CaM protein sequences from 10 different fungi is shown in Fig. 5.2. Six filamentous fungi (*N. crassa, A. nidulans, A. fumigatus, M. grisea, F. oxysporum Fo47* and *B. cinerea*), 2 diploid fungi (*U. maydis* and *C. albicans*), and two yeasts (*S. pombe* and *S. cerevisiae*) were chosen, of which four were model organisms and six were pathogens.

Most fungal CaMs, and 7 of the 10 analyzed here, contain 149 amino acids with four Ca^{2+}-binding motifs. Exceptions were the *F. oxysporum* CaM that has 220 amino acids because of an extra N-terminal part of the CaM, *S. pombe* with 150 amino acids and *S. cerevisiae* with 148 amino acids (Table 5.2). The four Ca^{2+}-binding loops are labelled in grey in Fig. 5.2. Each loop contains 12 amino acids that start with aspartic acid (D) and end at glutamic acid (E) (darker grey labelled). Interestingly, vertebrate and fungal CaMs bind four molecules of Ca^{2+} per molecule of CaM, whereas *S. cerevisiae* CaM binds a maximum of three molecules of Ca^{2+}. The *S. cerevisiae* CaM also exhibits the lowest similarity in this group of fungi compared to the *N. crassa* CaM (Table 5.1).

The 10^{th} amino acid of the CaM sequence in *N. crassa* is valine (V) which is the same in other filamentous fungi (first frame in Fig. 5.2), but different in diploid and yeast fungi in which it is isoleucine (I). Similarly, the 97^{th} amino acid of CaM sequence in *N. crassa* is asparagine (N), which is the same in other filamentous fungi (second frame in Fig. 5.2), but different in diploid and yeast fungi in which it is glycine (G). The filamentous fungus, *Trichoderma reesei* and the yeast, *Pichia pastoris* (*Komagataella pastoris*) also follow these rules (data not shown). These two conservative amino acid sites may be essential regions that distinguish different biological function of CaM in filamentous fungi and yeasts.

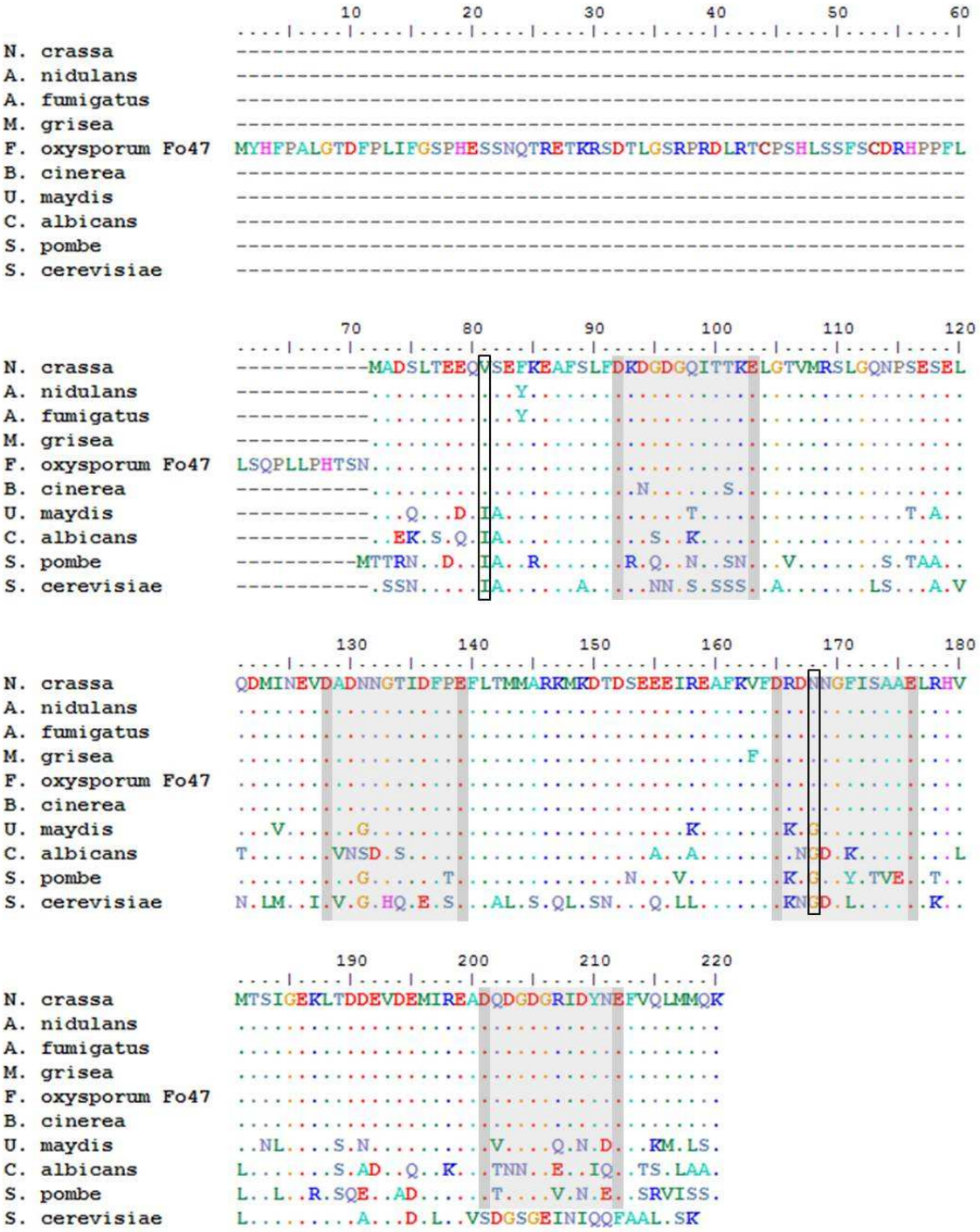

Figure 5.2 Protein sequence of CaM in different fungi

The CaM protein sequences in 10 different fungi including two yeasts (*S. pombe* and *S. cerevisiae*), two diploid fungi (*U. maydis* and *C. albicans*), and six filamentous fungi (*N. crassa, A. nidulans, A. fumigatus, M. grisea, F. oxysporum Fo47* and *B. cinerea*). Software BioEdit was used to produce the alignment. Colorful dots present the identical amino acids with the CaM sequence in *N. crassa*. Four Ca^{2+}-binding loops are marked in grey. Each loop contains 12 amino acids that start with aspartic acid (D) and end at glutamic acid (E) (dark grey). Black frames are two conservative regions for distinguishing filamentous fungi and yeasts.

Table 5.1 Comparative genetic analysis of CaM in different fungi

Organism	No. of gene	protein length (a.a.)[1]	No. of Ca^{2+} binding motifs	Similarity of CaM protein sequence to *N. crassa* CaM[2]
N. crassa	1	149	4	1
A. nidulans	1	149	4	0.99
A. fumigatus	1	149	4	0.99
M. grisea	1	149	4	0.99
F. oxysporum Fo47	1	220	4	0.68 / 1[3]
B. cinerea	1	149	4	0.99
U. maydis	1	149	4	0.84
C. albicans	1	149	4	0.74
S. pombe	1	150	4	0.68
S. cerevisiae	1	148	3	0.55

Note: 1. The protein length includes the first methionine from the start codon.

2. The similarity is the percentage of the same protein sequence of CaM compared to *N. crassa*..

3. The similarity of whole CaM sequence including the extra N-terminal part in *F. oxysporum* is 0.68 and the overlap part without N-terminal is 1.

5.2.2. Immuno-precipitation of CaM-binding protein complexes

To create a tagged-CaM mutant, two epitopes were used to label the *N. crassa* CaM (a V5 epitope, derived from the V5 simian virus and a poly-histidine sequence HAT from chicken lactate dehydrogenase), which are known to be a superior alternative to the commonly used 6xHis tag (Chaga et al., 1999). The double epitope tag was created using three overlapping synthetic oligonucleotides that were combined using yeast recombination cloning (YRC). Single native genomic loci of *cmd-1* were tagged by the introduction of an integration cassette containing the V5-HAT epitope and hygromycin selection marker (Fig. 5.3).

In V5-HAT-expressing strains, conidial germination, cell fusion, septation, and germ tube emergence was unchanged from the wild-type, suggesting that the V5-HAT tag does not interfere with normal cell function (data from Dr. A. Berepiki). SDS PAGE and western blot analysis of whole cell extracts with a monoclonal anti-V5 antibody demonstrated that the V5-HAT-tagged CaM was expressed as two isoforms in *N. crassa* (Fig. 5.4 A). The anti-V5 antibody showed a specific efficacy in the western blot reaction compared to a wild-type control (Fig. 5.4 B and C). Crude

protein extraction from both mature hyphae and germlings were separated using SDS PAGE (Fig. 5.4 D) and the protein profiles compared in western blots. Slight differences in the protein profile were shown in the western blot with the unspecific binding to the beads (Fig. 5.4 E). Thus, purified elution of the wild-type proteins were used as the control sample for the subsequent mass spectrometry analysis.

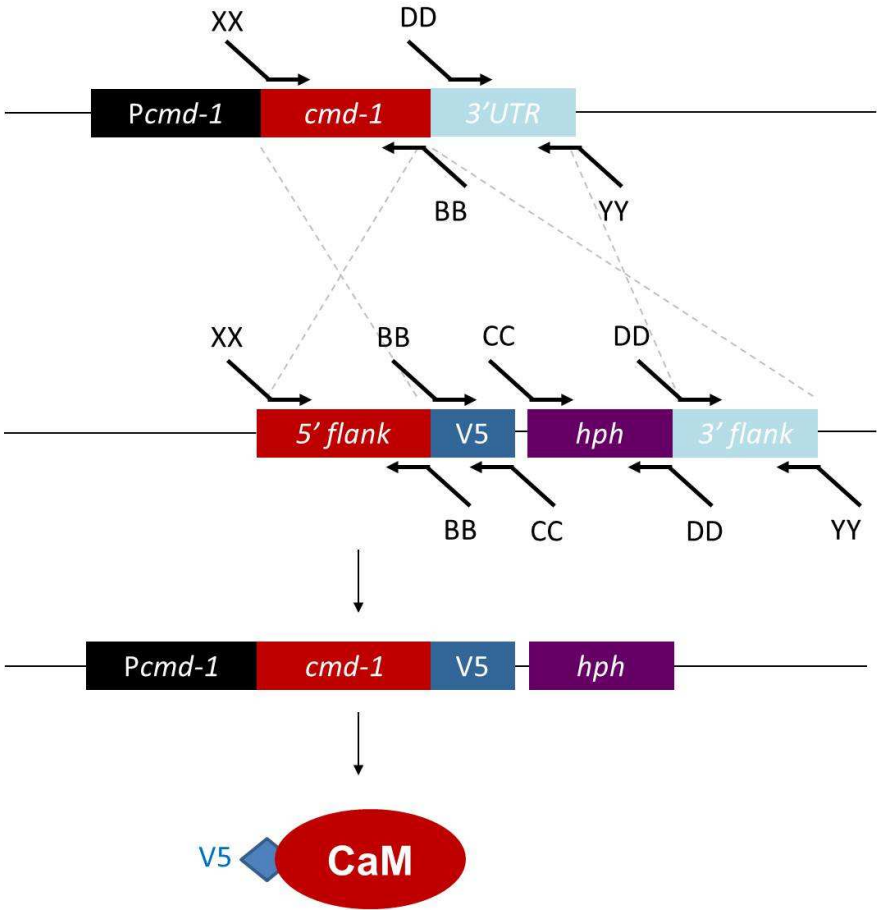

Figure 5.3 Schematic representation of CaM-V5 construction in *N. crassa*

Location of primer binding sites used to amplify fragments from genomic DNA or the plasmid template. Primers were used in the following combinations: CAM-KI-P1 and CAM-KI-P2 for the 5' flank , CAM-KI-P3 and CAM-KI-P4 for the 3' flank, V5-BB-F and V5-CC-R for the *v5* fragment, and HPH-CC-F and HPH-DD-R for the *hph* fragment with *trpC* promoter. Four PCR products and the linear vector RS426 were applied for the YRC to generate the whole plasmid.

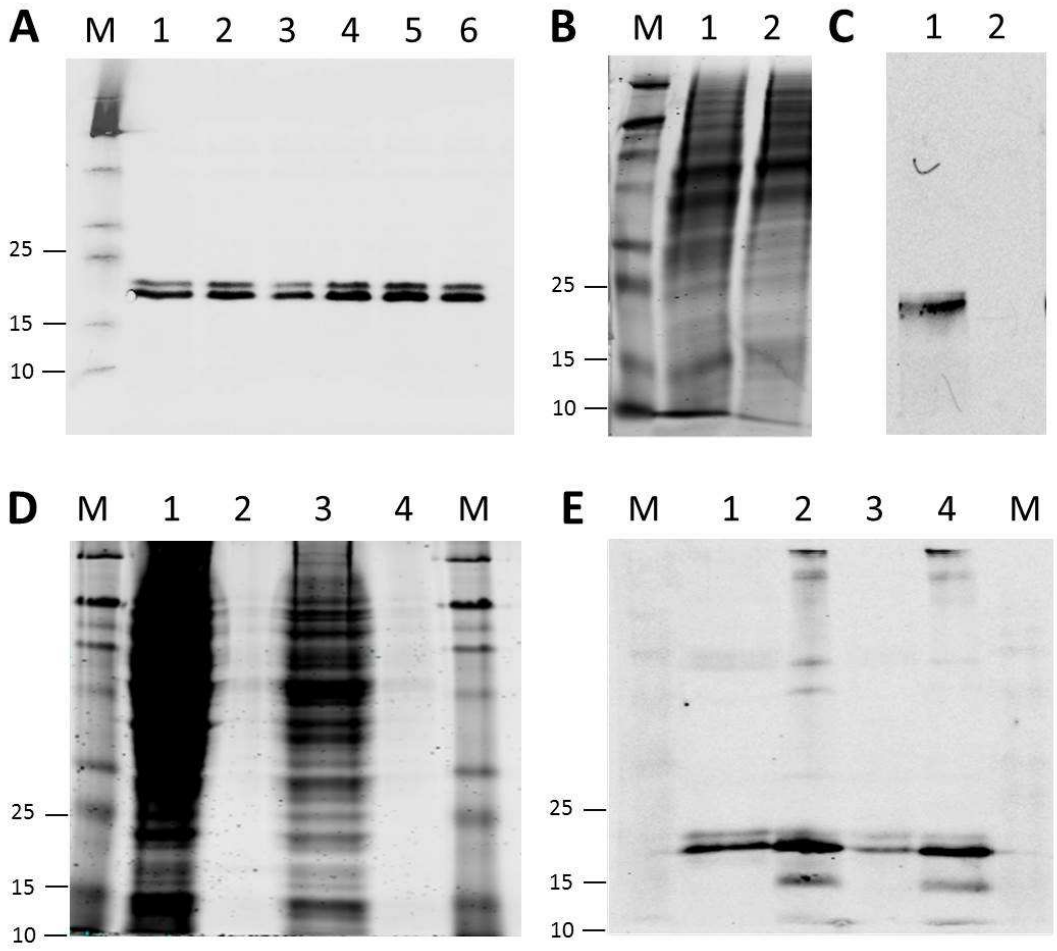

Figure 5.4 CaM-V5 expression and analysis in *N. crassa* (A) Western blot analysis of CaM-V5-HAT-expressing strains. Six CaM-V5 homokaryons were tested for the expression of CaM. All showed expression with two bands which are probably isoforms of CaM. (B) SDS PAGE of whole cell extracts from CaM-V5 (Lane 1) and wild-type (Lane 2) (C) Western blot of whole cell extracts from CaM-V5 (Lane 1) and wild-type (Lane 2) (D) Comparison of mature hyphae and 4 h old germlings in SDS PAGE. Lane 1: whole cell extracts of mature hyphae; Lane 2: purified elution of mature hyphae; Lane 3: whole cell extracts of germlings; Lane 4: purified elution of germlings. (E) Comparison of mature hyphae and 4 h old germlings in western blot. Lane 1: whole cell extracts of mature hyphae; Lane 2: purified elution of mature hyphae; Lane 3: whole cell extracts of germlings; Lane 4: purified elution of germlings. The positions of the molecular mass markers (M, in kDa) are shown at the left of the panel. SDS-PAGEs were visualised by coomassie blue stain. Mouse monoclonal anti-V5 antibody (Invitrogen; diluted to 1:10,000) and goat antimouse IgG- IRDye 800CW conjugate (LiCOR; diluted to 1:20,000) were used in these western blot.

A total of 10 g wet biomass of germlings were collected from the liquid culture incubated at 35°C, 180 rpm for 4 h and was frozen with liquid nitrogen to extract the crude protein (Fig. 5.5). The whole cell extract was used to purify the CaM-binding complex by the anti-V5 antibody conjugated Dynabeads with an altered elution buffer (0.1 M glycine-HCl, pH 2.5). Following elution, the purified protein complexes of both wild-type control and CaM-V5 sample were separated by SDS-PAGE and visualised by coomassie blue staining (Fig. 5.4 B). Each experiment was repeated three times and compared to the wild-type. Protein bands were excised then identified by tandem mass spectrometry by the SynthSys Institute at the University of Edinburgh.

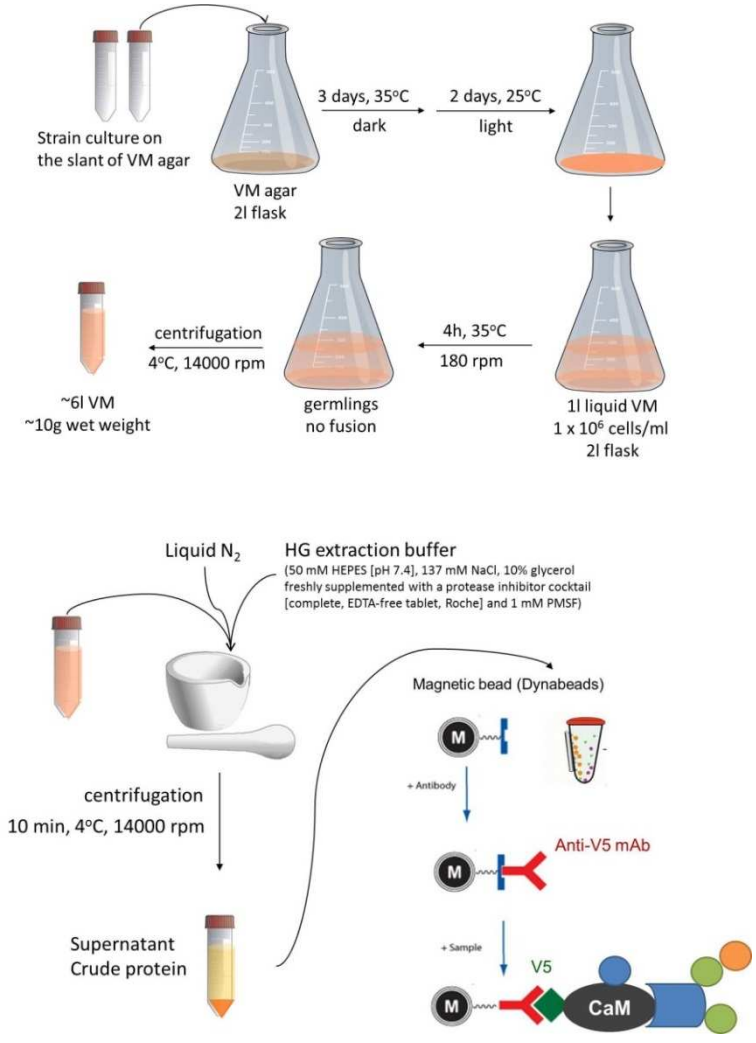

Figure 5.5 Protein purification process by Dynabeads

Large amount conidia were collected and inoculated into 1 l liquid VM to a final concentration of 1 x 10^6 cells/ml. Cultures were incubated in 35°C, 180 rpm for 4 h. 10 g wet conidia were collected from about 6 l of medium. Liquid nitrogen, extraction buffer and mechanical force were used to extract the crude protein. The Ca^{2+}/CaM-binding proteins were purified by anti-V5 antibody conjugated Dynabeads.

5.2.3. Identification and functional classification of CaM-interacting proteins obtained from mass spectrometry

A total of 318 putative CaM directly or indirectly interacting proteins were obtained from the mass spectrometry analysis of the CaM-V5 sample after repeating it three times. Peptides were eliminated when their signal intensities lower than wild-type to reduce the error from unspecific binding. The list of proteins was reduced to 286 proteins (Table A.3). Gene ontology (GO) and annotated information of the proteins were obtained using the databases listed below. Proteins were classified according to (1) the biological process they are involved in, (2) cell components they are part of, (3) whether they are a component of the Ca^{2+} signalling machinery, or (4) whether they are a component of another signalling pathway. The classification was made according to their GO term (Fig. 5.6) and online tools were used as listed:

Neurospora database – Broad Institute:
http://www.broad.mit.edu/annotation/genome/neurospora/
MNCDP Neurospora database:
http://mips.helmholtz-muenchen.de/genre/proj/ncrassa/
The Neurospora crassa e-Compendium:
http://www.bioinformatics.leeds.ac.uk/~gen6ar/newgenelist/genes/gene_list.htm
FungiDB:
http://fungidb.org/fungidb/
PANTHER:
http://www.pantherdb.org/
UniPro -- protein sequence and functional information.:
http://www.uniprot.org/
KEGG (Kyoto Encyclopedia of Genes and Genomes):
http://www.genome.jp/kegg/
RCSB Protein Data Bank:
http://www.rcsb.org/pdb/home/home.do
ProteomicsDB:
https://www.proteomicsdb.org/
Fungal Calcium Signalling Database
(FCSG):http://fcsd.ifungi.org/proteins.php?a=view

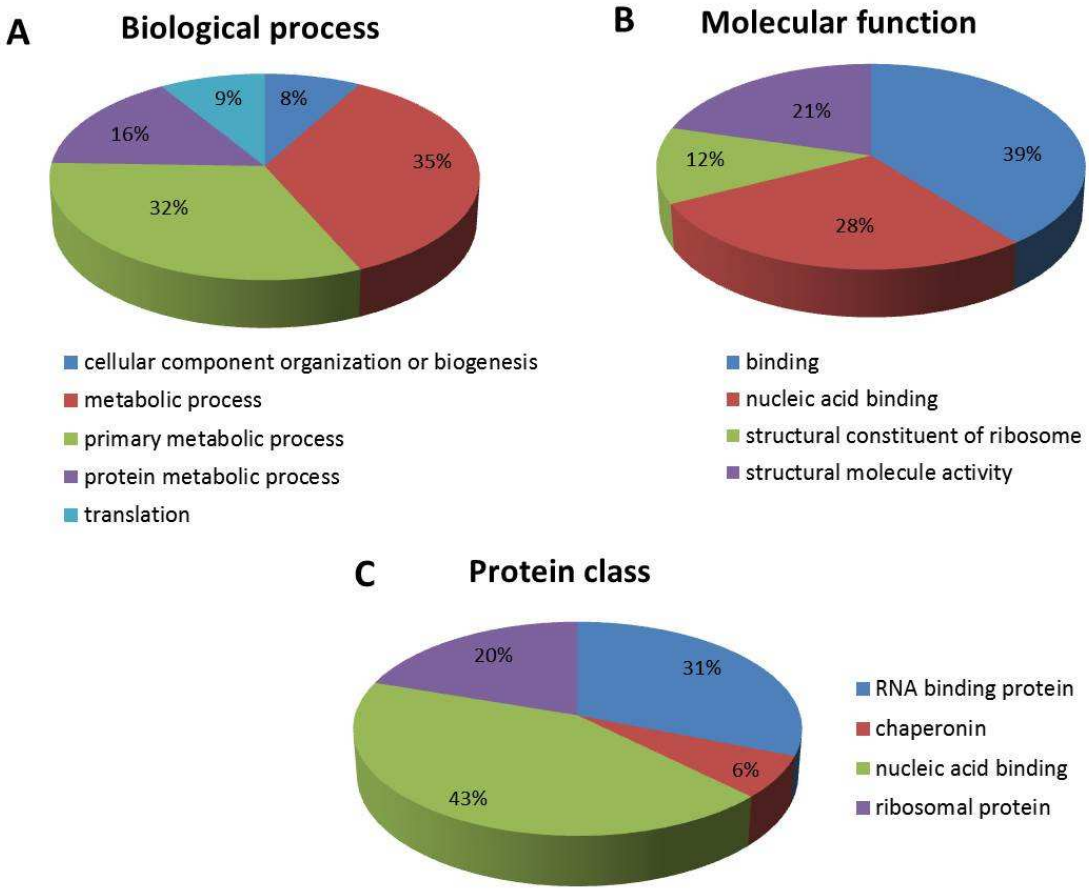

Figure 5.6 Pie chart depicting the functional classification of CaM-binding protein complexes

The CaM-binding proteome was characterized within the molecular function Gene Ontology (GO) category. Subcellular and functional categories were based on the annotations of GO using the online tool at www.pantherdb.org in the following categories: (a) biological process, (b) molecular function and (c) protein class.

In this chapter, I have only focused on those signalling pathways and biological processes that are likely to be associated with colony initiation, and cellular components associated with CaM localization described in Chapter 6 (Fig. 5.7).

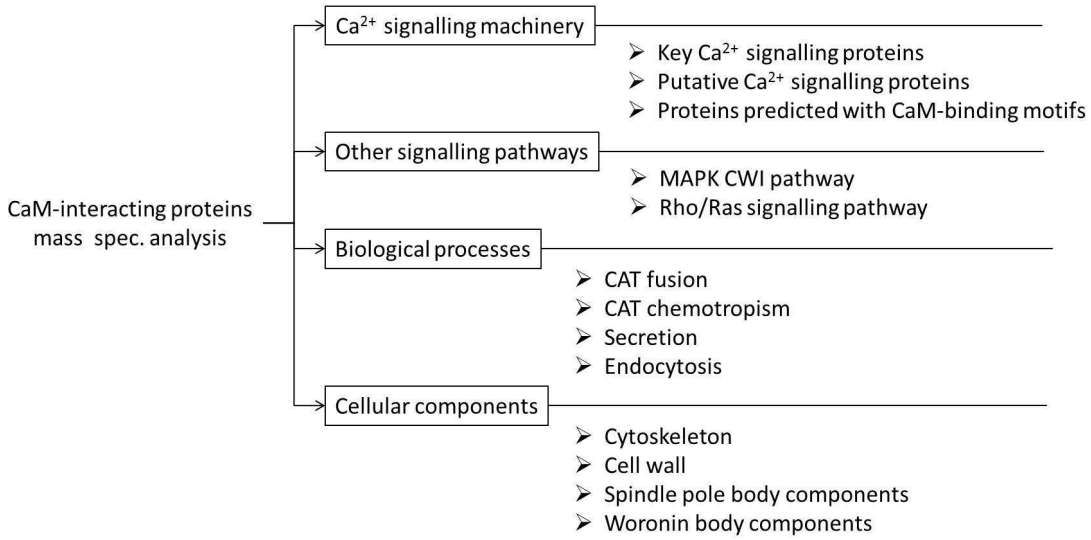

Figure 5.7 Protein classification of Ca^{2+}/CaM-binding complexes identified and analysed in this chapter. A total of 286 proteins were identified from the mass spectrometry analysis. To understand the CaM regulated mechanisms during colony initiation, sub-groups that may be associated with colony initiation were chosen under the following 4 main clusters Ca^{2+} signalling machinery, other signalling pathway, biological processes, and cellular components.

5.2.3.1 CaM-interacting proteins involved in the Ca^{2+} signalling machinery

5.2.3.2.1 Ca^{2+} signalling proteins

Among the Ca^{2+} signalling proteins which have been investigated in Chapter 4 (Table A.2), 9 key Ca^{2+} signalling proteins and 3 putative Ca^{2+} signalling regulators were shown to interact with CaM (Table 5.2), of which 3 proteins (CNA-1, CAMK-1, and CAMK-3) possessed a CaM-binding motif. Interestingly, only CaMK-4 did not show CaM-binding activity from the total of 4 CaMKs in *N. crassa*. Of 6 predicted Ca^{2+}-channel proteins, only CCH-1 and MID-1 interact with CaM. PMR-1 was the only Ca^{2+}-ATPase to bind CaM.

Table 5.2 Ca^{2+} signalling proteins interacting with CaM

Gene number	Gene name	Protein
Key Ca^{2+} signalling proteins		
NCU02762	*cch-1*	Ca^{2+} channel subunit Cch1
NCU06703	*mid-1*	Ca^{2+} channel subunit Mid1
NCU03292	*pmr-1*	Ca^{2+}-transporting ATPase type 2C member 1
NCU03804	*cna-1*	calcineurin catalytic subunit a
NCU03833	*cnb-1*	calcineurin regulatory subunit b

NCU07952	*crz-1*	calcineurin transcription factor
NCU09123	*camk-1*	Ca^{2+}/CaM-dependent kinase-1
NCU02283	*camk-2*	Ca^{2+}/CaM-dependent kinase-2
NCU06177	*camk-3*	Ca^{2+}/CaM -dependent kinase-3
Putative Ca^{2+} signalling proteins and regulators		
NCU02411	*nuf-1*	homolog of Spc110p in yeast
NCU06617	*cdc-4*	homolog of myosin Myo2p light chain; CDC4 in yeast
NCU00726	*cpr-1*	cyclosporin-resistant-1

5.2.3.2.2 Predicted CaM-interacting proteins with CaM-binding motifs

Proteins with specific CaM-binding motifs may play important roles in the Ca^{2+} signalling network. The calmodulin target database (http://calcium.uhnres.utoronto.ca/ctdb/ctdb/sequence.html) was used to search for CaM-binding motifs or putative CaM-binding sites within the 286 putative CaM-interacting proteins. About 90% proteins contained predictive CaM-binding sites with different scores (1-9). I only list a total 30 proteins with sequences included specific CaM-binding motifs in Table 5.3. This indicates that CaM may bind with these proteins directly to regulate other pathways.

Table 5.3 CaM-interacting proteins with CaM-binding motifs

Gene number	Gene name	Protein	CaM binding site (protein sequence loci)
NCU03804	*cna-1*	calcineurin catalytic subunit a	a 1-5-8-14 motif at 446, unclassified database CaM-binding motif at 324
NCU09123	*camk-1*	Ca^{2+}/CaM-dependent kinase-1	contains a 1-5-8-14 motif at 298
NCU06177	*camk-3*	Ca^{2+}/CaM -dependent kinase-3	unclassified CaM-binding motif at 711
NCU08332	*hex-1*	hexagonal-1	potential IQ motif at 711
NCU00352	-	phospholipid-transporting ATPase	potential IQ motif at 711
NCU04738	-	hypothetical protein	unclassified CaM-binding motif at 93
NCU03982	*grp78 / hsps-2*	glucose regulated protein 78	potential IQ motif at 114
NCU01440	*myo-5*	myosin-5	potential IQ motif at 788 potential IQ motif at 836 potential IQ motif at 907
NCU02003	-	translation elongation factor-1	unclassified CaM-binding motif at 453

NCU02075	*hsp70-2*	heat shock protein 70	unclassified CaM-binding motif at 232
NCU00212	*hH4-2*	histone h4	potential IQ motif at 23
NCU01659	-	dDENN domain-containing protein	potential IQ motif at 1189
NCU05837	-	vacuolar protein sorting-associated protein 13a	potential IQ motif at 147, potential IQ motif at 1000
NCU07721	-	26S proteasome regulatory subunit rpn1	unclassified CaM-binding motif at 731
NCU06733	*nkin-2*	kinesin	unclassified CaM-binding motif at 1585
NCU00018	-	cell division control protein Cdc48	unclassified CaM-binding motif at 709
NCU08957	-	hypothetical protein	unclassified CaM-binding motif at 292
NCU07700	*cot-3*	colonial temperature-sensitive-3 (845 aa)	potential IQ motif at 817
NCU04779	-	60S ribosomal protein L8	unclassified CaM-binding motif at 194
NCU07420	-	eIF4A	unclassified CaM-binding motif at 353
NCU08693	*hsp70-5*	heat shock protein 70-5	potential IQ motif at 121
NCU08409	*trp-3*	tryptophan synthetase	potential IQ motif at 237
NCU02514	*atp-1*	ATPase-1	unclassified CaM-binding motif at 248
NCU09602	*hsp70-1*	heat shock protein 70-1	unclassified CaM-binding motif at 255
NCU03972	*rpn-7*	proteasome regulatory particle	unclassified CaM-binding motif at 75
NCU04245	*tom70 / mom72*	translocase of outer mitochondrial membrane 70	potential IQ motif at 300
NCU02207	-	T-complex protein 1 subunit beta	unclassified CaM-binding motif at 426
NCU08480	*hssf-2*	HSF-type DNA-binding domain-containing protein	unclassified CaM-binding motif at 576
NCU09866	-	thyroid hormone receptor interactor 12	unclassified CaM-binding motif at 984
NCU06863	-	histone H1	unclassified CaM-binding motif at 58

5.2.3.2 CaM-interacting proteins in other signalling pathways

The MAPK CWI pathway and the Rho/Ras pathway have been previously shown to be involved in colony initiation (Read et al., 2012; Lichius et al., 2014) or in compatibly responses following cell fusion (Merlini et al., 2013). Of the 9 MAP kinases in the 3 MAK kinase pathways in *N. crassa*, only the MAK kinase kinase (MEK-2) in the CWI pathway was found to interact with CaM. The MAPK CWI pathway has been found to be involved in CAT chemotropism (Read et al., 2012).

Rho/Ras signalling regulates cell polarity, cell fusion, and septation in

filamentous fungi (Rasmussen et al., 2008; Rasmussen and Glass, 2005). Six proteins in the Rho/Ras signalling pathway that each interact with CaM are listed in Table 5.4.

Table 5.4 CaM-interacting proteins associated with other signalling pathways

Gene number	Gene name	Protein	Biological function
MAPK Cell wall integrity (CWI) signalling pathway			
NCU06419	*mek-1*	MAP kinase kinase-1	CAT induction CAT chemotropism (Fu et al., 2011; Lichius, 2010)
Rho/Ras signalling pathway			
NCU01484	*rho-1*	rho-type GTPase	Rho GTPase regulator; cytoskeletal regulation
NCU00895	-	RAB GTPase Ypt5	regulation of vesicle fusion
NCU11181	-	Ras superfamily GTPase (190 aa)	ER to Golgi vesicle-mediated transport
NCU04185	*prk-1*	protein kinase gsk3	Ras pathway
NCU03616	*smco-7*	semicolonial-7	Ras pathway
NCU07698	*sec5*	exocyst complex component Sec5	Ras pathway

5.2.3.3 CaM-interacting proteins involved in different biological processes

55 proteins have been identified as being involved in different stages of CAT fusion (Table 1.3). Eight of these proteins were identified as CaM-interacting proteins (Table 5.5). Of these 8 proteins, 2 (CNA-1 and CaMK-1) contain the CaM-binding motifs. Secretion and endocytosis play important roles during CAT induction, chemotropism and cell fusion. 9 CaM-interacting proteins were identified to be involved in secretion and 10 were in endocytosis according to their GO classification and the genomic analysis of *N. crassa* (Borkovich et al., 2004).

Table 5.5 CaM-interacting proteins associated with different biological processes

Gene number	Gene name	Protein	Biological function
CAT fusion process			
NCU02762	*cch-1*	Calcium channel subunit Cch1	CAT chemotropism (Chu, 2013)
NCU06703	*mid-1*	Calcium channel subunit Mid1	CAT chemotropism (Chu, 2013)
NCU03804	*cna-1*	Calcineurin catalytic subunit a	CAT chemotropism, this study
NCU03833	*cnb-1*	Calcineurin regulatory subunit b	CAT chemotropism, this study
NCU09123	*camk-1*	Ca^{2+}/CaM-dependent kinase-1	germination and CAT induction, this study
NCU06419	*mek-1*	MAP kinase kinase-1	CAT induction CAT chemotropism (Fu et al., 2011; Lichius, 2010)
NCU00421	*snf-5*	SWI-SNF complex subunit	CAT induction (Fu et al., 2011)
NCU03616	*smco-7*	Ras-2 protein	reduced CAT fusion (Lichius, 2010)
Secretion			
NCU02111	*myo-5*	Myosin-5 (MYO-5)	regulation of exocytosis
NCU09869	*sec-3*	exocyst complex component Sec3	cellular export and secretion
NCU04190	*sec-8*	exocyst complex component Sec8	cellular export and secretion
NCU07698	*sec-5*	exocyst complex component Sec5	cellular export and secretion
NCU00352	-	phospholipid-transporting ATPase	vesicle-mediated transport
NCU00018	-	cell division control protein Cdc48	vesicle fusion protein transport
NCU08477	*ypt-1*	small GTP-binding protein	ER to Golgi vesicle-mediated transport
NCU03509	*pmg* *naap* *nap-2*	amino acid permease NAAP1	ER to Golgi transport vesicle
NCU11181	-	Ras superfamily GTPase	ER to Golgi vesicle-mediated transport
Endocytosis			
NCU10073	-	actin binding protein	?
NCU02111	*myo-5*	Myosin-5 (MYO-5)	regulation of endocytosis
NCU09808	-	dynamin-1	GTPase activity
NCU04100	-	vacuolar sorting protein 1	vacuolar transport
NCU06177	*camk-3*	Ca^{2+}/CaM -dependent kinase-3	?
NCU00895	*ypt-5*	RAB GTPase Ypt5	regulation of vesicle fusion

NCU00352	-	phospholipid-transporting ATPase	vesicle-mediated transport
NCU07495	*lsp-1*	sphingolipid long chain base-responsive protein (LSP-1)	regulation of endocytosis
NCU01484	*rho-1*	rho-type GTPase (RHO-1)	regulation of endocytosis
NCU00566	-	synaptobrevin	vesicle-mediated transport

5.2.3.4 CaM-interacting proteins associated with different cellular components

This cluster was of particular interest in relation to CaM localization and dynamics during colony initiation (Chapter 6). CaM showed a dynamic association with the plasma membrane or cell wall, nucleus spindle pole bodies and septa. CaM-interacting proteins that were components of the cytoskeleton, cell wall, spindle pole body and septum-associated Woronin body were identified (Table 5.6).

The cytoskeleton provides a scaffold and a network of fibers composed of proteins in the cytoplasm. It also controls the intracellular transport as the movement of vesicles and organelles within the cell. Nine CaM-interacting cytoskeletal proteins were identified, of which 2 were actin-based myosin, 2 were microtubule-based motor proteins, 3 were tubulins, and 2 were actin-associated components. T-complex protein 1 is a molecular chaperone that folds various proteins, including actin and tubulin (Kubota, 1993; Sternlicht, 1995). Six different subunits of T-complex protein 1 showed CaM-interacting activity. Meanwhile, 8 cell wall synthesis proteins and regulators were identified.

The spindle pole body (SPB) is a microtubule organizing centre. Five SPB components and regulators were found to be CaM-interacting, of which NCU02411 is the homolog of Nuf1p/Spc110p that is thought to bind to CaM in *S. pombe* and *S. cerevisiae* (Flory et al., 2002; Okano and Ohya, 2003).The Woronin body is a peroxisome-derived dense-core intracellular vesicle that is found exclusively in filamentous fungi. It seals the septal pore in response to wounding, which restricts the loss of cytoplasm to the sites of injury (Liu et al., 2008). The hexagonal peroxisome (Hex1) protein has been identified as a major constituent of the Woronin body and shown to be responsible for self-assembly of the dense core of this organelle (Jedd and Chua, 2000). HEX-1 in *N. crassa* contains CaM-binding motif

(Table 5.3) and also showed a CaM-binding activity.

Table 5.6 CaM-interacting proteins associated with different cellular components

Gene number	Gene name	Protein	Biological function
Cytoskeleton			
NCU02111	*myo-1*	myosin-1 (homolog of Myo5p in yeast)	actin motor protein
NCU01440	*myo-5*	myosin-5 (homolog of Myo2p in yeast)	actin motor protein
NCU09468	*tba-2*	tubulin alpha-2	
NCU04054	*bml / tub-2*	tubulin beta chain	microtubule component
NCU06733	*nkin-2*	kinesin	microtubule motor protein
NCU06617	-	myosin regulatory light chain cdc4	actin motor protein
NCU04173	*act*	actin	actin component
NCU02555	*arp-4*	actin-related protein-4, actin	actin associated component
NCU09132	*tba-1*	alpha tubulin	microtubule component
NCU04448	-	T-complex protein 1 subunit alpha	actin and tubulin folding protein
NCU09700	-	T-complex protein 1 subunit beta	actin and tubulin folding protein
NCU02839	-	T-complex protein 1	actin and tubulin folding protein
NCU02207	-	T-complex protein 1 subunit beta	actin and tubulin folding protein
NCU07567	-	T-complex protein 1 subunit theta	actin and tubulin folding protein
NCU01843	-	T-complex protein 1 subunit gamma	actin and tubulin folding protein
Cell wall			
NCU03804	*cna-1*	calcineurin catalytic subunit A	cell wall synthesis
NCU03833	*cnb-1*	calcineurin regulatory subunit B	cell wall synthesis
NCU06871	*gls-1*	β-1,3-glucan synthase	β-1,3-glucan synthesis
NCU08132	*ags-2*	γ-1,3-glucan synthase Ags2	γ-1,3-glucan synthesis
NCU02478	*ags-2*	γ-1,3-glucan synthase Ags2	γ-1,3-glucan synthesis
NCU03611	*chs-1*	chitin synthase	chitin synthesis
NCU04251	*chs-3*	chitin synthase 3	chitin synthesis
NCU04352	*chs-5*	chitin synthase C	chitin synthesis
NCU01484	*rho-1*	rho-type GTPase	β-1,3-glucan synthesis
NCU02948	*ncw-4 / mig-1*	non-anchored cell wall protein-4	cell wall protein
NCU07366	*gfa1*	glucosamine-fructose-6-phosphate aminotransferase	chitin synthesis
NCU03616	*smco-7*	semicolonial-7	cell wall synthesis

NCU06003	-	mannose-1-phosphate guanyltransferase	mannoprotein synthesis
Spindle pole body components			
NCU09468	*tba-2*	tubulin alpha-2	spindle pole body component
NCU02411	-	hypothetical protein ; homolog of spindle pole body component NUF1p/Spc110p	spindle pole body component
NCU03616	*smco-7*	semicolonial-7	spindle organization
NCU07380		eukaryotic translation initiation factor 3	spindle assembly
NCU09132	*tba-1*	alpha tubulin	spindle pole body component
Woronin body components			
NCU08332	*hex-1*	hexagonal-1	Woronin body component

5.3. Discussion

Protein purification using magnetic beads offers several advantages over conventional column chromatography such as ease of use, rapidity and lower non-specific binding of proteins (Sousa et al., 2011; Trinkle-Mulcahy et al., 2008). Figure 5.1 summarizes the steps taken in this analysis. Using magnetic beads I identified 286 proteins that interact either directly or indirectly as part of a protein complex with CaM. However, this is still a significant underestimate of the number CaM-interacting proteins. This is particularly because many CaM-interacting proteins are large multimeric or transmembrane proteins which are difficult to extract for mass spectrometry analysis (Vetter and Leclerc, 2003). Thus, not many transmembrane proteins were identified as CaM-binding complexes, and of there only three were Ca^{2+}-transporters: CCH-1, MID-1, and PMR-1 (Table 5.2).

In Table 5.2-5.6, CaM-interacting proteins were classified according to their possible involvement in Ca^{2+} signalling, other signalling pathways, a range of different cellular processes, and components of different cell structures. My results further confirm the importance of Ca^{2+}/CaM signalling in the function of *N. crassa* cells.

5.3.1. Comparison of the interaction of novel CaM-interacting proteins identified in this chapter with known CaM-binding targets in *S. cerevisiae* and *N. crassa*

To compare my results on CaM-interacting proteins in *N. crassa* with those in *S. cerevisiae*, the online tool STRING 9.1 was used. The STRING database (http://string-db.org/) provides known and predicted associations of proteins in multiple organisms that are scored and integrated in a network of protein interaction (Franceschini et al., 2013). Figure 5.8 shows the known interaction between CaM and CaM-binding proteins in *S. cerevisiae* and *N. crassa*.

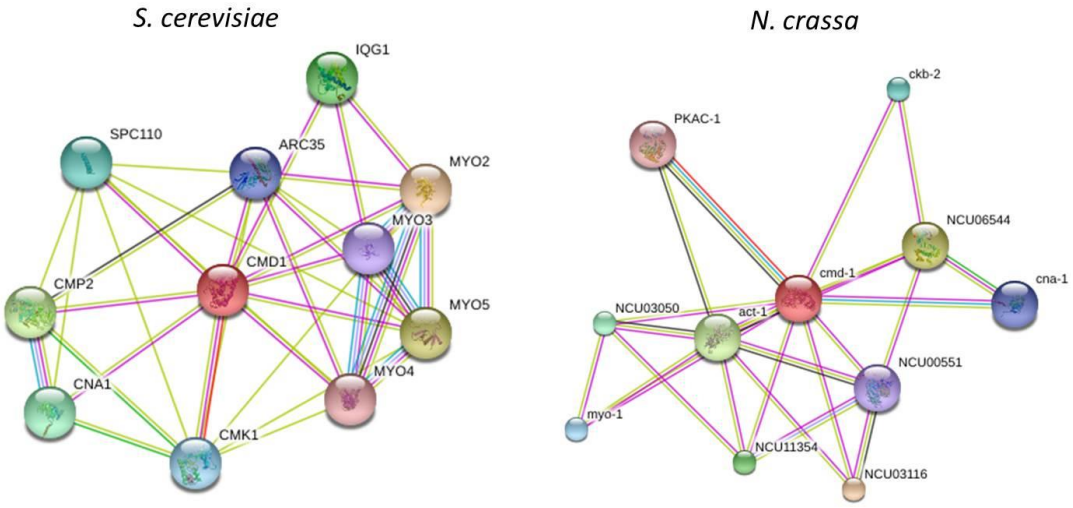

Figure 5.8 The comparison of CaM-binding proteins in *S. cerevisiae* and *N. crassa*. The online tool STRING 9.1 was used to analyse the network of protein-protein interactions with CaM. Ten proteins have been identified as CaM-binding proteins in both yeast and *N. crassa*.

S. cerevisiae is the sole known organism in which only the Ca^{2+}-independent functions of CaM are essential for cell viability (Geiser et al., 1991). The most C-terminal EF-hand in yeast CaM has a deletion of one residue in the Ca^{2+}-binding loop. It also contains a substitution of glutamine for a highly conserved glutamic acid at position 12 (Cyert, 2001). In *N. crassa*, 10 CaM-binding proteins were shown in the STRING database, of which 4 proteins, CNA-1, MYO-5, MYO-1, and ACT-1 (shown in bold in Table 5.8) I had identified as CaM-interacting proteins in *N. crassa* from my

proteomic analysis in section 5.2. With these known databases, novel CaM-interacting proteins can be defined and compared with other fungi in the future.

Table 5.7 CaM-binding proteins in *S. cerevisiae* and *N. crassa* from the STRING database

Gene number	Protein	
S. cerevisiae		
YNR035C	ARC35	ARP2/3 complex 34 kDa subunit
YPL242C	IQG1	Ras GTPase-activating-like protein
YOR326W	**MYO2**	**Myosin-2**
YKL129C	MYO3	Myosin-3
YMR109W	**MYO5**	**Myosin-5**
YAL029C	MYO4	Myosin-4
YFR014C	**CMK1**	**Calcium/calmodulin-dependent protein kinase I**
YLR433C	**CNA1**	**Serine/threonine-protein phosphatase 2B catalytic subunit A1**
YML057W	CMP2	Serine/threonine-protein phosphatase 2B catalytic subunit A2
YDR356W	**SPC110**	**Protein NUF1 (Spindle pole body spacer protein SPC110)**
N. crassa		
NCU02754	CKB-2	casein kinase II subunit beta-2
NCU06544	PKC	protein kinase C
NCU03804	**CNA-1**	**serine/threonine-protein phosphatase 2B catalytic subunit**
NCU00551	MYO-2	myosin type-2 heavy chain 2
NCU03116	RAS	Ras GTPase activating protein
NCU11354 (NCU01440)	**MYO-5**	**Homolog of Myo2p in yeast**
NCU02111	**MYO-1**	**Homolog of Myo5p in yeast)**
NCU03050	ARP2/3	ARP2/3 complex 34 kDa subunit
NCU04173	**ACT-1**	**actin**
NCU06240	PKAC-1	cAMP-dependent protein kinase type 3

5.3.2. CaM mediated Ca^{2+} signalling may regulate CAT chemotropism via the MEK-1 mediated MAP kinase CWI pathway

Numerous studies support an interaction between Ca^{2+}/CaM activated calcineurin signalling and the CWI pathway in yeast and yeast-like fungi.

Ca^{2+}/calcineurin signalling has been known to be involved in a number of cellular processes including cell wall remodelling, cell survival under stress conditions, such as high cation concentrations and antifungal treatment (Blankenship and Heitman, 2005; Cruz et al., 2002), and morphogenetic processes, such as yeast cell budding, mating and cytoskeletal reorganization (Cyert and Thorner, 1992; Popov et al., 2000). Three components of the CWI pathway, MIK1, MEK1 and MAK1, are present in *N. crassa* (Maerz et al., 2008; Park et al., 2008), and their deletion mutants exhibit defective phenotypes in vegetative hyphal fusion (Maerz et al., 2008), sexual development (Lichius et al., 2012a; Park et al., 2008), CAT formation and CAT chemotropism (Goryachev et al., 2012). CWI pathways in *Cochliobolus heterostrophus*, C*oniothyrium minitans*, *Fusarium graminearum*, and *Magnaporthe oryzae* have further been shown to be involved in female fertility, heterokaryon formation, mycoparasitism and pathogenicity (Eliahu et al., 2007; Hou et al., 2002; Zeng et al., 2012).

Protein kinase C (PKC1) functions upstream of the cell wall integrity MAP kinase pathway in yeast and filamentous fungi (Levin, 2011; Rispail et al., 2009). Mutations in the genes for yeast Pkc1 and a MAP kinase, Mpk1/Slt2 (homolog of MAK-1 in *N. crassa*), disrupts the Ca^{2+} signalling required to maintain a normal cell wall and cell integrity (Garrett-Engele et al., 1995). The single putative Δ*pkc-1* mutant in *N. crassa* is lethal as a homokaryon (Colot et al., 2006) and is reported to be involved in blue-light signalling (Arpaia et al., 1999).

In budding yeast, Rho1p co-ordinates the transcription of cell wall-specific enzymes through Pkc1p and directly functions in the MAP kinase CWI pathway by acting as the regulatory subunit of the β-1,3-glucan synthases, Fks1p and Fks2p (Levin, 2011; Park and Bi, 2007). In addition, *A. fumigatus* Rho1 was described as part of the β-1,3-glucan synthase complex (Beauvais et al., 2001) and *N. crassa* RHO-1 has been shown to interact with PKC1 using yeast two-hybrid analysis (Richthammer et al., 2012). Rho1, as a key regulator of hyphal growth and cell polarization, is essential for cell growth in various filamentous fungi, including the ascomycetes *A. niger* (Kwon et al., 2011), *C. albicans* (Smith et al., 2002) and *N. crassa* (Vogt and Seiler, 2008) and the basidiomycetes *C. neoformans* (Chang and Penoyer, 2000) and *U.*

maydis (Pham et al., 2009).

In the filamentous fungus, *S. macrospora* which is very closely related to *N. rassa*, the developmental protein PRO40 acts as a scaffold protein for MIK1, MEK1 and PKC1 links the MAPK module to its upstream activators. It has been shown that the PRO40 N-terminal disordered region and the central region encompassing a WW domain are sufficient to interact with MEK1 (Teichert et al., 2014). PRO40 in *S. macrospora* and its homolog, SO, in *N. crassa* are essential for sexual development and cell fusion (Engh et al., 2007b; Fleissner and Glass, 2007). SO has also been known to be involved in CAT fusion and exhibits anti-phase oscillatory recruitment with MAK-2 to CAT tips during CAT chemotropism (Fleissner and Glass, 2007; Fleissner et al., 2009b). I compared my CaM-interacting proteomic analysis in *N. crassa* with the PRO40 and MEK1-interacting proteomic analysis in *S. macrospora* (Teichert et al., 2014). In the 29 proteins which have been identified as MEK1 and PRO40-binding proteins, 8 of them were shown with CaM-interacting activity (Table 5.8). This indicates that the 8 proteins may be candidates that crosslink the Ca^{2+} signalling and the MAPK CWI pathway with CAT chemotropism. Especially, RHO-1 may play a key role to connect these pathways with Rho/Ras signalling.

Table 5.8 CaM-interacting proteins in *N. crassa* which interact with MEK1 and PRO40 in *S. macrospora*

Gene number	Gene name	Protein	Biological process
NCU01484	*rho-1*	rho-type GTPase	Rho GTPase regulator; cytoskeletal regulation
NCU06419	*mek-1*	MAP kinase kinase-1	CAT induction CAT chemotropism (Fu et al., 2011; Lichius, 2010)
NCU09602	*hsp70-1*	heat shock protein 70-1	establishment or maintenance of cell polarity
NCU02075	*hsp70-2*	heat shock protein 70-2	regulation of translation
NCU08693	*hsp70-5*	heat shock protein 70-5	protein folding
NCU01827	-	60S ribosomal protein L27	regulation of translation
NCU06783	-	ATP citrate lyase	?
NCU02435	-	histone H2B	?

The potential mechanism of CAT chemotropism and cell wall remodeling during CAT fusion being regulated via interacting Ca^{2+} signalling, MAPK CWI signalling and Rho/Ras signalling is summed up in Fig. 5.9. In this model, calcineurin, MIK-1, MEK-1, MAK-1, SO and MAK-2 have been shown to be involved in CAT chemotropism (labelled in red). MEK-1, MIK-1, PKC and Rho-1 are PRO40-binding proteins in *S. macrospora* (linked in dotted line; Teichert et al., 2014). HEX-1 has been known to be associated and co-localized with PRO40 (Engh et al., 2007). CaM, RHO-1, PKC, GLS-1 and HEX-1 are lethal in homokaryons (labelled in black). Of these proteins, calcineurin, MEK-1, RHO-1, GLS-1 and HEX-1 were found in my study to be CaM-interacting (bold).

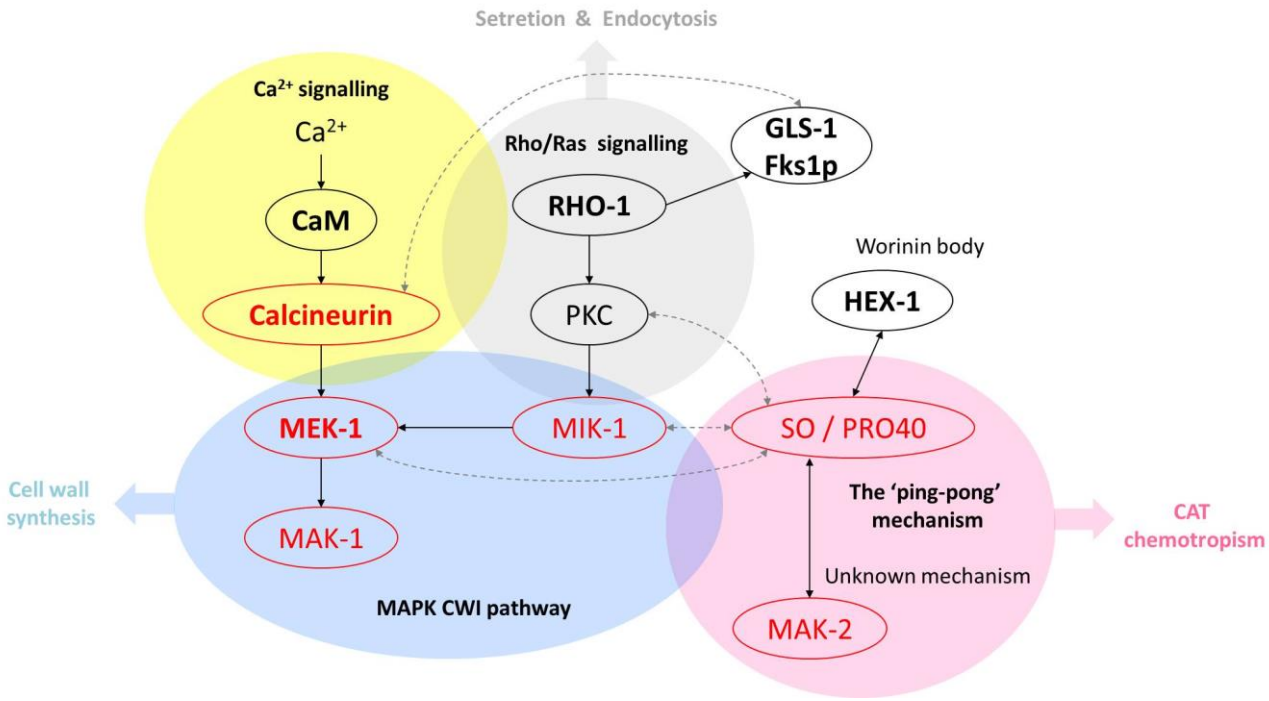

Figure 5.9 Potential interaction of Ca^{2+}/CaM signalling with MAPK CWI and Rho/Ras signalling pathways during colony initiation in *N. crassa*

Proteins involved in CAT chemotropism are labelled in red. CaM-interacting proteins analyzed in this study are labelled in bold. Abbreviations : CaM, calmodulin; MIK-1, MAP kinase kinase kinase; MEK-1, MAP kinase kinase; MAK-1/MAK-2, MAP kinase; PKC, protein kinase C; RHO-1, rho-type GTPase; GSL-1, β-1,3-glucan synthase; HEX-1, woronin body component hexagonal-1

5.3.3. CaM mediated Ca^{2+} signalling may regulate CAT fusion processes via secretion and endocytosis pathways

Fungi produce diffusible peptide mating pheromones as a prelude to mating and non-self fusion. Gradients in peptide mating pheromones are necessary for directional growth in yeast mating. These gradients are generated by secretion from signal-sending cells and degradation by receiving cells. In addition, endocytosis by regarding a high concentration of pheromone as well as released degradative proteases, and endocytosis by removing pheromone from the environment, will work in constant to amplify pheromone gradients in the external environment (Arkowitz, 2009). Although the chemotropic mechanism of self-fusion in *N. crassa* is still unknown, it has been hypothesized to involve a peptide chemoattractant and for secretory and endocytic recycling to play significant roles (Read et al., 2012).

Cell fusion events in diverse biological systems are preceded by specialized secretory processes. In *S. cerevisiae*, secretory vesicles are often found adjacent to the contact site in yeast mating pairs (Baba et al., 1989; Gammie et al., 1998) and the secretion is essential for late events in cell-fusion (Grote, 2010). A genome-scale model for the yeast secretory machinery has also been made to mimic this machinery and assign each secretory protein to a particular secretory class (Feizi et al., 2013). In *N. crassa*, there is a burst of endocytic and secretory traffic immediately before fusion between hyphal cells (Hickey et al., 2002a). There are 592 proteins of *N. crassa* that have been described in the Fungal Secretome Knowledge Base (FunSecKB; http://proteomics.ysu.edu/secretomes/fungi.php), which provides a resource of secreted fungal proteins (Lum and Min, 2011). In neurons and neuroendocrine cells, the release of neurotransmitters and hormones occurs by Ca^{2+}-regulated exocytosis (Bader et al., 2004) which is regulated by the binding of CaM and lipid to synaptobrevin (Quetglas et al., 2002). Exocytosis in neurons is directly triggered by a rapid increase in $[Ca^{2+}]_c$ which interactes with a number of different molecular targets located at or near to the site of fusion (Barclay et al., 2005).

Endocytosis is the process that eukaryotic cells used to internalize plasma membrane lipids, proteins, and extracellular molecules in vesicles that fuse with the endosomal system. This complicated process functions to recycle membrane proteins

and lipids, remove membrane proteins and lipids for degradation, and take up signal molecules from the external environment (Mellman, 1996). Although its occurrence of endocytosis in filamentous fungal hyphae was questioned (Read and Kalkman, 2003), there have been many studies which have provided convincing evidence for the existence and importance of endocytosis in yeast (Geli and Riezman, 1998; Geli et al., 1998) and filamentous fungi (Atkinson et al., 2002; Fischer-Parton et al., 2000; Hickey et al., 2002a; Hoffmann and Mendgen, 1998; Read and Kalkman, 2003). I identified 10 CaM-interacting proteins involved in endocytosis. The precise roles of possibly different secretion pathways and endocytic recycling in chemoattractant secretion, CAT chemotropic tip growth and adhesive secretion during CAT fusion will need to be investigated in the future.

5.3.4. CaM mediated Ca^{2+} signalling regulates CAT fusion processes via cell wall synthesis

My results provide evidence that CaM regulates glucan and chitin synthesis either by directly intereacting with the enzyme or indirectly via calcineurin. Further CaM-mediated regulation may occur by calcineurin activation of the transcription factor, CRZ-1.

The major fungal cell-wall polymer β-1,3-glucan is synthesized by the enzyme β-1,3-glucan synthase which is a complex composed of Rho1p and Fks1p (Mazur and Baginsky, 1996). Rho1p is a regulatory subunit which is required for the activity of β-1,3-glucan synthase (Inoue et al., 1999) and Fks1p acts as the catalytic subunit and appears to be the substrate-binding component of the enzyme (Cybulski and Hall, 2009). β-1,3-glucan synthase is known to be a downstream target regulated by the transcription factor, Crz1p. Crz1p is dephosphorylated by calcineurin and consequently binds to a promoter element called the calcineurin-dependent response element (Stathopoulos and Cyert, 1997). My result showed that treatment of caspofungin, a noncompetitive inhibitor of fungal β-1,3 glucan synthase, resulted in a similar inhibition of CAT chemotropism as defined as calcineurin inhibitors during colony initiation in *N. crassa* (Fig. 3.14). These results are consistent with calcineurin mediated β-1,3-glucan synthesis and being involved in CAT chemotropism.

Chitin is another important component of fungal cell walls. It has been known that chitin synthase is regulated by Ca^{2+} signalling. CaM-mediated phosphorylation of specific microsomal proteins has been shown to be important in the *in vivo* activation of chitin synthase in *N.crassa* (Suresh and Subramanyam, 1997). The calcineurin pathway is also required for upregulation of chitin synthase gene expression in response to cell wall damage in *C. albicans* (Munro et al., 2007). To sum up above, in *N. crassa*, CaM transmits the external Ca^{2+} signals to calcineurin and CRZ to induce the expression of β-1,3-glucan synthase or chitin synthase for the cell wall biogenesis.

5.4. Summary

- CaM protein of 10 different fungi were compared by sequence alignment. The specific amino acids at the 10^{th} and 97^{th} positions distinguish filamentous fungi from diploid fungi or yeast.
- A total of 286 proteins were identified as interacting either directly or indirectly with CaM. They were purified using anti-V5 antibody conjugated Dynabeads and analyzed by mass spectrometry.
- The CaM-interacting proteins were classified into 4 main clusters as being Ca^{2+} signalling proteins, proteins in other signalling pathways or cell components involved in different biological process.
- Evidence for Ca^{2+}-signalling interact with numerous other signalling pathways via CaM during colony initiation, including the MAP kinase CWI and Rho/Ras signalling pathways, were obtained. CaM-interacting proteins were also shown to be involved in numerous processes including secretion, cytoskeletal function, and cell wall synthesis and hyphal tip growthat different stages of the CAT fusion process.

Chapter 6

Live-cell imaging of proteins involved in Ca^{2+} signalling machinery

Chapter 6 – Live-cell imaging of proteins involved in Ca^{2+} signalling machinery

6.1. Introduction

Based on results described in chapter 3-5, gene deletion mutants of 5 Ca^{2+} signalling proteins showed defective phenotypes in germination or CAT furion (Fig. 4.6). There were: two calcineurin subunits (CNA-1 and CNB-1), Ca^{2+}/CaM dependent kinase I (CaMK-1), phospholipase C-2 (PLC-2) and homolog of regulator of G-protein signalling-1 (RGS-1). In this chapter, these 5 proteins and the main Ca^{2+} recepter, calmodulin (CaM), were chosen to be labelled with GFP to achieve the live-cell imaging for investigating protein-protein interaction and the dynamics of these proteins during CAT fusion.

CaM is a multifunctional intermediate messenger protein that transduces calcium signals by binding calcium ions and then modifying its interactions with various target proteins. Calcineurin is a CaM-dependent serine/threonine phosphatases consisting of a catalytic A subunit (CNA) and a regulatory B subunit (CNB). CAMKs are an enzyme group which can be activated by increases in the concentration of intracellular Ca^{2+} and transfers phosphates from ATP to defined serine or threonine residues in other proteins. PLC is a class of enzymes that cleave phospholipids before the phosphate group. Usually, it catalyses the hydrolysis of phosphatidylinositol 4,5-bisphosphate (PIP2) to produce a intracellular messengers inositol 1,4,5-trisphosphate (InsP3) for releasing intracellular Ca^{2+} from ER. RGS-1 is a homolog of the human regulator of G protein signalling 4 (RGS4), which regulates the G protein-mediated PLC pathway that releases Ca^{2+} from intracellular stores.

The aims of the research described in this chapter were:

- To label proteins involved in Ca^{2+} signalling with fluorescent proteins and localize their subcellular distribution in conidial germlings
- To analyse CaM dynamics in germlings and mature hyphal tips and determine the influence of extracellular Ca^{2+} on this localization
- To image CaM-GFP in the absence of target genes which are involved in CAT

fusion

- To co-localize CaM-GFP with F-actin during colony initiation

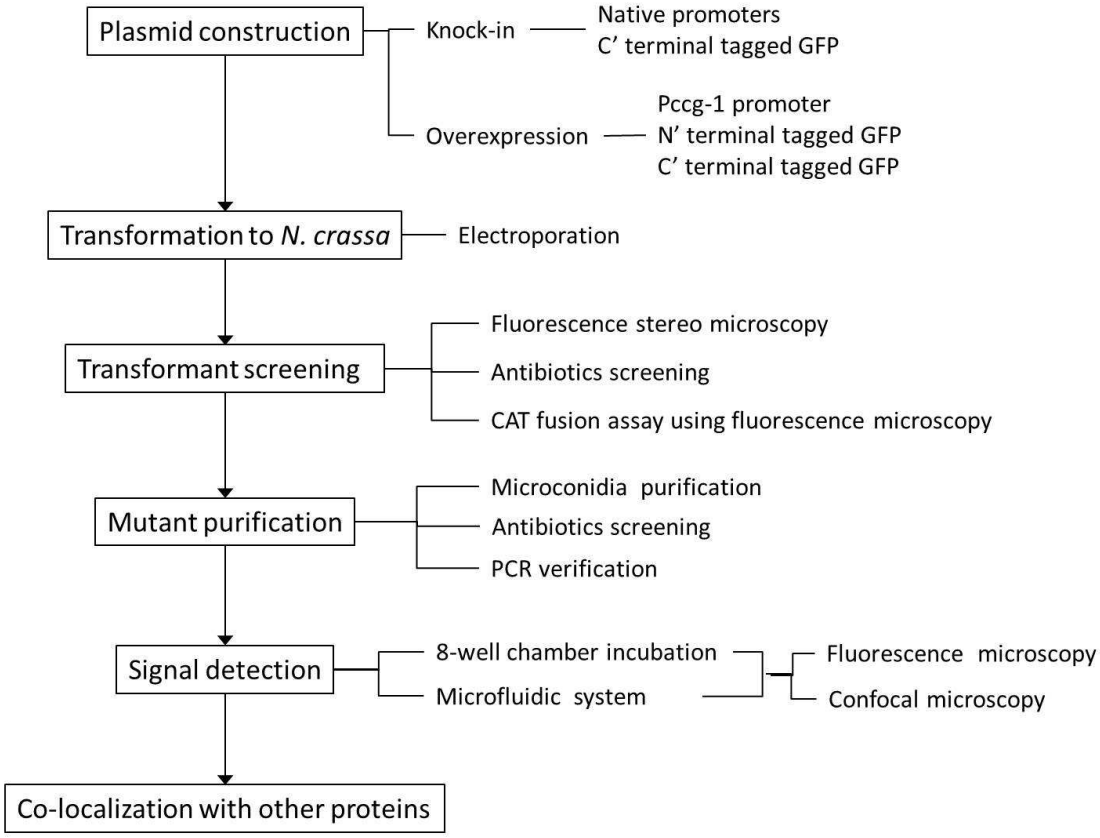

Figure 6.1 Flowchart of the live-cell imaging analysis in this chapter

To investigate the dynamics of 6 proteins which are involved in CAT fusion process, C'-terminal GFP-tagged fusion proteins were expressed by native promoters using knock-in strategy. For a better fluorescence eapression of CaM-GFP mutants, N'-terminal and C'-terminal were also tested with a stronger promoter, Pccg-1. Mutants were screened by antibiotics, fluorescence microscopy and PCR verification. Live-cell imaging was performed in two different incubation methods as 8-well chamber and microfluidic system.

6.2. Results

6.2.1. Plasmid construction

PCR cassettes were ligated by YRC (section 2.7.9) and transformed into *N. crassa* (section 2.8.1). These genes and proteins are shown in Table 6.1. A knock-in strategy was used to express the C' terminal GFP-fused proteins under the control of

their native promoters. For increasing fluorescence, both knock-in (native promoter) and overexpression (Pccg-1 promoter), C' terminal and N'terminal GFP-tagged fusion proteins were also tested in CaM GFP-labelled strains.

Table 6.1 Target proteins labelled with sGFP for the live-cell imaging

No.	Gene	Related protein	NCU number	Gene direction	Linkage	Gene size (gDNA)	Protein size (original)
1	***cmd-1***	Calmodulin (CaM)	NCU04120	+	5	1019 b.p.	150 a.a.
2	***cna-1***	Calcineurin subunit A (CnA-1)	NCU03804	+	5	2085 b.p.	559 a.a.
3	***cnb-1***	Calcineurin subunit B (CnB-1)	NCU03833	-	5	1181 b.p.	175 a.a.
4	***camk-1***	Ca^{2+}/CaM -dependent kinase-1 (CaMK-1)	NCU09123	+	1	1704 b.p.	414 a.a.
5	***plc-2***	Phospholipase C-2 (PLC-2)	NCU01266	+	5	3456	1152 a.a.
6	***rgs-1***	Homolog of developmental regulator flbA	NCU08319	+	4	2403	751 a.a.

6.2.2. GFP-labelled strain screening

Eight transformants were subcultured for each plasmid used to transform *N. crassa*. One heterokaryon was isolated for each gene construct that possessed a similar growth and morphological phenotypes as the wild-type, and expressed good fluorescence in germlings as detected by fluorescence microscopy. It was purified by microconidium isolation (section 2.8.1.4) to produce homokaryons. Homokaryons were subcultured twice on agar plates with antibiotics or specific selection medium. Fluorescence of 4 h germlings was detected by fluorescence microscopy according to the CAT fusion assay (section 2.5.2). The strain used for imaging was verified by the PCR-based genotyping. Table 6.2 shows a summary of the results.

No fluorescence was detected in PLC-2-GFP, and RGS-1-GFP strains. Small amont of protein expression or conformational problems may be the reasons. Using a stronger promoter or changing another GFP-tagged region may enhance their expression. In the following sections, I only discuss the live-cell imaging of CaM-GFP, CNA-1-GFP, CNB-1-GFP and CaMK-1-GFP.

Table 6.2 Plasmids and transformants created in this chapter

Plasmids	Genotype	Transformant	Result
pCC002	*cmd-1-5f-sgfp-hph-cmd-1-3f*	NCCC002	Dynamic dots and tip-focused gradient in polarized cells at different stages
pCC003	*cmd-1-5f-sgfp-nat-cmd-1-3f*	NCCC003	Dynamic dots and tip-focused gradient in polarized cells at different stages
pCC004	*his-3-Pccg-1- cmd-1-sgfp*	NCCC004	fluorescence accumulated in vacuoles
pCC005	*his-3-Pccg-1-sgfp-cmd-1*	NCCC005	fluorescence accumulated in vacuoles
pCC006	*cna-1-5f-sgfp-hph-cna-1-3f*	NCCC006	Fluorescence localized as punctate spots and at site of septa
pCC007	*cnb-1-5f-sgfp-hph-cnb-1-3f*	NCCC007	Fluorescence localized as punctate spots and at site of septa
pCC008	*camk-1-5f-sgfp-hph-camk-1-3f*	NCCC008	Fluorescence dispersed in the cytoplasm
pCC009	*plc-2-5f-sgfp-hph-plc-2-3f*	-	No fluorescence was detected
pCC010	*rgs-1-5f-sgfp-hph-rgs-1-3f*	-	No fluorescence was detected
-	*cmd-1-5f-sgfp-nat-cmd-1-3f ccg-1-fh4-2-dsred-ble*	NCCC0010	The cytoplasmic movement of CaM-GFP was associated with nuclei and spindle pole bodies.
-	*cmd-1-5f-sgfp-nat-cmd-1-3f, Δ myo-5::hph*	NCCC0011	Reduced CAT fusion. No pronounced accumulation of CaM-GFP at growing tips. The cytoplasmic movement of CaM-GFP was similar to NCCC002
-	*cmd-1-5f-sgfp-nat-cmd-1-3f; Δ so::hph*	NCCC0012	No CAT fusion. CaM-GFP localization was similar to NCCC002
-	*cmd-1-5f-sgfp-nat-cmd-1-3f; Δ rgs-1::hph*	NCCC0013	Reduced CAT fusion. CaM-GFP localization was similar to NCCC002

6.2.3. GFP-tagged CaM

6.2.3.1. CaM localizes dynamically in different structures at different stages

CaM-GFP localized to discrete spots in the cytoplasm, and in association with the plasma membrane, of the different cell types analyzed. The plasma membrane associated spots tended to accumulate towards the apical plasma membrane in growing germ tubes. CaM-GFP also accumulated at sites of septum formation, at both CAT tips homing towards each other, at the fusion pore between two fused CATs, and in the Spitzenkörper of growing vegetative hyphae (Fig. 6.2).

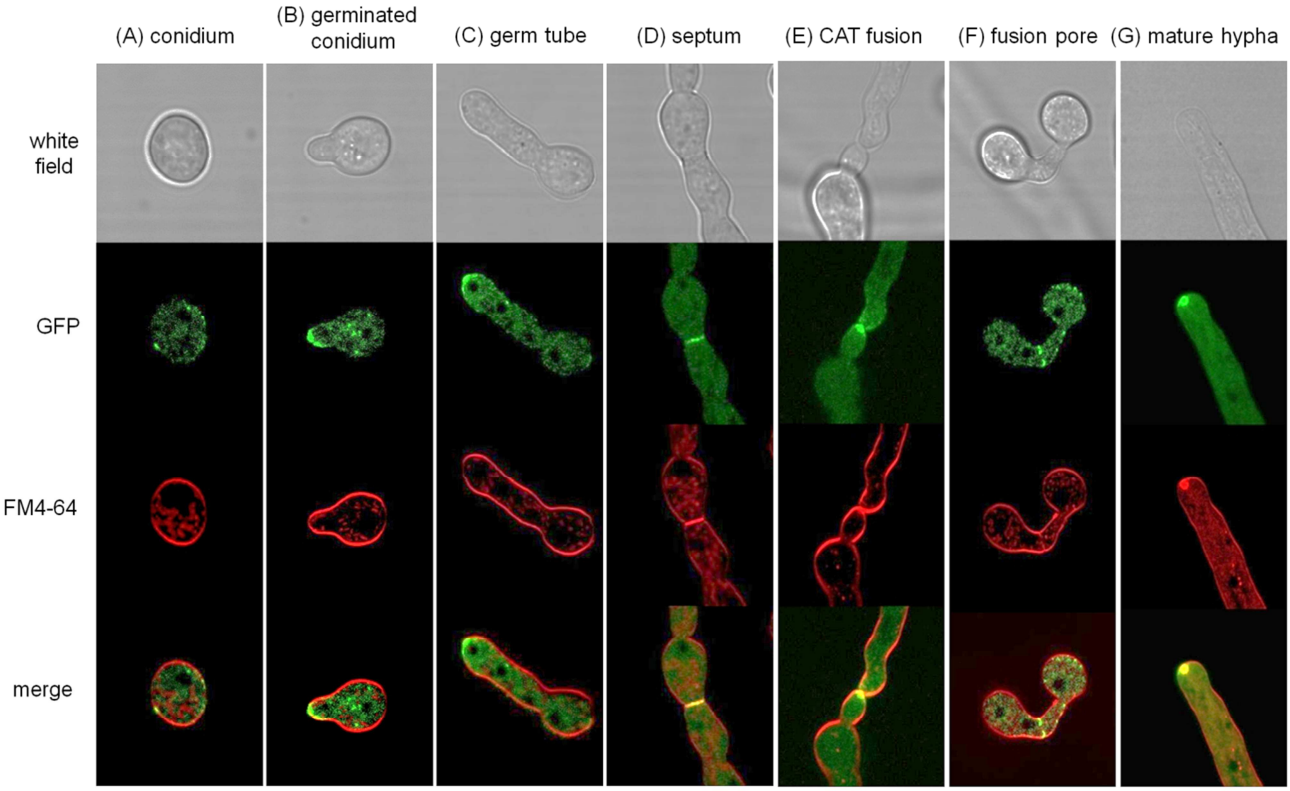

Figure 6.2 CaM localization at different stages of colony development. CaM-GFP expressing strains were stained with the membrane selective dye FM4-64 (red) and imaged by confocal microscopy.

6.2.3.1.1. CaM exhibits a dynamic localization in the growing tips of germ tubes and CATs not undergoing chemotropism

In germ tubes, live-cell imaging in time courses showed that the CaM-GFP was dispersed throughout the cytoplasm and also aggregated as small fluorescent dots moving in the cytoplasm. However, the majority of small fluorescent dots were relatively immobile and were associated with the plasma membrane (Fig. 6.3 A). CaM-GFP tended to focus as spots in association with the plasma membrane in the tips of CATs formed directly from conidia and from germ tubes that were not undergoing chemotropism (Fig. 6.3 B). The accumulation of CaM-GFP in the tips of germ tube and CATs was very dynamic and switched between being composed of numerous discrete spots and a single larger accumulation of the fusion protein (Fig. 6.3 C; supplementary movie 6).

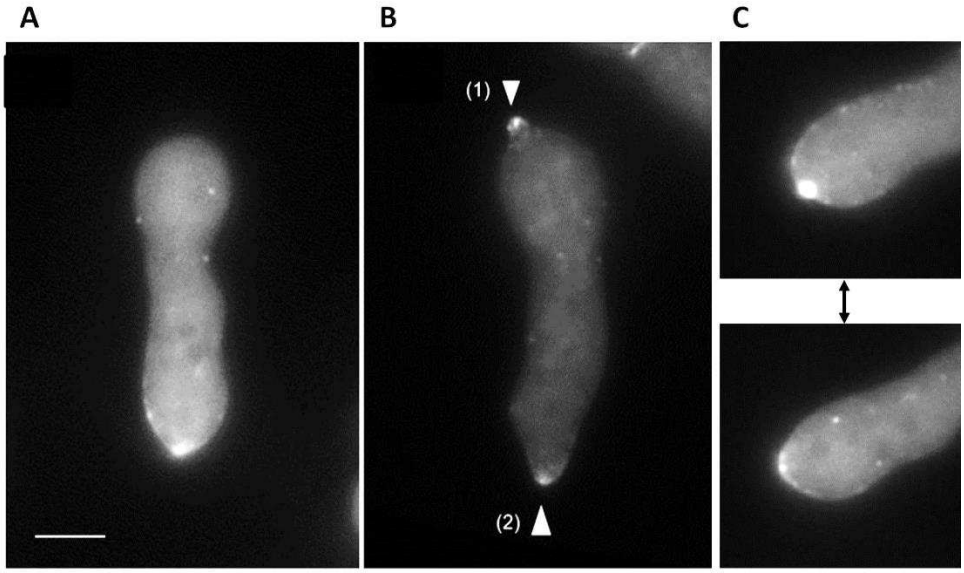

Figure 6.3 Live-cell imaging of GFP-tagged CaM in germ tubes (A) CaM-GFP accumulated at the tip of a growing germ tube, and dispersed dots moved in the cytoplasm. (B) CaM-GFP accumulated at both tips of a germ tube (2) and a CAT not undergoing chemotropism (1). (C) CaM-GFP accumulated at the tip of a germ tube showed a dynamic localization between a pronounced accumulation and small dots associated with the plasma membrane. Bar = 5 µm.

6.2.3.1.2. CaM complexes traffick in the cytoplasm, passed through septal pores, and move in association with nuclei

As the results from last section showed, CaM-GFP localized as fluorescent spots in the cytoplasm and moved around. Live-cell imaging showed that some spots moved in association with darker regions that had the appearance and behaviour of nuclei (Fig. 6.4 A and B; supplementary movie 7 and 8). The direction of movement of CaM-GFP spots in the cytoplasm was irregular and the velocity of their movement was typically 0.02-0.04 µm/sec (Fig. 6.4 B and C). Besides localizing at the developing septum, CaM-GFP also localized as discrete spots in the cytoplasm that passed through septal pores (Fig. 6.4 D and E; supplementary movie 9).

According to the results of CaM-binding proteome in chapter 5 (Table 5.6), five SPB components and regulators were found to be CaM-interacting, of which NCU02411 is the homolog of Nuf1p/Spc110p that is thought to bind to CaM in *S. pombe* and *S. cerevisiae* (Flory et al., 2002; Okano and Ohya, 2003). However, there was no fluorescence detected in the NUF-1-RFP strain. Thus, I used another nuclear

protein histone H4 to co-localize with CaM. In *S. cerevisiae*, Hhf2 (homolog of H4) has been known to follow nuclear dynamics (Wach et al., 1997) and to be associate with spindle pole body movement (Brachat et al., 1998).

The strain NCCC003 was sexually crossed with a strain in which nuclei were labelled with H4-tdimer-dsRed (Freitag and Selker, 2005) to generate the double labelled strain NCCC010 with CaM-GFP and H4-tdimerRFP. Live-cell imaging and co-localization of both proteins provided the evidence that the spots of CaM-GFP moving in the cytoplasm were associated with the spindle pole bodies of nuclei (Fig. 6.5; supplementary movie 10).

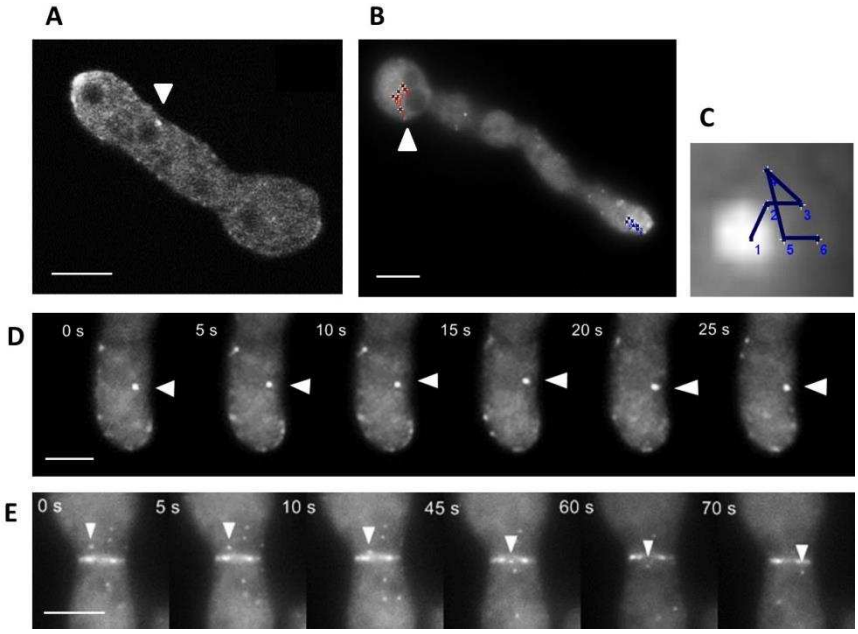

Figure 6.4 CaM complexes trafficked in the cytoplasm and passed through septal pores. Time-lapse imaging by confocal microscopy (A) and wide-field fluorescence microscopy (B-E). (A) CaM-GFP localized as discrete spots that moved around within the cytoplasm of germ tubes (arrow head) adjusted to dark regions (nuclei) or were associated more with the plasma membrane. (B) Tracking of dots pseudocolored (red and blue) associated with putative spindle pole bodies of nuclei over 10 sec. (C) Tracking of a single dot associated with a putative spindle pole body over 6 sec showing its irregular path (blue one from B). (D) Time-lapse imaging showing path of the movement of CaM-GFP dots associated with putative spindle pole bodies in the cytoplasm. Imaged at 5 second intervals. (E) CaM-GFP dots (arrowheads) moving through a septum in a germ tube. Bar = 5 µm.

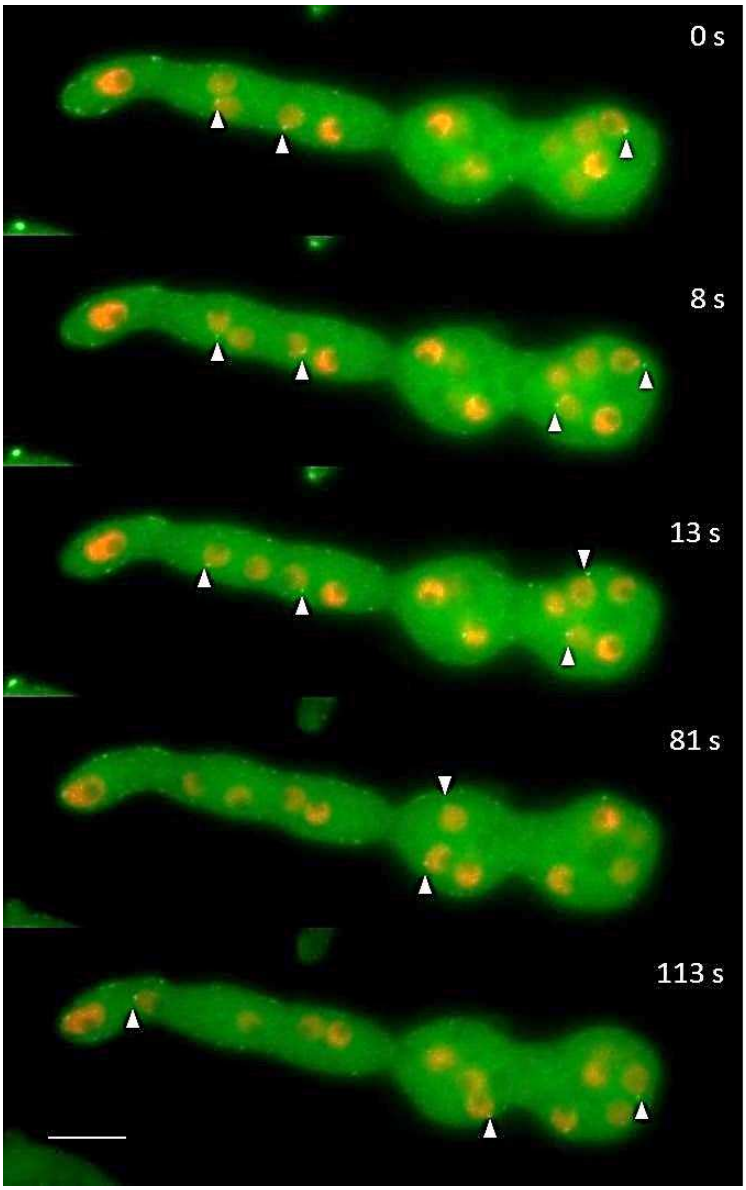

Figure 6.5 The movement of CaM spots in the cytoplasm is associated with nuclei. CaM-GFP spots co-localized with H4-tdimerRFP which labels nuclei. Time-lapse imaging by wide-field fluorescence microscopy with images captured at 1 sec intervals. CaM-GFP localized as single spots in association with the periphery of nucleus (arrowheads). Bar = 5 µm.

6.2.3.1.3. CaM accumulates at CAT tips during CAT chemoattraction and remaines at the fusion pore until fusion is completed

CaM-GFP accumulated at both tips of CATs during CAT chemotropism. CaM-GFP appeared before CAT formation and localized at the site of CAT formation, which was usually opposite another CAT formed from an adjacent spore or germling (Fig. 6.6 A).

Occasionally, the localization of CaM-GFP changed while CATs were homing towards each other. Sometimes the CaM-GFP interchangeably formed dispersed spots and then aggregated to accumulate as larger bright spots at the CAT tips (Fig. 6.6 B and C; supplementary movie 12). CaM-GFP often localized as larger spots in both CAT tips growing towards each other than those in single germ tube tips, and the large accumulation of CaM-GFP remained at the site of attachment and fusion pore formation for a period in excess of 30 min before it disappeared from that location following fusion (Fig. 6.6 D; supplementary movie 13).

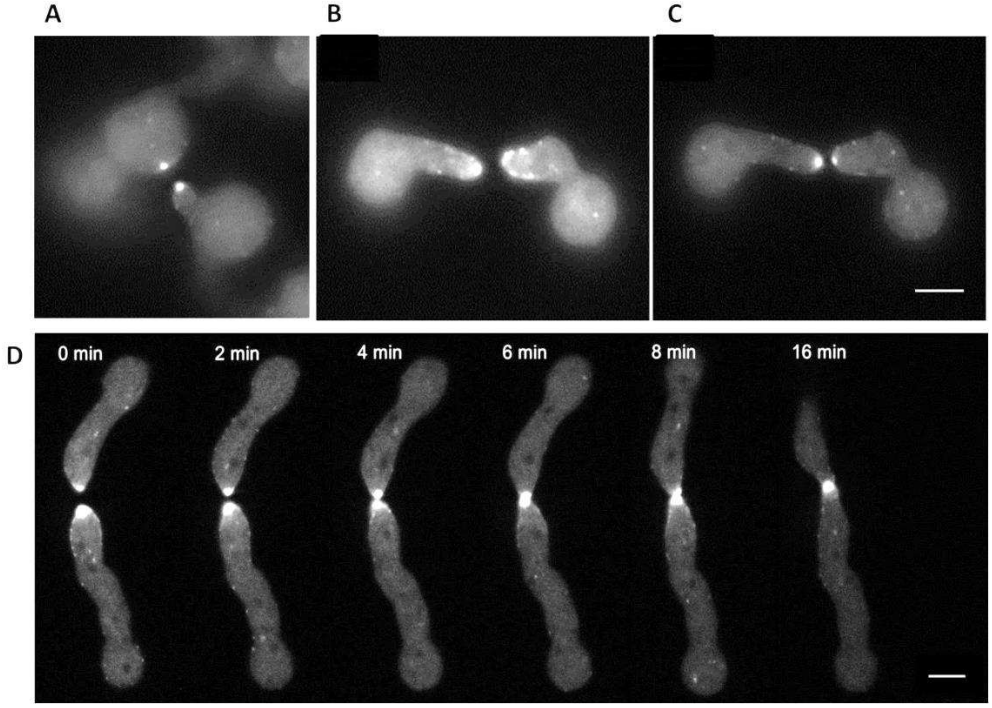

Figure 6.6 CaM-GFP localization during CAT chemoattraction and adhesion. Time-lapse imaging by wide-field fluorescence microscopy (A-C) and confocal microscopy (D) at 30 sec intervals. (A) CaM-GFP appeared at the site of CAT formation before CAT emergence and typically another CaM-GFP accumulation localized at the site where the opposing CAT tip would subsequently emerge. (B) and (C) CaM-GFP showed a dynamic pattern of accumulation at both CAT tips during CAT chemotropism. (D) CaM accumulated at CAT tips during CAT chemoattraction and remained at the fusion pore until fusion was completed. Bar = 5 μm.

6.2.3.1.1. CaM transiently accumulates at sites of septum formation

CaM-GFP accumulated at sites of fusion pore and septum formation, and then later disappeared within 15 min from these locations (Fig. 6.7; supplementary movie 11).

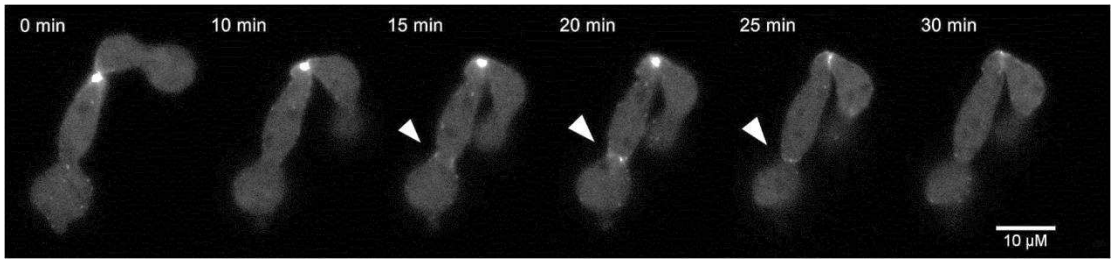

Figure 6.7 CaM localization during septum formation (arrowhead). Time-lapse imaging by confocal microscopy showing accumulation of CaM-GFP at the site of septum formation (arrowhead) and then its subsequent disappearance within 15 min from that location. Images captured at 30 sec intervals.

6.2.3.1.2. CaM exhibits a tip-focused gradient in growing vegetative hyphae

CaM-GFP was localized in a tip-focused gradient over a region of 25 µM from the apices of growing vegetative hyphae at the periphery of a mature colony (Fig. 6.8 A), and was strongly concentrated in the Spitzenkörper. This CaM-GFP gradient was absent in non-growing hyphae (Fig. 6.8 B).

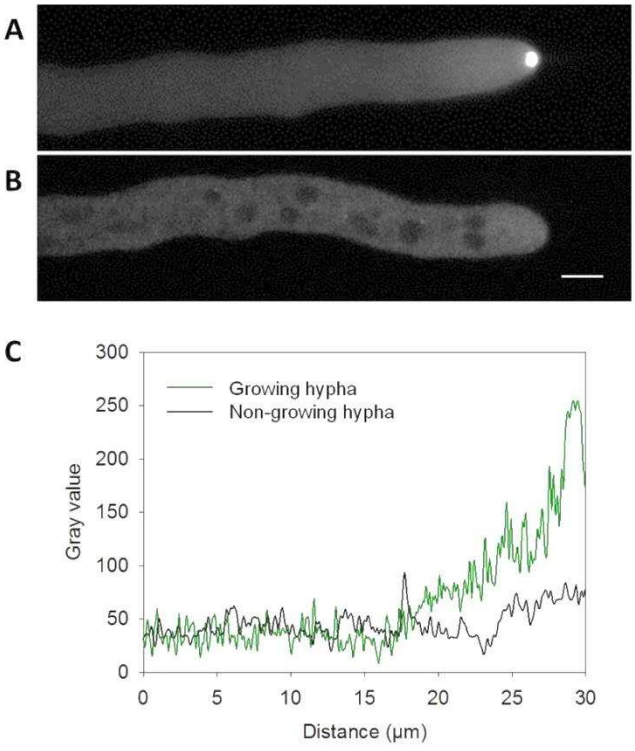

Figure 6.8 CaM-GFP localization in vegetative hyphae. (A) CaM-GFP concentrated in the Spitzenkörper of a growing hypha. (B) No accumulation of CaM-GFP in the tip of a non-growing hypha. (C) Grey level intensity transect along a midline through the hyphae in A and B showing a tip-focused gradient in CaM-GFP in a growing but not a non-growing hypha. Bar = 5 µm.

6.2.3.1.3. CaM appears in branch tips during the initiation of branch formation

During the branching of vegetative hyphae, CaM-GFP gradually accumulated at the site where a branch emerged (Fig. 6.9; supplementary movie 14). This accumulation of CaM-GFP was not evident until the first protrusion of the branch was evident (Fig. 6.9).

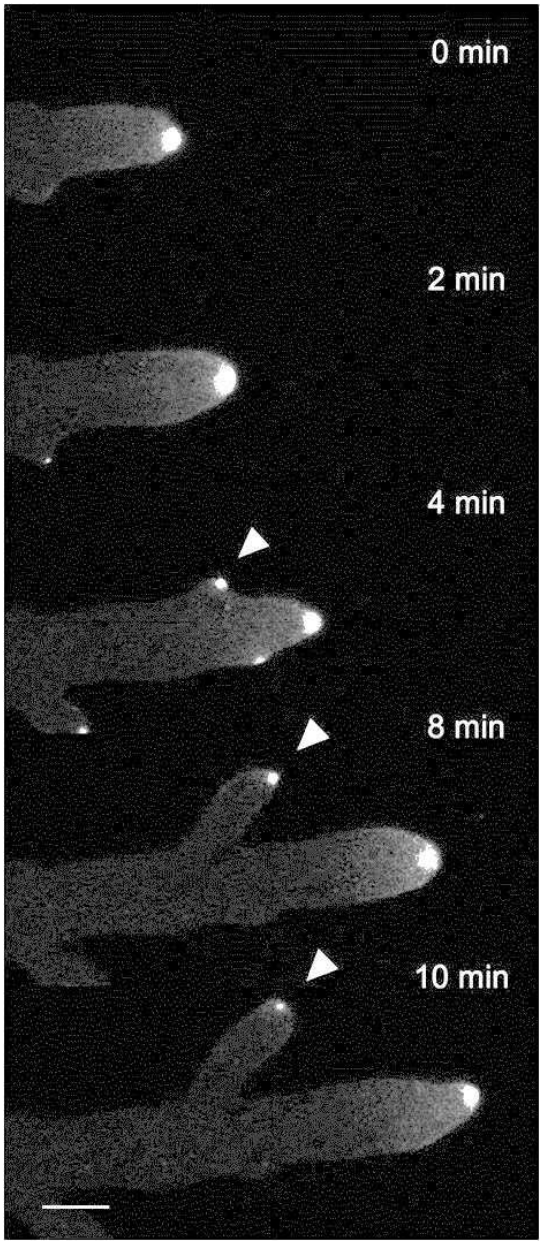

Figure 6.9 CaM-GFP localization in a hyphal branch (arrowhead) that has just emerged. Time-lapse imaging by confocal microscopy with images captured at 30 sec intervals. Bar = 5 µm.

6.2.3.2. Extracellular Ca^{2+} plays an important role in CAT chemoattraction and accumulation of CaM at tips

It has been known that the removal of Ca^{2+} from the growth medium inhibited CAT chemotropism, but had no obvious effects on CAT formation and conidial germination (see section 3.2.4). Conidia were incubated in growth medium at 35^{o}C in dark for 4 h. Compared to the control, the germ tube extension rate and the pronounced accumulation of CaM-GFP in tips was also influenced by the extracellular Ca^{2+}. The absence of extracellular Ca^{2+} inhibited both the germ tube extension rate and the number of germ tube tips with large accumulations of CaM-GFP (Fig. 6.10 C-D). Moreover, the large accumulation of CaM-GFP observed in CAT tips in the presence of extracellular Ca^{2+} was dramatically reduced in the absence of Ca^{2+} in CATs that were not undergoing chemotropism (Fig 6.10 B). The accumulation of CaM-GFP at the site of septum seem unaffected by the removal of Ca^{2+} from the external medium.

The pronounced recruitment of CaM at both CAT tips disappeared after adding 5 µM of the Ca^{2+} chelator, BAPTA, while CATs were homing towards each other (Fig. 6.11 B; supplementary movie 16). The experiment was repeated but with the additions of the same volume dH_2O instead of BAPTA, and the localization of CaM-GFP was unaffected and the CATs continued to grow towards each other and fused (Fig. 6.11 A; supplementary movie 15)..

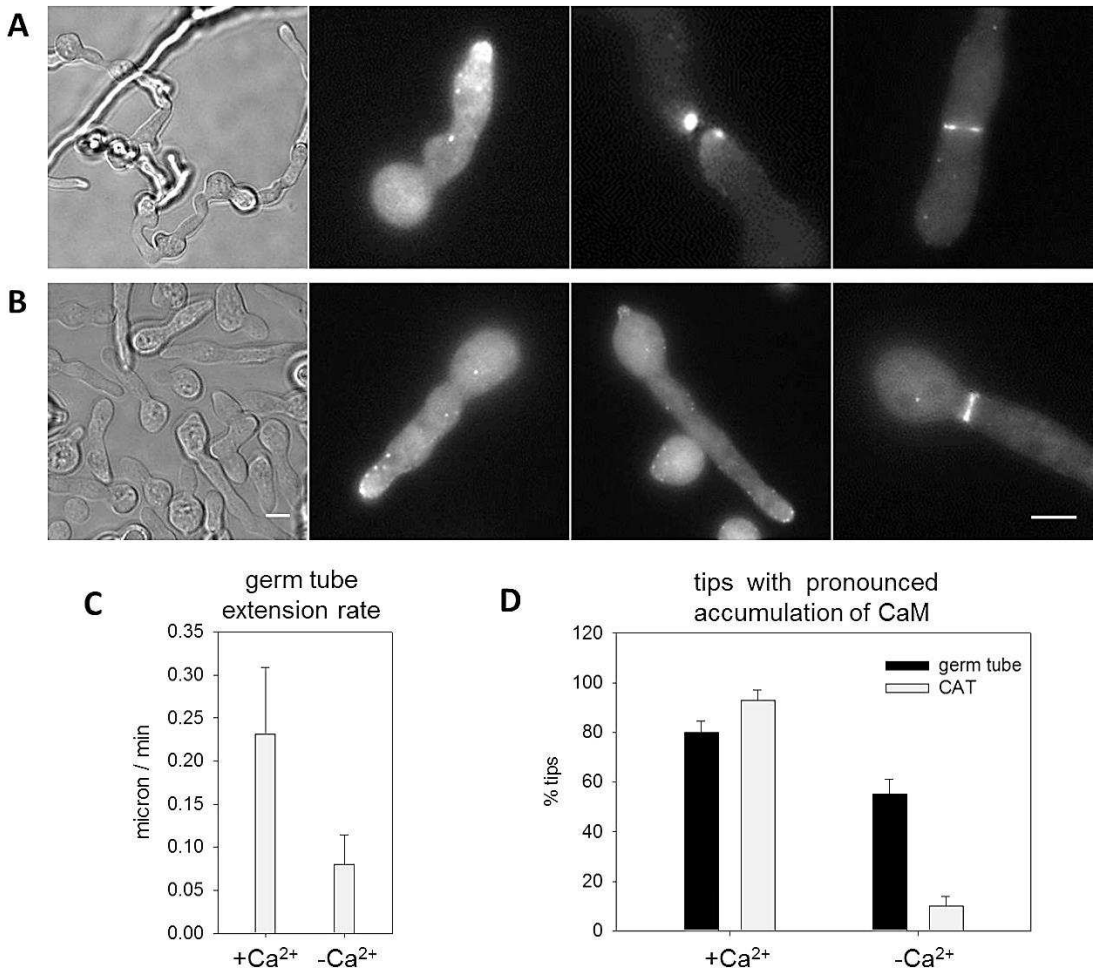

Figure 6.10 Extracellular Ca^{2+} influenced the localization of the tip-focused CaM. (A) CaM-GFP imaging in normal VM with 0.68 mM Ca^{2+} as a control. Cells underwent fusion and CaM-GFP localized at germ tube and CAT tips dynamically as large accumulations and as small spots. CaM-GFP also localized at septum. (B) CaM-GFP imaging in VM lacking Ca^{2+}. Cell fusion was inhibited and CaM-GFP did not localize as pronounced accumulations at tips but only as small dots. (C) The germ tube extension rate decreased in the absence of extracellular Ca^{2+} (n = 6; see section 3.2.2). (D) The tips of CATs with pronounced accumulation of CaM decreased more than the tips of germ tubes in Ca^{2+}-free medium (n=100). All cells incubated at 35°C for 4 h. Bar = 5 µm.

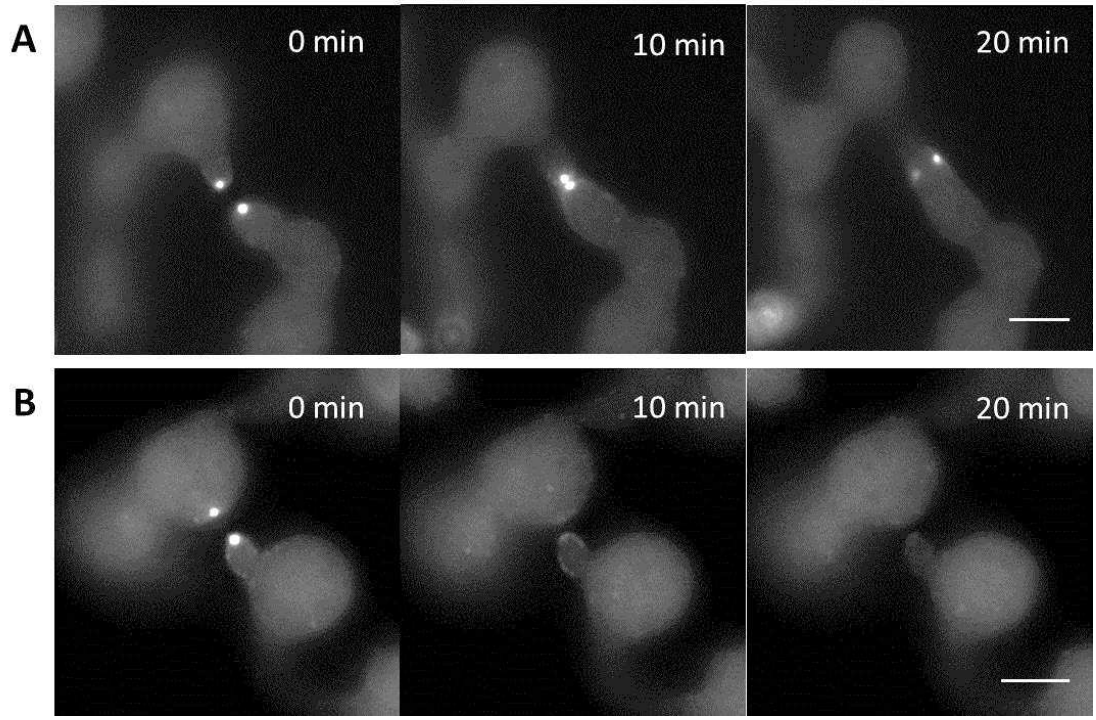

Figure 6.11 Extracellular Ca^{2+} is associated with the tip-focused CaM in CAT tips undergoing chemotropism. Time-lapse imaging by wide-field fluorescence microscopy with images captured at 30 sec intervals. (A) CaM-GFP imaging in normal VM with 0.68 mM Ca^{2+} as a control. CaM localized at both tips and the fusion pore during CAT fusion. (B) BAPTA was added at the 0 min time point. The pronounced accumulation of CaM-GFP at both tips of CAT decreased and the CATs stopped homing toward each other. Bar = 5 µm.

6.2.3.3. CaM trafficked along cytoskeletal elements

According to the proteomics analysis of CaM-binding complexes in chapter 5, cytoskeletal elements may play roles for the cytosolic movement of CaM (Table. 5.6). Thus, two drugs which target F-actin and microtubule were applied to CaM-GFP strain to investigate the protein-protein interaction between CaM and cytoskeletal components. In addition, 3 genes (*myo-5, so*, and *rgs-1*) were knocked-out in the CaM-GFP expressing strain to investigate the localization of CaM which is associated with plasma membrane, growing tips and cytosolic movement. Mutants Δ*myo-5,* Δ*so* and Δ*rgs-1* are defective in CAT fusion. GFP-MYO-5 acumulates at growing tips (Fig 6.20 A-F). Dot-loke SO-GFP presents an oscillation at CAT tips during CAT chemotropism (Fleissner et al., 2009b). It has been known that plasma membrane localization is required for RGS4 function in *S. cerevisiae* (Srinivasa et al., 1998).

6.2.3.3.1. MYO-5 and possibly F-actin are required for the pronounced accumulation of CaM at germ tube and CAT tips

The F-actin polymerization inhibitor, Latrunculin A (Lat A) causes a rapid loss of F-actin labelled with Lifeact-FP (Berepiki et al., 2010). The pronounced accumulation at tips of CATs and germ tubes disappeared when Lat A was added to the medium (Fig 6.12 B and C; supplementary movie 17). This was the same as the phenotype of the Δ*myo-5* mutant expressing CaM-GFP (NCCC011; Fig 6.13 B and C; supplementary movie 18). This suggests that F-actin and the actin motor protein myosin-5 may be required for the pronounced transient accumulation of CaM at CAT and germ tube tips.

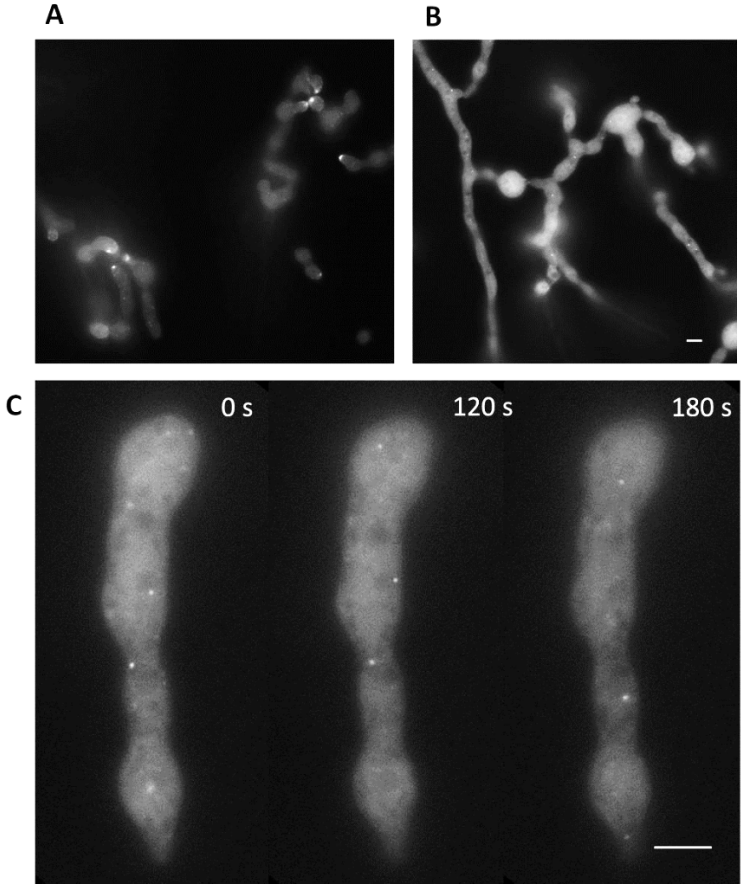

Figure 6.12 The pronounced accumulation of CaM-GFP at tips was sensitive to Latrunculin A. (A) CaM localized at the tips of germ tubes and CATs in VM. (B) The pronounced accumulation of CaM-GFP in germ tube and CAT tips disappeared within 5 min of adding Lat A. (C) The movement of CaM-GFP localized as spotsin the cytoplasm (1 and 2) was not influenced by Lat A. Three spots were associated with the spindle pole bodies of nuclei can be seen. Time-lapse imaging by fluorescence microscopy. Bar = 5 μm.

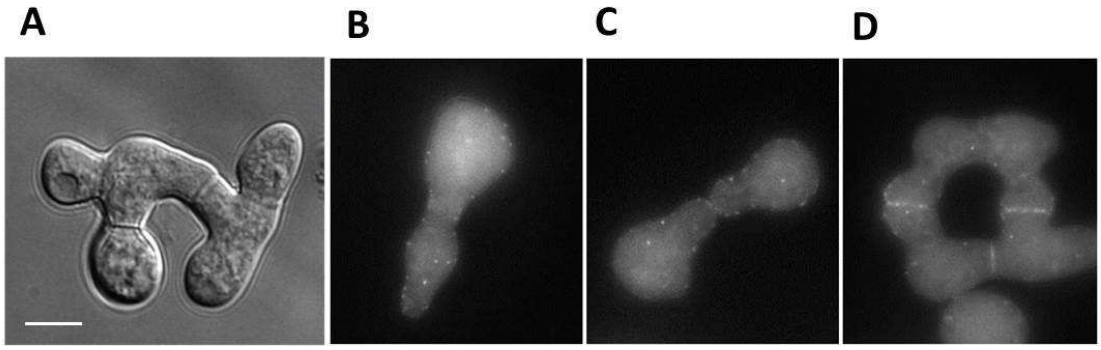

Figure 6.13 CaM localization in a *myo-5* gene deletion mutant. (A) The Δ*myo-5* strain expressing CaM-GFP possessed the following phenotypes : swollen conidia, reduced CAT fusion, slower CAT fusion, and shorter germ tubes. (B) CaM-GFP localization in a germ tube. No pronounced accumulation was evident at the germ tube tip. (C) CaM-GFP imaging when two CATs have attached prior to fusion. No pronounced accumulation was evident at both tips as occurs in the wild-type (Fig. 6.11 A). (D) CaM-GFP localized at the fusion pore or the site of septum formation. Bar = 5 µm.

6.2.3.3.2. Movement of CaM in the cytoplasm is microtubule-dependent

Treatment of germlings with 5 µM benomyl, a microtubule polymerization inhibitor, prevented the formation of long germ tubes (Fig 6.14 A), as previous by reported (Roca et al., 2010). The benomyl treatment did not affect the pronounced accumulation of CaM-GFP in CAT tips (Fig. 6.14 B). However, the cytoplasmic spots which associated with spindle pole bodies did not move in the presence of benomyl (Fig 6.14 C; supplementary movie 19). This demonstrates that the microtubules are required for the movement of CaM that is associated with spindle pole bodies in the cytoplasm.

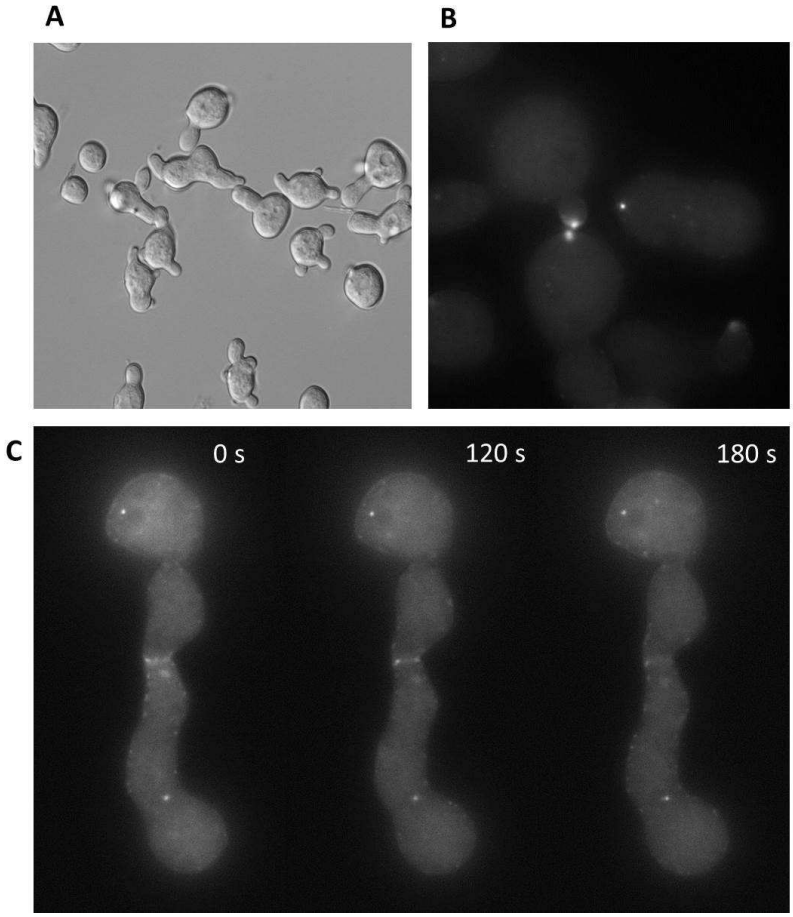

Figure 6.14 The movement of CaM-GFP in the cytoplasm is sensitive to Benomyl. (A) Benomyl inhibits long germ tube formation but not the formation of CATs. (B) CaM-GFP localized as a pronounced accumulation in CAT tips with 5 µM benomyl. (C) Time lapse imaging showed the inhibition of the movement of spots of CaM-GFP (arrows) in the cytoplasm. Time-lapse imaging by wild-field fluorescence microscopy. Bar = 5 µm.

6.2.3.4. SO is involved in CAT chemotropism but does not influence CaM localization

SO is known to play a role in CAT chemotropism and to exhibit oscillatory recruitment to CAT tips which is anti-phase to MAK-2 in opposing CATs (Fleissner et al., 2009b). The *so* gene deletion mutant is also significantly inhibited in CAT fusion. The KO cassette of *so* obtained from FGSC was transformed into the CaM-GFP expressing strain NCCC003 to generate NCCC012. No CAT fusion was observed in this strain. CaM-GFP localized the same as NCCC002 at the tips of germ tubes and CATs (not shown) and at the site of septum formation (Fig 6.15).

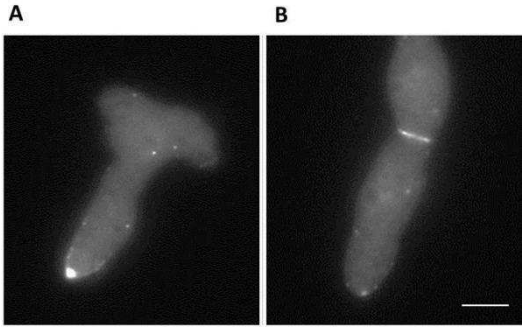

Fig. 6.15 CaM-GFP localization in a Δ*so* mutant background. (A) CaM-GFP localized at the tips of germ tubes and trafficked as spots in the cytoplasm. (B) CaM-GFP localized at the septum. Bar = 5 µm.

6.2.3.5. RGS-1 is involved in CAT formation but does not influence CaM localization

The gene deletion mutant of *rgs-1* showed a defective phenotype in CAT formation (section 4.2.2.2.1). The KO cassette of *rgs-1* obtained from FGSC was transformed into the CaM-GFP expressing strain NCCC003 to generate NCCC013. CaM-GFP in the Δ*rgs-1* background had the same localization at germ tube and CAT tips and septa as in the wild-type background (Fig 6.16).

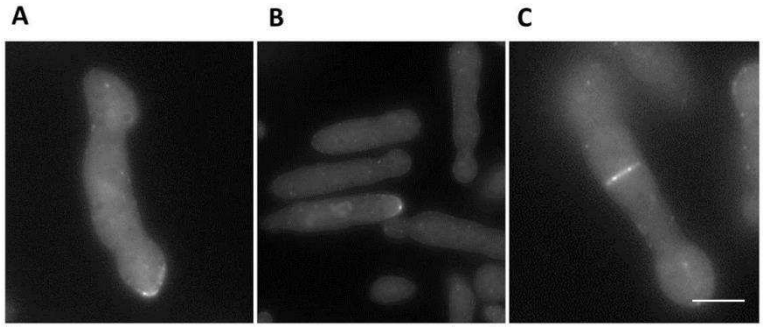

Figure 6.16 CaM-GFP localization in a Δ*rgs-1* background (A) and (B) CaM-GFP localized at the tips of germ tubes and trafficked as spots in the cytoplasm. (C) CaM-GFP localized at septa. Bar = 5 µm.

6.2.4. GFP-tagged CNA-1 and CNB-1

The labelled catalytic subunit of calcineurin, CNA-1-GFP, localized stably as a few static spots in the cytoplasm and accumulated at septa (NCCC006; Fig 6.17 A and B). The labelled regulatory subunit of calcineurin,CNB-1-GFP possessed the same localization as CNA-1-GFP (NCCC007; Fig. 6.17 C and D) and its fluorescence was much lower than CNA-1-GFP. Quick movement of dot-like CNA-1-GFP or CNB-1-GFP as CaM-GFP have not been observed in germling.

In *A. fumigatus*, it has been known that CnaA colocalizes to the contractile actin ring early during septtion and remains at the centre of the mature septum. CnaB's

septal localization is CnaA-dependent but CnaA's septal localization is CnaB-independent. CnaA also concentrates at the tip of germ tube emergence (Juvvadi et al., 2011). However, I did not observe any specific accumulation at tips or during CAT fusion process in both CNA-1-GFP and CNB-1-GFP in *N. crassa*. It may need further evidence to confirm the localization of calcineurin in *N.crassa*.

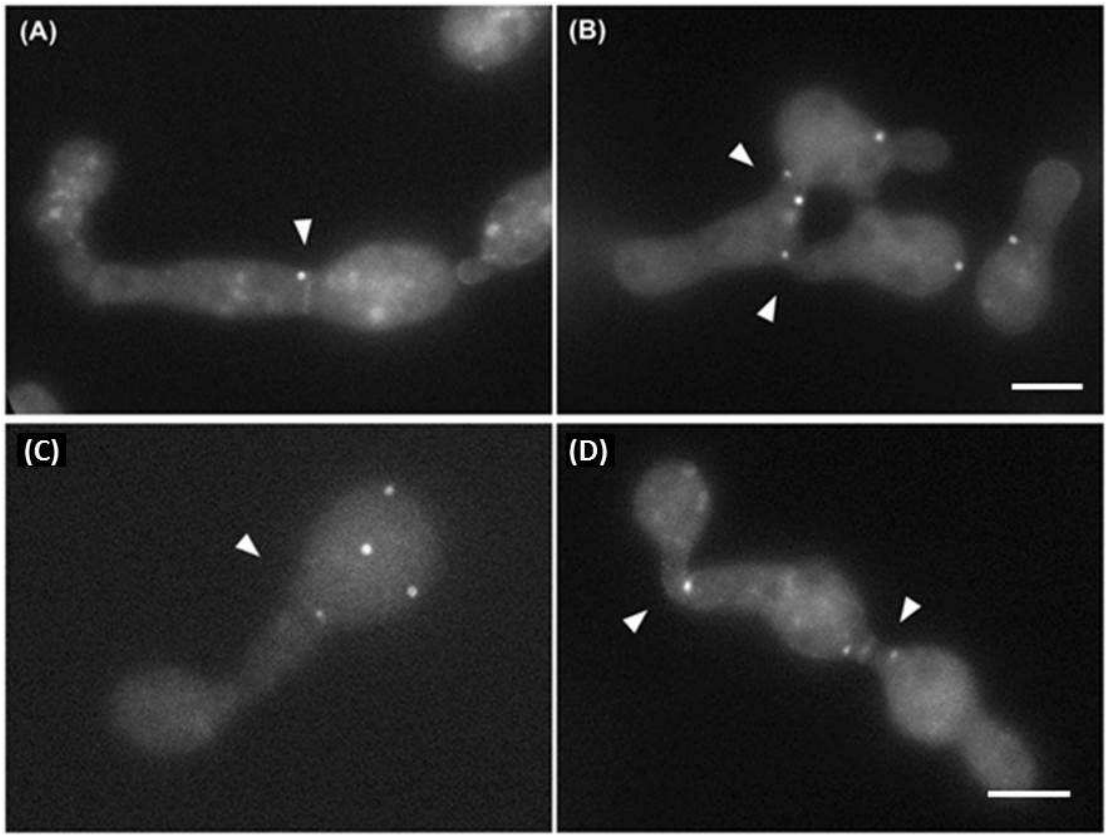

Figure 6.17 Live-cell imaging of GFP-tagged CNA-1 and CNB-1 during colony initiation. (A) CNA-1-GFP formed fluorescent spots in the cytoplasm and localized at the septum (arrowheaded). (B) No accumulation was observed at the fusion sites (arrowheaded). (C) CNB-1-GFP formed fluorescent spots in the cytoplasm and localized at the septum (arrowheaded). (D) No accumulation was observed at the fusion sites (arrowheaded). Bar = 5 µm. The contrast and brightness of Images were enhanced by ImageJ due to the weak fluorescence.

6.2.5. GFP-tagged CaMK-1

CaMK-1-GFP exhibited dispersed fluorescence throughout the cytoplasm of germlings. There was no specific accumulation at tips or in spots (NCCC008; Fig. 6.18).

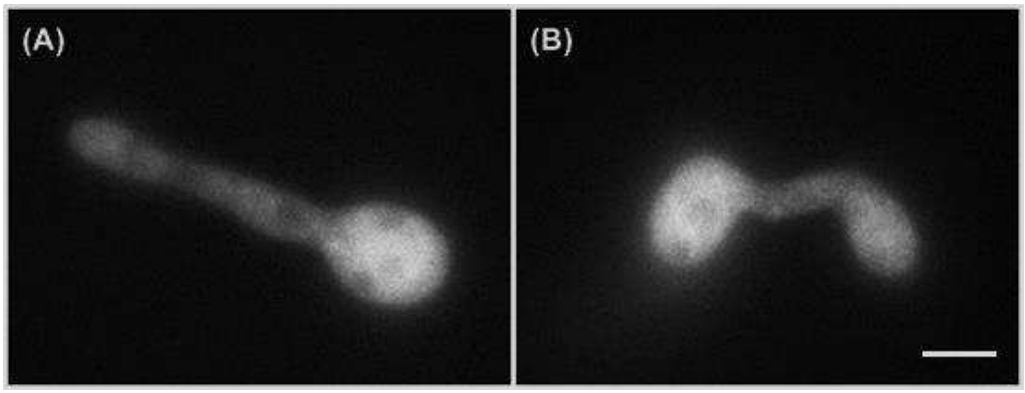

Figure 6.18 Live-cell imaging of GFP-tagged CaMK-1 during colony initiation. CaMK-1-GFP fluorescence was dispersed throughout the cytoplasm in (A) germ tubes and during (B) CAT fusion. Bar = 5 µm.

6.3. Discussion

6.3.1. Live-cell imaging GFP-tagged proteins in *N. crassa*

Fluorescent proteins, especially the green fluorescent protein (GFP), are useful and convenient tools for the localization of proteins in living cells. GFP is a comparatively stable and a powerful fluorescent protein that has been heterologously expressed in many different organisms. There have been numerous GFP-tagged plasmid systems and transformation methods applied to *N. crassa* to explore protein localization and function (Freitag et al., 2004; Honda and Selker, 2009). Two genetic strategies, knock-in (KI) and overexpression, were used in this study to express GFP-tagged proteins under the control of native promoters or other stronger promoters (Larrondo et al., 2009). Most of the fusion gene cassettes were constructed and inserted into a vector by yeast recombinant cloning (Oldenburg et al., 1997). This method for plasmid construction is cheaper and faster than more traditional methods.

Four different important proteins involved in Ca^{2+} signalling/homeostasis were labelled by C-terminal GFP-tagging. The transformants expressing CaM-GFP exhibited the strongest fluorescence. It was localized at the tips of growing germ tubes and CATs and reversibly localized as spots or larger accumulations. It was also localized as spots associated within the plasma membrane and with spindle pole bodies linked to nuclei. The CNA-1-GFP and CNB-1-GFP localized in the cytoplasm and septa. They

also formed static spots in the cytoplasm which did not exhibit a similar dynamic movement to CaM-GFP and no pronounced accumulation of the calcineurin subunits was observed at tips. In the CaMK-1-GFP transformants, the green fluorescence was also dispersed throughout the cytoplasm.

Generally, the knock-in strategy with native promoters provided better and more reliable localization patterns than overexpression in *N. crassa*. However, some problems and limitations with GFP labelling still occurred with some proteins. Some essential proteins (e.g. CaM, CNA-1, and CNB-1) tagged with GFP caused slightly defective phenotypes in the transformants possibly due to of the GFP inducing conformational changes in the protein it was fused to or due to problems associated with steric hindrance.

6.3.2. Comparison of CaM localization in *S. cerevisiae, S. pombe, A. nidulans* and *N. crassa*

As the main intracellular Ca^{2+} receptor, CaM has been imaged in several fungi. CaM typically displayed an asymmetric distribution in different organisms. In *S. cerevisiae*, CaM localizes at sites of cell growth and has been shown to be involved in the process of polarized growth. CaM concentrates at the presumptive site of bud formation about 10 minutes before bud emergence in unbudded cells, and accumulates throughout the bud in small budded cells. When the cell is growing, CaM concentrates at the tip and in the neck region before cytokinesis (Brockerhoff and Davis, 1992). The localization and functions of CaM in *S. pombe* strongly resemble those previously identified in *S. cerevisiae*. *S. pombe* Cam1 preferentially localizes at both sites of polarized cell growth and the spindle pole body (SPB) during meiosis and ascospore formation. The defects of a temperature-sensitive CaM mutant further substantiate a mitotic function for CaM during chromosome segregation in *S. pombe* (Moser et al., 1997). In the filamentous fungus *A. nidulans*, CaM localized dynamically throughout the hypha and concentrated in active growing sites during conidial germination, hyphal growth, septation and conidiation. CaM constantly was shown to accumulate in growing hyphal tips but was only transiently localized at developing septum during cytokinesis (Chen et al., 2010a).

In filamentous fungi, the live-cell imaging of CaM has only been performed in *A. nidulans* and *N. crassa*. However, the imaging of CaM in *N. crassa* showed a slightly different localization patterns to *A. nidulans*. Not only showing a single bright accumulation in polarized germlings and vegetative hyphae, CaM in *N. crassa* also formed multiple dynamic dots that associated with the plasma membrane, moved around in the cytoplasm, and concentrated more at growing tips. Similar to *A. nidulans*, CaM transiently appeared at sites of septum formation and constantly accumulated within the core region of the Spitzenkörper in vegetative hyphae of *N. crassa*. A summary comparing CaM localization in different fungi is shown in Table 6.3.

Table 6.3 Comparison of CaM localization in different fungi

Organism	Method of imaging CaM	Localization	Reference
S. cerevisiae	Immunofluorescence	Tips of growing cells and SPB	(Flory and Davis, 1999)
S. pombe	Immunofluorescence and N-terminus GFP-tagged fusion protein expressed under the control of the *cam1*$^{+}$ promoter	At sites of polarized cell growth and the SPB	(Itadani et al., 2010; Moser et al., 1997)
A. nidulans	N-terminus GFP-tagged and RFP-tagged fusion protein expressed under the control of the inducible *alcA* promoter or native *cam* promoter	At sites of polarized growth during conidium germination, hyphal growth, and conidiation; transiently located in forming septa.	(Chen et al., 2010a)
N. crassa	C-terminus GFP-tagged fusion protein expressed under the control of the native *cmd-1* promoter	At SPBs associated with nuclei; in association with the plasma membrane as dots; focused in the tips of CATs and germ tubes; within Spitzenkörper of vegetative hyphae; transiently located at developing septa and during fusion pore formation	This study

6.3.3. Extracellular Ca^{2+} plays a role in regulating the localization of CaM at growing tips in a MYO-5/F-actin-dependent manner

The results shown in Fig. 6.10 and 6.11 showed that the removal of extracellular Ca^{2+} caused a rapid loss of the tip-focused pronounced accumulation of CaM in the

tips and stopped the growth of germ tubes and CATs. Usually, after 6 h of incubation at room temperature, germ tubes started to grow again with a tip-focused CaM accumulation (data not shown), and CATs ceased to grow or developed into germ tubes (Fig 3.6 and 3.7).

A hypothesis to explain this phenomenon is that Ca^{2+} influx from the external medium may act as an inducer which by binding to CaM allows CaM-regulated protein complexes to transport CaM to the tips for the cell growth. This transport may be mediated by MYO-5 and F-actin. It has been previously shown that GFP-MYO-5 exhibited a similar localization (Fig 6.20 A-F) to the localization of CaM-GFP that I have shown in this chapter. Furthermore, occasionally I observed that CaM-GFP formed cable-like structures in the tip region (Fig. 6.20 J) which are similar to actin cables (Fig 6.20 G; Berepiki, 2012). In addition, MYO-5 has a CaM-binding motif and the proteomics analysis described in chapter 5 showed that it interacts either directly or indirectly with CaM. The recruitment of the Ca^{2+}/CaM/MYO-5 complex at tips may be necessary for germ tube and CAT growth.

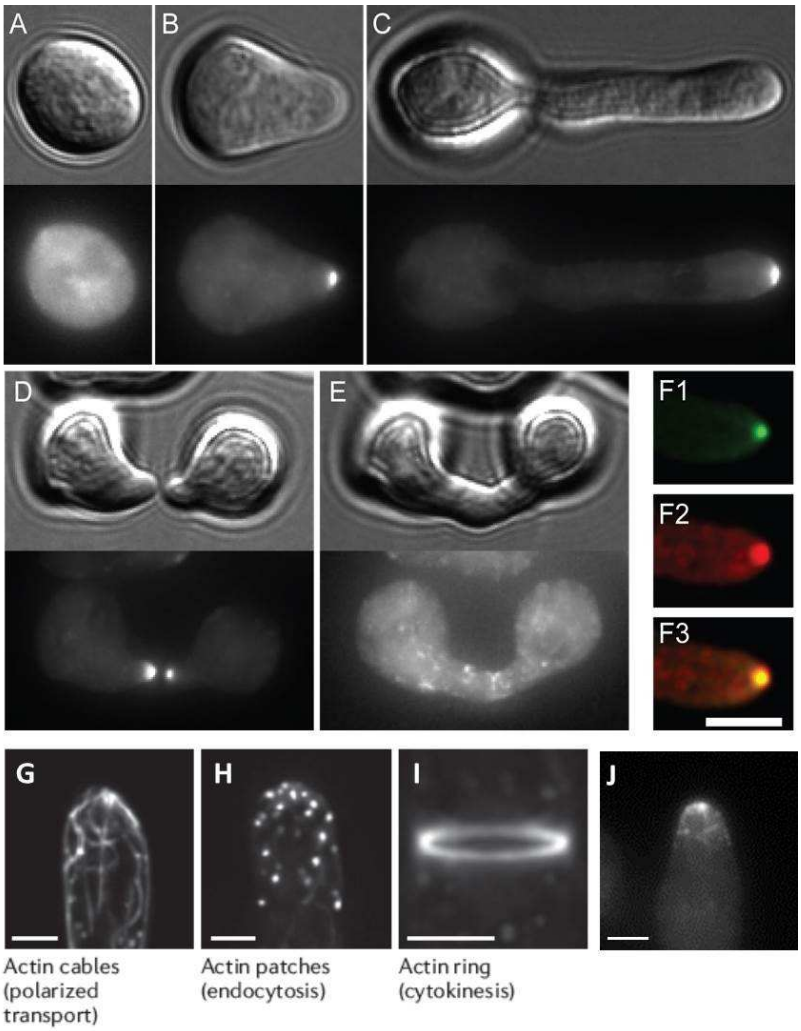

Fig. 6.20 MYO-5 showed the same localization with CaM. Adapted from Berepiki, 2010. Images A-I are from Berepiki, 2012**.** (A-E) GFP-MYO-5 localized as a crescent at tips of germ tubes and CATs. (F) F1: GFP-MYO-5 localized as a pronounced accumulation in the Spitzenkörper. F2: FM4-64 staining of Spitzenkörper from F1. F3: Merge of F1 and F2 showing GFP-MYO-5 localizes in the Spitzenkörper core. (G-I) Lifeact-GFP localized as patches and cables in the tip area and at the site of septum (Berepiki et al., 2010). (J) CaM-GFP occasionally localized as cables similar to F-actin in the tip region of a germ tube.

6.3.4. The movement of CaM-GFP in the cytoplasm may be regulated by the kinesin Nkin-2 along microtubules

Kinesins are a family, which share a conserved motor domain with ATP and microtubule binding activity, and regulate the plus-end-directed transport along microtubules (Lawrence et al., 2004). In *Ustilago maydis*, kinesin-3 (Kin3) is required for anterograde endosome movement (Schuster et al., 2011a; Schuster et al., 2011b;

Wedlich-Soldner et al., 2002), whereas retrograde movement of endosomes is accomplished by dynein (Steinberg, 2012). An additional role of Kin3 in mRNA transport has been demonstrated recently (Baumann et al., 2012; Konig et al., 2009). Some kinesins showed a Ca^{2+}-dependent manner as kinesin-like calmodulin-binding proteins (KCBP). Elevated levels of intracellular Ca^{2+} inhibits KCBP motor interaction with microtubules via CaM (Abdel-Ghany et al., 2005; Narasimhulu and Reddy, 1998; Reddy et al., 1996; Reddy et al., 2004; Reddy and Reddy, 2002).

In *N. crassa,* Nkin-2 has been known to be involved in polarized growth and early endosome transport (Seidel et al., 2013). It also appears to be associated with mitochondrial and plays some role in mitochondrial distribution (Fuchs and Westermann, 2005). From the proteomics analysis in chapter 5, Nkin2 (kinesin-3) is another motor protein, which has a CaM-binding motif and interacts with CaM. In this chapter I showed that the inhibition of microtubule polymerization with benomyl prevented the movement of CaM-GFP in nuclear spindle pole bodies (Fig. 6.14). This may be explained by nuclear movement being mediated by Nkin-2 along microtubules.

6.4. Summary

- CaM localized to growing tips of germ tubes and CATs not undergoing chemotropism with a dynamic localization that switched between being composed of small discrete spots and larger accumulations of the protein.
- CaM was associated with nuclear spindle pore bodies.
- CaM transiently accumulated at sites of septum formation.
- CaM accumulated pronouncedly at CAT tips during CAT chemoattraction and remained at the fusion pore until fusion was completed.
- CaM exhibited a tip-focused gradient in growing vegetative hyphae but not in non-growing hyphae.
- CaM appeared in branch tips during the initiation of branch formation.
- MYO-5 and possibly F-actin are required for the pronounced accumulation of CaM in growing germ tube and CAT tips.
- Extracellular Ca^{2+} may play an important role in regulating the localization of

CaM at growing tips in a MYO-5/F-actin-dependent manner.

- The CaM-GFP associated with spindle pole bodies may be related to the movement of nuclei being regulated by Nkin-2 transport along microtubules.
- SO is involved in CAT chemotropism but does not influence CaM localization.
- RGS-1 is involved in CAT formation but does not influence CaM localization.
- The calcineurin subunits, CNA-1-GFP and CNB-1-GFP, localized as a few static spots in the cytoplasm and at the sites of septa.
- CaMK-1-GFP showed dispersed fluorescence throughout the cytoplasm.

Chapter 7

Live-cell imaging of intracellular Ca^{2+} by the protein-based GCaMP Ca^{2+} sensors

Chapter 7 – Live-cell imaging of intracellular Ca^{2+} by the protein-based GCaMP Ca^{2+} sensors

7.1. Introduction

A variety of methods have been developed for measuring $[Ca^{2+}]_c$ that fall into two types: Ca^{2+}-sensitive microelectrodes (Miller, 1994) and Ca^{2+}-sensitive light emitting probes (Miyawaki et al., 1997; Parton and Read, 1999). Ca^{2+}-sensitive microelectrodes have not been widely applied to fungi because of technical difficulties (Miller et al., 1990). The Ca^{2+}-sensitive light emitting probes can be classified as: synthetic Ca^{2+} fluorescent indicators; bioluminescent proteins; FRET-based genetically encoded Ca^{2+} indicators (GECIs); and single-fluorophore GECIs (Grienberger and Konnerth, 2012).

A large number of synthetic Ca^{2+} fluorescent dyes are available for Ca^{2+} in cells and most of them are modified from the Ca^{2+} chelators EGTA or BAPTA (Grynkiewicz et al., 1985; Haugland, 1996; Minta and Tsien, 1989). Although some success in the measurement of $[Ca^{2+}]_c$ has been achieved in filamentous fungi using Ca^{2+} dyes, their utility has been limited due to various technical problems (Hickey et al., 2004; Nair et al., 2011b), including difficulties in dye loading (Parton et al., 1997; Silverman-Gavrila and Lew, 2001), and dye sequestration within organelles (e.g. vacuoles) (Parton et al., 1997; Hickey et al., 2005).

Several light emitting bioluminescent Ca^{2+}-binding proteins, which emit visible luminescence by an intramolecular reaction involving Ca^{2+}, have been described (e.g., aequorin and obelin) and some have been used to measure $[Ca^{2+}]_c$ (Shimomura, 1985; Tsuji et al., 1995). Aequorin, isolated from the jellyfish *Aequorea victoria*, is the most popular bioluminescent and is a 22 kDa photoprotein composed of apoaequorin, coelenterazine and bound oxygen (Inouye et al., 1985; Prasher et al., 1985). A major limitation of bioluminescent photoproteins are that they emit low Ca^{2+}-dependent light levels making them of little use for real-time imaging of Ca^{2+} dynamics (Kim et al., 2012). Aequorin has been expressed in a phytopathogenic fungus, *Phyllosticta ampelicida* (Shaw et al., 2001) and been codon optimized in *N. crassa*, *A. niger* and *A. awamori* for better expression (Nelson et al., 2004).

Cameleon is the most common FRET-based Ca^{2+} sensor that have been successfully expressed in animals (Diegelmann et al., 2002; Hasan et al., 2004; Higashijima et al., 2003) and plants (Allen et al., 1999; Iwano et al., 2004; Kosuta et al., 2008; Monshausen et al., 2008). Recently it has also been successfully used in three plant fungal pathogens, *M. oryzae*, *F. oxysporum*, and *F. graminearum* (Kim et al., 2012). However even after numerous modifications, cameleons have not been expressed in *N. crassa* (unpublished data from Read lab).

GCaMPs are a novel group of single-wavelength GECIs that consist of a CaM-interacting M13 peptide, a circularly permuted green fluorescent protein (cpGFP) and the Ca^{2+}-binding protein calmodulin (CaM) (Akerboom et al., 2012; Chen et al., 2013; Nakai et al., 2001; Tian et al., 2009). When Ca^{2+} binds with the C'-terminal CaM part, the N'-terminal M13 binds with the Ca^{2+}-activated CaM to change the comfromation of cpGFP for fluorescence expression. Several versions of the original GCaMP sensor (Nakai et al., 2001) have been published (Akerboom et al., 2009; Ohkura et al., 2005; Tallini et al., 2006). GCaMP3 has been used to detect Ca^{2+} in large neuronal populations in the motor cortex (Tian et al., 2009), barrel cortex (O'Connor et al., 2010), and hippocampus (Dombeck et al., 2010) of mice. GCaMP5s have been used with cultured neurons and astrocytes, mouse retina, *Caenorhabditis* chemosensory neurons, *Drosophila* larval neuromuscular junction and adult antennal lobe, zebrafish retina and tectum, and mouse visual cortex (Akerboom et al., 2012). The latest version, GCaMP6, was first described in 2013 for imaging neuronal activity (Chen et al., 2013). However, none of the GCaMPs have been previous reported to use for to Ca^{2+} imaging in fungal cells.

To create a novel toolkit for $[Ca^{2+}]_c$ live-cell imaging in *N. crassa*, the aims of the research described in this chapter were:

- To obtain GCaMP expressing strains in *N. crassa* and establish a routine screening method for GCaMP mutants
- To image $[Ca^{2+}]_c$ in living cells of *N. crassa* at different developmental stages by wild-field fluorescence microscopy
- To analysis the Ca^{2+} signatures in germlings and determine whether they play a role on Ca^{2+} signalling at different stages if CAT fusion

- To determine the influence of Ca^{2+} modulating pharmacological agents on these Ca^{2+} sgnatures

7.2. Results

7.3.1. Plasmid construction for GCaMPs expression strains

GCaMP5 and GCamP6s cassettes, amplified using the primer set GCaMP-PacI-F and GCaMP-EcoRI-R2, were ligated into the vectors pCCG1::C-Gly::GFP and pTEF1::C-Gly::GFP for his locus targeted transformation. GCaMP5 and GCamP6s cassettes, amplified using the primer set GCaMP-BamH1-F and GCaMP-EcoRV-R, were ligated into the vector pBARGRG-1 for the ectopically insertion. Plasmids were sequenced using the primers GCaMP-seq-F and GCaMP-seq-R.

7.3.2. Screening for GCaMPs expressing strains

Nine heterokaryotic transformants were selected and used to inoculate VM solid medium. These were incubated at 35^{o}C in dark for 3 days and 25^{o}C with light for 2 days. Conidia were collected and incubated in liquid VM at 35^{o}C for 4 h to test for transformants expressing GCaMPs that were responsive to changes in $[Ca^{2+}]_c$. For this purpose, high extracellular $CaCl_2$ (0.2M) was added to the sample wells before the time-lapse imaging by fluorescence microscopy because this stimulus has been previously shown to elicit a large transient increase in $[Ca^{2+}]_c$ (Nelson et al., 2004). CAT fusion in strains exhibiting transient $[Ca^{2+}]_c$ changes was quantified and compared with that of the wild-type. Nine homokaryons were purified from each heterokaryotic strain by the microconidiation method (section 2.8.1.4). This screening process was repeated with the homokaryotic mutants and the strain (Tef1-G6s-his-m1), which produced the greatest fluorescence and which exhibited similar levels of CAT fusion to the wild type, was used to generate all the results described in this chapter. The different plasmids and GCaMPs used, and the results of the screening, are summarized in Fig 7.1.

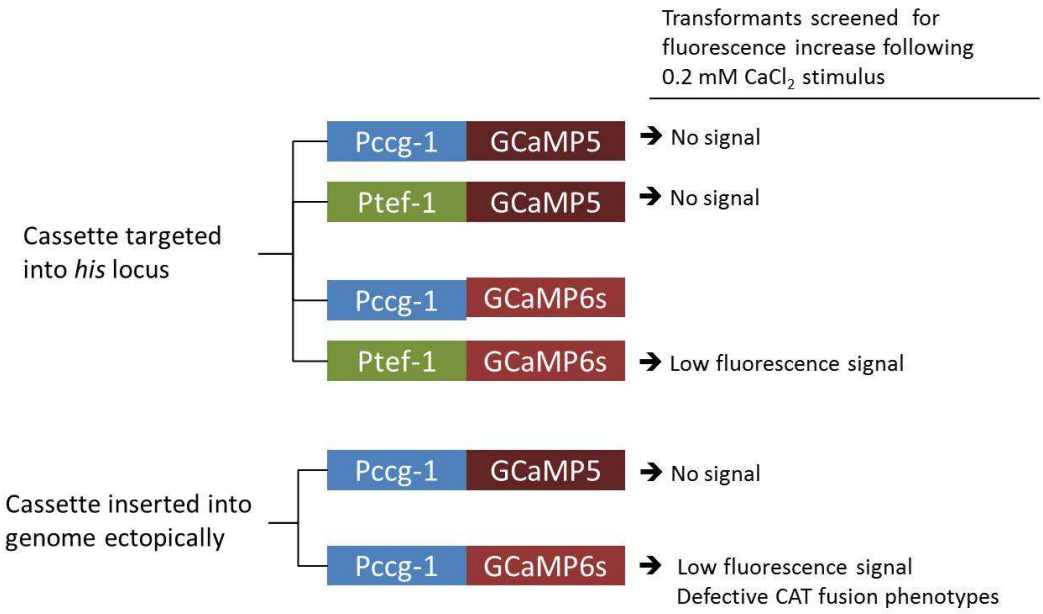

Figure 7.1 Summary of plasmid construction for GCaMP5 and GCaMP6s in *N. crassa* and the results of screening transformants. Two GCaMPs (GCaMP5 and GCaMP6s) were expressed using two different *N. crassa* promoters (*pccg-1* and *ptef-1*) with two transformation systems involving targeted to the *his* locus targeted and ectopically targeting. Ptef-1-G6s-his produced the best fluorescence for $[Ca^{2+}]_c$ imaging during colony initiation in *N. crassa*.

7.3.3. The optimization of imaging parameters in fluorescence microscopy

To determine suitable conditions for fluorescence microscopy to image $[Ca^{2+}]_c$ during colony initiation, several parameters (exposure time, LED intensity, interval time between images, and the length of imaging time available before bleaching) were optimized for detecting the Ca^{2+} signals. The total fluorescence per conidium/conidial germling was generated by selecting the whole cell area using a plugin (T-functions – intensity v time monitor) in ImageJ. The autofluorescence from wild type cells were measured with different parameters to be the control of peaks (Fig. 7.2). Time-lapse imaging was performed with a 1 sec interval time between images for measuring the length of an intracellular Ca^{2+} pulse. Each Ca^{2+} peak usually lasted for 5 - 50 sec (Fig. 7.3). To reduce photobleaching and maintain cells in a healthy state during the period of imaging, the combination of imaging parameters was experimentally found to be: 20 excitation LED intensity, 200 ms exposure time, 5 sec interval time, and a maximum imaging time of 20 min. Background subtraction

was performed on images in ImageJ to remove background noise. The intensity values represented in Figs. 7.3-7.7, 7.9, 7.11-7.17 show the total fluorescence intensity per cell and vary from cell to cell because the cells were of different sizes.

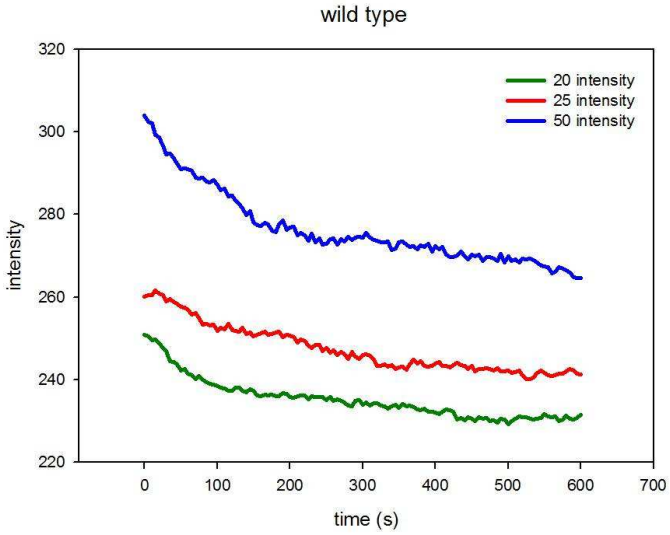

Figure 7.2 Photobleaching of the autofluorescence in the wild-type. Conidia were incubated in VM at 35°C for 4 h and imaged at room temperature. Time-lapse imaging was performed by wide-field fluorescence microscopy. Images were captured with a 200 ms exposure time at 5 sec intervals for 10 min with 3 different LED excitation intensities.

7.3.4. The Ca^{2+} spikes could not be correlated with germ tube extention rate or CAT fusion

Ca^{2+} imaging was performed either in 8-well chambers or microfluidic culture chambers (Millipore, CellASIC® ONIX Microfluidic Platform). In the 8-well chamber, conidia (1 x 10^5 cells/ml) were incubated in VM at 35°C for 4 h. A 60X objective was used for time-lapse imaging at room temperature. To avoid interfering fluorescence from surrounding cells isolated conidial germlings with germ tubes and CATs were selected for Ca^{2+} imaging. With the microfluidic system, conidia (1 x 10^7 cells/ml) were loaded into the cell chamber and cultured with a 2 psi medium flow rate at 35°C for 2.5 h. A 100X objective was used for time-lapse imaging at room temperature.

The Ca^{2+} traces of 10 germlings with germ tubes are presented in Fig. 7.4

(Supplementary movie 19-28). The frequency of Ca^{2+} spiking seemed random. The Ca^{2+} traces of 10 pairs of whole germlings with CATs are presented in Fig. 7.5 (Supplementary movie 29-38). They also showed random Ca^{2+} spiking. To examine the possible relationship between Ca^{2+} signalling and the ping-pong mechanism of oscillatory MAK-2 recruitment during CAT chemotropism, conidia of Tef1-G6s-his-m1 and MAK-2-GFP were mixed and two CATs homing towards each other, and which were expressing GCaMP6s and the other MAK-2-GFP, were selected. The MAK-2-GFP expressed significantly brighter fluorescence than Tef1-G6s-his-m1 in the cytoplasm. Three results are showed in Fig. 7.6 (Supplementary movie 39-41). No 'in-phase' or 'anti-phase' correlation between these two signals was observed.

Upon making contact with each other and during attachment, two CATs undergo twisting relative to each other, a phenomenon described as 'CAT torque' (Lichius et al., 2014). To determine if $[Ca^{2+}]_c$ increased in the tip region of CATs during attachment and fusion, the GCaMP6s signal was measured in a region of interest (a 2 x 2 µm box) over the tips of the CATs. From these measurements, no increase in $[Ca^{2+}]_c$ was observed during CAT contact or attachment (Fig 7.7; supplementary movie 42-44).

7.3.5. $[Ca^{2+}]_c$ increases in conidial germlings were localized and developed into $[Ca^{2+}]_c$ waves

Time-lapse imaging showed that the transient increases of $[Ca^{2+}]_c$ were very dynamic. The $[Ca^{2+}]_c$ increase were typically localized within the cytoplasm and from this localized region in which the $[Ca^{2+}]_c$ increased and they developed into $[Ca^{2+}]_c$ waves which moved bi-directionally along the germling. The localized $[Ca^{2+}]_c$ increases often occurred in more than one region of a single germling. These features are all shown in Fig. 7.8 (Supplementary movie 45) in which two germlings with CATs growing towards each other have been imaged in the microfluidic culture system. These subcellular dynamics in $[Ca^{2+}]_c$ were averaged in the whole germlings (Figs. 7.3-7.7).

7.3.6. $[Ca^{2+}]_c$ waves are generated from localized $[Ca^{2+}]_c$ increases in vegetative hyphae and can move uni- or bi-directionally

Conidia were incubated in VM at 35^{o}C for 10 h to produce mature vegetative hyphae longer than 150 µm. The first 100 µm from the tips was visualized by time-lapse imaging and the total fluorescence intensity of GCaMP6s fluorescence for this region was measured (Fig 7.9). Interestingly, although most of the Ca^{2+} waves started from the tips and moved towards the base of each hypha (Fig. 7.10 A; supplementary movie 46), some $[Ca^{2+}]_c$ waves started subapically and moved bi-directionally along the hyphae (Fig. 7.10 B and C; supplementary movie 47 and 48).

7.3.7. The influence of pharmacological agents on Ca^{2+} spiking

To determine possible links between Ca^{2+} spiking, extracellular Ca^{2+} and other components of the Ca^{2+} signalling machinery, several Ca^{2+}-modulating pharmacological agents were applied to the germlings at close to their IC50 concentrations. These drugs were: the Ca^{2+} chelator BAPTA (5 µM); the CaM antagonist TFP (Fig. 3.11); the calcineurin inhibitor FK506 (Fig. 3.12); and the antifungal drug caspofungin (Fig. 3.14). All of the drugs had previously shown to inhibit CAT fusion (section 3.2.5-3.2.7) . BAPTA completely suppressed all Ca^{2+} spiking when cells were either incubated continuously over 4 h with the chelator or by adding it just before imaging (Fig. 7.11 and 7.12). The other 3 chemicals, on the contrary, generally increased the frequency of Ca^{2+} peaks compared to the untreated cells in normal VM (Figs 7.13-16).

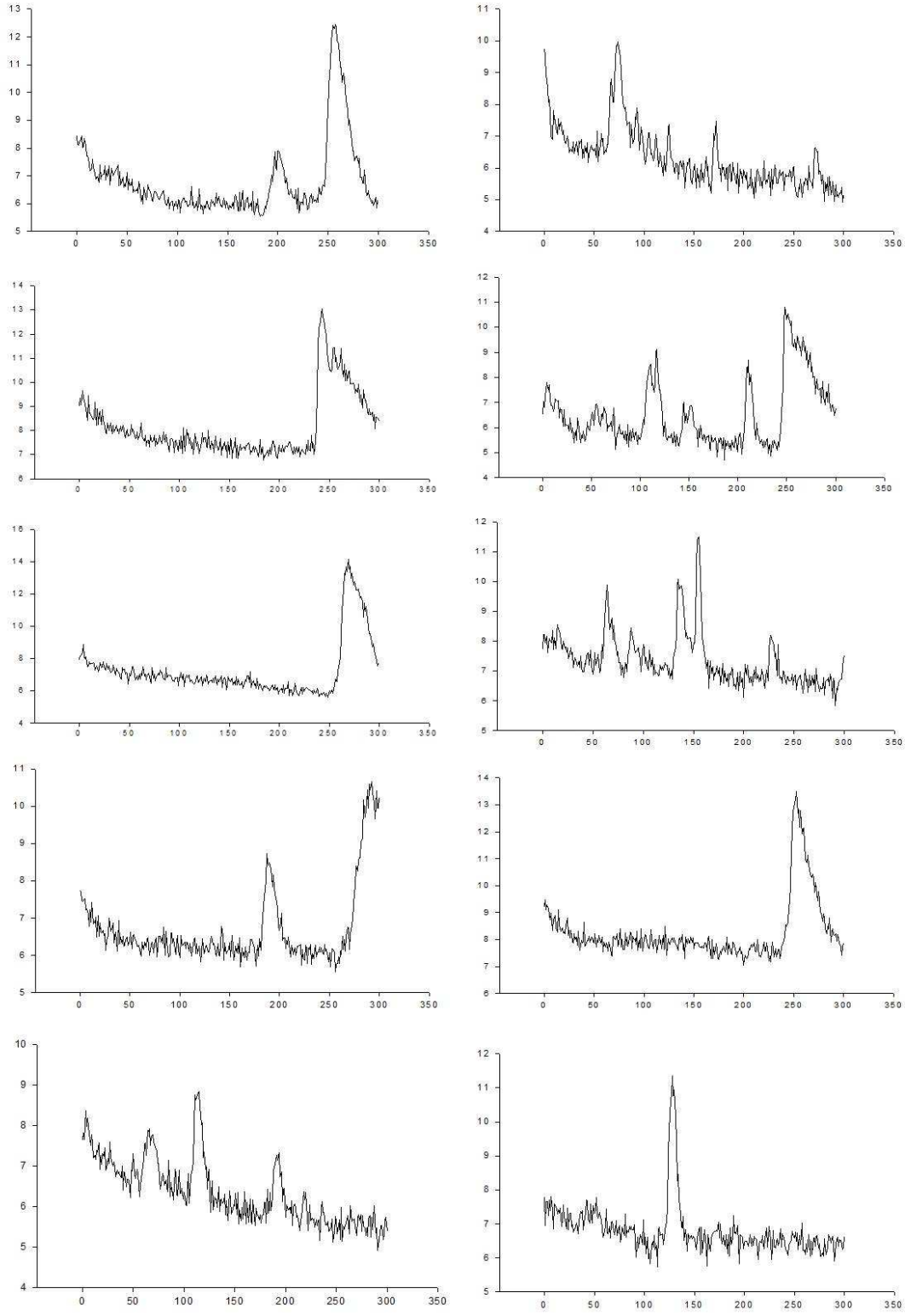

Figure 7.3 The length of $[Ca^{2+}]_c$ pulse was usually between 5 s and 50 s. Conidia were incubated in VM at 35^{o}C for 4 h and imaged at room temperature. Time-lapse Images captured with a 200 ms exposure time and 20 LED excitation intensity at 1 sec intervals for 5 min. The X axis represents time (s) and the Y axis represent fluorescence intensity.

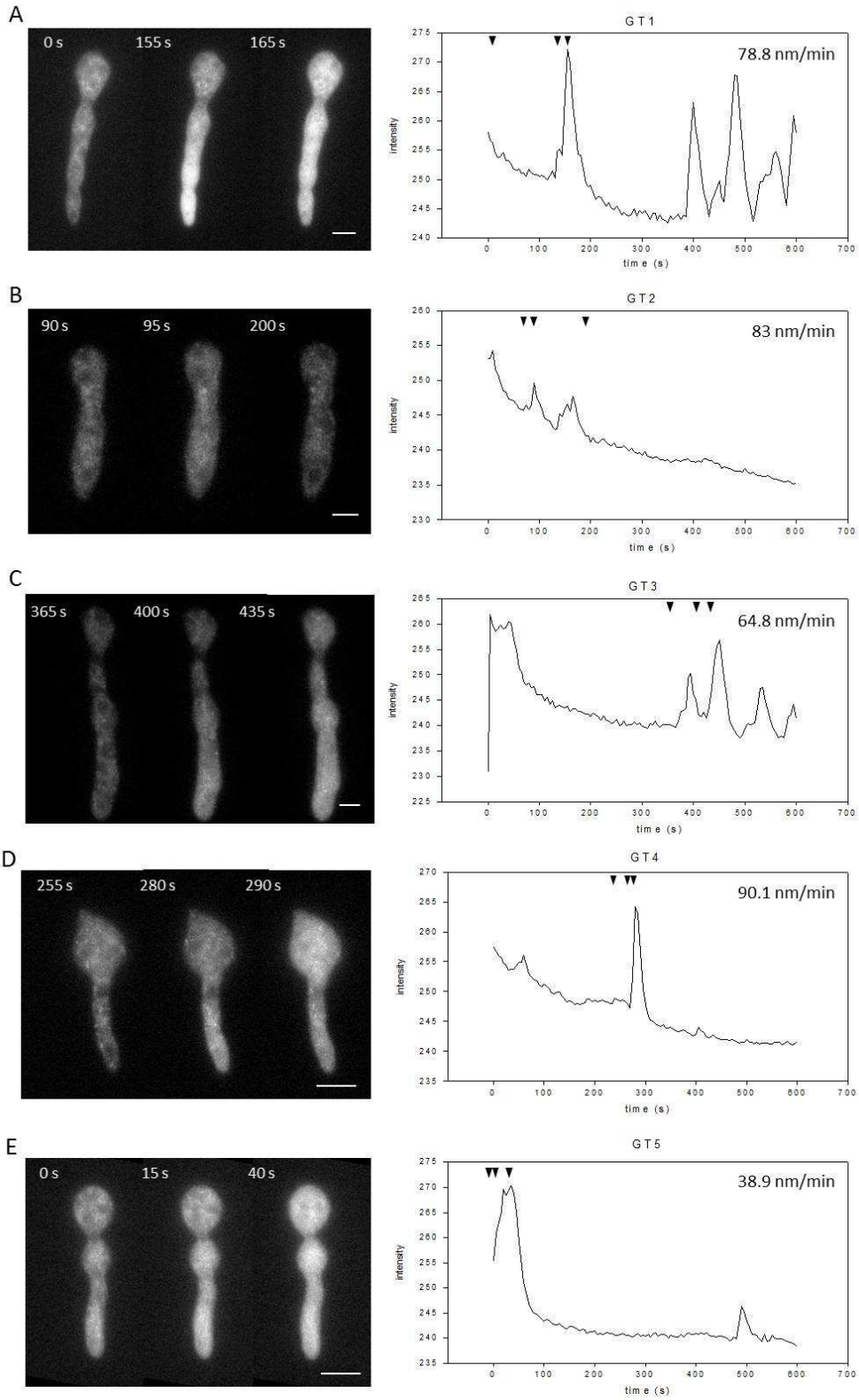

Figure 7.4 Ca^{2+} traces from whole germlings with germ tubes. Conidia were incubated in VM at 35^{o}C for 4 h and imaged at room temperature. Time-lapse Images were captured with a 200 ms exposure time and 20 LED excitation intensity at 1 sec intervals for 5 min. The time points of the images shown on the left are arrowed in the figure. The germ tube extension rates are shown in the top right corner of each figure. Bar = 5 µm.

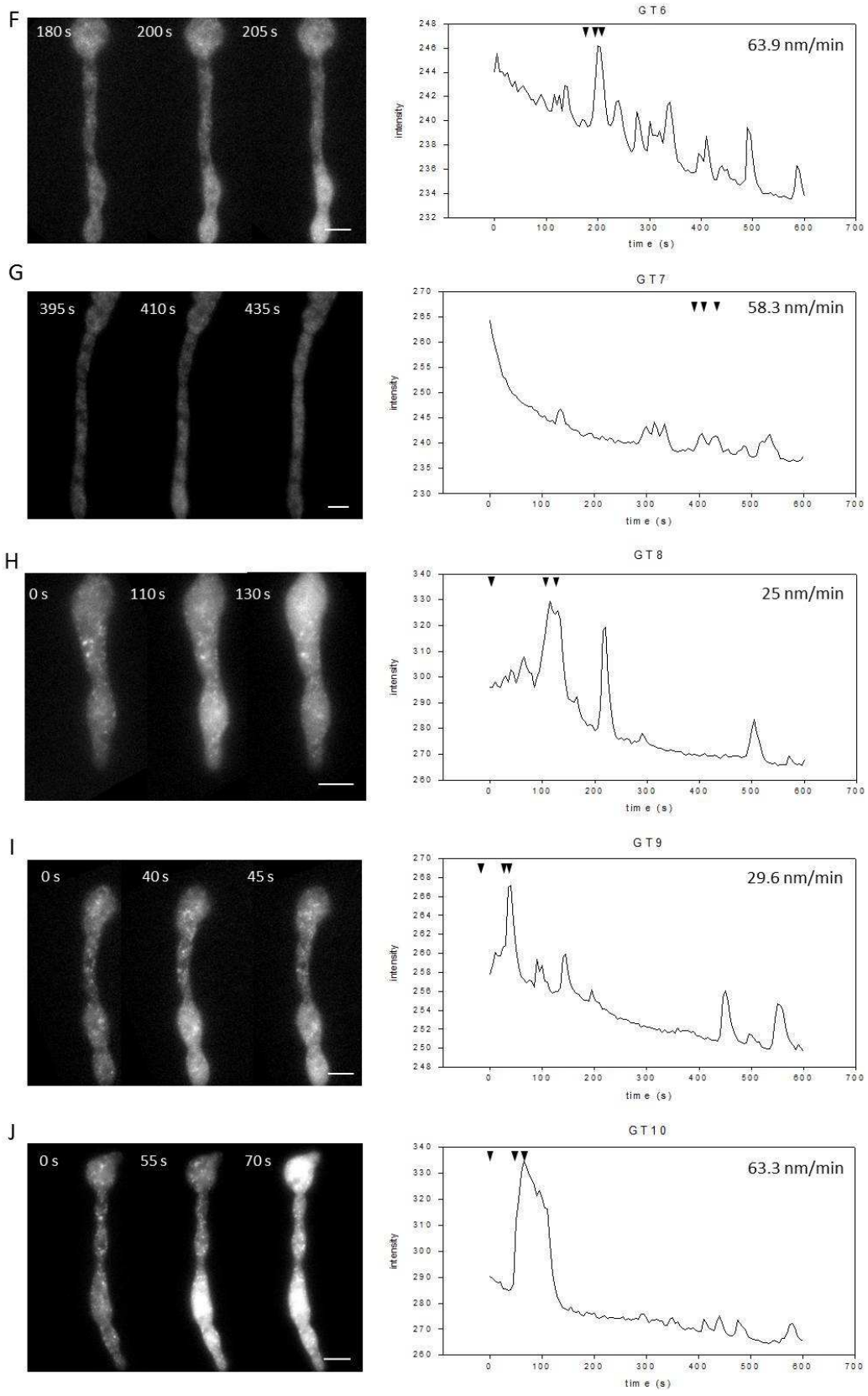

Figure 7.4 Ca^{2+} traces in whole germlings with in germ tubes (continued).

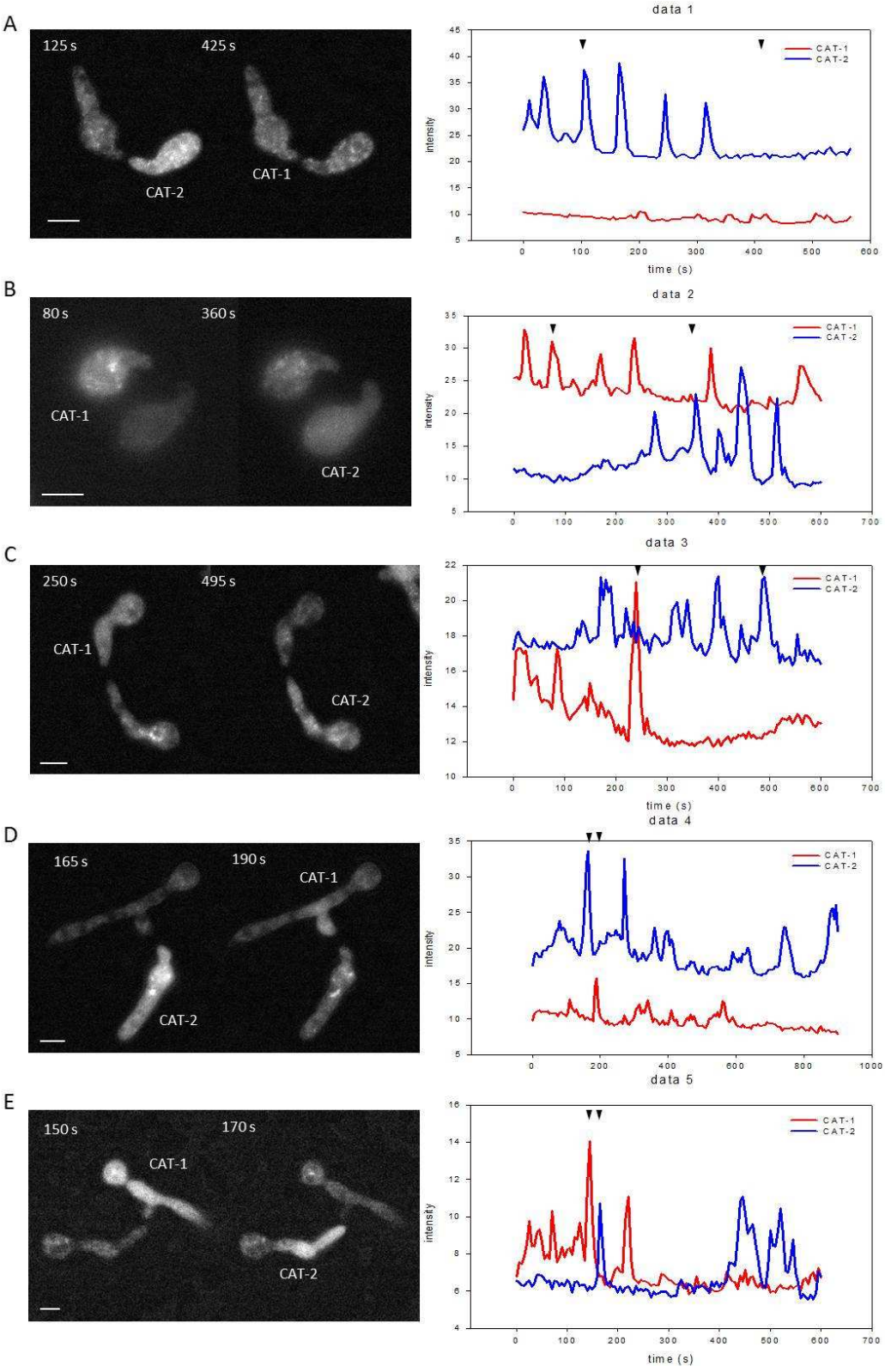

Figure 7.5 Ca^{2+} traces of two whole germlings (red and blue) undergoing CAT chemotropism. Conidia were incubated in VM at 35°C for 4 h and imaged at room temperature. Time-lapse Images captured with a 200 ms exposure time and 20 LED excitation intensity at 1 sec intervals for 5 min. The time points of the images shown on the left are arrowed in the figure. Bar = 5 µm.

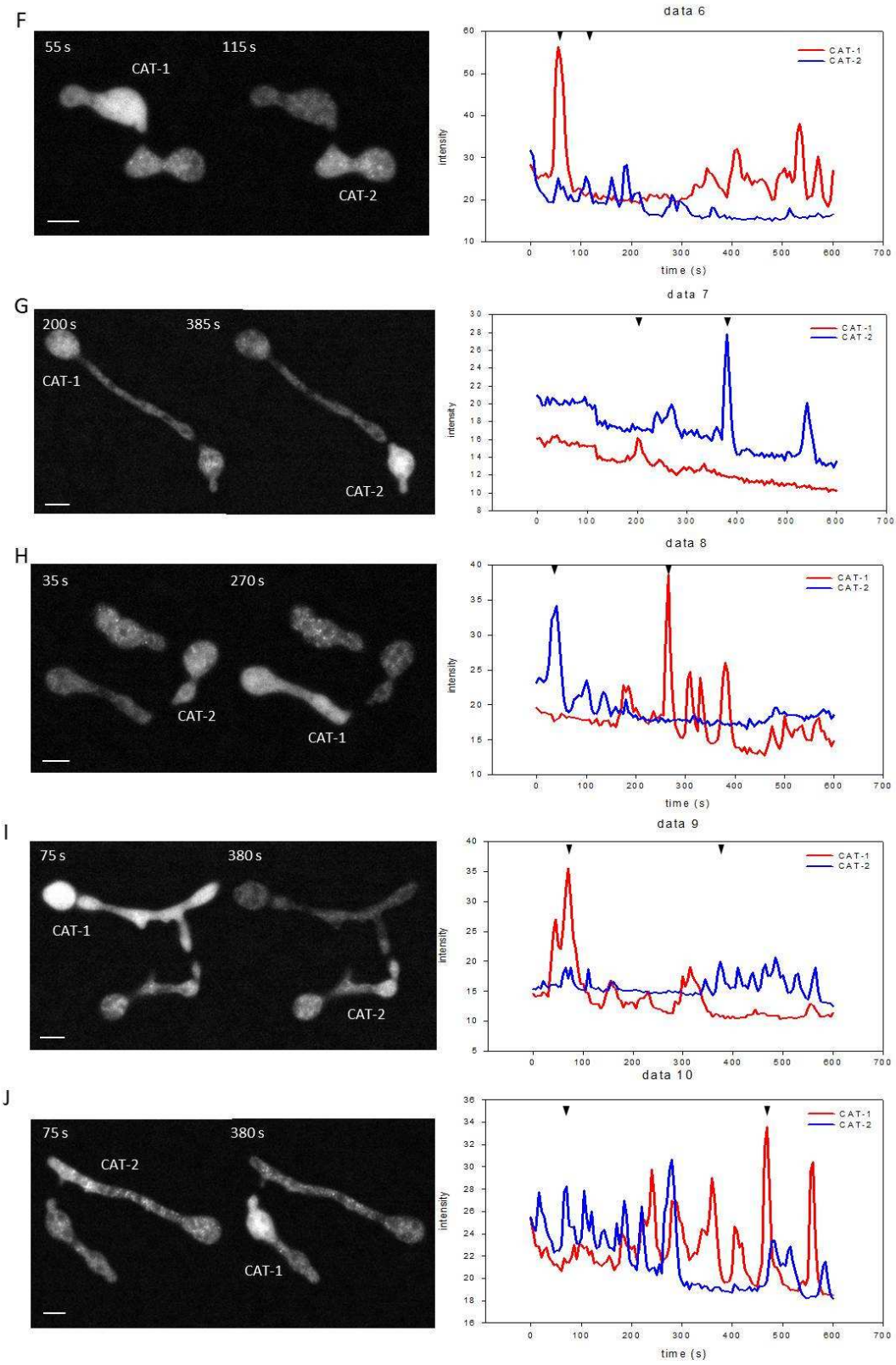

Figure 7.5 The Ca^{2+} traces of two whole germlings (red and blue) undergoing CAT chemotropism (continued).

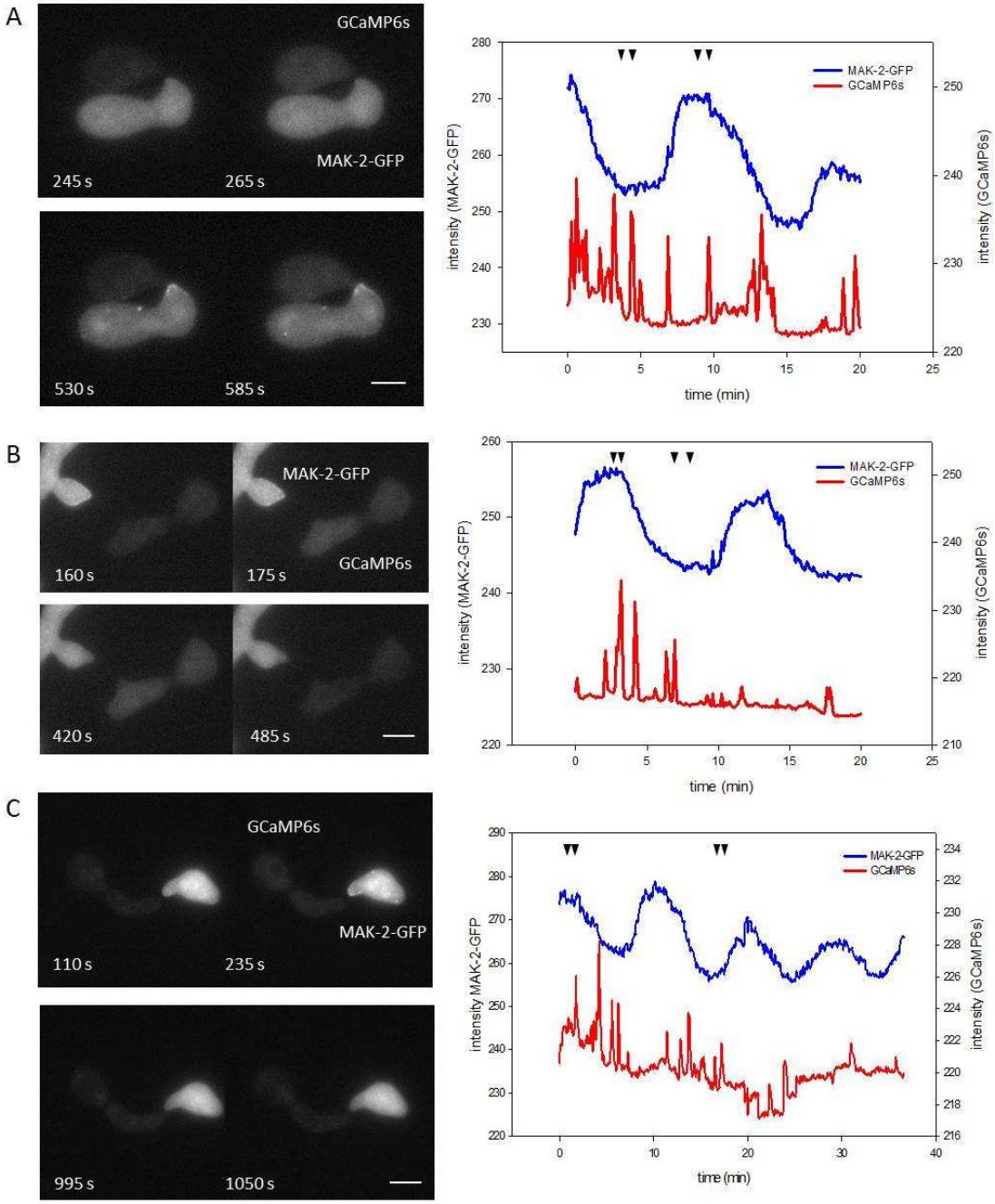

Figure 7.6 Ca^{2+} traces within whole germlings with CATs undergoing chemotropism to corresponding CATs exhibiting oscillatory of MAK-2. Conidia of GCaM6s and MAK-2-GFP were mixed in equal quantities (total cell density = 10^6 cells/ml). The cell suspension was incubated in VM at 35^{o}C for 4 h and imaged at room temperature. Time-lapse Images captured with a 200 ms exposure time and 20 LED excitation intensity at 5 sec intervals for 20-37 min. The time points of the images shown on the left are arrowed in the figures on the right. Bar = 5 µm.

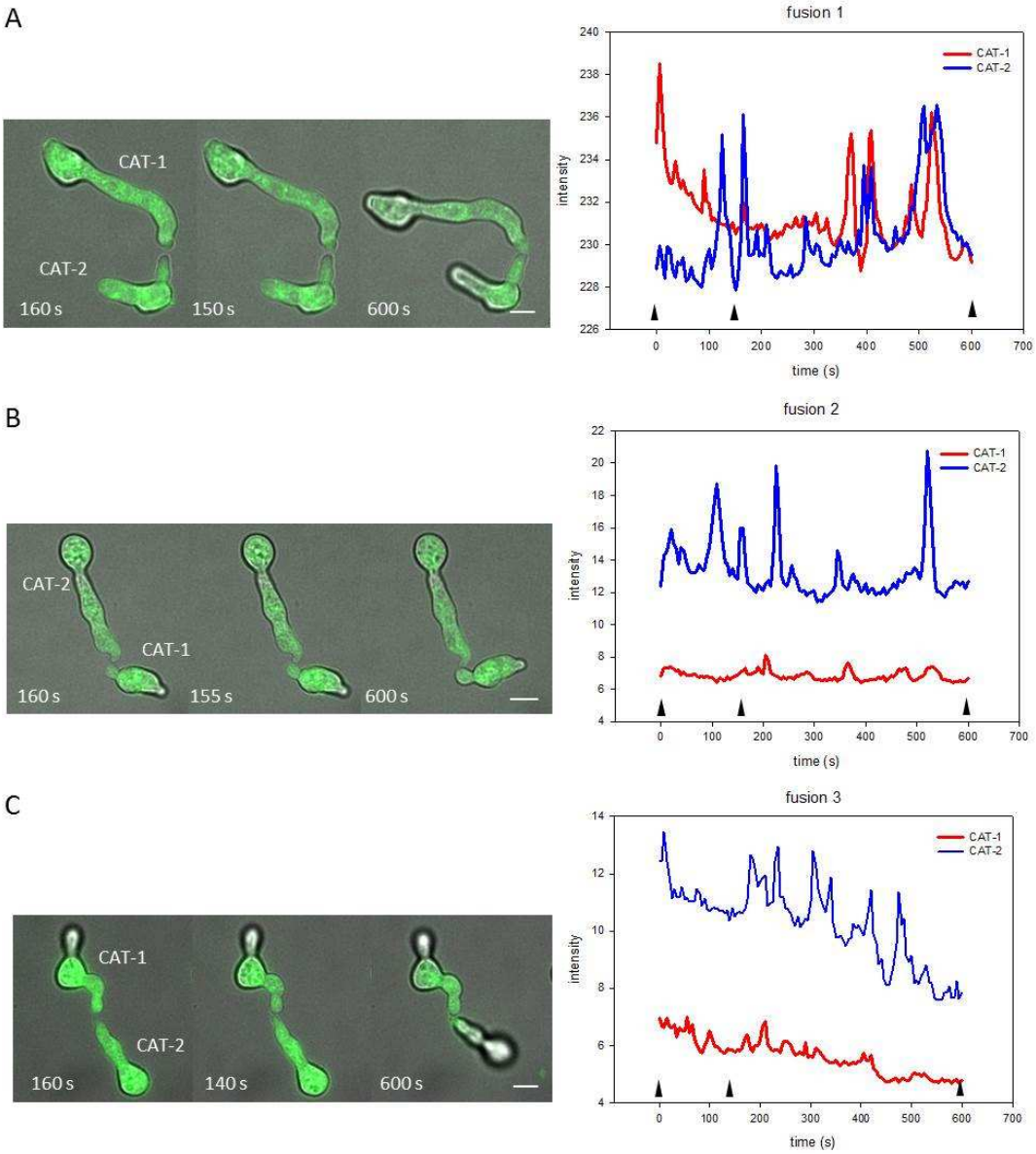

Figure 7.7 Ca^{2+} traces of two whole germlings undergoing CAT fusion. Conidia were incubated in VM at 35°C for 4 h and imaged at room temperature. Time-lapse Images captured with a 200 ms exposure time and 20 LED excitation intensity at 5 sec intervals for 20-37 min. The time points of the images shown on the left are arrowed in the figures on the right. A region including the whole germling during CAT torque was selected to measure the intensity. Bar = 5 µm.

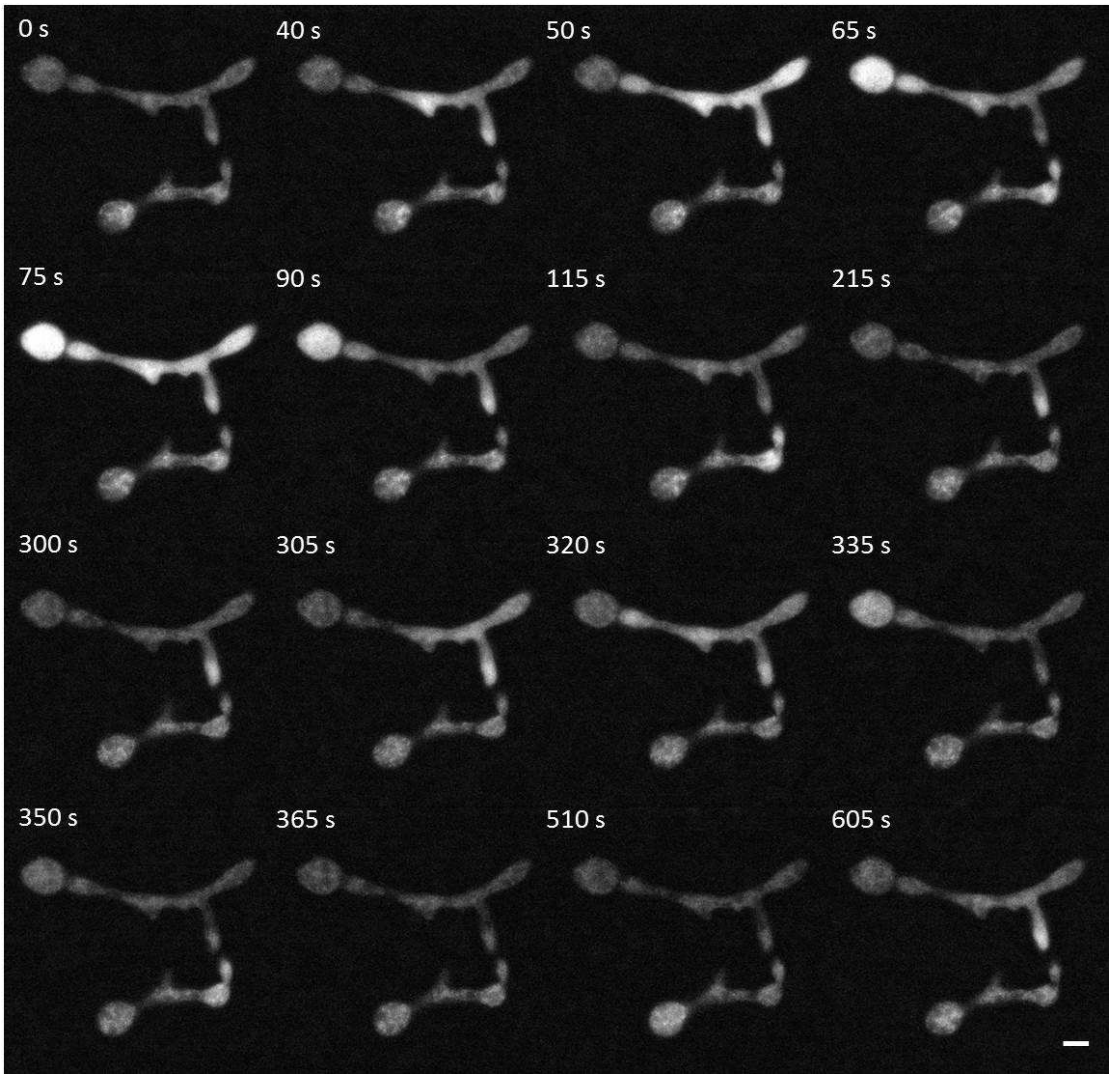

Figure 7.8 $[Ca^{2+}]_c$ increases in germlings are very dynamic and localized, and also occur in the form of $[Ca^{2+}]_c$ waves. Conidia were incubated in VM at 35^{o}C for 4 h and imaged at room temperature. Time-lapse Images were captured with a 200 ms exposure time and 20 LED excitation intensity at 5 sec intervals for 20 min. The two germlings shown in this time course possess CATs that have formed from germ tubes. The CATs are undergoing chemotropism towards each other. Bar = 5 µm.

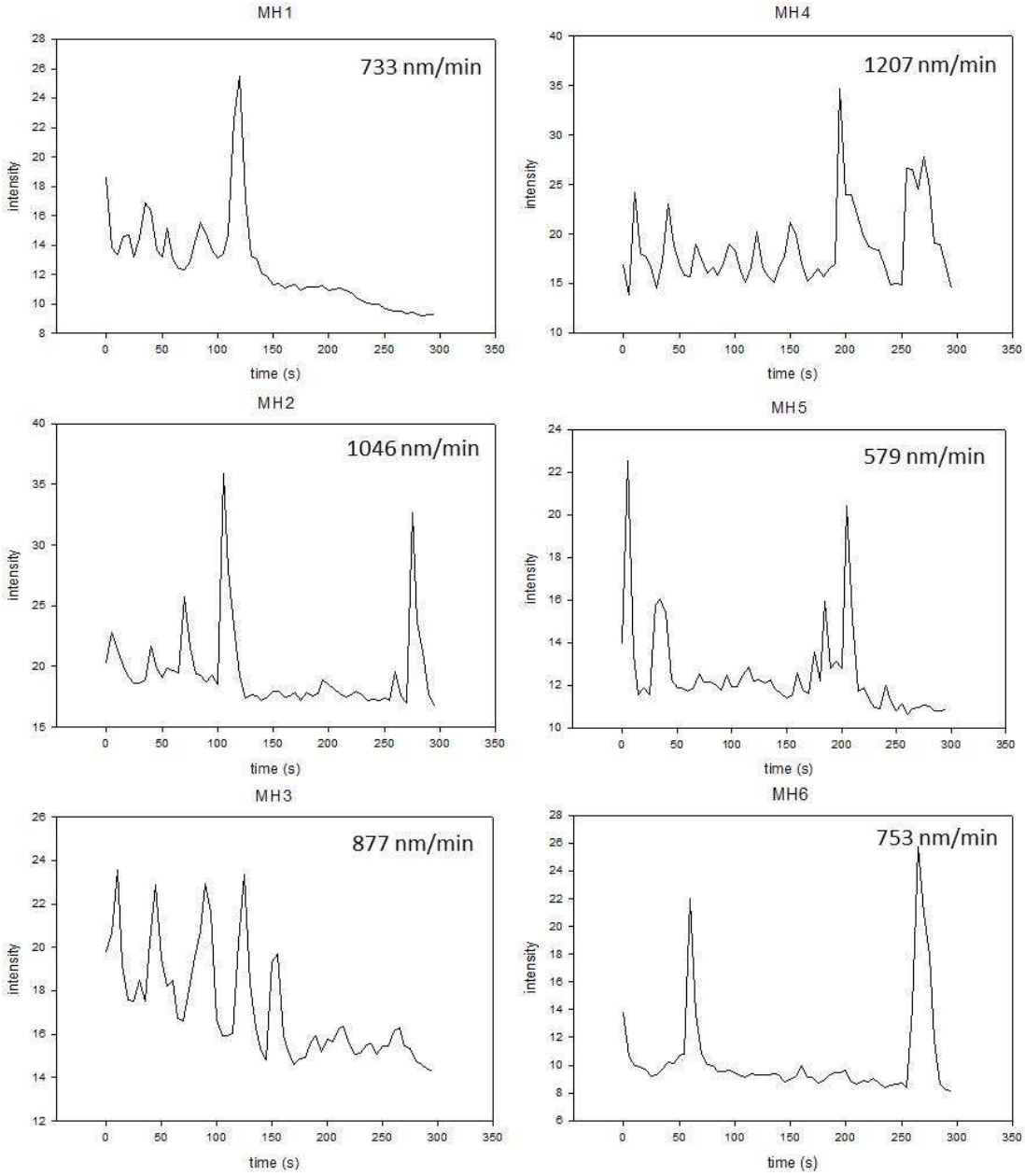

Figure 7.9 Timecourses of the Ca^{2+} spiking (GCaMP6s fluorescence) over the first 100 µm of growing tips of vegetative hyphae. Measurements represent the total GCaMP6s fluorescence over the first 100 µM region of the hyphal tips. Conidia were incubated in VM at 35^{o}C for 10 h and imaged at room temperature. Time-lapse images were captured with a 200 ms exposure time and 20 LED excitation intensity at 5 sec intervals for 5 min. The hyphal extension rates are shown in the top right corner of each figure.

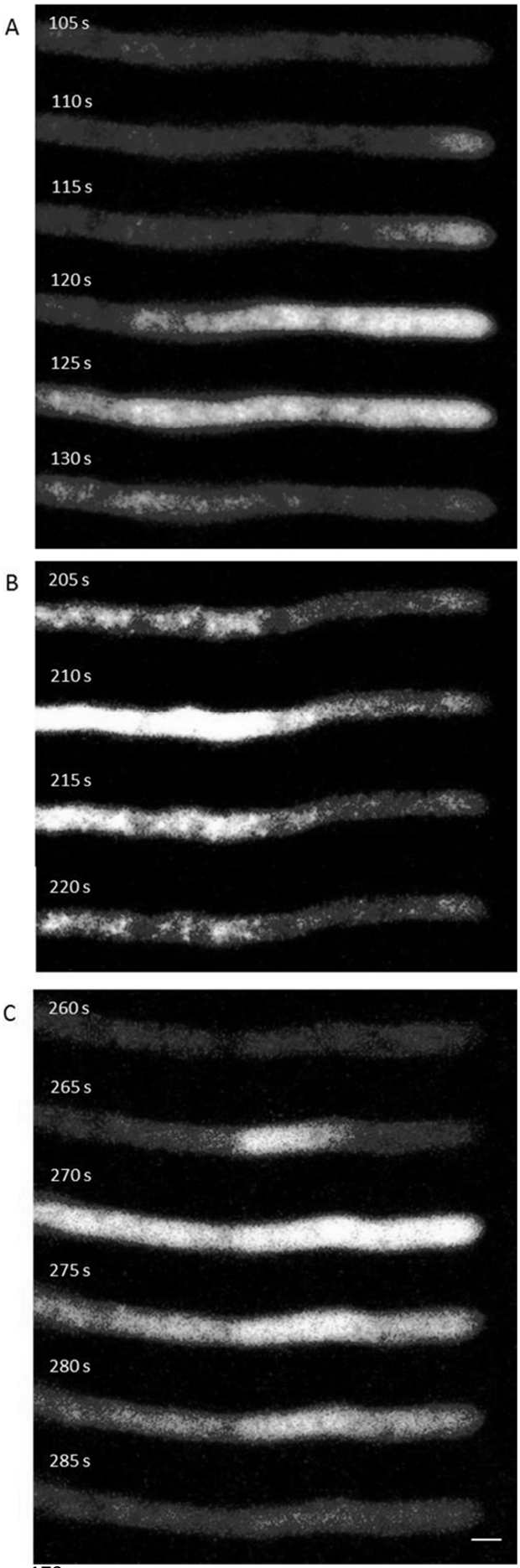

Figure 7.10 Time-lapse imaging of $[Ca^{2+}]_c$ waves in vegetative hyphae. Conidia were incubated in VM at 35°C for 10 h and imaged at room temperature. Time-lapse images were captured with a 200 ms exposure time and 20 LED excitation intensity at 5 sec intervals for 5 min. (A) Localized $[Ca^{2+}]_c$ increase occurred at the tip (110 s) and then moved in a wave basically. (B) A localized transient increase of $[Ca^{2+}]_c$ occurred subsequently and moved apically. Bar = 10 µm.

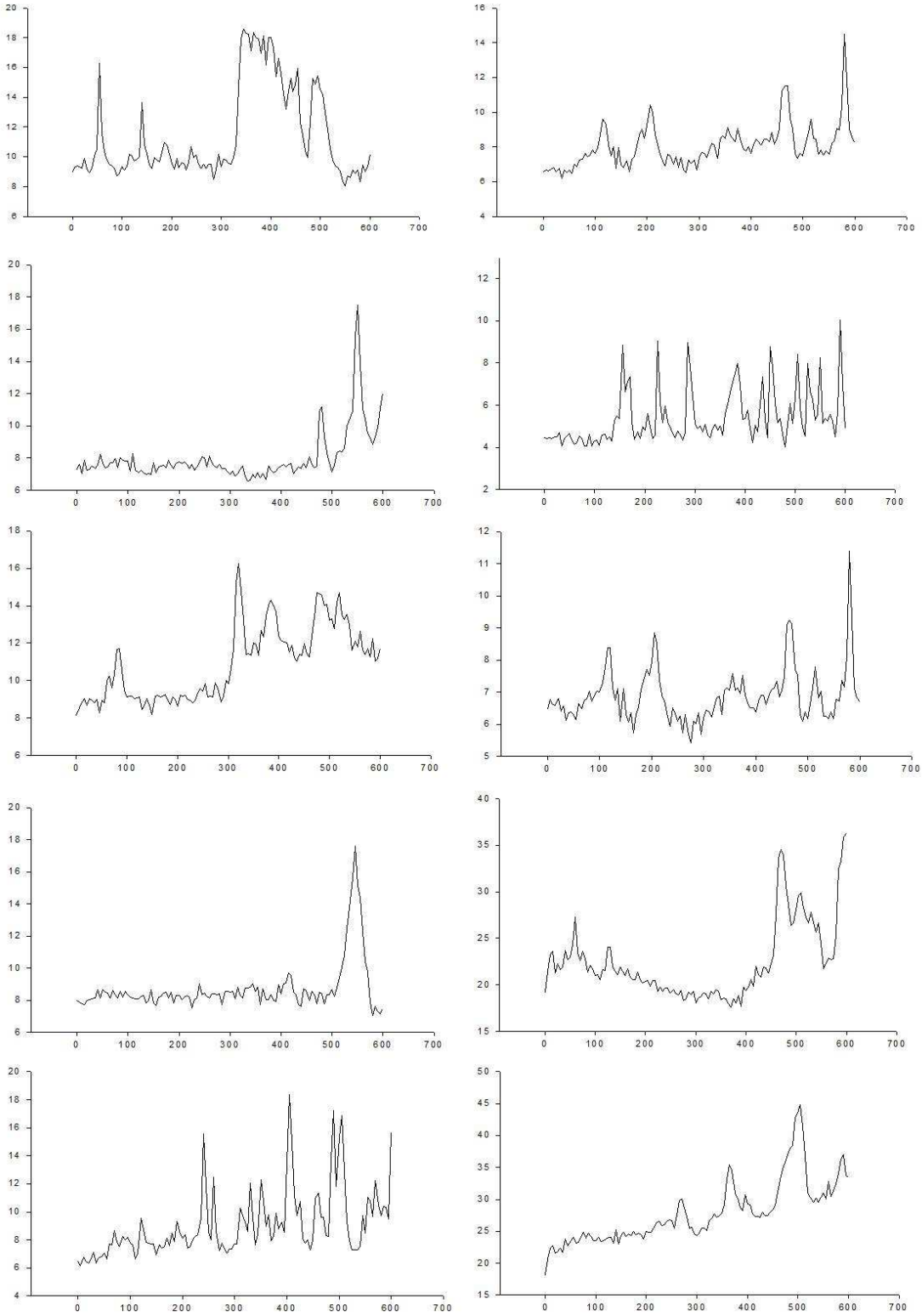

Figure 7.11 Ca^{2+} traces of untreated whole germlings as controls. Conidia were incubated in VM at 35^{o}C for 4 h and imaged at room temperature. Time-lapse Images captured with a 200 ms exposure time and 20 LED excitation intensity at 1 sec intervals for 10 min. The X axis represents time (s) and the Y axis represent fluorescence intensity.

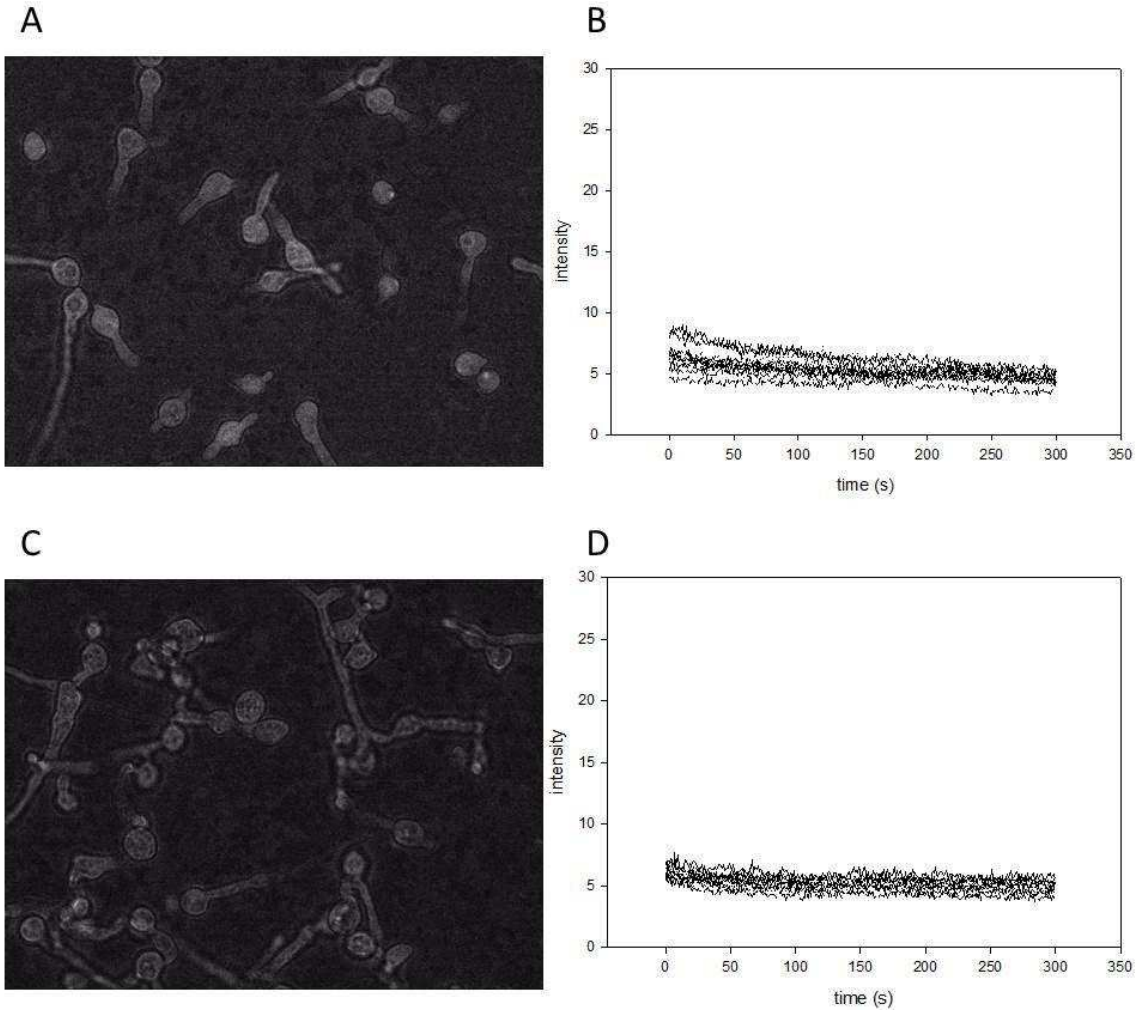

Figure 7.12 The removal of extracellular Ca^{2+} prevents Ca^{2+} spiking in germlings. Time-lapse Images captured with a 200 ms exposure time and 20 LED excitation intensity at 5 sec intervals for 5 min. (A) Conidia were incubated in VM with 3 µM BAPTA at 35^{o}C for 4 h and imaged at room temperature. (B) Ten germlings were chosen randomly from A to measure the fluorescent intensity (10 traces). (C) Conidia were incubated in VM at 35^{o}C for 4h. Three µM BAPTA was added just before the imaging at room temperature. (D) Ten germlings were chosen randomly from C to measure the fluorescent intensity (10 traces).

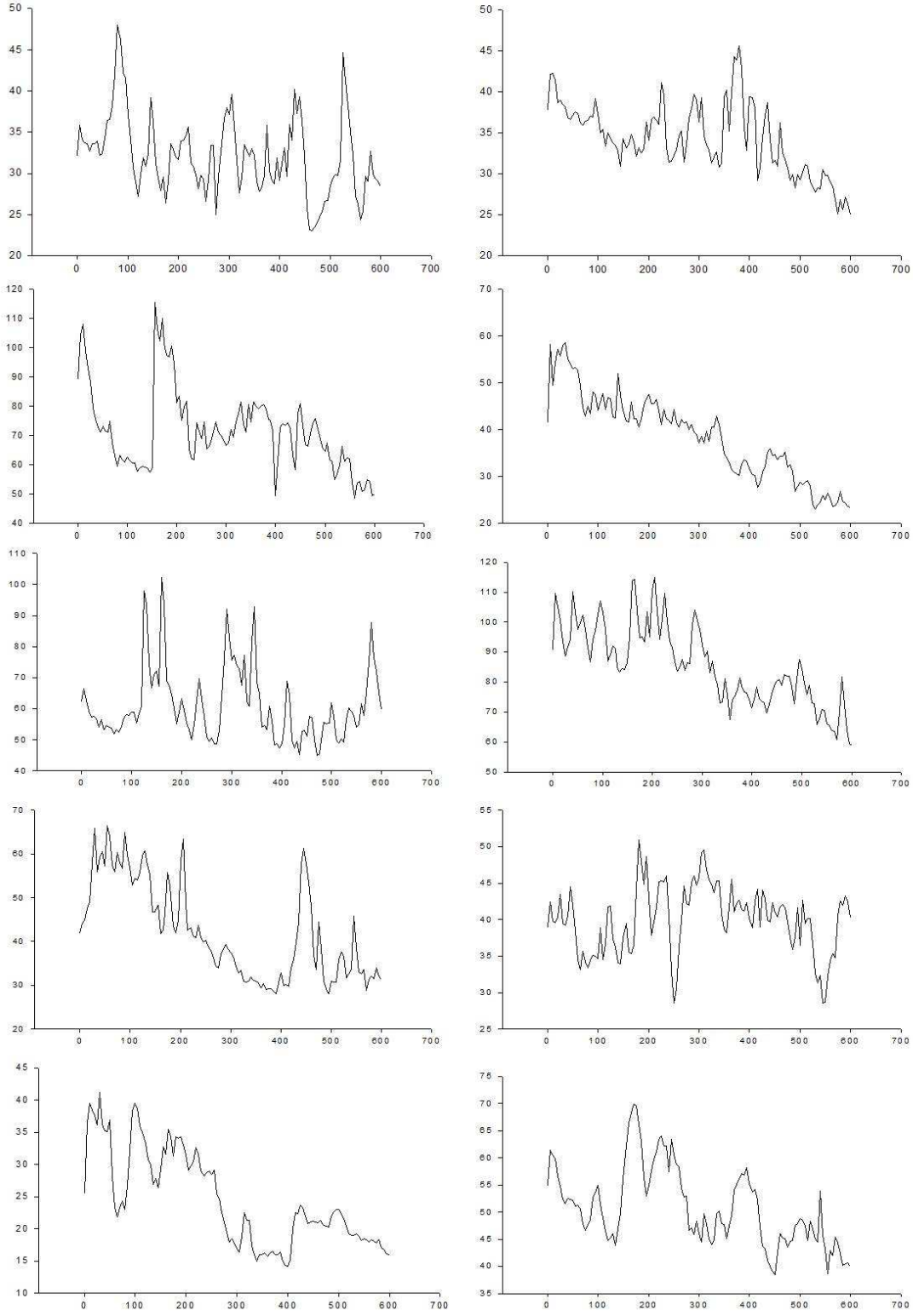

Figure 7.13 Examples of Ca^{2+} traces from whole germlings treated with 25 µM TFP. Conidia were incubated in VM with 25 µM TFP at 35°C for 4 h and imaged at room temperature. Time-lapse images were captured with a 200 ms exposure time and 20 LED excitation intensity at 5 sec intervals for 10 min. The X axis represents time (s) and the Y axis represents signal intensity.

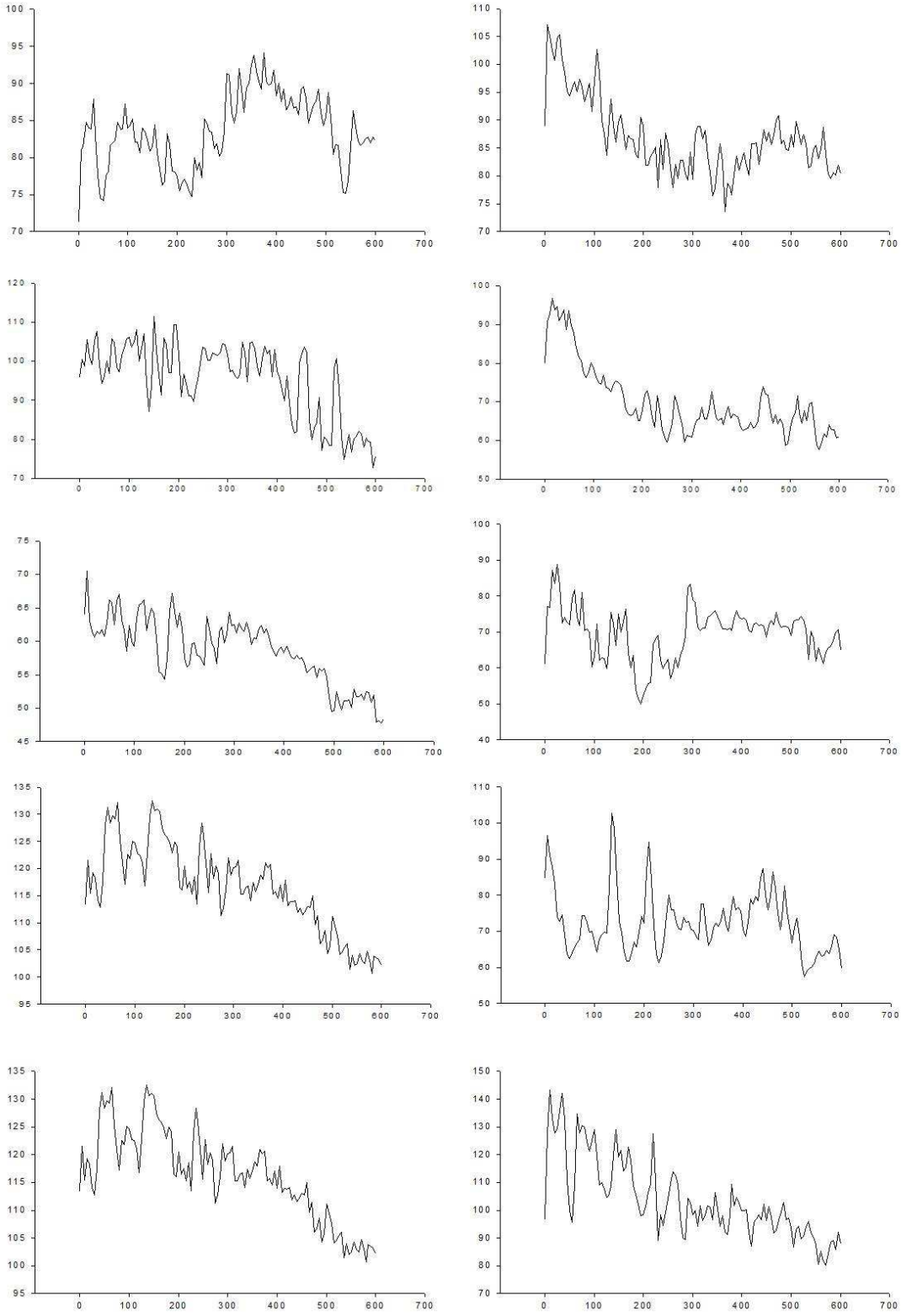

Figure 7.14 Examples of Ca^{2+} traces from whole germlings treated with 5 µg/ml FK506. Conidia were incubated in VM with 5 µg/ml FK506 at 35^{o}C for 4 h and imaged at room temperature. Time-lapse images were captured with a 200 ms exposure time and 20 LED excitation intensity at 5 sec intervals for 10 min. The X axis represents time (s) and the Y axis represents signal intensity.

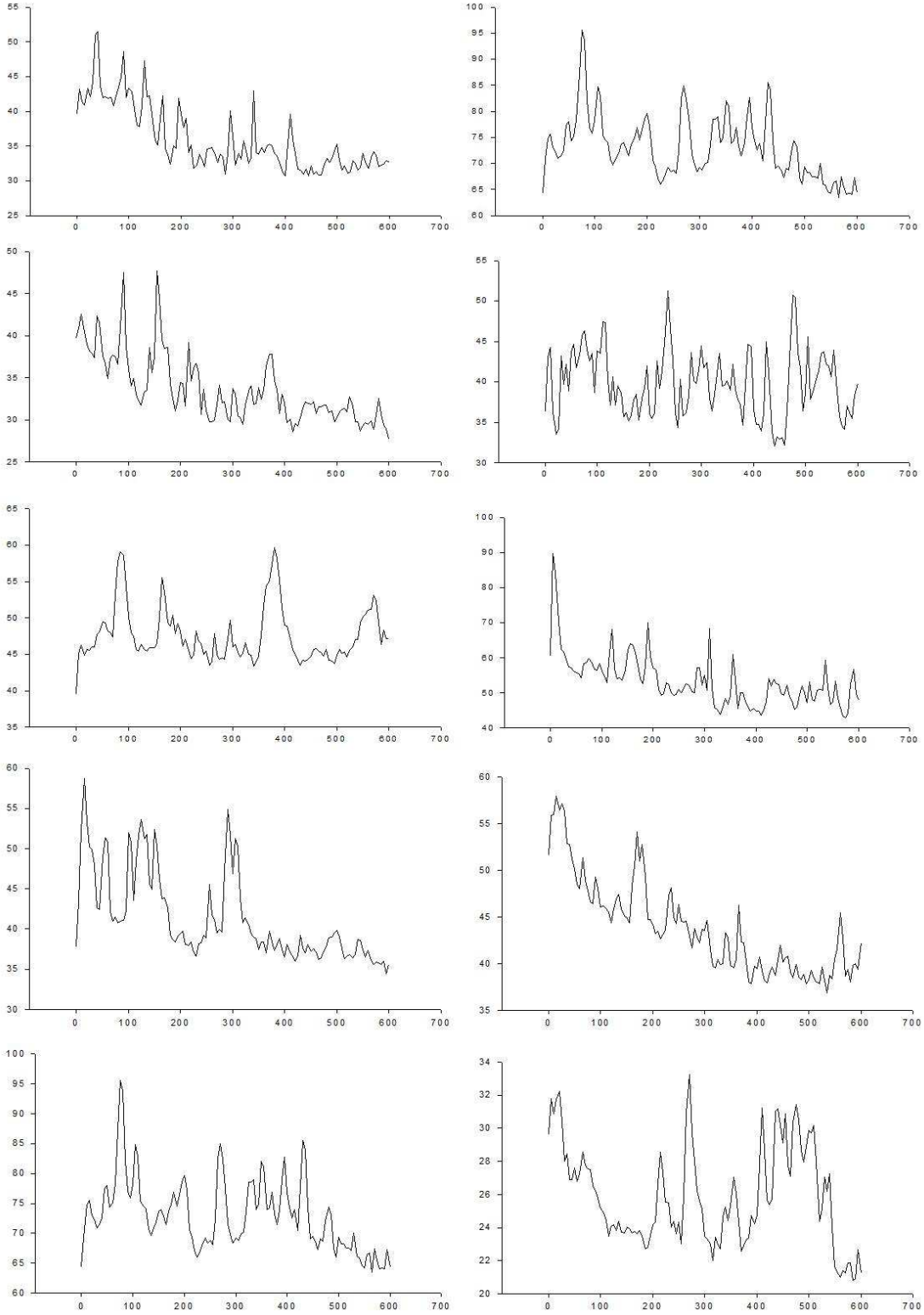

Figure 7.15 Examples of Ca^{2+} traces from whole germlings treated with 5 µg/ml caspofungin. Conidia were incubated in VM with 5 µg/ml caspofungin at 35^{o}C for 4 h and imaged at room temperature. Time-lapse images were captured with a 200 ms exposure time and 20 LED excitation intensity at 5 sec intervals for 10 min. The X axis represents time (s) and the Y axis represents signal intensity.

7.3. Discussion

7.3.1. GCamP6s provides a novel Ca^{2+} reporter for live-cell imaging of Ca^{2+} in filamentous fungi

Several versions of GCaMPs with different protein sequences were analyzed using BioEdit software (Fig. 7.16 C). The most recently developed GCaMP6 family have been reported to outperform other GCaMPs sensors in cultured neurons and in zebrafish, flies and mice (Chen et al., 2013). GCaMP6s, which has 4 mutated sites on the interface between cpGFP and CaM relative to GCaMP5G (Fig. 7.16 A) was chosen to be tested in *N.crassa* because of its highest sensitivity (Fig. 7.16 B). GCaMP6s produced sevenfold larger signals than GCaMP5 and > 10-fold larger signals than GCaMP3 in neurons. Compared to GCaMP5G, GCaMP6s also exhibited a threefold higher affinity for Ca^{2+} and a 1.3-fold higher Ca^{2+} saturated fluorescence, but with a similar baseline fluorescence (Chen et al., 2013).

Two different promoters (*pccg-1* and *ptef-1*) and two methods of gene targeting (*his* locus and ectopic insertion) were used to construct plasmids and transform *N. crassa* (Fig. 7.1). In germlings, GCaMP6s, but not GCaMP5, produced detectable Ca^{2+} spikes using widefield fluorescence microscopy. In addition, the *tef-1* promoter performed better than the *ccg-1* promoter for GCaMP6s during colony initiation. Mutants with the ectopic targeting influenced phenotypes more than targeting in his loci. Other unpublished results from the Read lab have shown reasonable expression of GCaMP5 and very strong expression of GCaMP6s in *A. fumigatus*. This indicates that the level of GCaMP expression varies between different filamentous fungi. Due to the low level of expression of GCaMP6s in *N. crassa*, it was not possible to image $[Ca^{2+}]_c$ for period longer than 30 min because of the photobleaching and phototoxicity.

7.3.2. The internal Ca^{2+} spikes were positively correlated with extracellular Ca^{2+}

In this chapter, I have reported the first imaging of $[Ca^{2+}]_c$ dynamics in *N. crassa.* Localized increases in $[Ca^{2+}]_c$ and $[Ca^{2+}]_c$ waves were routinely observed in conidial germlings and vegetative hyphae growing in Vogel's medium. Ca^{2+} spiking was observed within germlings possessing germ tubes or CATs and there was no clear

indication that any of the Ca^{2+} spiking or tip localized increases in CAT $[Ca^{2+}]_c$ were related to CAT chemotropism or CAT fusion. However, when Ca^{2+} was removed from the medium the Ca^{2+} spiking disappeared. It was shown in chapter 3 that CAT chemotropism is extracellular Ca^{2+}-dependent. One interpretation, therefore, is that extracellular Ca^{2+} is required for the activity of the chemoattractant or receptor on their own. With regard to the Ca^{2+} spiking, unpublished results from the Read's lab suggest that internal Ca^{2+}-spike frequency and extracellular Ca^{2+} (75 – 1000 μM) are does-dependent (P. Hernande-Ortiz and N. D. Read, unpublished). Removal of extracellular Ca^{2+} also decreased the $[Ca^{2+}]_c$ waves which in animal cells involves Ca^{2+}-induced Ca^{2+} release from ER (Endo, 1977). Assuming that Ca^{2+} waves in fungal cells are propagated in a similar manner, my results suggest that the extracellular Ca^{2+} is required as an initial stimulus for the Ca^{2+} waves to be initiated. Meanwhile, tools of mathematical analysis are required for further analysis of peak frequency.

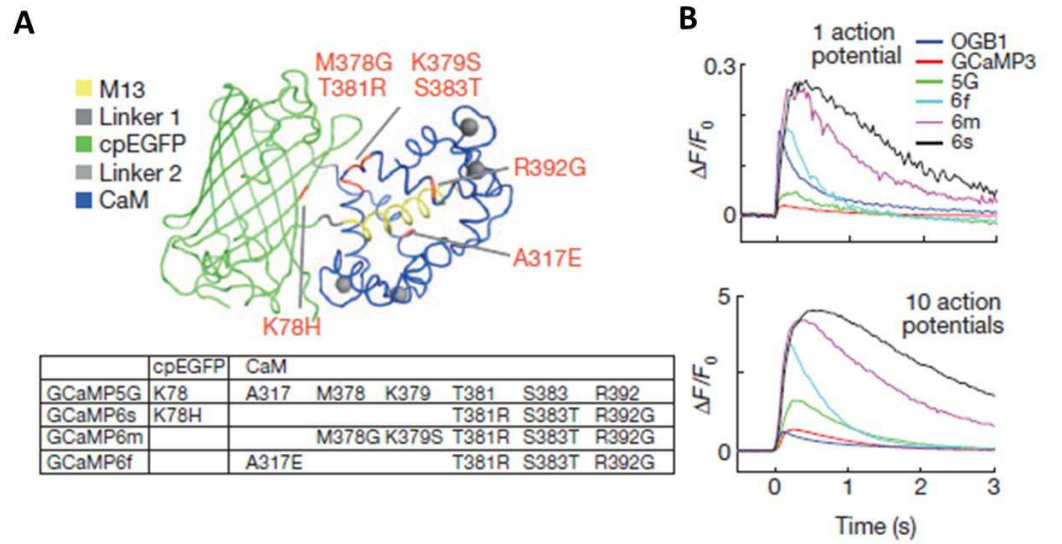

	cpEGFP	CaM					
GCaMP5G	K78	A317	M378	K379	T381	S383	R392
GCaMP6s	K78H				T381R	S383T	R392G
GCaMP6m			M378G	K379S	T381R	S383T	R392G
GCaMP6f		A317E			T381R	S383T	R392G

C

```
                    10        20        30        40        50        60        70        80        90       100
                    ....|....|....|....|....|....|....|....|....|....|....|....|....|....|....|....|....|....|
GCaMP3              MGSHHHHHHGMASMTGGQQMGRDLYDDDDKDLATMVDSSRRKWNKTGHAVRAIGRLSSLENVYIKADKQKNGIKANFKIRHNIEDGGVQLAYHYQQNTPI
GCaMP5              ..........................................................................................
GCaMP6s             ..........................................................H.......................................
GCaMP6m             ..........................................................................................
GCaMP6f             ..........................................................................................

                   110       120       130       140       150       160       170       180       190       200
                    ....|....|....|....|....|....|....|....|....|....|....|....|....|....|....|....|....|....|
GCaMP3              GDGPVLLPDNHYLSVQSKLSKDPNEKRDHMVLLEFVTAAGITLGMDELYKGGTGGSMVSKGEELFTGVVPILVELDGDVNGHKFSVSGEGEGDATYGKLT
GCaMP5              ..........................................................................................
GCaMP6s             ..........................................................................................
GCaMP6m             ..........................................................................................
GCaMP6f             ..........................................................................................

                   210       220       230       240       250       260       270       280       290       300
                    ....|....|....|....|....|....|....|....|....|....|....|....|....|....|....|....|....|....|
GCaMP3              LKFICTTGKLPVPWPTLVTTLTYGVQCFSRYPDHMRQHDFFKSAMPEGYIQERTIFFKDDGNYKTRAEVKFEGDTLVNRIELKGIDFKEDGNILGHKLEY
GCaMP5              ..........................................................................................
GCaMP6s             ..........................................................................................
GCaMP6m             ..........................................................................................
GCaMP6f             ..........................................................................................

                   310       320       330       340       350       360       370       380       390       400
                    ....|....|....|....|....|....|....|....|....|....|....|....|....|....|....|....|....|....|
GCaMP3              NTRDQLTEEQIAEFKEAFSLFDKDGDGTITTKELGTVMRSLGQNPTEAELQDMINEVDADGDGTIDFPEFLTMMARRMKDTDSEEEIREAFRVFDKDGNG
GCaMP5              .LP.....................................................................Y.................
GCaMP6s             .LP.....................................................................YR.T.....G.........
GCaMP6m             .LP.....................................................................GSYR.T.....G.........
GCaMP6f             .LP.............E.......................................................YR.T.....G.........

                   410       420       430       440       450
                    ....|....|....|....|....|....|....|....|....|.
GCaMP3              YISAAELRHVMTNLGEKLTDEEVDEMIREADIDGDGQVNYEEFVQMMTAK*
GCaMP5              ..................................................*
GCaMP6s             ..................................................*
GCaMP6m             ..................................................*
GCaMP6f             ..................................................*
```

Figure 7.16 GCaMP mutagenesis and screening in dissociated neurons. (A) GCaMP structure (Akerboom et al., 2009; Wang et al., 2008) and mutations in different GCaMP variants relative to GCaMP5G. (B) Responses averaged across multiple neurons and wells for GCaMP3, 5G, 6f, 6m, 6s, and a synthetic calcium dye, OGB1-AM. Top, fluorescence changes in response to 1 action potential. Bottom, 10 action potentials (Chen et al., 2013). Images (A and B) were copied from Chen et al., 2013 (C) The comparison of protein sequences in different GCaMPs. Sequences were from NCBI database and analyzed by BioEdit software.

7.4. Summary

- GCaMP6s has been used for the first time to image $[Ca^{2+}]_c$ dynamics in *N. crassa.*
- GCaMP6s under the control of the *tef-1* promoter produced the best expression in germlings, although the expression was not very high.
- Localized, transient increases in $[Ca^{2+}]_c$ occurred in germlings grown in Vogel's media which was manifested as Ca^{2+} spikes lasting 5 s to 50 s when total GCaMP6s fluorescence was measured in a single germling.
- The localized $[Ca^{2+}]_c$ increases developed into Ca^{2+} waves in both germlings and vegetative hyphae.
- The removal of extracellular Ca^{2+} by BAPTA abolished the $[Ca^{2+}]_c$ spiking in germlings growing in Vogel's medium.
- The Ca^{2+}-modulating drugs TFP, FK506 and caspofungin increased the frequency of Ca^{2+} spiking in Vogel's medium.
- No evidence for $[Ca^{2+}]_c$ transients associated with the 'ping-pong' mechanism of CAT chemotropism was obtained
- Extracellular Ca^{2+} may be involved in the interaction of the CAT chemoattractant with its receptor or is required for the activity of the CAT chemoattractant or receptor

Chapter 8

General discussion and future work

Chapter 8 – General discussion and future work

8.1. General discussion and future work

Ca^{2+} signalling plays a significant role in eukaryotic cells. Ca^{2+} signalling has been previously shown to be involved in regulating numerous processes in filamentous fungi based on genomic analyses, pharmacological studies, and the imaging and measurement of intracellular Ca^{2+}. However, we still know very little about Ca^{2+} signalling in filamentous fungi compared to what is known in animals and plants. The primary goal of my PhD research was to provide a comprehensive identification of the Ca^{2+}/CaM signalling machinery in *N. crassa* and analyze the role of Ca^{2+} signalling during colony initiation. The formation of germ tubes, which are involved in colony establishment (Araujo-Palomares et al., 2007), and conidial anastomosis tube (CAT)-mediated fusion, which is involved the production of cell networks (Poggeler and Kuck, 2004), are two developmental pathways that occur during colony initiation.

In Chapter 3, to further analyze the potential role of extracellular Ca^{2+} previously shown to be involved in CAT chemotropism (Chu, 2013), Ca^{2+} was added back to the non-fused germlings in Ca^{2+}-free growth medium for 4 h. This resulted in CATs growing towards each other chemotropically and fusing again. The long-term (> 6 h) absence of extracellular Ca^{2+} caused CATs to develop into germ tubes. Adding the Ca^{2+} chelator, BAPTA, whilst two CATs were homing towards each other immediately inhibited CAT chemotropism and the oscillatory recruitment of MAK-2 in CATs tips (the ping-pong mechanism). This provides further strong evidence that extracellular Ca^{2+} is required for CAT chemotropism and also is reqired for CATs to be developmentally committed to remain as CATs. The CaM antagonists (TFP and calmidazolium), Ca^{2+} channel blockers (verapamil and diltiazem, Chu, 2013), calcineurin inhibitors (FK506 and cyclosporine A) and an antifungal drug (caspofungin), which has been known to target β-1,3 glucan synthase and to be regulated by calcineurin, all inhibited CAT chemotropism. These data provide clear evidence that Ca^{2+} signalling is involved in the regulation of CAT chemotropism. The results from chapter 3 are summarized in Figs 8.1 and 8.2.

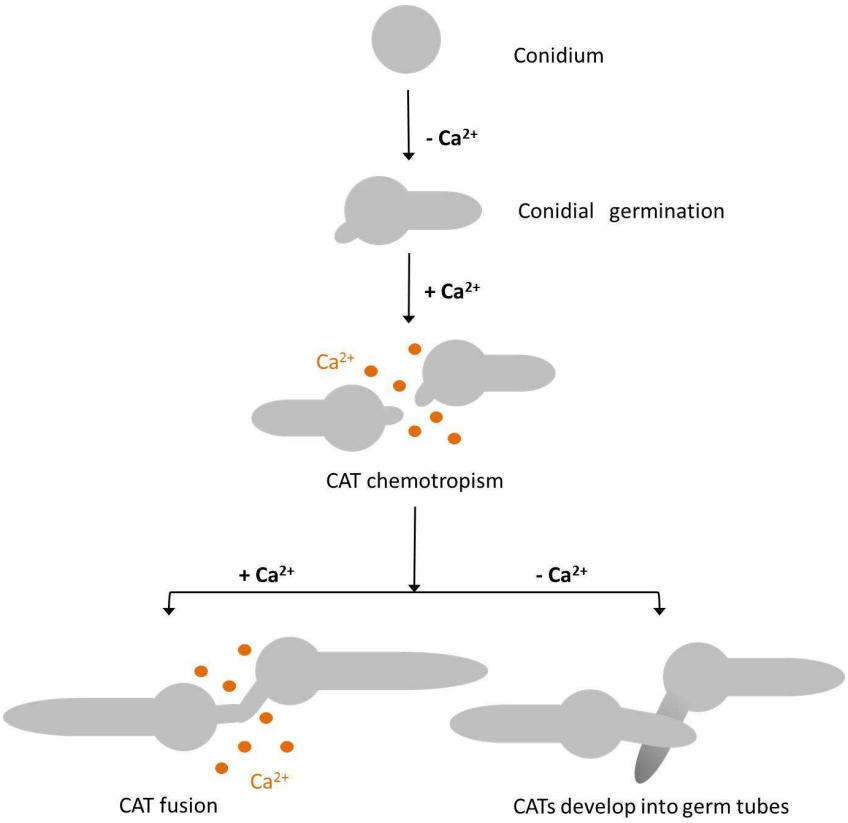

Figure 8.1 Summary of the Ca^{2+}-dependent steps during colony initiation

The conidial germination is extracellular Ca^{2+}-independent. CAT chemotropism and CAT fusion are Ca^{2+}-dependent. The long-term (> 6 h) absence of extracellular Ca^{2+} caused CATs to develop into germ tubes.

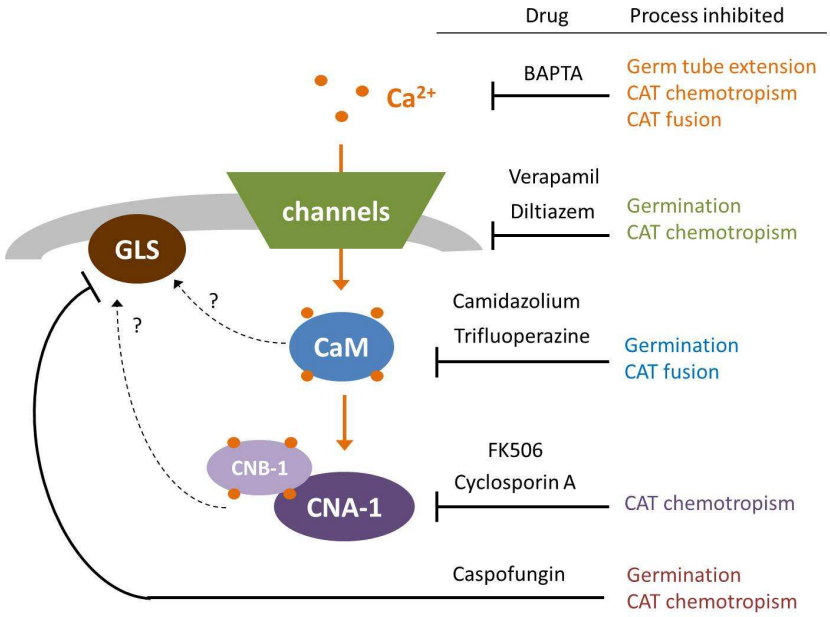

Figure 8.2 Summary of the results of the influence of different Ca^{2+} modulators on conidial germination, germ tube extension, CAT chemotropism and CAT fusion during colony initiation. Abbreviations: GLS, β-1,3 glucan synthase; CaM, calmodulin; CNA-1, calcineurin catalytic subunit; CNB-1, calcineurin regulatory subunit.

In Chapter 4, to provide a comprehensive identification of the Ca^{2+} signalling components of *N. crassa* and further analyze the role of Ca^{2+} signalling in colony initiation, a comparative genomics and mutant phenotype analysis was performed. In this analysis, different functional groups of Ca^{2+} signalling proteins were identified: Ca^{2+}-channels, Ca^{2+}-ATPases, other Ca^{2+}-transporters, key Ca^{2+} or Ca^{2+}/CaM-binding proteins, putative Ca^{2+} or Ca^{2+}/CaM-binding proteins, and other Ca^{2+} signalling regulators. This study initially involved a comparative genomics analysis of the 4 fungal genome databases of *N. crassa*, *S. cerevisiae*, *A. fumigatus*, and *C. albicans.* The phenotypes of 29 homokaryotic gene deletion mutants were analyzed by comparing the morphology of 16 h young colonies, 5 d mature colonies, and the results of CAT fusion assay using mutants obtained from the gene deletion mutant collection from the FGSC. The phenotypic analysis provided evidence that *plc-2*, *camk-1*, and *rgs-1* were involved in conidial germination (germination and/or CAT formation), and that *cna-1, cnb-1*, and *cch-1*/*mid-1* (Chu, 2013) were involved in CAT chemotropism. The phenotypic analysis of mutants in which each of the calcineurin subunits (CNA-1 and CNB-1) had been deleted were consistent with the results obtained after using the calcineurin inhibitors which further supports a role for calcineurin regulating CAT chemotropism.

In Chapter 5, the protein sequence of the main intracellular Ca^{2+} receptor, CaM, was compared in 10 different fungi. Four Ca^{2+}-binding motifs were shown to be conserved in 6 filamentous fungi (*N. crassa, A. nidulans, A. fumigatus, M. grisea, F. oxysporum Fo47* and *B. cinerea*), 2 diploid fungi (*U. maydis* and *C. albicans*), and the fission yeast *S. pombe*. The CaM in *S. cerevisiae* was markedly different by possessing only 3 Ca^{2+}-binding sites. Interestingly, the 10th and the 97th amino acids. of the CaM sequences were consistently conserved in all the filamentous fungi as valine and asparagine, and in diploid fungi and yeasts as isoleucine and glycine. This may be useful as a potential bio-marker for the identification of filamentous fungi. To analyze the Ca^{2+}/CaM-binding proteome during colony initiation in *N. crassa*, immunoprecipitation was performed using V5-tagged CaM followed by mass spectrometry analysis. A total of 286 proteins were identified and cross-analyzed with gene oncology (GO) using proteomic databases and the online software

PANTHER. The results provided evidence that CaM plays a role in regulating important pathways including the MAPK CWI and Rho/Ras signalling pathways. CaM was also associated with numerous cellular components and biological processes which are listed in Fig. 5.1. Thirty proteins were identified with CaM-binding motifs by using a calmodulin target database. This provided further evidence of protein-protein interactions which may link the Ca^{2+} signalling machinery with other cellular pathways. In addition, 8 proteins (for which evidence has been obtained for being involved in CAT fusion Table. 5.5), were identified as forming CaM-binding complexes. These were CCH-1, MID-1, CNA-1, CNB-1, CaMK-1, MEK-1, SNF-5, and SMCO-7. Of these proteins, CNA-1 and CaMK-1 contain CaM-binding motifs.

In Chapter 6, live-cell imaging of CaM, calcineurin and CaMK-1 was performed by GFP tagging of these proteins using native promoters. CaM-GFP localized dynamically moving between numerous spots and larger single accumulations in the growing tips of germ tubes and CATs. In vegetative hyphae, CaM concentrated in the Spitzenkörper, and exhibited a tip-focused gradient in growing hyphae. It also appeared in branch tips during the initiation of branch formation (Fig. 8.3). The two subunits of calcineurin, CNA-1 and CNB-1, showed a similar localization to CaM at sites of septum but formed static spots in the cytoplasm without movement and large accumulation at tips. The CaM-dependent kinase, CaMK-1, in contract to CaM was not localized to specific regions but was formed throughout the cytoplasm.

The tip-focused CaM became reduced in growing vegetative hyphae when Ca^{2+} was absent from the growth medium. It disappeared altogether when the Ca^{2+} chelator, BAPTA, was added whilst two CATs were homing towards each other. The tip-focused CaM in CATs was also inhibited in the *myo-5* deletion mutant and in the presence of the F-actin inhibitor, Latrunculin A. These results are consistent with the accumulation of CaM at CAT tips requiring extracellular Ca^{2+} and being transported to CAT tips by the motor protein MYO-5 along the F-actin cytoskeleton. Spots of CaM-GFP trafficked in the cytoplasm in multiple directions and passed through septal pores. The co-localization of CaM-GFP and H1-RFP showed that the mobile CaM spots in the cytoplasm wereassociated with the nuclear spindle pore bodies (SPB). Adding the microtubule polymerization inhibitor, benomyl, to growing cells inhibited

the movement of SPB-associated CaM-GFP in the cytoplasm. This is consistent with the transport of nuclei in germlings being microtubule-dependent. Further supportive evidence for CaM being associated with F-actin and microtubule transport processes was the finding that MYO-5, actin proteins, Nkin2, and tubulin proteins formed CaM-interacting complexes (Fig. 5.8). Furthermore, MYO-5 and Nkin2 contain CaM-binding motifs.

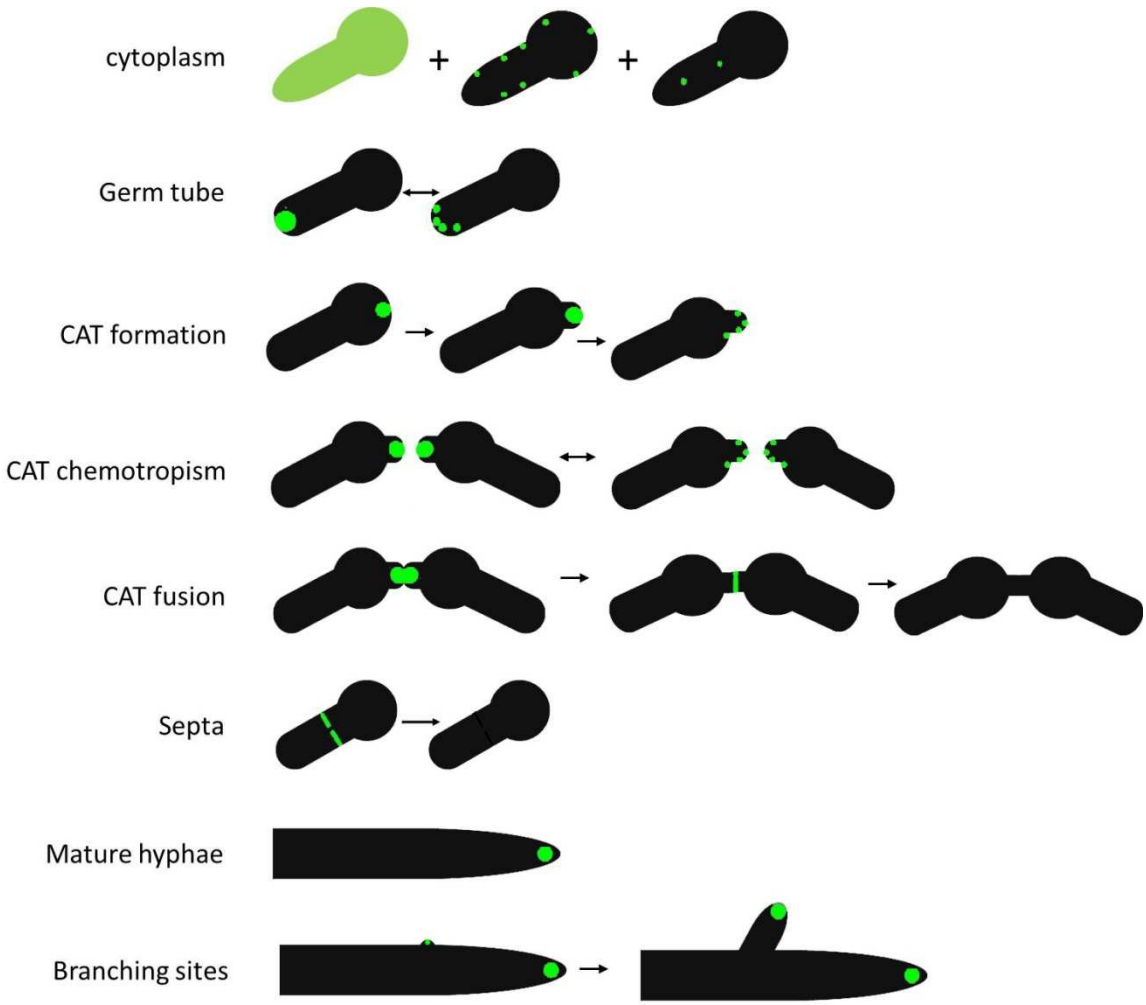

Figure 8.3 Schematic representation of CaM localization in *N. crassa*
Green labelled regions show sites of CaM accumulation in the cell.

In Chapter 7, $[Ca^{2+}]_c$ dynamics were imaged for the first time in *N. crassa* by live-cell imaging using GCaMP6s Ca^{2+}-reporter driven by the *tef-1* promoter and targeted into *his* locus. The microscopy parameters and cell culture conditions were optimized for Ca^{2+} imaging in both 8-well chambers and microfluidic chambers.

Conidia were cultured in the *N. crassa* growth medium, Vogel's medium, which contains 680 µM Ca^{2+}, at 35^{o}C for 4 h. 2-10 Ca^{2+} pulses, which last for 5-50 s, were produced in 10 min by each germling. The removal of extracellular Ca^{2+} by adding BAPTA caused the Ca^{2+} spikes to disappear. CaM and calcineurin inhibitors and the antifungal drug, caspofungin, all increased the frequency of Ca^{2+} spikes in Vogel's medium suggesting roles for CaM and calcineurin in regulating these repeated increases in $[Ca^{2+}]_c$. No clear correlation between the Ca^{2+} spiking and the oscillatory recruitment of MAK-2 was observed indicating the Ca^{2+} signalling may not directly regulate the ping-pong mechanism of CAT chemotropism. Several key issues arising from the results described in chapter 3-7 are discussed in the following paragraghs.

8.1.1. Extracellular Ca^{2+} is required for CAT chemotropism but the intracellular Ca^{2+} spiking is not directly associated with CAT chemotropism or CAT fusion.

From Chapters 3, 5 and 7, a summary of the effect of extracellular Ca^{2+} and Ca^{2+} modulating drugs on Ca^{2+} spiking, CaM localization and CAT fusion is presented in Table 8.1. These results show that Ca^{2+} spiking requires the presence of extracellular Ca^{2+}. CAT chemotropism also requires extracellular Ca^{2+} as well as CaM and calcineurin activity. However, Ca^{2+} spiking is not required for CAT chemotropism because Ca^{2+} spiking was present in germlings in which CAT chemotropism was inhibited with CaM and calcineurin inhibitors. Nevertheless, CaM and calcineurin do seem to play a role in regulating the frequency of Ca^{2+} spiking. Other interacting observations were that increased extracellular Ca^{2+} increases the extension rate of germ tubes and that extracellular Ca^{2+} is required for the accumulation of CaM in growing CAT tips. The mechanistic basis of these latter processes is not understood.

My results point to extracellular Ca^{2+} playing a role in one or more of the following processes that regulate CAT chemotropism: (a) regulation of the activity of the chemoattractants; (b) regulation of the interaction between the chemoattractants and their regulators; and/or (c) the regulation of the activity of the receptors. Intracellular CaM and calcineurin also seem to play a role in CAT chemotropism but their activation is not dependent on the frequency of Ca^{2+} spiking

increasing during CAT homing towards each other.

Table 8.1 Summary of the effects of extracellular Ca^{2+} and Ca^{2+}-modulating drugs on Ca^{2+} spiking, CaM localization and CAT fusion.

Extracellular Ca^{2+} concentration in VM	Drug treatment	Ca^{2+} spiking	CaM localization	CAT fusion assay
Normal Ca^{2+} concentration (680 μM Ca^{2+})	-	Normal frequency (2-10 spikes per 10 min)	At tips of both CATs and germ tubes	Normal CAT fusion (65-75%)
High Ca^{2+} concentration (200 mM Ca^{2+})	-	Increased frequency	At tips of both CATs and germ tubes	Normal CAT fusion; higher germ tube extension rate
No Ca^{2+}	BAPTA (Ca^{2+} chelator)	Inhibited	At tips of germ tubes but not CATs	No CAT chemotropism
Normal Ca^{2+} concentration	TFP (CaM antagonist)	Increased frequency	At tips of growing CATs and germ tubes	conidial germination and CAT fusion inhibited
Normal Ca^{2+} concentration	FK506 (calcineurin inhibitor)	Increased frequency	At tips of growing CATs and germ tubes	CAT chemotropism inhibited
Normal Ca^{2+} concentration	Caspofungin (antifungal drug; 1,3-β-glucan synthase inhibitor)	Increased frequency	At tips of growing CATs and germ tubes	CAT chemotropism inhibited

8.1.2. The Ca^{2+} signalling machinery is involved in colony initiation, and especially, calcineurin may be the target which is linked to CAT chemotropism.

Ca^{2+} signalling components involved in the CAT fusion process are summarized in Fig. 8.4. Calcineurin is known to mediate the cell wall integrity (CWI) pathway via the transcription factor CRZ and β-1,3-glucan synthase in yeast (Stathopoulos and Cyert, 1997; Zhao et al., 1998). In *C. neoformans*, Crz1 is selectively activated by Ca^{2+}/calcineurin-dependent and independent signals depending on the environmental conditions, and it regulates cell wall integrity (Lev et al., 2012). In Chapter 5 (Table 5.4), CaM-interacting proteins that were identified from the

proteomic analysis included calcineurin (CNA-1 and CNB-1 subunits), β-1,3-glucan synthase (GLS-1), RHO-1 (which interacts with GLS-1) and the MAP Kinase in the CWI pathway (MEK-1). It has previously been shown that gene deletion mutants of the 3 MAP kinases (*mik-1, mek-1*, and *mak-1*) in the CWI MAPK pathway are defective in CAT chemotropism (Galagan et al., 2003). CaM activated calcineurin may therefore play an important role in regulating the crosstalk between Ca^{2+} signalling and the CWI MAPK signalling pathway. Whether transcription regulation via the transcriptor factor CRZ-1 plays a role in this process is unclear at this stage.

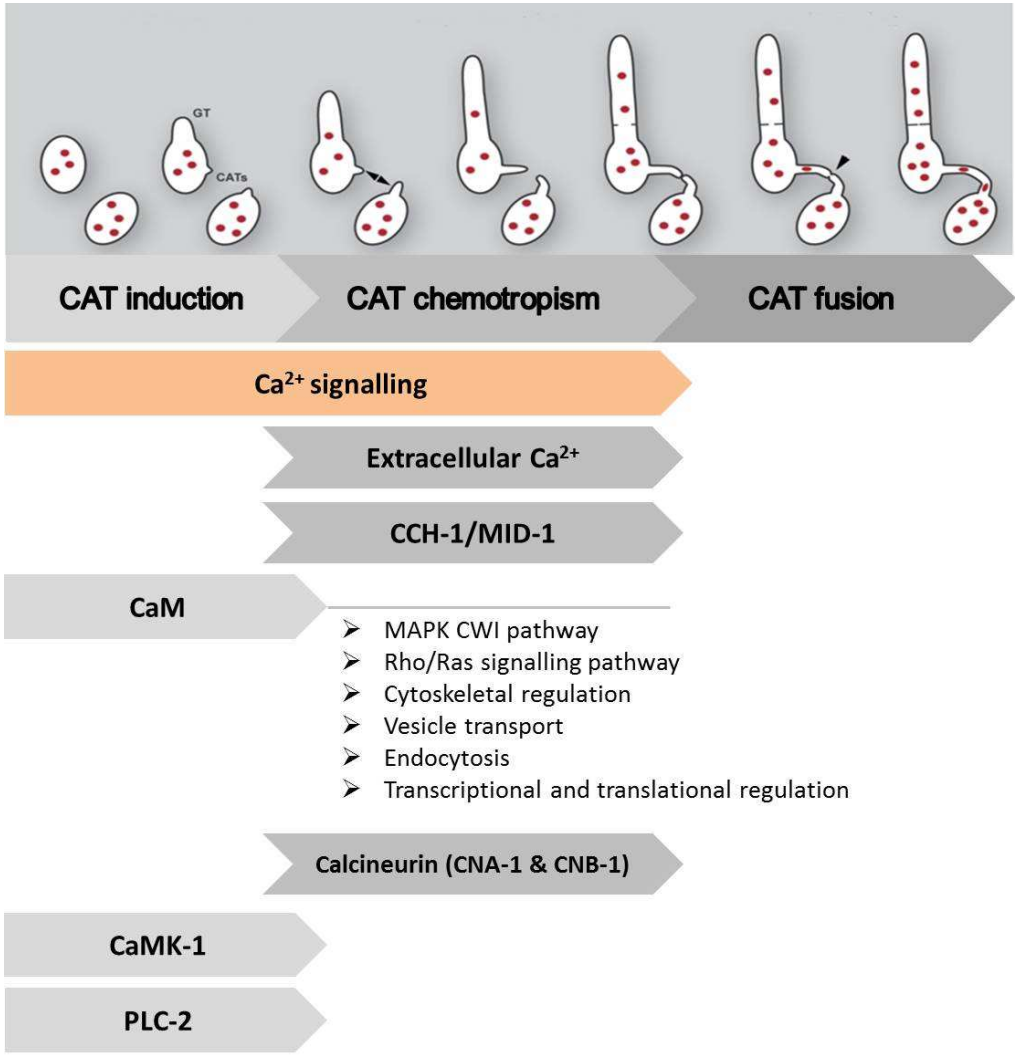

Figure 8.4 Schematic view of Ca^{2+} signalling components involved in the CAT fusion process in *N. crassa*.

In section 3.3, 5 hypotheses of how Ca^{2+} may regulate CAT chemotropism in *N. crassa* were presented. These different hypotheses have been converted into 4

models shown schematically in Fig. 8.5. The first model (A) is considered unlikely because any gradient in Ca^{2+} between 2 homing CAT tips would probably be disrupted by the presence of a high extracellular Ca^{2+} (200 mM) in the external medium (Table 8.1). Model (B) combines the 3 hypotheses that Ca^{2+} is involved in the external activation of the chemoattractant, the chemoattractant receptors or the interaction of the chemoattractant with the receptor. My results reported in sections 3.2.2-4 support the involvement of one or more aspects of this model. Model (C) involves 'ping-pong' spiking of $[Ca^{2+}]_c$ which alternates back and forth between each opposing CAT. In this model Ca^{2+} will be regulating either the 'signal sending' or 'signal receiving' pathway. My Ca^{2+} imaging data presented in chapter 7 provides strong evidence against this hypothesis. The final model (D) proposes that a steady influx of Ca^{2+} which activates CaM and calcineurin-regulated processes is required for chemotropism. My data supports this model even though no tip-focused $[Ca^{2+}]_c$ gradient was detected in my study (possibly the Ca^{2+} flux is not great enough to produce a gradient). In conclusion, my results support both model (B) and (D) playing a role in CAT chemotropism.

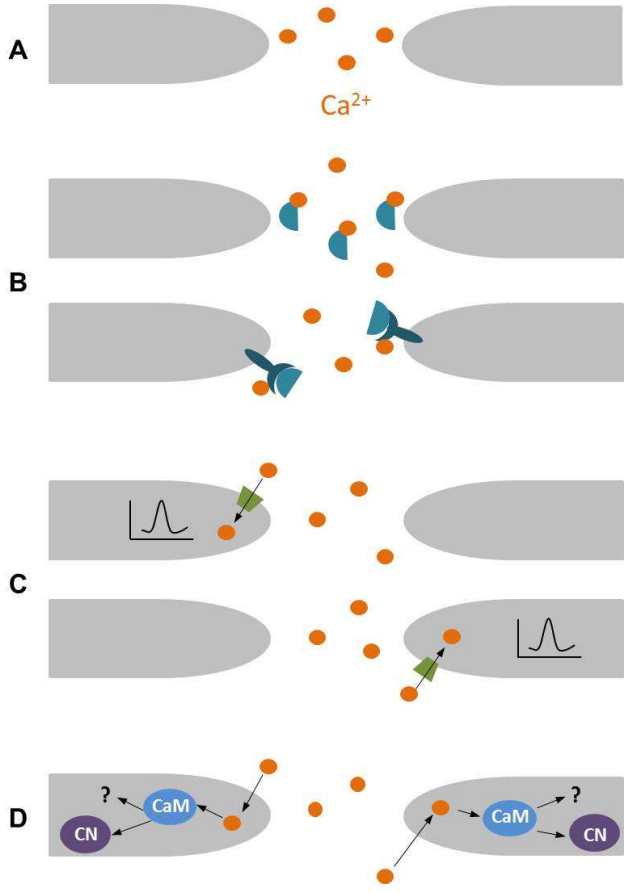

Figure 8.5 Schematic presentation of 4 hypotheses of the Ca^{2+}-dependent mechanism during CAT chemotropism in *N. crassa*.

(A) Ca^{2+} acts as a chemotractant (B) Extracellular Ca^{2+} is an activator of the chemotractant and the receptors or is required for chemotractant-receptor interation (C) Ca^{2+} influx alternates between CAT tips in a 'ping-pong' fashion. (D) Simultaneous Ca^{2+} influx into both CATs tips is required for the continuous activation of CaM-calcineurin pathway to drive CAT chemotropism.

8.2. Future work

- Investigation of the biological role of the Ca^{2+} spiking in *N. crassa*. These studies will require appropriate software to analyse the amplitudes and frequency of the Ca^{2+} spiking in germlings under different conditions (e.g. different nutrient medium or inhibitor treatments).
- Investigation of the Ca^{2+} spiking in different gene deletion mutants such as Δcch-1, Δmid-1, Δcna-1 and Δcnb-1 to analysis the regulation of Ca^{2+} homeostasis.
- Live-cell imaging of Ca^{2+} spiking in CaM-GFP strain and co-localization of CaM-GFP and MAK-2-RFP to determine whether the dynamic accumulation of CaM at tips of homing CATs are associated with Ca^{2+} spiking and the osillation of SO and MAK-2.
- Determination of whether transcriptional regulation via the calcineurin-activated transcription factor, CRZ-1, is involved in CAT fusion. A first step here will be to label CRZ-1 with GFP and determine whether it is recruited to nuclei at any stage during CAT induction, chemotropism or fusion.
- Identification of the chemoattractant, which has been proposed to be a peptide (Read et al., 2012), and determination of whether its activity is Ca^{2+}-dependent. One experimental approach here would be to use liquid chromatography and mass spectrometry of the medium around CATs and determination of whether different fraction have CAT chemoattractant properties.
- Identification of the chemoattractant receptor and determination of whether its activity or its interaction with the chemoattractant is Ca^{2+}-dependent. A means to this end will be to perform a genome-wide screen of mutants that are predicted to be defective in plasma membrane associated proteins.
- Determine what roles endocytic recycling plays during the CAT fusion. Various endocytic mutants can be used to analyse the role of endocytosis during this process. Once the chemoattractant has been identified it may be possible to fluorescently label it and directly visualize its internalization by endocytosis

8.3. References

Abdel-Ghany, S.E., I.S. Day, M.P. Simmons, P. Kugrens, and A.S. Reddy. 2005. Origin and evolution of Kinesin-like calmodulin-binding protein. *Plant Physiol*. 138:1711-1722.

Aguilar, P.S., A. Engel, and P. Walter. 2007. The plasma membrane proteins Prm1 and Fig1 ascertain fidelity of membrane fusion during yeast mating. *Mol Biol Cell*. 18:547-556.

Akerboom, J., T.W. Chen, T.J. Wardill, L. Tian, J.S. Marvin, S. Mutlu, N.C. Calderon, F. Esposti, B.G. Borghuis, X.R. Sun, A. Gordus, M.B. Orger, R. Portugues, F. Engert, J.J. Macklin, A. Filosa, A. Aggarwal, R.A. Kerr, R. Takagi, S. Kracun, E. Shigetomi, B.S. Khakh, H. Baier, L. Lagnado, S.S. Wang, C.I. Bargmann, B.E. Kimmel, V. Jayaraman, K. Svoboda, D.S. Kim, E.R. Schreiter, and L.L. Looger. 2012. Optimization of a GCaMP calcium indicator for neural activity imaging. *J Neurosci*. 32:13819-13840.

Akerboom, J., J.D. Rivera, M.M. Guilbe, E.C. Malave, H.H. Hernandez, L. Tian, S.A. Hires, J.S. Marvin, L.L. Looger, and E.R. Schreiter. 2009. Crystal structures of the GCaMP calcium sensor reveal the mechanism of fluorescence signal change and aid rational design. *J Biol Chem*. 284:6455-6464.

Aldabbous, M.S., M.G. Roca, A. Stout, I.C. Huang, N.D. Read, and S.J. Free. 2010. The ham-5, rcm-1 and rco-1 genes regulate hyphal fusion in Neurospora crassa. *Microbiology*. 156:2621-2629.

Allen, G.J., J.M. Kwak, S.P. Chu, J. Llopis, R.Y. Tsien, J.F. Harper, and J.I. Schroeder. 1999. Cameleon calcium indicator reports cytoplasmic calcium dynamics in Arabidopsis guard cells. *Plant J*. 19:735-747.

Antebi, A., and G.R. Fink. 1992. The yeast Ca(2+)-ATPase homologue, PMR1, is required for normal Golgi function and localizes in a novel Golgi-like distribution. *Mol Biol Cell*. 3:633-654.

Aramburu, J., A. Rao, and C.B. Klee. 2000. Calcineurin: from structure to function. *Curr Top Cell Regul*. 36:237-295.

Araujo-Palomares, C.L., E. Castro-Longoria, and M. Riquelme. 2007. Ontogeny of the Spitzenkorper in germlings of Neurospora crassa. *Fungal Genet Biol*. 44:492-503.

Araujo-Palomares, C.L., C. Richthammer, S. Seiler, and E. Castro-Longoria. 2011. Functional characterization and cellular dynamics of the CDC-42 - RAC - CDC-24 module in Neurospora crassa. *PLoS One*. 6:e27148.

Arkowitz, R.A. 2009. Chemical gradients and chemotropism in yeast. *Cold Spring Harb Perspect Biol*. 1:a001958.

Arnaudeau, S., M. Frieden, K. Nakamura, C. Castelbou, M. Michalak, and N. Demaurex. 2002. Calreticulin differentially modulates calcium uptake and release in the endoplasmic reticulum and mitochondria. *J Biol Chem*. 277:46696-46705.

Arpaia, G., F. Cerri, S. Baima, and G. Macino. 1999. Involvement of protein kinase C in the response of Neurospora crassa to blue light. *Mol Gen Genet*. 262:314-322.

Atkinson, H.A., A. Daniels, and N.D. Read. 2002. Live-cell imaging of endocytosis during conidial germination in the rice blast fungus, Magnaporthe grisea. *Fungal Genet Biol*. 37:233-244.

Audhya, A., R. Loewith, A.B. Parsons, L. Gao, M. Tabuchi, H. Zhou, C. Boone, M.N. Hall, and S.D. Emr. 2004. Genome-wide lethality screen identifies new PI4,5P2 effectors that regulate the actin cytoskeleton. *EMBO J*. 23:3747-3757.

Awata, H., C. Huang, M.E. Handlogten, and R.T. Miller. 2001. Interaction of the calcium-sensing receptor and filamin, a potential scaffolding protein. *J Biol Chem*. 276:34871-34879.

Baba, M., N. Baba, Y. Ohsumi, K. Kanaya, and M. Osumi. 1989. Three-dimensional analysis of morphogenesis induced by mating pheromone alpha factor in Saccharomyces cerevisiae. *J Cell Sci*. 94 (Pt 2):207-216.

Babu, Y.S., C.E. Bugg, and W.J. Cook. 1988. Structure of calmodulin refined at 2.2 A resolution. *J Mol Biol*. 204:191-204.

Bader, M.F., F. Doussau, S. Chasserot-Golaz, N. Vitale, and S. Gasman. 2004. Coupling actin and membrane dynamics during calcium-regulated exocytosis: a role for Rho and ARF GTPases. *Biochim Biophys Acta*. 1742:37-49.

Bar-Sagi, D., and J. Prives. 1983. Trifluoperazine, a calmodulin antagonist, inhibits muscle cell fusion. *J Cell Biol*. 97:1375-1380.

Barbara, J.G. 2002. IP3-dependent calcium-induced calcium release mediates bidirectional calcium waves in neurones: functional implications for synaptic plasticity. *Biochim Biophys Acta*. 1600:12-18.

Barclay, J.W., A. Morgan, and R.D. Burgoyne. 2005. Calcium-dependent regulation of exocytosis. *Cell Calcium*. 38:343-353.

Baumann, S., T. Pohlmann, M. Jungbluth, A. Brachmann, and M. Feldbrugge. 2012. Kinesin-3 and dynein mediate microtubule-dependent co-transport of mRNPs and endosomes. *J Cell Sci*. 125:2740-2752.

Beauvais, A., J.M. Bruneau, P.C. Mol, M.J. Buitrago, R. Legrand, and J.P. Latge. 2001. Glucan synthase complex of Aspergillus fumigatus. *J Bacteriol*. 183:2273-2279.

Bencina, M., T. Bagar, L. Lah, and N. Krasevec. 2009. A comparative genomic analysis of calcium and proton signaling/homeostasis in Aspergillus species. *Fungal Genet Biol*. 46 Suppl 1:S93-S104.

Bennett, J., and A. Weeds. 1986. Calcium and the cytoskeleton. *Br Med Bull*. 42:385-390.

Benoist, M., S. Gaillard, and F. Castets. 2006. The striatin family: a new signaling platform in dendritic spines. *J Physiol Paris*. 99:146-153.

Berepiki, A., A. Lichius, and N.D. Read. 2011. Actin organization and dynamics in filamentous fungi. *Nat Rev Microbiol*. 9:876-887.

Berepiki, A., A. Lichius, J.Y. Shoji, J. Tilsner, and N.D. Read. 2010. F-actin dynamics in

Neurospora crassa. *Eukaryot Cell*. 9:547-557.

Bernards, A., and J. Settleman. 2004. GAP control: regulating the regulators of small GTPases. *Trends Cell Biol*. 14:377-385.

Berridge, M.J., M.D. Bootman, and H.L. Roderick. 2003. Calcium signalling: dynamics, homeostasis and remodelling. *Nat Rev Mol Cell Biol*. 4:517-529.

Berridge, M.J., P. Lipp, and M.D. Bootman. 2000. The versatility and universality of calcium signalling. *Nat Rev Mol Cell Biol*. 1:11-21.

Bistis, G.N., D.D. Perkins, and N.D. Read. 2003. Different cell types in Neurospora crassa. *Fungal Genetics Newsletter*. 50:17-19.

Bkaily, G., and N. Sperelakis. 1986. Calmodulin is required for a full activation of the calcium slow channels in heart cells. *J Cyclic Nucleotide Protein Phosphor Res*. 11:25-34.

Blankenship, J.R., and J. Heitman. 2005. Calcineurin is required for Candida albicans to survive calcium stress in serum. *Infect Immun*. 73:5767-5774.

Bloemendal, S., K.M. Lord, C. Rech, B. Hoff, I. Engh, N.D. Read, and U. Kuck. 2010. A mutant defective in sexual development produces aseptate ascogonia. *Eukaryot Cell*. 9:1856-1866.

Bootman, M.D., T.J. Collins, C.M. Peppiatt, L.S. Prothero, L. MacKenzie, P. De Smet, M. Travers, S.C. Tovey, J.T. Seo, M.J. Berridge, F. Ciccolini, and P. Lipp. 2001. Calcium signalling--an overview. *Semin Cell Dev Biol*. 12:3-10.

Bootman, M.D., D. Thomas, S.C. Tovey, M.J. Berridge, and P. Lipp. 2000. Nuclear calcium signalling. *Cell Mol Life Sci*. 57:371-378.

Borkovich, K.A., L.A. Alex, O. Yarden, M. Freitag, G.E. Turner, N.D. Read, S. Seiler, D. Bell-Pedersen, J. Paietta, N. Plesofsky, M. Plamann, M. Goodrich-Tanrikulu, U. Schulte, G. Mannhaupt, F.E. Nargang, A. Radford, C. Selitrennikoff, J.E. Galagan, J.C. Dunlap, J.J. Loros, D. Catcheside, H. Inoue, R. Aramayo, M. Polymenis, E.U. Selker, M.S. Sachs, G.A. Marzluf, I. Paulsen, R. Davis, D.J. Ebbole, A. Zelter, E.R. Kalkman, R. O'Rourke, F. Bowring, J. Yeadon, C. Ishii, K. Suzuki, W. Sakai, and R. Pratt. 2004. Lessons from the genome sequence of Neurospora crassa: tracing the path from genomic blueprint to multicellular organism. *Microbiol Mol Biol Rev*. 68:1-108.

Bowman, S.M., A. Piwowar, M. Al Dabbous, J. Vierula, and S.J. Free. 2006. Mutational analysis of the glycosylphosphatidylinositol (GPI) anchor pathway demonstrates that GPI-anchored proteins are required for cell wall biogenesis and normal hyphal growth in Neurospora crassa. *Eukaryot Cell*. 5:587-600.

Brachat, A., J.V. Kilmartin, A. Wach, and P. Philippsen. 1998. Saccharomyces cerevisiae cells with defective spindle pole body outer plaques accomplish nuclear migration via half-bridge-organized microtubules. *Mol Biol Cell*. 9:977-991.

Brand, A., and N.A. Gow. 2009. Mechanisms of hypha orientation of fungi. *Curr Opin Microbiol*. 12:350-357.

Brand, A., K. Lee, V. Veses, and N.A. Gow. 2009. Calcium homeostasis is required for contact-dependent helical and sinusoidal tip growth in Candida albicans hyphae. *Mol Microbiol*. 71:1155-1164.

Brand, A., S. Shanks, V.M. Duncan, M. Yang, K. Mackenzie, and N.A. Gow. 2007. Hyphal orientation of Candida albicans is regulated by a calcium-dependent mechanism. *Curr Biol*. 17:347-352.

Braun, A.P., and H. Schulman. 1995. The multifunctional calcium/calmodulin-dependent protein kinase: from form to function. *Annu Rev Physiol*. 57:417-445.

Braun, E.L., A.L. Halpern, M.A. Nelson, and D.O. Natvig. 2000. Large-scale comparison of fungal sequence information: mechanisms of innovation in Neurospora crassa and gene loss in Saccharomyces cerevisiae. *Genome Res*. 10:416-430.

Braun, E.L., S. Kang, M.A. Nelson, and D.O. Natvig. 1998. Identification of the first fungal annexin: analysis of annexin gene duplications and implications for eukaryotic evolution. *J Mol Evol*. 47:531-543.

Brockerhoff, S.E., and T.N. Davis. 1992. Calmodulin concentrates at regions of cell growth in Saccharomyces cerevisiae. *J Cell Biol*. 118:619-629.

Brown, E.M., and R.J. MacLeod. 2001. Extracellular calcium sensing and extracellular calcium signaling. *Physiol Rev*. 81:239-297.

Burgoyne, R.D. 2007. Neuronal calcium sensor proteins: generating diversity in neuronal Ca2+ signalling. *Nat Rev Neurosci*. 8:182-193.

Cai, X., and J. Lytton. 2004. The cation/Ca(2+) exchanger superfamily: phylogenetic analysis and structural implications. *Mol Biol Evol*. 21:1692-1703.

Carafoli, E. 2002. Calcium signaling: a tale for all seasons. *Proc Natl Acad Sci U S A*. 99:1115-1122.

Chaga, G., D.E. Bochkariov, G.G. Jokhadze, J. Hopp, and P. Nelson. 1999. Natural poly-histidine affinity tag for purification of recombinant proteins on cobalt(II)-carboxymethylaspartate crosslinked agarose. *J Chromatogr A*. 864:247-256.

Chang, Y.C., and L.A. Penoyer. 2000. Properties of various Rho1 mutant alleles of Cryptococcus neoformans. *J Bacteriol*. 182:4987-4991.

Chen, R.E., and J. Thorner. 2007. Function and regulation in MAPK signaling pathways: lessons learned from the yeast Saccharomyces cerevisiae. *Biochim Biophys Acta*. 1773:1311-1340.

Chen, S., Y. Song, J. Cao, G. Wang, H. Wei, X. Xu, and L. Lu. 2010a. Localization and function of calmodulin in live-cells of Aspergillus nidulans. *Fungal Genet Biol*. 47:268-278.

Chen, S.L., J. Yan, and F.S. Wang. 2010b. Two topical calcineurin inhibitors for the treatment of atopic dermatitis in pediatric patients: a meta-analysis of randomized clinical trials. *J Dermatolog Treat*. 21:144-156.

Chen, Y., X. Song, S. Ye, L. Miao, Y. Zhu, R.G. Zhang, and G. Ji. 2013. Structural insight into

enhanced calcium indicator GCaMP3 and GCaMPJ to promote further improvement. *Protein Cell*. 4:299-309.

Chin, D., and A.R. Means. 2000. Calmodulin: a prototypical calcium sensor. *Trends Cell Biol*. 10:322-328.

Chitaev, N.A., and S.M. Troyanovsky. 1998. Adhesive but not lateral E-cadherin complexes require calcium and catenins for their formation. *J Cell Biol*. 142:837-846.

Chu, M. 2013a. Ca2+ signalling and homeostasis during colony initiation in Neurospora crassa. Vol. Ph.D. The University of Edinburgh.

Chu, M. 2013b. Ca2+ signalling and homeostasis during colony initiation in Neurospora crassa. *In* Institute of Cell biology. University of Edinburgh.

Clapham, D.E. 2007. Calcium signaling. *Cell*. 131:1047-1058.

Clapham, D.E., L.W. Runnels, and C. Strubing. 2001. The TRP ion channel family. *Nat Rev Neurosci*. 2:387-396.

Colot, H.V., G. Park, G.E. Turner, C. Ringelberg, C.M. Crew, L. Litvinkova, R.L. Weiss, K.A. Borkovich, and J.C. Dunlap. 2006. A high-throughput gene knockout procedure for Neurospora reveals functions for multiple transcription factors. *Proc Natl Acad Sci U S A*. 103:10352-10357.

Coppin, E., R. Debuchy, S. Arnaise, and M. Picard. 1997. Mating types and sexual development in filamentous ascomycetes. *Microbiol Mol Biol Rev*. 61:411-428.

Cramer, R.A., Jr., B.Z. Perfect, N. Pinchai, S. Park, D.S. Perlin, Y.G. Asfaw, J. Heitman, J.R. Perfect, and W.J. Steinbach. 2008. Calcineurin target CrzA regulates conidial germination, hyphal growth, and pathogenesis of Aspergillus fumigatus. *Eukaryot Cell*. 7:1085-1097.

Crivici, A., and M. Ikura. 1995. Molecular and structural basis of target recognition by calmodulin. *Annu Rev Biophys Biomol Struct*. 24:85-116.

Cruz, M.C., A.L. Goldstein, J.R. Blankenship, M. Del Poeta, D. Davis, M.E. Cardenas, J.R. Perfect, J.H. McCusker, and J. Heitman. 2002. Calcineurin is essential for survival during membrane stress in Candida albicans. *EMBO J*. 21:546-559.

Cui, J., J.A. Kaandorp, P.M. Sloot, C.M. Lloyd, and M.V. Filatov. 2009. Calcium homeostasis and signaling in yeast cells and cardiac myocytes. *FEMS Yeast Res*. 9:1137-1147.

Cunningham, K.W., and G.R. Fink. 1994. Ca2+ transport in Saccharomyces cerevisiae. *J Exp Biol*. 196:157-166.

Cunningham, K.W., and G.R. Fink. 1996. Calcineurin inhibits VCX1-dependent H+/Ca2+ exchange and induces Ca2+ ATPases in Saccharomyces cerevisiae. *Mol Cell Biol*. 16:2226-2237.

Cybulski, N., and M.N. Hall. 2009. TOR complex 2: a signaling pathway of its own. *Trends Biochem Sci*. 34:620-627.

Cyert, M.S. 2001. Genetic analysis of calmodulin and its targets in Saccharomyces cerevisiae.

Annu Rev Genet. 35:647-672.

Cyert, M.S., R. Kunisawa, D. Kaim, and J. Thorner. 1991. Yeast has homologs (CNA1 and CNA2 gene products) of mammalian calcineurin, a calmodulin-regulated phosphoprotein phosphatase. *Proc Natl Acad Sci U S A*. 88:7376-7380.

Cyert, M.S., and J. Thorner. 1992. Regulatory subunit (CNB1 gene product) of yeast Ca2+/calmodulin-dependent phosphoprotein phosphatases is required for adaptation to pheromone. *Mol Cell Biol*. 12:3460-3469.

d'Enfert, C. 1997. Fungal Spore Germination: Insights from the Molecular Genetics ofAspergillus nidulansandNeurospora crassa. *Fungal Genetics and Biology*. 21:163–172.

Davis, R.H. 2000. Neurospora: contributions of a model organism. Oxford [Oxfordshire]: Oxford University Press. ISBN 0-19-512236-4. .

Davis, R.H., and D.D. Perkins. 2002. Timeline: Neurospora: a model of model microbes. *Nat Rev Genet*. 3:397-403.

Dayton, J.S., and A.R. Means. 1996. Ca(2+)/calmodulin-dependent kinase is essential for both growth and nuclear division in Aspergillus nidulans. *Mol Biol Cell*. 7:1511-1519.

Dayton, J.S., M. Sumi, N.N. Nanthakumar, and A.R. Means. 1997. Expression of a constitutively active Ca2+/calmodulin-dependent kinase in Aspergillus nidulans spores prevents germination and entry into the cell cycle. *J Biol Chem*. 272:3223-3230.

De Koninck, P., and H. Schulman. 1998. Sensitivity of CaM kinase II to the frequency of Ca2+ oscillations. *Science*. 279:227-230.

Decottignies, A., I. Sanchez-Perez, and P. Nurse. 2003. Schizosaccharomyces pombe essential genes: a pilot study. *Genome Res*. 13:399-406.

Demidchik, V., and F.J. Maathuis. 2007. Physiological roles of nonselective cation channels in plants: from salt stress to signalling and development. *New Phytol*. 175:387-404.

Denis, V., and M.S. Cyert. 2002. Internal Ca(2+) release in yeast is triggered by hypertonic shock and mediated by a TRP channel homologue. *J Cell Biol*. 156:29-34.

Deresinski, S.C., and D.A. Stevens. 2003. Caspofungin. *Clin Infect Dis*. 36:1445-1457.

Dettmann, A., J. Illgen, S. Marz, T. Schurg, A. Fleissner, and S. Seiler. 2012. The NDR kinase scaffold HYM1/MO25 is essential for MAK2 map kinase signaling in Neurospora crassa. *PLoS Genet*. 8:e1002950.

Diegelmann, S., A. Fiala, C. Leibold, T. Spall, and E. Buchner. 2002. Transgenic flies expressing the fluorescence calcium sensor Cameleon 2.1 under UAS control. *Genesis*. 34:95-98.

Diverse-Pierluissi, M.A., T. Fischer, J.D. Jordan, M. Schiff, D.F. Ortiz, M.G. Farquhar, and L. De Vries. 1999. Regulators of G protein signaling proteins as determinants of the rate of desensitization of presynaptic calcium channels. *J Biol Chem*. 274:14490-14494.

Dolphin, A.C. 2003. G protein modulation of voltage-gated calcium channels. *Pharmacol Rev*.

55:607-627.

Dombeck, D.A., C.D. Harvey, L. Tian, L.L. Looger, and D.W. Tank. 2010. Functional imaging of hippocampal place cells at cellular resolution during virtual navigation. *Nat Neurosci*. 13:1433-1440.

Dunlap, J.C., J.J. Loros, H.V. Colot, A. Mehra, W.J. Belden, M. Shi, C.I. Hong, L.F. Larrondo, C.L. Baker, C.H. Chen, C. Schwerdtfeger, P.D. Collopy, J.J. Gamsby, and R. Lambreghts. 2007. A circadian clock in Neurospora: how genes and proteins cooperate to produce a sustained, entrainable, and compensated biological oscillator with a period of about a day. *Cold Spring Harb Symp Quant Biol*. 72:57-68.

Dunn, T., K. Gable, and T. Beeler. 1994. Regulation of cellular Ca2+ by yeast vacuoles. *J Biol Chem*. 269:7273-7278.

Egan, J.D., M.D. Garcia-Pedrajas, D.L. Andrews, and S.E. Gold. 2009. Calcineurin is an antagonist to PKA protein phosphorylation required for postmating filamentation and virulence, while PP2A is required for viability in Ustilago maydis. *Mol Plant Microbe Interact*. 22:1293-1301.

Eilam, Y., J. El-On, and D.T. Spira. 1985. Leishmania major: excreted factor, calcium ions, and the survival of amastigotes. *Exp Parasitol*. 59:161-168.

Eliahu, N., A. Igbaria, M.S. Rose, B.A. Horwitz, and S. Lev. 2007. Melanin biosynthesis in the maize pathogen Cochliobolus heterostrophus depends on two mitogen-activated protein kinases, Chk1 and Mps1, and the transcription factor Cmr1. *Eukaryot Cell*. 6:421-429.

Endo, M. 1977. Calcium release from the sarcoplasmic reticulum. *Physiol Rev*. 57:71-108.

Engh, I., M. Nowrousian, and U. Kuck. 2007a. Regulation of melanin biosynthesis via the dihydroxynaphthalene pathway is dependent on sexual development in the ascomycete Sordaria macrospora. *FEMS Microbiol Lett*. 275:62-70.

Engh, I., C. Wurtz, K. Witzel-Schlomp, H.Y. Zhang, B. Hoff, M. Nowrousian, H. Rottensteiner, and U. Kuck. 2007b. The WW domain protein PRO40 is required for fungal fertility and associates with Woronin bodies. *Eukaryot Cell*. 6:831-843.

Fadri, M., A. Daquinag, S. Wang, T. Xue, and J. Kunz. 2005. The pleckstrin homology domain proteins Slm1 and Slm2 are required for actin cytoskeleton organization in yeast and bind phosphatidylinositol-4,5-bisphosphate and TORC2. *Mol Biol Cell*. 16:1883-1900.

Feizi, A., T. Osterlund, D. Petranovic, S. Bordel, and J. Nielsen. 2013. Genome-scale modeling of the protein secretory machinery in yeast. *PLoS One*. 8:e63284.

Fischer-Parton, S., R.M. Parton, P.C. Hickey, J. Dijksterhuis, H.A. Atkinson, and N.D. Read. 2000. Confocal microscopy of FM4-64 as a tool for analysing endocytosis and vesicle trafficking in living fungal hyphae. *J Microsc*. 198:246-259.

Fischer, M., N. Schnell, J. Chattaway, P. Davies, G. Dixon, and D. Sanders. 1997. The Saccharomyces cerevisiae CCH1 gene is involved in calcium influx and mating. *FEBS*

Lett. 419:259-262.

Fleissner, A., S. Diamond, and N.L. Glass. 2009a. The Saccharomyces cerevisiae PRM1 homolog in Neurospora crassa is involved in vegetative and sexual cell fusion events but also has postfertilization functions. *Genetics*. 181:497-510.

Fleissner, A., and N.L. Glass. 2007. SO, a protein involved in hyphal fusion in Neurospora crassa, localizes to septal plugs. *Eukaryot Cell*. 6:84-94.

Fleissner, A., A.C. Leeder, M.G. Roca, N.D. Read, and N.L. Glass. 2009b. Oscillatory recruitment of signaling proteins to cell tips promotes coordinated behavior during cell fusion. *Proc Natl Acad Sci U S A*. 106:19387-19392.

Fleissner, A., S. Sarkar, D.J. Jacobson, M.G. Roca, N.D. Read, and N.L. Glass. 2005. The so locus is required for vegetative cell fusion and postfertilization events in Neurospora crassa. *Eukaryot Cell*. 4:920-930.

Fleissner, A., A.R. Simonin, and N.L. Glass. 2008. Cell fusion in the filamentous fungus, Neurospora crassa. *Methods Mol Biol*. 475:21-38.

Flick, J.S., and J. Thorner. 1993. Genetic and biochemical characterization of a phosphatidylinositol-specific phospholipase C in Saccharomyces cerevisiae. *Mol Cell Biol*. 13:5861-5876.

Flory, M.R., and T.N. Davis. 1999. Localization of calmodulin in budding yeast and fission yeast using green fluorescent protein. *Methods Enzymol*. 302:87-102.

Franceschini, A., D. Szklarczyk, S. Frankild, M. Kuhn, M. Simonovic, A. Roth, J. Lin, P. Minguez, P. Bork, C. von Mering, and L.J. Jensen. 2013. STRING v9.1: protein-protein interaction networks, with increased coverage and integration. *Nucleic Acids Res*. 41:D808-815.

Freitag, M., P.C. Hickey, N.B. Raju, E.U. Selker, and N.D. Read. 2004. GFP as a tool to analyze the organization, dynamics and function of nuclei and microtubules in Neurospora crassa. *Fungal Genet Biol*. 41:897-910.

Freitag, M., and E.U. Selker. 2005. Controlling DNA methylation: many roads to one modification. *Curr Opin Genet Dev*. 15:191-199.

Frieman, M.B., and B.P. Cormack. 2004. Multiple sequence signals determine the distribution of glycosylphosphatidylinositol proteins between the plasma membrane and cell wall in Saccharomyces cerevisiae. *Microbiology*. 150:3105-3114.

Fu, C., P. Iyer, A. Herkal, J. Abdullah, A. Stout, and S.J. Free. 2011. Identification and characterization of genes required for cell-to-cell fusion in Neurospora crassa. *Eukaryot Cell*. 10:1100-1109.

Fuchs, F., and B. Westermann. 2005. Role of Unc104/KIF1-related motor proteins in mitochondrial transport in Neurospora crassa. *Mol Biol Cell*. 16:153-161.

Galagan, J.E., S.E. Calvo, K.A. Borkovich, E.U. Selker, N.D. Read, D. Jaffe, W. FitzHugh, L.J. Ma, S. Smirnov, S. Purcell, B. Rehman, T. Elkins, R. Engels, S. Wang, C.B. Nielsen, J. Butler,

M. Endrizzi, D. Qui, P. Ianakiev, D. Bell-Pedersen, M.A. Nelson, M. Werner-Washburne, C.P. Selitrennikoff, J.A. Kinsey, E.L. Braun, A. Zelter, U. Schulte, G.O. Kothe, G. Jedd, W. Mewes, C. Staben, E. Marcotte, D. Greenberg, A. Roy, K. Foley, J. Naylor, N. Stange-Thomann, R. Barrett, S. Gnerre, M. Kamal, M. Kamvysselis, E. Mauceli, C. Bielke, S. Rudd, D. Frishman, S. Krystofova, C. Rasmussen, R.L. Metzenberg, D.D. Perkins, S. Kroken, C. Cogoni, G. Macino, D. Catcheside, W. Li, R.J. Pratt, S.A. Osmani, C.P. DeSouza, L. Glass, M.J. Orbach, J.A. Berglund, R. Voelker, O. Yarden, M. Plamann, S. Seiler, J. Dunlap, A. Radford, R. Aramayo, D.O. Natvig, L.A. Alex, G. Mannhaupt, D.J. Ebbole, M. Freitag, I. Paulsen, M.S. Sachs, E.S. Lander, C. Nusbaum, and B. Birren. 2003. The genome sequence of the filamentous fungus Neurospora crassa. *Nature*. 422:859-868.

Gammie, A.E., V. Brizzio, and M.D. Rose. 1998. Distinct morphological phenotypes of cell fusion mutants. *Mol Biol Cell*. 9:1395-1410.

Garcia-Effron, G., S. Lee, S. Park, J.D. Cleary, and D.S. Perlin. 2009. Effect of Candida glabrata FKS1 and FKS2 mutations on echinocandin sensitivity and kinetics of 1,3-beta-D-glucan synthase: implication for the existing susceptibility breakpoint. *Antimicrob Agents Chemother*. 53:3690-3699.

Garrett-Engele, P., B. Moilanen, and M.S. Cyert. 1995. Calcineurin, the Ca2+/calmodulin-dependent protein phosphatase, is essential in yeast mutants with cell integrity defects and in mutants that lack a functional vacuolar H(+)-ATPase. *Mol Cell Biol*. 15:4103-4114.

Geiser, J.R., D. van Tuinen, S.E. Brockerhoff, M.M. Neff, and T.N. Davis. 1991. Can calmodulin function without binding calcium? *Cell*. 65:949-959.

Geisow, M.J. 1986. Common domain structure of Ca2+ and lipid-binding proteins. *FEBS Lett*. 203:99-103.

Geli, M.I., and H. Riezman. 1998. Endocytic internalization in yeast and animal cells: similar and different. *J Cell Sci*. 111 (Pt 8):1031-1037.

Geli, M.I., A. Wesp, and H. Riezman. 1998. Distinct functions of calmodulin are required for the uptake step of receptor-mediated endocytosis in yeast: the type I myosin Myo5p is one of the calmodulin targets. *EMBO J*. 17:635-647.

Geng, F., Y. Cao, and B.C. Laurent. 2001. Essential roles of Snf5p in Snf-Swi chromatin remodeling in vivo. *Mol Cell Biol*. 21:4311-4320.

Gerke, V., C.E. Creutz, and S.E. Moss. 2005. Annexins: linking Ca2+ signalling to membrane dynamics. *Nat Rev Mol Cell Biol*. 6:449-461.

Gietzen, K., I. Sadorf, and H. Bader. 1982. A model for the regulation of the calmodulin-dependent enzymes erythrocyte Ca2+-transport ATPase and brain phosphodiesterase by activators and inhibitors. *Biochem J*. 207:541-548.

Gilkey, J.C., L.F. Jaffe, E.B. Ridgway, and G.T. Reynolds. 1978. A free calcium wave traverses the

activating egg of the medaka, Oryzias latipes. *J Cell Biol*. 76:448-466.

Gillis, T.E., D.A. Martyn, A.J. Rivera, and M. Regnier. 2007. Investigation of thin filament near-neighbour regulatory unit interactions during force development in skinned cardiac and skeletal muscle. *J Physiol*. 580:561-576.

Gilroy, S., N.D. Read, and A.J. Trewavas. 1990. Elevation of cytoplasmic calcium by caged calcium or caged inositol triphosphate initiates stomatal closure. *Nature*. 346:769-771.

Gingras, A.C., M. Gstaiger, B. Raught, and R. Aebersold. 2007. Analysis of protein complexes using mass spectrometry. *Nat Rev Mol Cell Biol*. 8:645-654.

Glass, N.L., D.J. Jacobson, and P.K. Shiu. 2000. The genetics of hyphal fusion and vegetative incompatibility in filamentous ascomycete fungi. *Annu Rev Genet*. 34:165-186.

Gnegy, M.E. 1993. Calmodulin in neurotransmitter and hormone action. *Annu Rev Pharmacol Toxicol*. 33:45-70.

Goryachev, A.B., A. Lichius, G.D. Wright, and N.D. Read. 2012. Excitable behavior can explain the "ping-pong" mode of communication between cells using the same chemoattractant. *Bioessays*. 34:259-266.

Goudreault, M., L.M. D'Ambrosio, M.J. Kean, M.J. Mullin, B.G. Larsen, A. Sanchez, S. Chaudhry, G.I. Chen, F. Sicheri, A.I. Nesvizhskii, R. Aebersold, B. Raught, and A.C. Gingras. 2009. A PP2A phosphatase high density interaction network identifies a novel striatin-interacting phosphatase and kinase complex linked to the cerebral cavernous malformation 3 (CCM3) protein. *Mol Cell Proteomics*. 8:157-171.

Green, M.S., and E. Jucha. 1987. Interrelationships between blood pressure, serum calcium and other biochemical variables. *Int J Epidemiol*. 16:532-536.

Grienberger, C., and A. Konnerth. 2012. Imaging calcium in neurons. *Neuron*. 73:862-885.

Griffin, D. 1994. Fungal Physiology.

Griffith, L.C., and H. Schulman. 1988. The multifunctional Ca2+/calmodulin-dependent protein kinase mediates Ca2+-dependent phosphorylation of tyrosine hydroxylase. *J Biol Chem*. 263:9542-9549.

Groll, A.H., and T.J. Walsh. 2001. Caspofungin: pharmacology, safety and therapeutic potential in superficial and invasive fungal infections. *Expert Opin Investig Drugs*. 10:1545-1558.

Groppi, S., F. Belotti, R.L. Brandao, E. Martegani, and R. Tisi. 2011. Glucose-induced calcium influx in budding yeast involves a novel calcium transport system and can activate calcineurin. *Cell Calcium*. 49:376-386.

Grote, E. 2010. Secretion is required for late events in the cell-fusion pathway of mating yeast. *J Cell Sci*. 123:1902-1912.

Grynkiewicz, G., M. Poenie, and R.Y. Tsien. 1985. A new generation of Ca2+ indicators with greatly improved fluorescence properties. *J Biol Chem*. 260:3440-3450.

Harmon, A.C., M. Gribskov, and J.F. Harper. 2000. CDPKs - a kinase for every Ca2+ signal? *Trends Plant Sci*. 5:154-159.

Hasan, M.T., R.W. Friedrich, T. Euler, M.E. Larkum, G. Giese, M. Both, J. Duebel, J. Waters, H. Bujard, O. Griesbeck, R.Y. Tsien, T. Nagai, A. Miyawaki, and W. Denk. 2004. Functional fluorescent Ca2+ indicator proteins in transgenic mice under TET control. *PLoS Biol*. 2:e163.

Haugland, R.P. 1996. Handbook of fluorescent probes and research chemicals. Molecular Probes Inc., Eugene, Oregon. .

Heath, V.L., S.L. Shaw, S. Roy, and M.S. Cyert. 2004. Hph1p and Hph2p, novel components of calcineurin-mediated stress responses in Saccharomyces cerevisiae. *Eukaryot Cell*. 3:695-704.

Hennings, H., D. Michael, C. Cheng, P. Steinert, K. Holbrook, and S.H. Yuspa. 1980. Calcium regulation of growth and differentiation of mouse epidermal cells in culture. *Cell*. 19:245-254.

Hepler, J.R. 1999. Emerging roles for RGS proteins in cell signalling. *Trends Pharmacol Sci*. 20:376-382.

Hetherington, A.M., and C. Brownlee. 2004. The generation of Ca(2+) signals in plants. *Annu Rev Plant Biol*. 55:401-427.

Hickey, P.C., D. Jacobson, N.D. Read, and N.L. Glass. 2002a. Live-cell imaging of vegetative hyphal fusion in Neurospora crassa. *Fungal Genet Biol*. 37:109-119.

Hickey, P.C., D. Jacobson, N.D. Read, and N.L. Louise Glass. 2002b. Live-cell imaging of vegetative hyphal fusion in Neurospora crassa. *Fungal Genet Biol*. 37:109-119.

Hickey, P.C., S.M. Swift, M.G. Roca, and N.D. Read. 2004. Live-cell Imaging of Filamentous Fungi Using Vital Fluorescent Dyes and Confocal Microscopy. *Methods in Microbiology*. 24:63-87.

Hidalgo, F.J., and R. Zamora. 2007. Conversion of phenylalanine into styrene by 2,4-decadienal in model systems. *J Agric Food Chem*. 55:4902-4906.

Higashijima, S., M.A. Masino, G. Mandel, and J.R. Fetcho. 2003. Imaging neuronal activity during zebrafish behavior with a genetically encoded calcium indicator. *J Neurophysiol*. 90:3986-3997.

Hirano, S., A. Nose, K. Hatta, A. Kawakami, and M. Takeichi. 1987. Calcium-dependent cell-cell adhesion molecules (cadherins): subclass specificities and possible involvement of actin bundles. *J Cell Biol*. 105:2501-2510.

Hirschi, K.D., M.L. Miranda, and N.L. Wilganowski. 2001. Phenotypic changes in Arabidopsis caused by expression of a yeast vacuolar Ca2+/H+ antiporter. *Plant Mol Biol*. 46:57-65.

Hjalm, G., R.J. MacLeod, O. Kifor, N. Chattopadhyay, and E.M. Brown. 2001. Filamin-A binds to the carboxyl-terminal tail of the calcium-sensing receptor, an interaction that

participates in CaR-mediated activation of mitogen-activated protein kinase. *J Biol Chem*. 276:34880-34887.

Hofer, A.M., and E.M. Brown. 2003. Extracellular calcium sensing and signalling. *Nat Rev Mol Cell Biol*. 4:530-538.

Hoffmann, J., and K. Mendgen. 1998. Endocytosis and membrane turnover in the germ tube of uromyces fabae. *Fungal Genet Biol*. 24:77-85.

Holda, J.R., A. Klishin, M. Sedova, J. Huser, and L.A. Blatter. 1998. Capacitative Calcium Entry. *News Physiol Sci*. 13:157-163.

Honda, S., and E.U. Selker. 2009. Tools for fungal proteomics: multifunctional neurospora vectors for gene replacement, protein expression and protein purification. *Genetics*. 182:11-23.

Hong-Geller, E., and R.A. Cerione. 2000. Cdc42 and Rac stimulate exocytosis of secretory granules by activating the IP(3)/calcium pathway in RBL-2H3 mast cells. *J Cell Biol*. 148:481-494.

Hou, Z., C. Xue, Y. Peng, T. Katan, H.C. Kistler, and J.R. Xu. 2002. A mitogen-activated protein kinase gene (MGV1) in Fusarium graminearum is required for female fertility, heterokaryon formation, and plant infection. *Mol Plant Microbe Interact*. 15:1119-1127.

Hrabak, E.M., L.J. Dickmann, J.S. Satterlee, and M.R. Sussman. 1996. Characterization of eight new members of the calmodulin-like domain protein kinase gene family from Arabidopsis thaliana. *Plant Mol Biol*. 31:405-412.

Hwang, J., and D.C. Pallas. 2014. STRIPAK complexes: structure, biological function, and involvement in human diseases. *Int J Biochem Cell Biol*. 47:118-148.

Iida, H., H. Nakamura, T. Ono, M.S. Okumura, and Y. Anraku. 1994. MID1, a novel Saccharomyces cerevisiae gene encoding a plasma membrane protein, is required for Ca2+ influx and mating. *Mol Cell Biol*. 14:8259-8271.

Iida, H., Y. Yagawa, and Y. Anraku. 1990. Essential role for induced Ca2+ influx followed by [Ca2+]i rise in maintaining viability of yeast cells late in the mating pheromone response pathway. A study of [Ca2+]i in single Saccharomyces cerevisiae cells with imaging of fura-2. *J Biol Chem*. 265:13391-13399.

Inoue, S.B., H. Qadota, M. Arisawa, T. Watanabe, and Y. Ohya. 1999. Prenylation of Rho1p is required for activation of yeast 1, 3-beta-glucan synthase. *J Biol Chem*. 274:38119-38124.

Inouye, S., M. Noguchi, Y. Sakaki, Y. Takagi, T. Miyata, S. Iwanaga, and F.I. Tsuji. 1985. Cloning and sequence analysis of cDNA for the luminescent protein aequorin. *Proc Natl Acad Sci U S A*. 82:3154-3158.

Itadani, A., T. Nakamura, A. Hirata, and C. Shimoda. 2010. Schizosaccharomyces pombe calmodulin, Cam1, plays a crucial role in sporulation by recruiting and stabilizing the

spindle pole body components responsible for assembly of the forespore membrane. *Eukaryot Cell*. 9:1925-1935.

Iwano, M., H. Shiba, T. Miwa, F.S. Che, S. Takayama, T. Nagai, A. Miyawaki, and A. Isogai. 2004. Ca2+ dynamics in a pollen grain and papilla cell during pollination of Arabidopsis. *Plant Physiol*. 136:3562-3571.

Jaffe, A.B., A. Hall, and A. Schmidt. 2005. Association of CNK1 with Rho guanine nucleotide exchange factors controls signaling specificity downstream of Rho. *Curr Biol*. 15:405-412.

Jaffe, L.F. 2010. Fast calcium waves. *Cell Calcium*. 48:102-113.

Janmey, P.A. 1994. Phosphoinositides and calcium as regulators of cellular actin assembly and disassembly. *Annu Rev Physiol*. 56:169-191.

Janssens, V., and J. Goris. 2001. Protein phosphatase 2A: a highly regulated family of serine/threonine phosphatases implicated in cell growth and signalling. *Biochem J*. 353:417-439.

Jurado, L.A., P.S. Chockalingam, and H.W. Jarrett. 1999. Apocalmodulin. *Physiol Rev*. 79:661-682.

Juvvadi, P.R., J.R. Fortwendel, L.E. Rogg, K.A. Burns, S.H. Randell, and W.J. Steinbach. 2011. Localization and activity of the calcineurin catalytic and regulatory subunit complex at the septum is essential for hyphal elongation and proper septation in Aspergillus fumigatus. *Mol Microbiol*. 82:1235-1259.

Karamushka, V.I., and G.M. Gadd. 1994. Influence of copper on proton efflux from Saccharomyces cerevisiae and the protective effect of calcium and magnesium. *FEMS Microbiol Lett*. 122:33-38.

Kawano, C.Y., and S. Said. 2002. Morphological alterations induced by cold-shock in Neurospora crassa. *J Basic Microbiol*. 42:381-387.

Kawano, S., S. Okajima, A. Mizoguchi, K. Tamai, Y. Hirasawa, and C. Ide. 1997. Immunocytochemical distribution of Ca(2+)-independent protein kinase C subtypes (delta, epsilon, and zeta) in regenerating axonal growth cones of rat peripheral nerve. *Neuroscience*. 81:263-273.

Kean, M.J., D.F. Ceccarelli, M. Goudreault, M. Sanches, S. Tate, B. Larsen, L.C. Gibson, W.B. Derry, I.C. Scott, L. Pelletier, G.S. Baillie, F. Sicheri, and A.C. Gingras. 2011. Structure-function analysis of core STRIPAK Proteins: a signaling complex implicated in Golgi polarization. *J Biol Chem*. 286:25065-25075.

Keith, C.H., A.S. Bajer, R. Ratan, F.R. Maxfield, and M.L. Shelanski. 1986. Calcium and calmodulin in the regulation of the microtubular cytoskeleton. *Ann N Y Acad Sci*. 466:375-391.

Kemler, R., M. Ozawa, and M. Ringwald. 1989. Calcium-dependent cell adhesion molecules. *Curr Opin Cell Biol*. 1:892-897.

Khalaj, V., L. Smith, J. Brookman, and D. Tuckwell. 2004. Identification of a novel class of annexin genes. *FEBS Lett*. 562:79-86.

Kim, B.J., J.H. Jeon, S.J. Kim, and I. So. 2007. Role of calmodulin and myosin light chain kinase in the activation of carbachol-activated cationic current in murine ileal myocytes. *Can J Physiol Pharmacol*. 85:1254-1262.

Kim, C.K., J.S. Han, H.S. Lee, J.Y. Oh, T. Shigaki, S.H. Park, and K. Hirschi. 2006. Expression of an Arabidopsis CAX2 variant in potato tubers increases calcium levels with no accumulation of manganese. *Plant Cell Rep*. 25:1226-1232.

Kim, H.S., K.J. Czymmek, A. Patel, S. Modla, A. Nohe, R. Duncan, S. Gilroy, and S. Kang. 2012. Expression of the Cameleon calcium biosensor in fungi reveals distinct Ca(2+) signatures associated with polarized growth, development, and pathogenesis. *Fungal Genet Biol*. 49:589-601.

Kinnunen, P.K., and J.M. Holopainen. 2000. Mechanisms of initiation of membrane fusion: role of lipids. *Biosci Rep*. 20:465-482.

Kinsey, J.A., P.W. Garrett-Engele, E.B. Cambareri, and E.U. Selker. 1994. The Neurospora transposon Tad is sensitive to repeat-induced point mutation (RIP). *Genetics*. 138:657-664.

Klee, C.B., T.H. Crouch, and M.H. Krinks. 1979. Calcineurin: a calcium- and calmodulin-binding protein of the nervous system. *Proc Natl Acad Sci U S A*. 76:6270-6273.

Klee, C.B., H. Ren, and X. Wang. 1998. Regulation of the calmodulin-stimulated protein phosphatase, calcineurin. *J Biol Chem*. 273:13367-13370.

Klockner, U., and G. Isenberg. 1987. Calmodulin antagonists depress calcium and potassium currents in ventricular and vascular myocytes. *Am J Physiol*. 253:H1601-1611.

Knight, M.R., A.K. Campbell, S.M. Smith, and A.J. Trewavas. 1991. Recombinant aequorin as a probe for cytosolic free Ca2+ in Escherichia coli. *FEBS Lett*. 282:405-408.

Ko, K.S., P.D. Arora, and C.A. McCulloch. 2001. Cadherins mediate intercellular mechanical signaling in fibroblasts by activation of stretch-sensitive calcium-permeable channels. *J Biol Chem*. 276:35967-35977.

Konig, J., S. Baumann, J. Koepke, T. Pohlmann, K. Zarnack, and M. Feldbrugge. 2009. The fungal RNA-binding protein Rrm4 mediates long-distance transport of ubi1 and rho3 mRNAs. *EMBO J*. 28:1855-1866.

Kontoyiannis, D.P., R.E. Lewis, N. Osherov, N.D. Albert, and G.S. May. 2003. Combination of caspofungin with inhibitors of the calcineurin pathway attenuates growth in vitro in Aspergillus species. *J Antimicrob Chemother*. 51:313-316.

Kornstein, L.B., M.L. Gaiso, R.L. Hammell, and D.C. Bartelt. 1992. Cloning and sequence determination of a cDNA encoding Aspergillus nidulans calmodulin-dependent multifunctional protein kinase. *Gene*. 113:75-82.

Kosuta, S., S. Hazledine, J. Sun, H. Miwa, R.J. Morris, J.A. Downie, and G.E. Oldroyd. 2008.

Differential and chaotic calcium signatures in the symbiosis signaling pathway of legumes. *Proc Natl Acad Sci U S A*. 105:9823-9828.

Kraus, P.R., D.S. Fox, G.M. Cox, and J. Heitman. 2003. The Cryptococcus neoformans MAP kinase Mpk1 regulates cell integrity in response to antifungal drugs and loss of calcineurin function. *Mol Microbiol*. 48:1377-1387.

Krumlauf, R., and G.A. Marzluf. 1979. Characterization of the sequence complexity and organization of the Neurospora crassa genome. *Biochemistry*. 18:3705-3713.

Krumlauf, R., and G.A. Marzluf. 1980. Genome organization and characterization of the repetitive and inverted repeat DNA sequences in Neurospora crassa. *J Biol Chem*. 255:1138-1145.

Kwon, M.J., M. Arentshorst, E.D. Roos, C.A. van den Hondel, V. Meyer, and A.F. Ram. 2011. Functional characterization of Rho GTPases in Aspergillus niger uncovers conserved and diverged roles of Rho proteins within filamentous fungi. *Mol Microbiol*. 79:1151-1167.

Larrondo, L.F., H.V. Colot, C.L. Baker, J.J. Loros, and J.C. Dunlap. 2009. Fungal functional genomics: tunable knockout-knock-in expression and tagging strategies. *Eukaryot Cell*. 8:800-804.

Lawrence, C.J., R.K. Dawe, K.R. Christie, D.W. Cleveland, S.C. Dawson, S.A. Endow, L.S. Goldstein, H.V. Goodson, N. Hirokawa, J. Howard, R.L. Malmberg, J.R. McIntosh, H. Miki, T.J. Mitchison, Y. Okada, A.S. Reddy, W.M. Saxton, M. Schliwa, J.M. Scholey, R.D. Vale, C.E. Walczak, and L. Wordeman. 2004. A standardized kinesin nomenclature. *J Cell Biol*. 167:19-22.

Lee, B.N., and T.H. Adams. 1994. Overexpression of flbA, an early regulator of Aspergillus asexual sporulation, leads to activation of brlA and premature initiation of development. *Mol Microbiol*. 14:323-334.

Leeder, A.C., W. Jonkers, J. Li, and N.L. Glass. 2013. Early colony establishment in Neurospora crassa requires a MAP kinase regulatory network. *Genetics*. 195:883-898.

Lev, S., D. Desmarini, M. Chayakulkeeree, T.C. Sorrell, and J.T. Djordjevic. 2012. The Crz1/Sp1 transcription factor of Cryptococcus neoformans is activated by calcineurin and regulates cell wall integrity. *PLoS One*. 7:e51403.

Levin, D.E. 2011. Regulation of cell wall biogenesis in Saccharomyces cerevisiae: the cell wall integrity signaling pathway. *Genetics*. 189:1145-1175.

Li, J., A. Negro, J. Lopez, A.L. Bauman, E. Henson, K. Dodge-Kafka, and M.S. Kapiloff. 2010. The mAKAPbeta scaffold regulates cardiac myocyte hypertrophy via recruitment of activated calcineurin. *J Mol Cell Cardiol*. 48:387-394.

Lichius, A. 2010. Cell Fusion in Neurospora crassa. Vol. Ph.D. The University of Edinburgh.

Lichius, A., A.B. Goryachev, M.D. Fricker, B. Obara, E. Castro-Longoria, and N.D. Read. 2014. CDC-42 and RAC-1 regulate opposite chemotropisms in Neurospora crassa. *J Cell Sci*.

127:1953-1965.

Lichius, A., K.M. Lord, C.E. Jeffree, R. Oborny, P. Boonyarungsrit, and N.D. Read. 2012a. Importance of MAP kinases during protoperithecial morphogenesis in Neurospora crassa. *PLoS One*. 7:e42565.

Lichius, A., M.E. Yanez-Gutierrez, N.D. Read, and E. Castro-Longoria. 2012b. Comparative live-cell imaging analyses of SPA-2, BUD-6 and BNI-1 in Neurospora crassa reveal novel features of the filamentous fungal polarisome. *PLoS One*. 7:e30372.

Liu, M., P. Du, G. Heinrich, G.M. Cox, and A. Gelli. 2006a. Cch1 mediates calcium entry in Cryptococcus neoformans and is essential in low-calcium environments. *Eukaryot Cell*. 5:1788-1796.

Liu, Q., B.J. Wilkins, Y.J. Lee, H. Ichijo, and J.D. Molkentin. 2006b. Direct interaction and reciprocal regulation between ASK1 and calcineurin-NFAT control cardiomyocyte death and growth. *Mol Cell Biol*. 26:3785-3797.

Locke, E.G., M. Bonilla, L. Liang, Y. Takita, and K.W. Cunningham. 2000. A homolog of voltage-gated Ca(2+) channels stimulated by depletion of secretory Ca(2+) in yeast. *Mol Cell Biol*. 20:6686-6694.

Lum, G., and X.J. Min. 2011. FunSecKB: the Fungal Secretome KnowledgeBase. *Database (Oxford)*. 2011:bar001.

Lydan, M.A., and D.H. O'Day. 1993. Calmodulin and calmodulin-binding proteins during cell fusion in Dictyostelium discoideum: developmental regulation by calcium ions. *Exp Cell Res*. 205:134-141.

MacRobbie, E.A. 2000. ABA activates multiple Ca(2+) fluxes in stomatal guard cells, triggering vacuolar K(+)(Rb(+)) release. *Proc Natl Acad Sci U S A*. 97:12361-12368.

Maerz, S., A. Dettmann, C. Ziv, Y. Liu, O. Valerius, O. Yarden, and S. Seiler. 2009. Two NDR kinase-MOB complexes function as distinct modules during septum formation and tip extension in Neurospora crassa. *Mol Microbiol*. 74:707-723.

Maerz, S., Y. Funakoshi, Y. Negishi, T. Suzuki, and S. Seiler. 2010. The Neurospora peptide:N-glycanase ortholog PNG1 is essential for cell polarity despite its lack of enzymatic activity. *J Biol Chem*. 285:2326-2332.

Maerz, S., C. Ziv, N. Vogt, K. Helmstaedt, N. Cohen, R. Gorovits, O. Yarden, and S. Seiler. 2008. The nuclear Dbf2-related kinase COT1 and the mitogen-activated protein kinases MAK1 and MAK2 genetically interact to regulate filamentous growth, hyphal fusion and sexual development in Neurospora crassa. *Genetics*. 179:1313-1325.

Mahs, A., T. Ischebeck, Y. Heilig, I. Stenzel, F. Hempel, S. Seiler, and I. Heilmann. 2012. The essential phosphoinositide kinase MSS-4 is required for polar hyphal morphogenesis, localizing to sites of growth and cell fusion in Neurospora crassa. *PLoS One*. 7:e51454.

Masloff, S., S. Poggeler, and U. Kuck. 1999. The pro1(+) gene from Sordaria macrospora

encodes a C6 zinc finger transcription factor required for fruiting body development. *Genetics*. 152:191-199.

Matheos, D.P., T.J. Kingsbury, U.S. Ahsan, and K.W. Cunningham. 1997. Tcn1p/Crz1p, a calcineurin-dependent transcription factor that differentially regulates gene expression in Saccharomyces cerevisiae. *Genes Dev*. 11:3445-3458.

Matsumoto, T.K., A.J. Ellsmore, S.G. Cessna, P.S. Low, J.M. Pardo, R.A. Bressan, and P.M. Hasegawa. 2002. An osmotically induced cytosolic Ca2+ transient activates calcineurin signaling to mediate ion homeostasis and salt tolerance of Saccharomyces cerevisiae. *J Biol Chem*. 277:33075-33080.

Matthiesen, R. 2007. Useful mass spectrometry programs freely available on the internet. *Methods Mol Biol*. 367:303-305.

Mayor, S., and H. Riezman. 2004. Sorting GPI-anchored proteins. *Nat Rev Mol Cell Biol*. 5:110-120.

Mazur, P., and W. Baginsky. 1996. In vitro activity of 1,3-beta-D-glucan synthase requires the GTP-binding protein Rho1. *J Biol Chem*. 271:14604-14609.

McAinsh, M.R., and J.K. Pittman. 2009. Shaping the calcium signature. *New Phytol*. 181:275-294.

Mellman, I. 1996. Endocytosis and molecular sorting. *Annu Rev Cell Dev Biol*. 12:575-625.

Merlini, L., O. Dudin, and S.G. Martin. 2013. Mate and fuse: how yeast cells do it.

Metzenberg, R.L., and N.L. Glass. 1990. Mating type and mating strategies in Neurospora. *Bioessays*. 12:53-59.

Michard, E., P.T. Lima, F. Borges, A.C. Silva, M.T. Portes, J.E. Carvalho, M. Gilliham, L.H. Liu, G. Obermeyer, and J.A. Feijo. 2011. Glutamate receptor-like genes form Ca2+ channels in pollen tubes and are regulated by pistil D-serine. *Science*. 332:434-437.

Miller, A.J., G. Vogg, and D. Sanders. 1990. Cytosolic calcium homeostasis in fungi: roles of plasma membrane transport and intracellular sequestration of calcium. *Proc Natl Acad Sci U S A*. 87:9348-9352.

Miller, K.D. 1994. A model for the development of simple cell receptive fields and the ordered arrangement of orientation columns through activity-dependent competition between ON- and OFF-center inputs. *J Neurosci*. 14:409-441.

Minta, A., and R.Y. Tsien. 1989. Fluorescent indicators for cytosolic sodium. *J Biol Chem*. 264:19449-19457.

Missiaen, L., L. Dode, J. Vanoevelen, L. Raeymaekers, and F. Wuytack. 2007. Calcium in the Golgi apparatus. *Cell Calcium*. 41:405-416.

Miyawaki, A., J. Llopis, R. Heim, J.M. McCaffery, J.A. Adams, M. Ikura, and R.Y. Tsien. 1997. Fluorescent indicators for Ca2+ based on green fluorescent proteins and calmodulin. *Nature*. 388:882-887.

Monshausen, G.B., M.A. Messerli, and S. Gilroy. 2008. Imaging of the Yellow Cameleon 3.6

indicator reveals that elevations in cytosolic Ca2+ follow oscillating increases in growth in root hairs of Arabidopsis. *Plant Physiol*. 147:1690-1698.

Moser, M.J., M.R. Flory, and T.N. Davis. 1997. Calmodulin localizes to the spindle pole body of Schizosaccharomyces pombe and performs an essential function in chromosome segregation. *J Cell Sci*. 110 (Pt 15):1805-1812.

Muller, E.M., E.G. Locke, and K.W. Cunningham. 2001. Differential regulation of two Ca(2+) influx systems by pheromone signaling in Saccharomyces cerevisiae. *Genetics*. 159:1527-1538.

Muller, E.M., N.A. Mackin, S.E. Erdman, and K.W. Cunningham. 2003. Fig1p facilitates Ca2+ influx and cell fusion during mating of Saccharomyces cerevisiae. *J Biol Chem*. 278:38461-38469.

Munro, C.A., S. Selvaggini, I. de Bruijn, L. Walker, M.D. Lenardon, B. Gerssen, S. Milne, A.J. Brown, and N.A. Gow. 2007. The PKC, HOG and Ca2+ signalling pathways co-ordinately regulate chitin synthesis in Candida albicans. *Mol Microbiol*. 63:1399-1413.

Nair, R., S. Raina, T. Keshavarz, and M.J. Kerrigan. 2011a. Application of fluorescent indicators to analyse intracellular calcium and morphology in filamentous fungi. *Fungal Biol*. 115:326-334.

Nair, R., S. Raina, T. Keshavarz, and M.J. Kerrigan. 2011b. Application of fluorescent indicators to analyse intracellular calcium and morphology in filamentous fungi. *Fungal biology*. 115:326-334.

Nakai, J., M. Ohkura, and K. Imoto. 2001. A high signal-to-noise Ca(2+) probe composed of a single green fluorescent protein. *Nat Biotechnol*. 19:137-141.

Nakajima-Shimada, J., H. Iida, F.I. Tsuji, and Y. Anraku. 1991. Monitoring of intracellular calcium in Saccharomyces cerevisiae with an apoaequorin cDNA expression system. *Proc Natl Acad Sci U S A*. 88:6878-6882.

Nakazawa, K., K. Higo, K. Abe, Y. Tanaka, H. Saito, and N. Matsuki. 1993. Blockade by calmodulin inhibitors of Ca2+ channels in smooth muscle from rat vas deferens. *Br J Pharmacol*. 109:137-141.

Nalefski, E.A., and J.J. Falke. 1996. The C2 domain calcium-binding motif: structural and functional diversity. *Protein Sci*. 5:2375-2390.

Naor, Z., M.S. Shearman, A. Kishimoto, and Y. Nishizuka. 1988. Calcium-independent activation of hypothalamic type I protein kinase C by unsaturated fatty acids. *Mol Endocrinol*. 2:1043-1048.

Narasimhulu, S.B., and A.S. Reddy. 1998. Characterization of microtubule binding domains in the Arabidopsis kinesin-like calmodulin binding protein. *Plant Cell*. 10:957-965.

Nelson, G., O. Kozlova-Zwinderman, A.J. Collis, M.R. Knight, J.R. Fincham, C.P. Stanger, A. Renwick, J.G. Hessing, P.J. Punt, C.A. van den Hondel, and N.D. Read. 2004. Calcium

measurement in living filamentous fungi expressing codon-optimized aequorin. *Mol Microbiol*. 52:1437-1450.

Nguyen, Q.B., N. Kadotani, S. Kasahara, Y. Tosa, S. Mayama, and H. Nakayashiki. 2008. Systematic functional analysis of calcium-signalling proteins in the genome of the rice-blast fungus, Magnaporthe oryzae, using a high-throughput RNA-silencing system. *Mol Microbiol*. 68:1348-1365.

Ninomiya, Y., K. Suzuki, C. Ishii, and H. Inoue. 2004. Highly efficient gene replacements in Neurospora strains deficient for nonhomologous end-joining. *Proc Natl Acad Sci U S A*. 101:12248-12253.

Nishizuka, Y. 1986. Studies and perspectives of protein kinase C. *Science*. 233:305-312.

O'Connor, R.P., S.D. Madison, P. Leveque, H.L. Roderick, and M.D. Bootman. 2010. Exposure to GSM RF fields does not affect calcium homeostasis in human endothelial cells, rat pheocromocytoma cells or rat hippocampal neurons. *PLoS One*. 5:e11828.

Ohkura, M., M. Matsuzaki, H. Kasai, K. Imoto, and J. Nakai. 2005. Genetically encoded bright Ca2+ probe applicable for dynamic Ca2+ imaging of dendritic spines. *Anal Chem*. 77:5861-5869.

Oldenburg, K.R., K.T. Vo, S. Michaelis, and C. Paddon. 1997. Recombination-mediated PCR-directed plasmid construction in vivo in yeast. *Nucleic Acids Res*. 25:451-452.

Paidhungat, M., and S. Garrett. 1997. A homolog of mammalian, voltage-gated calcium channels mediates yeast pheromone-stimulated Ca2+ uptake and exacerbates the cdc1(Ts) growth defect. *Mol Cell Biol*. 17:6339-6347.

Palma-Guerrero, J., A.C. Leeder, J. Welch, and N.L. Glass. 2014. Identification and characterization of LFD1, a novel protein involved in membrane merger during cell fusion in Neurospora crassa. *Mol Microbiol*. 92:164-182.

Palmer, C.P., X.L. Zhou, J. Lin, S.H. Loukin, C. Kung, and Y. Saimi. 2001. A TRP homolog in Saccharomyces cerevisiae forms an intracellular Ca(2+)-permeable channel in the yeast vacuolar membrane. *Proc Natl Acad Sci U S A*. 98:7801-7805.

Pandey, A., M.G. Roca, N.D. Read, and N.L. Glass. 2004. Role of a mitogen-activated protein kinase pathway during conidial germination and hyphal fusion in Neurospora crassa. *Eukaryot Cell*. 3:348-358.

Parent, S.A., J.B. Nielsen, N. Morin, G. Chrebet, N. Ramadan, A.M. Dahl, M.J. Hsu, K.A. Bostian, and F. Foor. 1993. Calcineurin-dependent growth of an FK506- and CsA-hypersensitive mutant of Saccharomyces cerevisiae. *J Gen Microbiol*. 139:2973-2984.

Park, G., S. Pan, and K.A. Borkovich. 2008. Mitogen-activated protein kinase cascade required for regulation of development and secondary metabolism in Neurospora crassa. *Eukaryot Cell*. 7:2113-2122.

Park, H.O., and E. Bi. 2007. Central roles of small GTPases in the development of cell polarity

in yeast and beyond. *Microbiol Mol Biol Rev*. 71:48-96.

Parton, R.M., S. Fischer, R. Malho, O. Papasouliotis, T.C. Jelitto, T. Leonard, and N.D. Read. 1997. Pronounced cytoplasmic pH gradients are not required for tip growth in plant and fungal cells. *J Cell Sci*. 110:1187-1198.

Parton, R.M., and N.D. Read. 1999. Calcium and pH imaging in living cells. Oxford University Press, Oxford, UK.

Payne, W.E., and M. Fitzgerald-Hayes. 1993. A mutation in PLC1, a candidate phosphoinositide-specific phospholipase C gene from Saccharomyces cerevisiae, causes aberrant mitotic chromosome segregation. *Mol Cell Biol*. 13:4351-4364.

Pei, Z.M., Y. Murata, G. Benning, S. Thomine, B. Klusener, G.J. Allen, E. Grill, and J.I. Schroeder. 2000. Calcium channels activated by hydrogen peroxide mediate abscisic acid signalling in guard cells. *Nature*. 406:731-734.

Perkins, D.D. 1992. Neurospora: the organism behind the molecular revolution. *Genetics*. 130:687-701.

Perkins, D.D., and R.H. Davis. 2000. Evidence for safety of Neurospora species for academic and commercial uses. *Appl Environ Microbiol*. 66:5107-5109.

Pham, C.D., Z. Yu, B. Sandrock, M. Bolker, S.E. Gold, and M.H. Perlin. 2009. Ustilago maydis Rho1 and 14-3-3 homologues participate in pathways controlling cell separation and cell polarity. *Eukaryot Cell*. 8:977-989.

Poggeler, S., and U. Kuck. 2004. A WD40 repeat protein regulates fungal cell differentiation and can be replaced functionally by the mammalian homologue striatin. *Eukaryot Cell*. 3:232-240.

Popov, S.G., U.M. Krishna, J.R. Falck, and T.M. Wilkie. 2000. Ca2+/Calmodulin reverses phosphatidylinositol 3,4, 5-trisphosphate-dependent inhibition of regulators of G protein-signaling GTPase-activating protein activity. *J Biol Chem*. 275:18962-18968.

Pottosin, II, and G. Schonknecht. 2007. Vacuolar calcium channels. *J Exp Bot*. 58:1559-1569.

Pozos, T.C., I. Sekler, and M.S. Cyert. 1996. The product of HUM1, a novel yeast gene, is required for vacuolar Ca2+/H+ exchange and is related to mammalian Na+/Ca2+ exchangers. *Mol Cell Biol*. 16:3730-3741.

Prasher, D., R.O. McCann, and M.J. Cormier. 1985. Cloning and expression of the cDNA coding for aequorin, a bioluminescent calcium-binding protein. *Biochem Biophys Res Commun*. 126:1259-1268.

Price, A.H., A. Taylor, S.J. Ripley, A. Griffiths, A.J. Trewavas, and M.R. Knight. 1994. Oxidative Signals in Tobacco Increase Cytosolic Calcium. *Plant Cell*. 6:1301-1310.

Prole, D.L., and C.W. Taylor. 2012. Identification and analysis of cation channel homologues in human pathogenic fungi. *PLoS One*. 7:e42404.

Qi, M., and E.A. Elion. 2005. MAP kinase pathways. *J Cell Sci*. 118:3569-3572.

Quetglas, S., C. Iborra, N. Sasakawa, L. De Haro, K. Kumakura, K. Sato, C. Leveque, and M.

Seagar. 2002. Calmodulin and lipid binding to synaptobrevin regulates calcium-dependent exocytosis. *EMBO J*. 21:3970-3979.

Read, N., Fleißner A, Roca GM, and G. NL. 2010. Hyphal Fusion. American Society of Microbiology.

Read, N.D., A.B. Goryachev, and A. Lichius. 2012. The mechanistic basis of self-fusion between conidial anastomosis tubes during fungal colony initiation. *Fungal Biology Reviews*. 26:1-11.

Read, N.D., and E.R. Kalkman. 2003. Does endocytosis occur in fungal hyphae? *Fungal Genet Biol*. 39:199-203.

Read, N.D., A. Lichius, J.Y. Shoji, and A.B. Goryachev. 2009. Self-signalling and self-fusion in filamentous fungi. *Curr Opin Microbiol*. 12:608-615.

Reddy, A.S., S.B. Narasimhulu, F. Safadi, and M. Golovkin. 1996. A plant kinesin heavy chain-like protein is a calmodulin-binding protein. *Plant J*. 10:9-21.

Reddy, V.S., I.S. Day, T. Thomas, and A.S. Reddy. 2004. KIC, a novel Ca2+ binding protein with one EF-hand motif, interacts with a microtubule motor protein and regulates trichome morphogenesis. *Plant Cell*. 16:185-200.

Reddy, V.S., and A.S. Reddy. 2002. The calmodulin-binding domain from a plant kinesin functions as a modular domain in conferring Ca2+-calmodulin regulation to animal plus- and minus-end kinesins. *J Biol Chem*. 277:48058-48065.

Reedy, J.L., S.G. Filler, and J. Heitman. 2010. Elucidating the Candida albicans calcineurin signaling cascade controlling stress response and virulence. *Fungal Genet Biol*. 47:107-116.

Reissig, J.L., and S.G. Kinney. 1983. Calcium as a branching signal in Neurospora crassa. *J Bacteriol*. 154:1397-1402.

Rescher, U., and V. Gerke. 2004. Annexins--unique membrane binding proteins with diverse functions. *J Cell Sci*. 117:2631-2639.

Rho, H.S., J. Jeon, and Y.H. Lee. 2009. Phospholipase C-mediated calcium signalling is required for fungal development and pathogenicity in Magnaporthe oryzae. *Mol Plant Pathol*. 10:337-346.

Rhoads, A.R., and F. Friedberg. 1997. Sequence motifs for calmodulin recognition. *FASEB J*. 11:331-340.

Richthammer, C., M. Enseleit, E. Sanchez-Leon, S. Marz, Y. Heilig, M. Riquelme, and S. Seiler. 2012. RHO1 and RHO2 share partially overlapping functions in the regulation of cell wall integrity and hyphal polarity in Neurospora crassa. *Mol Microbiol*. 85:716-733.

Ringer, S. 1883. A further Contribution regarding the influence of the different Constituents of the Blood on the Contraction of the Heart. *J Physiol*. 4:29-42 23.

Rispail, N., D.M. Soanes, C. Ant, R. Czajkowski, A. Grunler, R. Huguet, E. Perez-Nadales, A. Poli, E. Sartorel, V. Valiante, M. Yang, R. Beffa, A.A. Brakhage, N.A. Gow, R. Kahmann, M.H.

Lebrun, H. Lenasi, J. Perez-Martin, N.J. Talbot, J. Wendland, and A. Di Pietro. 2009. Comparative genomics of MAP kinase and calcium-calcineurin signalling components in plant and human pathogenic fungi. *Fungal Genet Biol*. 46:287-298.

Rivera-Rodriguez, N., and N. Rodriguez-del Valle. 1992. Effects of calcium ions on the germination of Sporothrix schenckii conidia. *J Med Vet Mycol*. 30:185-195.

Roca, M., N.D. Read, and A.E. Wheals. 2005a. Conidial anastomosis tubes in filamentous fungi. *FEMS Microbiol Lett*. 249:191-198.

Roca, M.G., J. Arlt, C.E. Jeffree, and N.D. Read. 2005b. Cell biology of conidial anastomosis tubes in Neurospora crassa. *Eukaryot Cell*. 4:911-919.

Roca, M.G., H.C. Kuo, A. Lichius, M. Freitag, and N.D. Read. 2010. Nuclear dynamics, mitosis, and the cytoskeleton during the early stages of colony initiation in Neurospora crassa. *Eukaryot Cell*. 9:1171-1183.

Roca, M.G., M. Weichert, U. Siegmund, P. Tudzynski, and A. Fleissner. 2012. Germling fusion via conidial anastomosis tubes in the grey mould Botrytis cinerea requires NADPH oxidase activity. *Fungal Biol*. 116:379-387.

Roelants, F.M., P.D. Torrance, N. Bezman, and J. Thorner. 2002. Pkh1 and Pkh2 differentially phosphorylate and activate Ypk1 and Ykr2 and define protein kinase modules required for maintenance of cell wall integrity. *Mol Biol Cell*. 13:3005-3028.

Rogers, K.L., S. Picaud, E. Roncali, R. Boisgard, C. Colasante, J. Stinnakre, B. Tavitian, and P. Brulet. 2007. Non-invasive in vivo imaging of calcium signaling in mice. *PLoS One*. 2:e974.

Rosen, L.B., D.D. Ginty, M.J. Weber, and M.E. Greenberg. 1994. Membrane depolarization and calcium influx stimulate MEK and MAP kinase via activation of Ras. *Neuron*. 12:1207-1221.

Ross, A.C. 2011. The 2011 report on dietary reference intakes for calcium and vitamin D. *Public Health Nutr*. 14:938-939.

Rudolph, H.K., A. Antebi, G.R. Fink, C.M. Buckley, T.E. Dorman, J. LeVitre, L.S. Davidow, J.I. Mao, and D.T. Moir. 1989. The yeast secretory pathway is perturbed by mutations in PMR1, a member of a Ca2+ ATPase family. *Cell*. 58:133-145.

Sanchez-Mir, L., A. Franco, R. Martin-Garcia, M. Madrid, J. Vicente-Soler, T. Soto, M. Gacto, P. Perez, and J. Cansado. 2014a. Rho2 palmitoylation is required for plasma membrane localization and proper signaling to the fission yeast cell integrity mitogen- activated protein kinase pathway. *Mol Cell Biol*. 34:2745-2759.

Sanchez-Mir, L., T. Soto, A. Franco, M. Madrid, R.A. Viana, J. Vicente, M. Gacto, P. Perez, and J. Cansado. 2014b. Rho1 GTPase and PKC ortholog Pck1 are upstream activators of the cell integrity MAPK pathway in fission yeast. *PLoS One*. 9:e88020.

Sanders, D., C. Brownlee, and J.F. Harper. 1999. Communicating with calcium. *Plant Cell*. 11:691-706.

Sanders, D., J. Pelloux, C. Brownlee, and J.F. Harper. 2002. Calcium at the crossroads of signaling. *Plant Cell*. 14 Suppl:S401-417.

Schmidt, A., and A. Hall. 2002. Guanine nucleotide exchange factors for Rho GTPases: turning on the switch. *Genes Dev*. 16:1587-1609.

Schroeder, J.E., P.S. Fischbach, and E.W. McCleskey. 1990. T-type calcium channels: heterogeneous expression in rat sensory neurons and selective modulation by phorbol esters. *J Neurosci*. 10:947-951.

Schumaker, K.S., and H. Sze. 1987. Inositol 1,4,5-trisphosphate releases Ca2+ from vacuolar membrane vesicles of oat roots. *J Biol Chem*. 262:3944-3946.

Schurg, T., U. Brandt, C. Adis, and A. Fleissner. 2012. The Saccharomyces cerevisiae BEM1 homologue in Neurospora crassa promotes co-ordinated cell behaviour resulting in cell fusion. *Mol Microbiol*. 86:349-366.

Schuster, M., S. Kilaru, G. Fink, J. Collemare, Y. Roger, and G. Steinberg. 2011a. Kinesin-3 and dynein cooperate in long-range retrograde endosome motility along a nonuniform microtubule array. *Mol Biol Cell*. 22:3645-3657.

Schuster, M., R. Lipowsky, M.A. Assmann, P. Lenz, and G. Steinberg. 2011b. Transient binding of dynein controls bidirectional long-range motility of early endosomes. *Proc Natl Acad Sci U S A*. 108:3618-3623.

Seidel, C., S.D. Moreno-Velasquez, M. Riquelme, and R. Fischer. 2013. Neurospora crassa NKIN2, a kinesin-3 motor, transports early endosomes and is required for polarized growth. *Eukaryot Cell*. 12:1020-1032.

Seiler, S., and M. Plamann. 2003. The genetic basis of cellular morphogenesis in the filamentous fungus Neurospora crassa. *Mol Biol Cell*. 14:4352-4364.

Selker, E.U. 1990. Premeiotic instability of repeated sequences in Neurospora crassa. *Annu Rev Genet*. 24:579-613.

Shaw, B.D., O. Kozlova, N.D. Read, B.G. Turgeon, and H.C. Hoch. 2001. Expression of recombinant aequorin as an intracellular calcium reporter in the phytopathogenic fungus Phyllosticta ampelicida. *Fungal Genet Biol*. 34:207-215.

Shimomura, O. 1985. Bioluminescence in the sea: photoprotein systems. *Symp Soc Exp Biol*. 39:351-372.

Silverman-Gavrila, L.B., and R.R. Lew. 2001. Regulation of the tip-high [Ca2+] gradient in growing hyphae of the fungus Neurospora crassa. *Eur J Cell Biol*. 80:379-390.

Silverman-Gavrila, L.B., and R.R. Lew. 2002. An IP3-activated Ca2+ channel regulates fungal tip growth. *J Cell Sci*. 115:5013-5025.

Silverman-Gavrila, L.B., and R.R. Lew. 2003. Calcium gradient dependence of Neurospora crassa hyphal growth. *Microbiology*. 149:2475-2485.

Simonin, A.R., C.G. Rasmussen, M. Yang, and N.L. Glass. 2010. Genes encoding a striatin-like protein (ham-3) and a forkhead associated protein (ham-4) are required for hyphal

fusion in Neurospora crassa. *Fungal Genet Biol*. 47:855-868.

Smith, S.E., C. Csank, G. Reyes, M.A. Ghannoum, and V. Berlin. 2002. Candida albicans RHO1 is required for cell viability in vitro and in vivo. *FEMS Yeast Res*. 2:103-111.

Snedden, W.A., and H. Fromm. 2001. Calmodulin as a versatile calcium signal transducer in plants. *New Phytologist*. 151:35-66.

Soderling, T.R., B. Chang, and D. Brickey. 2001. Cellular signaling through multifunctional Ca2+/calmodulin-dependent protein kinase II. *J Biol Chem*. 276:3719-3722.

Sorin, A., G. Rosas, and R. Rao. 1997. PMR1, a Ca2+-ATPase in yeast Golgi, has properties distinct from sarco/endoplasmic reticulum and plasma membrane calcium pumps. *J Biol Chem*. 272:9895-9901.

Sousa, A., C.T. Tomaz, F. Sousa, and J.A. Queiroz. 2011. Successful application of monolithic innovative technology using a carbonyldiimidazole disk to purify supercoiled plasmid DNA suitable for pharmaceutical applications. *J Chromatogr A*. 1218:8333-8343.

Srinivasa, S.P., L.S. Bernstein, K.J. Blumer, and M.E. Linder. 1998. Plasma membrane localization is required for RGS4 function in Saccharomyces cerevisiae. *Proc Natl Acad Sci U S A*. 95:5584-5589.

Stathopoulos, A.M., and M.S. Cyert. 1997. Calcineurin acts through the CRZ1/TCN1-encoded transcription factor to regulate gene expression in yeast. *Genes Dev*. 11:3432-3444.

Steinberg, G. 2012. The transport machinery for motility of fungal endosomes. *Fungal Genet Biol*. 49:675-676.

Stie, J., and D. Fox. 2008. Calcineurin regulation in fungi and beyond. *Eukaryot Cell*. 7:177-186.

Stolz, B., and J. Bereiter-Hahn. 1988. Increase of cytosolic calcium results in formation of F-actin aggregates in endothelial cells. *Cell Biol Int Rep*. 12:321-329.

Suresh, K., and C. Subramanyam. 1997. A putative role for calmodulin in the activation of Neurospora crassa chitin synthase. *FEMS Microbiol Lett*. 150:95-100.

Sze, H., X. Li, and M.G. Palmgren. 1999. Energization of plant cell membranes by H+-pumping ATPases. Regulation and biosynthesis. *Plant Cell*. 11:677-690.

Szlufcik, K., G. Bultynck, G. Callewaert, L. Missiaen, J.B. Parys, and H. De Smedt. 2006. The suppressor domain of inositol 1,4,5-trisphosphate receptor plays an essential role in the protection against apoptosis. *Cell Calcium*. 39:325-336.

Takeuchi, Y., J. Schmid, J.H. Caldwell, and F.M. Harold. 1988. Transcellular ion currents and extension of Neurospora crassa hyphae. *J Membr Biol*. 101:33-41.

Tallini, Y.N., M. Ohkura, B.R. Choi, G. Ji, K. Imoto, R. Doran, J. Lee, P. Plan, J. Wilson, H.B. Xin, A. Sanbe, J. Gulick, J. Mathai, J. Robbins, G. Salama, J. Nakai, and M.I. Kotlikoff. 2006. Imaging cellular signals in the heart in vivo: Cardiac expression of the high-signal Ca2+ indicator GCaMP2. *Proc Natl Acad Sci U S A*. 103:4753-4758.

Teichert, I., E.K. Steffens, N. Schnass, B. Franzel, C. Krisp, D.A. Wolters, and U. Kuck. 2014.

PRO40 is a scaffold protein of the cell wall integrity pathway, linking the MAP kinase module to the upstream activator protein kinase C. *PLoS Genet*. 10:e1004582.

Thion, L., C. Mazars, P. Nacry, D. Bouchez, M. Moreau, R. Ranjeva, and P. Thuleau. 1998. Plasma membrane depolarization-activated calcium channels, stimulated by microtubule-depolymerizing drugs in wild-type Arabidopsis thaliana protoplasts, display constitutively large activities and a longer half-life in ton 2 mutant cells affected in the organization of cortical microtubules. *Plant J*. 13:603-610.

Tian, L., S.A. Hires, T. Mao, D. Huber, M.E. Chiappe, S.H. Chalasani, L. Petreanu, J. Akerboom, S.A. McKinney, E.R. Schreiter, C.I. Bargmann, V. Jayaraman, K. Svoboda, and L.L. Looger. 2009. Imaging neural activity in worms, flies and mice with improved GCaMP calcium indicators. *Nat Methods*. 6:875-881.

Tisi, R., F. Belotti, S. Wera, J. Winderickx, J.M. Thevelein, and E. Martegani. 2004. Evidence for inositol triphosphate as a second messenger for glucose-induced calcium signalling in budding yeast. *Curr Genet*. 45:83-89.

Tonelli, F.M., A.K. Santos, D.A. Gomes, S.L. da Silva, K.N. Gomes, L.O. Ladeira, and R.R. Resende. 2012. Stem cells and calcium signaling. *Adv Exp Med Biol*. 740:891-916.

Trinkle-Mulcahy, L., S. Boulon, Y.W. Lam, R. Urcia, F.M. Boisvert, F. Vandermoere, N.A. Morrice, S. Swift, U. Rothbauer, H. Leonhardt, and A. Lamond. 2008. Identifying specific protein interaction partners using quantitative mass spectrometry and bead proteomes. *J Cell Biol*. 183:223-239.

Tsuji, F.I., Y. Ohmiya, T.F. Fagan, H. Toh, and S. Inouye. 1995. Molecular evolution of the Ca(2+)-binding photoproteins of the Hydrozoa. *Photochem Photobiol*. 62:657-661.

Turner, B.C., D.D. Perkins, and A. Fairfield. 2001. Neurospora from natural populations: a global study. *Fungal Genet Biol*. 32:67-92.

Vandonselaar, M., R.A. Hickie, J.W. Quail, and L.T. Delbaere. 1994. Trifluoperazine-induced conformational change in Ca(2+)-calmodulin. *Nat Struct Biol*. 1:795-801.

Very, A.A., and J.M. Davies. 2000. Hyperpolarization-activated calcium channels at the tip of Arabidopsis root hairs. *Proc Natl Acad Sci U S A*. 97:9801-9806.

Vetter, S.W., and E. Leclerc. 2003. Novel aspects of calmodulin target recognition and activation. *Eur J Biochem*. 270:404-414.

Viladevall, L., R. Serrano, A. Ruiz, G. Domenech, J. Giraldo, A. Barcelo, and J. Arino. 2004. Characterization of the calcium-mediated response to alkaline stress in Saccharomyces cerevisiae. *J Biol Chem*. 279:43614-43624.

Virag, A., M.P. Lee, H. Si, and S.D. Harris. 2007. Regulation of hyphal morphogenesis by cdc42 and rac1 homologues in Aspergillus nidulans. *Mol Microbiol*. 66:1579-1596.

Vogt, N., and S. Seiler. 2008. The RHO1-specific GTPase-activating protein LRG1 regulates polar tip growth in parallel to Ndr kinase signaling in Neurospora. *Mol Biol Cell*. 19:4554-4569.

Volberg, T., B. Geiger, J. Kartenbeck, and W.W. Franke. 1986. Changes in membrane-microfilament interaction in intercellular adherens junctions upon removal of extracellular Ca2+ ions. *J Cell Biol*. 102:1832-1842.

Wach, A., A. Brachat, C. Alberti-Segui, C. Rebischung, and P. Philippsen. 1997. Heterologous HIS3 marker and GFP reporter modules for PCR-targeting in Saccharomyces cerevisiae. *Yeast*. 13:1065-1075.

Wang, Q., B. Shui, M.I. Kotlikoff, and H. Sondermann. 2008. Structural basis for calcium sensing by GCaMP2. *Structure*. 16:1817-1827.

Watkinson, M.C.a.S. 1994. The Fungi.

Wedlich-Soldner, R., I. Schulz, A. Straube, and G. Steinberg. 2002. Dynein supports motility of endoplasmic reticulum in the fungus Ustilago maydis. *Mol Biol Cell*. 13:965-977.

White, P.J., and M.R. Broadley. 2003. Calcium in plants. *Ann Bot*. 92:487-511.

Wu, H., C.L. He, and R.A. Fissore. 1997. Injection of a porcine sperm factor triggers calcium oscillations in mouse oocytes and bovine eggs. *Mol Reprod Dev*. 46:176-189.

Xiang, Q., C. Rasmussen, and N.L. Glass. 2002. The ham-2 locus, encoding a putative transmembrane protein, is required for hyphal fusion in Neurospora crassa. *Genetics*. 160:169-180.

Xiong, T.C., S. Bourque, D. Lecourieux, N. Amelot, S. Grat, C. Briere, C. Mazars, A. Pugin, and R. Ranjeva. 2006. Calcium signaling in plant cell organelles delimited by a double membrane. *Biochim Biophys Acta*. 1763:1209-1215.

Yanez, M., J. Gil-Longo, and M. Campos-Toimil. 2012. Calcium binding proteins. *Adv Exp Med Biol*. 740:461-482.

Yang, M., A. Brand, T. Srikantha, K.J. Daniels, D.R. Soll, and N.A. Gow. 2011. Fig1 facilitates calcium influx and localizes to membranes destined to undergo fusion during mating in Candida albicans. *Eukaryot Cell*. 10:435-444.

Yang, Y., P. Cheng, G. Zhi, and Y. Liu. 2001. Identification of a calcium/calmodulin-dependent protein kinase that phosphorylates the Neurospora circadian clock protein FREQUENCY. *J Biol Chem*. 276:41064-41072.

Yokoyama, H., M. Mizunuma, M. Okamoto, J. Yamamoto, D. Hirata, and T. Miyakawa. 2006. Involvement of calcineurin-dependent degradation of Yap1p in Ca2+-induced G2 cell-cycle regulation in Saccharomyces cerevisiae. *EMBO Rep*. 7:519-524.

Yoshimura, H., T. Tada, and H. Iida. 2004. Subcellular localization and oligomeric structure of the yeast putative stretch-activated Ca2+ channel component Mid1. *Exp Cell Res*. 293:185-195.

Zelter, A., M. Bencina, B.J. Bowman, O. Yarden, and N.D. Read. 2004. A comparative genomic analysis of the calcium signaling machinery in Neurospora crassa, Magnaporthe grisea, and Saccharomyces cerevisiae. *Fungal Genet Biol*. 41:827-841.

Zeng, F., X. Gong, M.I. Hamid, Y. Fu, X. Jiatao, J. Cheng, G. Li, and D. Jiang. 2012. A fungal cell

wall integrity-associated MAP kinase cascade in Coniothyrium minitans is required for conidiation and mycoparasitism. *Fungal Genet Biol*. 49:347-357.

Zhao, C., U.S. Jung, P. Garrett-Engele, T. Roe, M.S. Cyert, and D.E. Levin. 1998. Temperature-induced expression of yeast FKS2 is under the dual control of protein kinase C and calcineurin. *Mol Cell Biol*. 18:1013-1022.

Zhou, X.L., A.F. Batiza, S.H. Loukin, C.P. Palmer, C. Kung, and Y. Saimi. 2003. The transient receptor potential channel on the yeast vacuole is mechanosensitive. *Proc Natl Acad Sci U S A*. 100:7105-7110.

Appendices

Table A.1 Oligonucleotide primers used in this study

Primer name	Sequence
RS426-EcoR1-F	GAATTCCTGCAGCCCGGGGGA
RS426-Xho1-R	CTCGAGGGGGGGCCCGGTAC
NAT Y HR Fw CC	TACAAGTAAGAATTCGATATCAAGCTTATCGCAACTGATATTGAAGGAGCATTTT
NAT Y HR Rv DD	GTACCGAGCTCGGATCCATAACTTCGTATAGCCTTGTCGACGAATTCAGATG
HPH Y HR Fw CC	TACAAGTAAGAATTCGATATCAAGC
HPH Y HR Rv DD	GTACCGAGCTCGGATCC
YRC BB GFP TAGT Fw	GGCGGAGGCGGCGGAGGCGGAGGCGGAGGCATGGTG
YRC CC Rv	CGATAAGCTTGATATCGAATTCTTACTTGTA
MCHERRY Fw BB YRC	GGCGGAGGCGGCGGAGGCGGAGGCGGAGGCATGGTGAGCAAGGGCGAGG
MCHERRY Rv CC YRC	CGATAAGCTTGATATCGAATTCTTACTTGTACAGCTCGTCCATGCC
mCh-PacI-F	ATCCCCGGGTTAATTAAGGGCGGAGGCGGCGGAGGCGGAGGCGGAGGCATGGTGAGCAAGGGCGAG
mCh-EcoRI-R	CTTGATATCGAATTCTTACTTGTACAGCTCGTCCATGC
CNA-1 KI P1	GTAATACGACTCACTATAGGGCGAATTGGGGCGGCCGCTCTAACAGCCACTTGACTGCC
CNA-1 KI P2	GCCTCCGCCTCCGCCTCCGCCGCCTCCGCCAGAACTACACCCTCATAAAACCAGAAA
CNA-1 KI P3	GCTATACGAAGTTATGGATCCGAGCTCGGTACGCGAGTTTACATACCTCAGCGA
CNA-1 KI P4	CAAAAGCTGGAGCTCCACCGCGGTGGCGGCCGCCCCTTTCTCTTCCTCCTCATCC
CNB-1 KI P1	GTAATACGACTCACTATAGGGCGAATTGGGGCGGCCGCGATCCAACTGTACGTTTCGCTC
CNB-1 KI P2	GCCTCCGCCTCCGCCTCCGCCGCCTCCGCCGAATTGATCTGTTAAAGCGTCGACT
CNB-1 KI P3	GCTATACGAAGTTATGGATCCGAGCTCGGTACATCTCAATTGAGGCGCTGG
CNB-1 KI P4	CAAAAGCTGGAGCTCCACCGCGGTGGCGGCCGCTGGATGTGGATTACCGGACA
CaM KI P1	GTAATACGACTCACTATAGGGCGAATTGGGGCGGCCGCATGGTATGCTCATTCCTTATCTCG
CaM KI P2	GCCTCCGCCTCCGCCTCCGCCGCCTCCGCCCTTCTGCATCATGAGCTGGA
CaM KI P3	GCTATACGAAGTTATGGATCCGAGCTCGGTACGCGTTATGCTGGACTGTTACC
CaM KI P4	CAAAAGCTGGAGCTCCACCGCGGTGGCGGCCGCTACAGTACTGGGACTCGTGGC
G-CaM-OE-AscI-P1	CGGAGGCGGCGCGCCAGTATGCTCATTCCTTATCTCGG
G-CaM-OE-XbaI-P2	GGCGGCCGCTCTAGATTACTTCTGCATCATGAGCTG

Primer name	Sequence
CaM-G-OE-XbaI-P1	TCAACCAAATCTAGAATGGTATGCTCATTCCTTATCTC
CaM-G-OE-PacI-P2	TCCGCCCTTAATTAACTTCTGCATCATGAGCTGG
V5 HAT YRC A Fw	GGCGGAGGCGGCGGAGGCGGAGGCGGAGGCGGCAAGCCCATCCCCAACCCCCT CCTCGGACTCGACAGCACCGGACTCGACAGCACC
CaMK1 KI P1	GTAATACGACTCACTATAGGGCGAATTGGGGCGGCCGCAAGTCTTGGGTGCCGTC A
CaMK1 KI P2	GCCTCCGCCTCCGCCTCCGCCGCCTCCGCCGGCTTGGAAACTCTTCGC
CaMK1 KI P3	GCTATACGAAGTTATGGATCCGAGCTCGGTACGCGGATATGGAGTGAGTGTACG
CaMK1 KI P4	CAAAAGCTGGAGCTCCACCGCGGTGGCGGCCGCGACGAAGAGTCAGAACCTAGC TTTACA
GCaMP-PacI-F	CCCCGGGTTAATTAAATGGGTTCTCATCATCATCATC
GCaMP-EcoRI-R	CTTGATATCGAATTCTTACTTCGCTGTCATCATTTGTA
GCaMP-EcoRV-F	ATCGATAAGCTTGATATCATGGGTTCTCATCATCATCATC
GCaMP-BamHI-R	TTTCCTCGACGGATCCTTACTTCGCTGTCATCATTTGTA
CaM-5f-XX-F	GTAATACGACTCACTATAGGGCGAATTGGGGCGGCCGCCGAACGACTCTCATCTCC G
M13-F	GTAAAACGACGGCCAGT
GFP-seq-rv	ATGTGGTCGGGGTAGCGG
HPH 1 Fw	TCACTGGCAAACTGTGATG
HPH 2 Rv	ACACATGGGGATCAGCAATC
NAT 1 Fw	CTTCGTGGTCGTCTCGTA
NAT 2 Rv	CGCCAGGTCGCCGTCG
HIS-3 3' Fw	TTGCCATCTCCACCATCC
HIS-3 5' Rv	GCTGTAGACCAGACCCAGAGC
GFP Fw	CAAGATCCGCCACAACATCG
GFP Rv	ATGTGGTCGGGGTAGCGG

Table A.2 Gene deletion mutant analysis of Ca^{2+} signalling machinery in *N. crassa*

No	gene[1]	BLAST against *S. cerevisiae* (or other organisms)	protein[2]	gene locus	FGSC number	Read lab stock	mating type	strain type	Phenotype[3]
		Ca^{2+} channels							
1	*cch-1*	Cch1p	**Ca^{2+}-channel pore-forming subunit (CCH-1)**	**NCU02762**	(Chu, 2013)	-	-	homokaryon	Slower colony extension, **Reduced CAT fusion,** Reduced sporulation
2	*mid-1*	Mid1p	**Ca^{2+}-channel protein (MID-1)**	**NCU06703.2**	FGSC11708	273	A	homokaryon	Slower colony extension, Reduced sporulation **Reduced CAT fusion with Δ*cch-1***
3	*yvc-1*	Yvc1p	Ca^{2+}-channel protein (YVC-1)	NCU07605.2	FGSC11253	274	A	homokaryon	No obvious phenotype
4	*fig-1*	Fig1p	Ca^{2+}-channel protein (FIG-1)	NCU02219.2	FGSC17273	735	a	homokaryon	Slower colony extension
5	-	AFUA_ 6g11300 (from *A. fumigatus*)	Integral membrane channel protein, transient receptor potential Ca^{2+} channel family	NCU08283.2	FGSC11860	-	A	homokaryon	No obvious phenotype
6	-	AFUA_6g11180 (from *A. fumigatus*)	Integral membrane channel protein, transient receptor potential Ca^{2+} channel family	NCU06601.2	FGSC11858	-	A	homokaryon	No obvious phenotype
		Ca^{2+} ATPases							
7	*nca-1*	Pmr1p	Ca^{2+} - ATPase (NCA-1)	NCU03305.2	FGSC13287	473	a	homokaryon	No obvious phenotype
8	*nca-2*	Pmc1p	Ca^{2+} - ATPase (NCA-2)	NCU04736.2	FGSC13071	471	A	homokaryon	Reduced sporulation
9	*nca-3*	Pmc1p	Ca^{2+} - ATPase (NCA-3)	NCU05154.2	FGSC13037	468	A	homokaryon	No obvious phenotype
10	*pmr-1*	Pmr1p	**Ca^{2+} - ATPase (PMR-1)**	**NCU03292.2**	FGSC11616	449	a	heterokaryon	**can't survive in homokaryon**
11	*ph-7*	Ena2p (Na^{+}-ATPase)	Ca^{2+} - ATPase (PH-7)	NCU08147.2	FGSC11256	275	A	homokaryon	No obvious phenotype

No	gene[1]	BLAST against *S. cerevisiae* (or other organisms)	protein[2]	gene locus	FGSC number	Read lab stock	mating type	strain type	Phenotype[3]
12	-	Spf1p	cation-transporting ATPase 4	NCU04898.2	FGSC13040	469	A	homokaryon	Slower colony extension, **Reduced CAT fusion**
13	-	Neo1p, Ena2p(Na^+-ATPase)	phospholipid-translocating P-type ATPase	NCU03818.2	FGSC16010 **This study**	480	a	heterokaryon homokaryon	No obvious phenotype
14	-	Cta3p (from *S. pombe)*	Ca^{2+}-transporting ATPase 3	NCU07966.2	FGSC11409	289	A	homokaryon	No obvious phenotype
15	-	YOR291W (Undefined cation-ATPase), Ena5p (Na^+-ATPase)	ATPase type 13A2	NCU10143	FGSC12645	878	A	homokaryon	No obvious phenotype
16	*ena-1*	Ena1	Na^+ P-type ATPase (ENA-1)	NCU05046	FGSC11237	-	A	homokaryon	No obvious phenotype
		Ca^{2+} antiporters							
17	*cax*	Mnr1p	Ca^{2+}/H^+ exchanger (CAX)	NCU07075.2	FGSC11249	433	A	homokaryon	No obvious phenotype
18	-	Vcx1p	Ca^{2+}/H^+ exchanger	NCU00916	FGSC11686	288	A	homokaryon	No obvious phenotype
19	-	Vcx1p	Ca^{2+}/H^+ exchanger	NCU00795.2	FGSC12375	333	A	homokaryon	No obvious phenotype
20	-	Mnrp	Ca^{2+}/H^+ exchanger	NCU06366.2	FGSC11408	290	A	homokaryon	No obvious phenotype
21	-	Hum1p	Ca^{2+}/H^+ exchanger	NCU07711	Not available	-	-	-	Not tested
22	-	Rpd3p	Ca^{2+}/H^+ exchanger	NCU05360.2	FGSC11619 **This study**	451	a	heterokaryon homokaryon	No obvious phenotype
23	-	YDL206W, Ecm27p	Ca^{2+}/H^+ exchanger	NCU02826.2	FGSC11529	291	A	homokaryon	No obvious phenotype
24	-	EAA01911 (from *Anopheles gambiae*)	Ca^{2+}/Na^+ exchanger	NCU08490.2	FGSC12468	465	a	homokaryon	No obvious phenotype
25	-	MCU (from *Homo sapiens*)	mitochondrial Ca^{2+} uniporter (MCU)	NCU08166	Not available	-	-	-	Not tested

No	gene[1]	BLAST against *S. cerevisiae* (or other organisms)	protein[2]	gene locus	FGSC number	Read lab stock	mating type	strain type	Phenotype[3]
	Key Ca^{2+} or Ca^{2+}/CaM binding proteins								
26	*cmd-1*	Cmd1p	**Calmodulin A (CaM)**	**NCU04120.2**	FGSC11618	450	a	heterokaryon	**can't survive in homokaryon**
27	*cna-1*	Cna1p, Cna2p	**Calcineurin catalytic subunit a**	**NCU03804.2**	FGSC17929 **This study**	736	a	heterokaryon homokaryon	Slower colony extension, Reduced sporulation **Delayed CAT chemotropism**
28	*cnb-1*	Cnb1p	**Calcineurin regulatory subunit b**	**NCU03833.2**	**This study**	-	-	homokaryon	Slower colony extension, Reduced sporulation, **Delayed germination** **Delayed CAT chemotropism**
29	*crz-1*	Crz1p	**Calcineurin transcription factor**	**NCU07952.2**	FGSC11494 **This study**	565	a	heterokaryon homokaryon	Slower colony extension
30	*camk-1*	Cmk1p, Cmk2p	**Ca^{2+}/CaM-dependent kinase-1**	**NCU09123.1**	FGSC12548	514	a	homokaryon	Slower colony extension, Reduced sporulation **Reduced germination** **Reduced CAT fusion**
31	*camk-2*	Cmk1p, Cmk2p	**Ca^{2+}/CaM-dependent kinase-2**	**NCU02283.2**	FGSC12448	725	a	homokaryon	No obvious phenotype
32	*camk-3*	Pak1p	**Ca^{2+}/CaM -dependent kinase-3**	**NCU06177.2**	FGSC11536	496	A	homokaryon	No obvious phenotype
33	*camk-4*	Rck1p, Rck2p	Ca^{2+}/CaM -dependent kinase-4	NCU09212.2	FGSC11545	499	a	homokaryon	No obvious phenotype
	Putative Ca^{2+} or Ca^{2+}/CaM binding proteins								
34	-	Cne1p	Calnexin / Calreticulin	NCU09265	Not available	-	-	-	Not tested
35	-	Cmd1p	Ca^{2+}/CaM binding protein	NCU03750.1	FGSC11531	928	a	homokaryon	No obvious phenotype
36	-	AGC1 (aspartate-glutamate transporter)	Ca^{2+}/CaM binding protein	NCU01241.2	FGSC11613		a	heterokaryon	**can't survive in homokaryon**

No	gene[1]	BLAST against *S. cerevisiae* (or other organisms)	protein[2]	gene locus	FGSC number	Read lab stock	mating type	strain type	Phenotype[3]
37	-	SAL1 (Ca^{2+}-binding mitochondrial carrier)	Ca^{2+}/CaM binding protein	NCU01564.2	FGSC15898	933	a	homokaryon	No obvious phenotype
38	-	-	Ca^{2+}/CaM binding protein	NCU02115.2	FGSC13049	930	a	homokaryon	No obvious phenotype
39	*(nuf-1)*	NUF1	**Ca^{2+}/CaM binding protein**	**NCU02411.2**	FGSC11615	181	a	heterokaryon	**can't survive in homokaryon**
40	-	-	Ca^{2+}/CaM binding protein	NCU02738.2	FGSC15890	932	a	homokaryon	No obvious phenotype
41	-	Dun1p, Rad53p	Ca^{2+}/CaM binding protein	NCU02814.2	FGSC11169	491	a	homokaryon	No obvious phenotype
42	-	Hypothetical protein	Ca^{2+}/CaM binding protein	NCU04265.2	FGSC15488	931	a	heterokaryon	**can't survive in homokaryon**
43	*ncs-1*	Frequenin-like protein (Frq1p)	Neuronal Ca^{2+} sensor 1 (NCS-1)	NCU04379	FGSC11403	-	a	homokaryon	No obvious phenotype
44	-	Type II NAD(P)H:quinone oxidoreductase	Ca^{2+}/CaM binding protein	NCU05225.2	FGSC11405	926	a	homokaryon	No obvious phenotype
45	*end-3*	End3p	Ca^{2+}/CaM binding protein	NCU06347.2	FGSC11502 **This study**	496	a	heterokaryon homokaryon	No obvious phenotype
46	-	Myosin Myo2p light chain (CDC4)	**Ca^{2+}/CaM binding protein**	**NCU06617.2**	FGSC11503	207	a	heterokaryon	**can't survive in homokaryon**
47	-	-	Ca^{2+}/CaM binding protein	NCU06650.2	FGSC11246	825	a	homokaryon	No obvious phenotype
48	-	-	Ca^{2+}/CaM binding protein	NCU06948.2	FGSC11541	929	a	homokaryon	No obvious phenotype
49	-	Cell division control protein 31	Ca^{2+}/CaM binding protein	NCU09871.2	FGSC11504	927	a	heterokaryon	**can't survive in homokaryon**
50	*nde-1*	NADH:ubiquinone oxidoreductase	Ca^{2+}/CaM binding protein (NDE-1)	NCU08980	Not available	-	-	-	Not tested
51	*stk-16*	Kin4p, Arp8p	serine/threonine protein kinase-16	NCU00914.2	FGSC13072	518	a	homokaryon	No obvious phenotype
52	-	-	annexin XIV	NCU04421.2	FGSC11887	588	a	homokaryon	No obvious phenotype
53	-	-	annexin ANXC4	NCU02139.7	FGSC14861		a	homokaryon	Not tested

No	gene[1]	BLAST against *S. cerevisiae* (or other organisms)	protein[2]	gene locus	FGSC number	Read lab stock	mating type	strain type	Phenotype[3]
54	*ham-3*	Striatin Pro11	HAM-3	NCU08741	FGSC11300		a	homokaryon	**Reduced CAT fusion** Reduced hyphal fusion[4]
55	*ham-10*	-	HAM-10, C2 domain-containing protein	NCU02833	FGSC21395	-	a	homokaryon	**Reduced CAT fusion** Reduced hyphal fusion[5]
56	*rgs-1*	RGS4 (from *Homo sapiens*)	Regulator of G protein signalling; Developmental regulator flbA (*A. nidulans*)	NCU08319.7	FGSC12372	460	a	homokaryon	**Reduced CAT fusion**
	Other Ca^{2+}/CaM signalling regulators								
57	*plc-1*	Plc1p	Phospholipase C	NCU06245.2	FGSC11411	328	a	homokaryon	No obvious phenotype
58	*plc-2*	Plc1p	Phospholipase C	NCU01266.2	FGSC12022	331	a	homokaryon	Slower colony extension, **Reduced germination** **Reduced CAT fusion**
59	*plc-3*	Plc1p	Phospholipase C	NCU11415	FGSC11271	329	a	homokaryon	No obvious phenotype
60	*plc-4*	Plc1p	Phospholipase C	NCU02175.2	FGSC12023	332	a	homokaryon	No obvious phenotype
61	-	RCN1	calcineurin binding protein calcipressin homolog	NCU01504	Not available	-	-	-	Not tested
62	-	FPR1	FK506-binding protein 4 (binds to calcineurin inhibitor FK506)	NCU03241	FGSC12177	-	a	homokaryon	No obvious phenotype
63	-	FPR1	peptidyl-prolyl cis-trans isomerase fkr-3 (binds to calcineurin inhibitor FK506)	NCU04371	FGSC15832	-	a	homokaryon	No obvious phenotype
64	-	CPR1	**Cyclosporin-resistant-1** **(binds to calcineurin inhibitor CysA)**	**NCU00726**	FGSC14340	795	a	homokaryon	No obvious phenotype
65	-	CPR1	Peptidyl-prolyl cis-trans isomerase (binds to calcineurin inhibitor cyclosporin A)	NCU03853	FGSC11560	-	a	homokaryon	No obvious phenotype

Notes:

1. ‘ – ‘ indicates that this gene has not been given a name in *N. crassa*. The names of genes in bracket were given from Read’s lab temporarily.
2.
3. Phenotypes analyzed and compared with the wild type for all the mutants were (1) colony extension rate; (2) colony morphology in 16 h and 5 d old plates; (3) conidiation in 5 days old plates; (4) percentage of conidial germination at 35^{o}C for 4 h in liquid Vogel’s medium; (5) percentage of CAT fusion at 35^{o}C for 4 h in liquid Vogel’s medium.
4. Simonin, A.R., Rasmussen, C.G., Yang, M., and Glass, N.L. (2010). HAM-3, a striatin-like protein, is required for hyphal fusion in *N. crassa*.
5. Fu, C., Ao, J., Dettmann, A., Seiler, S., Free S. J. (2014). HAM-10 is required for cell growth and development in *N. crassa*.

Table A.3 Proteomic analysis of CaM-interacting proteins

Gene No.	Gene	Protein	Biological Process	Molecular Function	Cellular Component	functional catalog	Pathway
NCU00959	*tca-10*	succinate dehydrogenase iron-sulfur protein (283 aa)	tricarboxylic acid cycle	succinate dehydrogenase (ubiquinone) activity	mitochondrion	01.05 - C-compound and carbohydrate metabolism	TCA cycle variation III (eukaryotic)
			mitochondrial electron transport, succinate to ubiquinone		mitochondrial respiratory chain complex II	02.10 - tricarboxylic-acid pathway (citrate cycle, Krebs cycle, TCA cycle)	aerobic respiration -- electron donor II
			cellular response to glucose starvation			70.16 - mitochondrion	aerobic respiration -- electron donor III
							superpathway of glyoxylate cycle
NCU08946		hypothetical protein (277 aa)	protein folding		mitochondrion	10.01.03 - DNA synthesis and replication	
			inner mitochondrial membrane organization		mitochondrial inner membrane	10.03.01 - mitotic cell cycle and cell cycle control	
			negative regulation of proteolysis		mitochondrial membrane		
			mitochondrion morphogenesis				
NCU05064		C2H2 transcription factor (786 aa)				11.02.03.04 - transcriptional control	
NCU08681		hypothetical protein (403 aa)					
NCU09123	*camk-1*	Ca/CaM-dependent kinase-1 (414 aa)	sporocarp development involved in sexual reproduction				
			protein phosphorylation				
			ascospore formation				
			hyphal growth				
			regulation of growth rate				
			regulation of circadian rhythm				
			conidium formation				
			conidiophore development				
NCU01160	*dbp-5*	ATP-dependent RNA helicase dbp-5 (484 aa)	mRNA export from nucleus	inositol hexakisphosphate binding	nucleus	11 - TRANSCRIPTION	
			translational termination	RNA helicase activity	nuclear pore	20.01.21 - RNA transport	
					cytoplasm	20.09.01 - nuclear transport	
					polysome		
NCU08332	*hex-1*	hexagonal-1 (177 aa)	response to pH	structural molecule activity	peroxisome	01.03.16 - polynucleotide degradation	
			cytolysis		glyoxysome	12.04.01 - translation initiation	
			conidium formation		cell part	16.01 - protein binding	
						41.05 - animal development	
						43.01.03 - fungal and other eukaryotic cell type differentiation	
NCU06177	*camk-3*	calcium/calmodulin-dependent protein kinase (773 aa)					

Gene No.	Gene	Protein	Biological Process	Molecular Function	Cellular Component	functional catalog	Pathway
NCU02111	*myo-5*	myosin-5 (1236 aa)	exocytosis	microfilament motor activity	actin cortical patch	20.09.14 - cytoskeleton-dependent transport	
			endocytosis			43.01.03.05 - budding, cell polarity and filament formation	
			receptor-mediated endocytosis				
			response to osmotic stress				
			cellular cell wall organization				
			actin cortical patch localization				
NCU03804	*cna-1*	serine/threonine-protein phosphatase 2B catalytic subunit (559 aa)	establishment or maintenance of cell polarity	phosphoprotein phosphatase activity	cytosol	14.07 - protein modification	
			hyphal growth	calcium-dependent protein serine/threonine phosphatase activity	calcineurin complex	14.07.03 - modification by phosphorylation, dephosphorylation, autophosphorylation	
			cellular chloride ion homeostasis			30.01 - cellular signalling	
			fungal-type cell wall organization				
NCU00352		phospholipid-transporting ATPase (1361 aa)	ribosomal small subunit assembly	phospholipid-translocating ATPase activity	trans-Golgi network	20.01.01.01 - cation transport (H+, Na+, K+, Ca2+ , NH4+, etc.)	
			intracellular protein transport			20.03.22 - transport ATPases	
			post-Golgi vesicle-mediated transport			20.09.07 - vesicular transport (Golgi network, etc.)	
			endocytosis			70.08 - Golgi	
			establishment or maintenance of cell polarity				
			vesicle-mediated transport				
			phospholipid translocation				
NCU09468	*tba-2*	tubulin alpha-2 (450 aa)	establishment or maintenance of cell polarity	protein heterodimerization activity	nucleus	10.03.04.05 - chromosome segregation/division	
			mitochondrion distribution		cytosol	10.03.05.01 - spindle pole body/centrosome and microtubule	
					microtubule	16.19.05 - GTP binding	
						42.04.05 - microtubule cytoskeleton	
						70.04.05 - microtubule cytoskeleton	

Gene No.	Gene	Protein	Biological Process	Molecular Function	Cellular Component	functional catalog	Pathway
NCU03463	*vph-1*	vacuolar pH-sensitive ATPase-1 (857 aa)	protein complex assembly	proton-transporting ATPase activity, rotational mechanism	vacuolar proton-transporting V-type ATPase, V0 domain	02.13.03 - aerobic respiration	aerobic xylose fermentation
			polyphosphate metabolic process		fungal-type vacuole		aerobic xylose fermentation
			vacuolar acidification		fungal-type vacuole membrane		aerobic respiration
NCU03702		rRNA 2'-O-methyltransferase fibrillarin (324 aa)	ribosomal large subunit assembly	methyltransferase activity	nucleolus	11.02.01 - rRNA synthesis	
			rRNA modification		ribosome	11.04.01 - rRNA processing	
			RNA methylation		box C/D snoRNP complex	70.10 - nucleus	
			rRNA processing		small-subunit processome		
			snoRNA 3'-end processing				
			ribosome biogenesis				
NCU08515	*vma-2*	vacuolar membrane ATPase-2 (514 aa)	cellular calcium ion homeostasis	proton-transporting ATPase activity, rotational mechanism	vacuolar proton-transporting V-type ATPase, V1 domain	16.19.03 - ATP binding	aerobic xylose fermentation
			vacuolar acidification		fungal-type vacuole	20.01.01.01 - cation transport (H+, Na+, K+, Ca2+ , NH4+, etc.)	aerobic xylose fermentation
					cytoplasm	20.03.22 - transport ATPases	aerobic respiration
						20.09.13 - vacuolar/lysosomal transport	
						34.01.01.03 - homeostasis of protons	
						70.25 - vacuole or lysosome	
NCU09559	*ccg-9*	clock-controlled gene-9 (866 aa)	trehalose biosynthetic process				
			cellular response to nitrogen starvation				
			response to heat				
			response to salt stress				
			regulation of growth rate				
			cellular response to glucose starvation				
			conidium formation				
			cellular response to osmotic stress				
NCU04738		hypothetical protein (939 aa)				10.01.03 - DNA synthesis and replication	
						70.10 - nucleus	
NCU03982	*grp78 / hsps-2*	glucose regulated protein 78 (662 aa)	SRP-dependent cotranslational protein targeting to membrane, translocation	ATPase activity	endoplasmic reticulum	32.01 - stress response	
			response to stress	unfolded protein binding		70.07 - endoplasmic reticulum	
			response to unfolded protein				
			response to heat				
			ER-associated protein catabolic process				

Gene No.	Gene	Protein	Biological Process	Molecular Function	Cellular Component	functional catalog	Pathway
			posttranslational protein targeting to membrane, translocation response to starvation				
NCU07590		Ser/Thr protein phosphatase (711 aa)				01.03 -nucleotide / nucleoside / nucleobase metabolism	
NCU09032		hypothetical protein (894 aa)					
NCU01765	*nuo78*	NADH:ubiquinone oxidoreductase 78 (745 aa)	NADH oxidation	electron carrier activity	mitochondrion		aerobic respiration -- electron donor II
			mitochondrial electron transport, NADH to ubiquinone		mitochondrial respiratory chain complex I		aerobic respiration -- electron donor III
			ascospore formation				aerobic xylose fermentation
			regulation of oxygen and reactive oxygen species metabolic process				PWY2T-21
NCU00571		hypothetical protein (209 aa)					
NCU04553	*ubi-3 / crp-6*	ubiquitin/cytoplasmic ribosomal protein-6 (155 aa)	ribosomal small subunit assembly	structural constituent of ribosome	cytoplasm	12.01.01 - ribosomal proteins	
			translation		cytosolic small ribosomal subunit	14.07.05 - modification by ubiquitination, deubiquitination	
			protein ubiquitination			14.13.01 - cytoplasmic and nuclear protein degradation	
			ribosome biogenesis			70.03 - cytoplasm	
NCU03837		Snf1 kinase complex beta-subunit Gal83 (482 aa)					aerobic respiration
NCU01440	*myo-2*	myosin-2 (1595 aa)				20.09.14 - cytoskeleton-dependent transport 70.04.03 - actin cytoskeleton	
NCU04258	*dap-1*	dim-2-associated protein-1 (1753 aa)	DNA methylation				
NCU00775	*tca-6*	isocitrate dehydrogenase subunit 1 (386 aa)	tricarboxylic acid cycle	isocitrate dehydrogenase (NAD+) activity	cytoplasm	01.05 - C-compound and carbohydrate metabolism	TCA cycle variation III (eukaryotic)
			isocitrate metabolic process		mitochondrion	02.10 - tricarboxylic-acid pathway (citrate cycle, Krebs cycle, TCA cycle)	
			glutamate biosynthetic process			70.16 - mitochondrion	
NCU02283	*camk-2*	calcium/calmodulin-dependent protein kinase type I (298 aa)	protein phosphorylation	calmodulin-dependent protein kinase activity	nucleus	14.07.03 - modification by phosphorylation, dephosphorylation, autophosphorylation	
			ascospore formation		cytosol	30.01.05 - enzyme mediated signal transduction	
						34.11.11 - rhythm (e.g. circadian, ultradian)	

Gene No.	Gene	Protein	Biological Process	Molecular Function	Cellular Component	functional catalog	Pathway
NCU02957		hypothetical protein (487 aa)					
NCU06691		hypothetical protein (410 aa)				01.01.13 - regulation of amino acid metabolism 11.02.03.04 - transcriptional control 70.10 - nucleus	
NCU01288		hypothetical protein (1485 aa)					
NCU04054	*bml / tub-2*	tubulin beta chain (448 aa)			astral microtubule microtubule	10.03.01 - mitotic cell cycle and cell cycle control 10.03.02 - meiosis 70.04 - cytoskeleton	
NCU06110		thiazole biosynthetic enzyme (345 aa)	thiamine biosynthetic process response to vitamin B1	protein binding	mitochondrion cytosol	16.01 - protein binding	PWY3O-17 THISYNARA-PWY
NCU01895	*rrg-1*	response regulator (1115 aa)	sporocarp development involved in sexual reproduction conidium formation osmosensory signaling pathway via two-component system response to light stimulus phosphorylation ascospore formation regulation of cytolysis regulation of phosphorylation hyperosmotic salinity response regulation of circadian rhythm regulation of MAPKKK cascade	two-component response regulator activity		30.01.05 - enzyme mediated signal transduction	
NCU06989		hypothetical protein (519 aa)					
NCU03038		40S ribosomal protein S13 (152 aa)	translation	structural constituent of ribosome	cytosolic small ribosomal subunit	12.01.01 - ribosomal proteins 70.03 - cytoplasm	
NCU00127		hypothetical protein (593 aa)					
NCU06199		RNA binding protein Jsn1 (1219 aa)				11.04.03.11 - control of mRNA stability 16.03.03 - RNA binding	
NCU02972		hypothetical protein (764 aa)					
NCU03611	*chs-1*	chitin synthase (918 aa)			fungal-type vacuole porous cell septum spitzenkorper	42.01 - cell wall	PWY2T-19
NCU08132		alpha-1,3-glucan synthase Ags2 (2375 aa)					

Gene No.	Gene	Protein	Biological Process	Molecular Function	Cellular Component	functional catalog	Pathway
NCU02003		translation elongation factor-1 (461 aa)	tRNA export from nucleus translational elongation	translation elongation factor activity	ribosome eukaryotic translation elongation factor 1 complex	12.04 - translation	
NCU02478		alpha-1,3-glucan synthase Ags2 (2391 aa)				42.01 - cell wall	
NCU06095	*csp-2 / ghh*	grainy-head homolog (795 aa)	circadian rhythm response to light stimulus carotenoid biosynthetic process conidiophore development	sequence-specific DNA binding		11.02.03.04 - transcriptional control	
NCU08502		40S ribosomal protein S6 (240 aa)	translation	RNA binding structural constituent of ribosome protein binding	nucleus cytosolic small ribosomal subunit	12.01.01 - ribosomal proteins 70.03 - cytoplasm	
NCU09861		Ser/Thr protein phosphatase (696 aa)					
NCU02075	*hsp70-2*	heat shock protein 70 (586 aa)	translation regulation of translational fidelity de novo' cotranslational protein folding	ATPase activity unfolded protein binding	soluble fraction polysome		
NCU00212	*hH4-2*	histone h4 (104 aa)	chromatin assembly or disassembly	DNA binding	nuclear nucleosome	11.02.03.04 - transcriptional control 70.10.03 - chromosome	
NCU02657	*eth-1*	ethionine resistant-1 (396 aa)	methionine metabolic process S-adenosylmethionine biosynthetic process regulation of DNA methylation	methionine adenosyltransferase activity	cytoplasm mitochondrion	01.01.06.05.02 - degradation of methionine 01.20.21 - metabolism of sulfuric acid and L-cysteine derivatives	methionine degradation I (to homocysteine) S-adenosyl-L-methionine cycle II PWY2T-24 S-adenosylmethionine biosynthesis
NCU07495		sphingolipid long chain base-responsive protein LSP1 (375 aa)	endocytosis response to heat	protein kinase inhibitor activity	cytoplasm mitochondrion mitochondrial outer membrane eisosome	01.04.04 - regulation of phosphate metabolism 18.02.01.02.05 - kinase inhibitior 32.01.05 - heat shock response 34.11.09 - temperature perception and response	

Gene No.	Gene	Protein	Biological Process	Molecular Function	Cellular Component	functional catalog	Pathway
NCU01659		dDENN domain-containing protein (1227 aa)					
NCU09475		40s ribosomal protein s5 (214 aa)	translation	RNA binding structural constituent of ribosome	cytosolic small ribosomal subunit	12.01.01 - ribosomal proteins	
NCU04331	*crp-4*	cytoplasmic ribosomal protein-4 (302 aa)	ribosomal large subunit assembly translation	RNA binding structural constituent of ribosome	cytosolic large ribosomal subunit	12.01 - ribosome biogenesis	
NCU01680	*pma-1*	plasma membrane ATPase-1 (921 aa)	regulation of pH response to osmotic proton transport	hydrogen-exporting ATPase activity, phosphorylative mechanism ATPase activity	membrane fraction mitochondrion plasma membrane membrane raft	20.03.22 - transport ATPases	
NCU05837		vacuolar protein sorting-associated protein 13a (3210 aa)				14.04 - protein targeting, sorting and translocation	
NCU07721		26S proteasome regulatory subunit rpn1 (903 aa)					
NCU06733	*nkin-2*	kinesin (1878 aa)	mitochondrion transport along microtubule				
NCU02236		hypothetical protein (578 aa)					
NCU04448		T-complex protein 1 subunit alpha (567 aa)	protein folding cytoskeleton organization	unfolded protein binding	cytoplasm chaperonin-containing T-complex cytoskeleton	14.01 - protein folding and stabilization 70.03 - cytoplasm	
NCU06617		myosin regulatory light chain cdc4 (140 aa)		calcium ion binding protein binding	nucleus cytosol myosin II complex		
NCU10073		actin binding protein (806 aa)					
NCU00018		cell division control protein Cdc48 (825 aa)	ubiquitin-dependent protein catabolic process vesicle fusion protein transport ER-associated protein catabolic process	ATPase activity	nucleus endoplasmic reticulum membrane cytosol	14.13.01.01 - proteasomal degradation (ubiquitin/proteasomal pathway)	
NCU09869		exocyst complex component Sec3 (1509 aa)				20.09.16 - cellular export and secretion 43.01.03.05 - budding, cell polarity and filament formation	

Gene No.	Gene	Protein	Biological Process	Molecular Function	Cellular Component	functional catalog	Pathway
NCU08957		hypothetical protein (1402 aa)					
NCU07700	*cot-3*	colonial temperature-sensitive-3 (845 aa)	translational elongation hyphal growth	translation elongation factor activity	ribosome	12.04.02 - translation elongation	
NCU02793		hypothetical protein (10739 aa)	response to wounding hyphal growth organelle inheritance		porous cell septum hyphal tip		
NCU00420		hypothetical protein (523 aa)					
NCU00823	*rpn-11*	26S proteasome regulatory subunit RPN11 (339 aa)	ubiquitin-dependent protein catabolic process	protein binding	proteasome complex nucleus cytoplasm sytosol	20.01.27 - drug/toxin transport 32.05.01 - resistance proteins	
NCU08477	*ypt-1*	small GTP-binding protein (204 aa)	protein complex assembly ER to Golgi vesicle-mediated transport	GTPase activity	Golgi membrane mitochondrion mitochondrial outer membrane endoplasmic reticulum membrane	16.19.05 - GTP binding 30.01 - cellular signalling	
NCU01549		hypothetical protein (749 aa)				20.09.07 - vesicular transport (Golgi network, etc.) 20.09.14 - cytoskeleton-dependent transport 70.08 - Golgi	
NCU03757		60S ribosomal protein L4-A (362 aa)	translation response to light stimulus	structural constituent of ribosome	cytoplasm cytosolic large ribosomal subunit	12.01 - ribosome biogenesis 70.03 - cytoplasm	
NCU04779		60S ribosomal protein L8 (263 aa)	translation	structural constituent of ribosome	cytosolic large ribosomal subunit	12.01 - ribosome biogenesis 70.03 - cytoplasm	
NCU07420		eIF4A (398 aa)	telomere maintenance translational initiation	translation initiation factor activity ATP-dependent RNA helicase activity	ribosome eukaryotic translation initiation factor 4F complex		
NCU10067	*rpn-12*	26S proteasome non-ATPase regulatory subunit 8 (290 aa)				10.03.01 - mitotic cell cycle and cell cycle control 14.07.11 - protein processing (proteolytic) 14.13.01.01 - proteasomal degradation (ubiquitin/proteasomal pathway) 32.01 - stress response	

Gene No.	Gene	Protein	Biological Process	Molecular Function	Cellular Component	functional catalog	Pathway
NCU09127		hypothetical protein (424 aa)					
NCU05488		RNA-binding protein Vip1 (284 aa)			mitochondrion		
NCU01528	*gpd-1 / ccg-7*	glyceraldehyde-3-phosphate dehydrogenase-1 (339 aa)	gluconeogenesis glycolysis cellular response to glucose starvation	glyceraldehyde-3-phosphate dehydrogenase (phosphorylating) activity	cytoplasm mitochondrion fungal-type cell wall glyoxysome	02.01 - glycolysis and gluconeogenesis	gluconeogenesis I glycolysis I glycolysis II xylose fermentation
NCU03559		ubiquinol-cytochrome c reductase complex core protein 2 precursor (455 aa)	regulation of growth rate conidium formation		mitochondrion	02.13.03 - aerobic respiration 20.01.15 - electron transport 20.03 - transport facilities	aerobic xylose fermentation aerobic xylose fermentation PWY2T-21 aerobic respiration aerobic respiration -- electron donor II
NCU04173	*act*	actin (376 aa)			glyoxysome actin filament bundle cell cortex of cell tip	70.04 - cytoskeleton	
NCU02905		60S ribosomal protein L23 (140 aa)	translation	structural constituent of ribosome	cytosolic large ribosomal subunit	12.01.01 - ribosomal proteins 70.03 - cytoplasm	
NCU08693	*hsp70-5*	heat shock protein 70-5 (669 aa)	protein folding response to pH protein import into mitochondrial matrix protein refolding	protein transporter activity ATPase activity enzyme regulator activity	presequence translocase-associated import motor mitochondrion mitochondrial inner membrane mitochondrial membrane mitochondrial nucleoid		
NCU06783		ATP citrate lyase (488 aa)				01.06.05 - fatty acid metabolism	acetyl-CoA biosynthesis (from citrate)
NCU06226		60S ribosomal protein L25 (157 aa)	translation	structural constituent of ribosome protein binding	cytosolic large ribosomal subunit	12.01.01 - ribosomal proteins 70.03 - cytoplasm	
NCU02411	*(nuf-1)*	hypothetical protein (1492 aa)				16.01 - protein binding	
NCU02549	*pep*	processing enhancing protein (477 aa)	protein processing involved in protein targeting to mitochondrion	metalloendopeptidase activity mitochondrial processing peptidase activity ATP binding	mitochondrion mitochondrial inner membrane mitochondrial processing peptidase complex	14.07.11 - protein processing (proteolytic) 70.16 - mitochondrion	

Gene No.	Gene	Protein	Biological Process	Molecular Function	Cellular Component	functional catalog	Pathway
NCU01207	*vma-1*	vacuolar membrane ATPase-1 (608 aa)	intron homing	endodeoxyribonuclease activity	vacuolar proton-transporting V-type ATPase, V1 domain	20.01.01.01 - cation transport (H+, Na+, K+, Ca2+ , NH4+, etc.)	aerobic xylose fermentation
			vacuolar acidification	proton-transporting ATPase activity, rotational mechanism	fungal-type vacuole	20.03.22 - transport ATPases	aerobic xylose fermentation
			protein metabolic process		mitochondrion	20.09.13 - vacuolar/lysosomal transport	aerobic respiration
			methylamine metabolic process		vacuolar membrane vacuolar proton-transporting V-type ATPase complex		
NCU08409	*trp-3*	tryptophan synthetase (709 aa)	tryptophan biosynthetic process	tryptophan synthase activity	nucleus cytoplasm		tryptophan biosynthesis
NCU01754	*adh-1*	alcohol dehydrogenase I (354 aa)	amino acid catabolic process to alcohol via Ehrlich pathway	alcohol dehydrogenase (NAD) activity	soluble fraction	02.01 - glycolysis and gluconeogenesis	mixed acid fermentation
			NADH oxidation		mitochondrion	02.16.01 - alcohol fermentation	valine degradation II
			response to light stimulus		mitochondrial matrix		leucine degradation III
			cellular response to glucose starvation				isoleucine degradation II phenylalanine degradation III tryptophan degradation VIII (to tryptophol) methionine degradation III pyruvate fermentation to ethanol II xylose conversion to ethanol xylose fermentation cellulose conversion to ethanol PWY3O-4108-1 oxidative ethanol degradation I
NCU01484	*rho-1*	rho-type GTPase (196 aa)	endocytosis	GTPase activity	signal transducer activity		PWY2T-19
			actin filament organization	signal transducer activity	membrane fraction		
			cellular cell wall organization		mitochondrion		
			establishment or maintenance of cell polarity		mitochondrial outer membrane		
			small GTPase mediated signal transduction		peroxisome		
			fungal-type cell wall organization		spitzenkorper		
			regulation of MAP kinase activity				

Gene No.	Gene	Protein	Biological Process	Molecular Function	Cellular Component	functional catalog	Pathway
NCU06661		60S ribosomal protein L22 (127 aa)				12.01 - ribosome biogenesis	
NCU09477	*aac / acp*	ADP, ATP carrier protein (314 aa)	mitochondrial transport response to oxidative stress aerobic respiration response to pH	ATP:ADP antiporter activity	mitochondrion mitochondrial inner membrane	20.01.17 - nucleotide/nucleoside/nucleobase transport 20.09.04 - mitochondrial transport 70.16 - mitochondrion	aerobic respiration -- electron donor II aerobic respiration -- electron donor III aerobic xylose fermentation PWY2T-21 aerobic respiration
NCU11708 (NCU16773)		hypothetical protein (569 aa)					
NCU02152		RRM domain-containing protein (380 aa)					
NCU01004		phosphatidylserine decarboxylase proenzyme (1063 aa)				01.06 - lipid, fatty acid and isoprenoid metabolism 70.08 - Golgi	phosphatidylethanolamine biosynthesis I
NCU02514	*atp-1*	ATPase-1 (552 aa)		hydrogen ion transporting ATP synthase activity, rotational mechanism	mitochondrion mitochondrial proton-transporting ATP synthase, catalytic core mitochondrial membrane mitochondrial nucleoid	02.11 - electron transport and membrane-associated energy conservation 02.45.15 - energy generation (e.g. ATP synthase) 20.01.01.01 - cation transport (H+, Na+, K+, Ca2+ , NH4+, etc.) 20.03.22 - transport ATPases 20.09.04 - mitochondrial transport 34.01.01.03 - homeostasis of protons	aerobic xylose fermentation aerobic xylose fermentation aerobic respiration
NCU09119		ATP synthase subunit gamma (300 aa)	ATP synthesis coupled proton transport	ATPase activity hydrogen ion transporting ATP synthase activity, rotational mechanism	mitochondrion mitochondrial proton-transporting ATP synthase, central stalk proton-transporting ATP synthase complex, catalytic core F(1)	02.13.03 - aerobic respiration 02.45.15 - energy generation (e.g. ATP synthase) 20.03.22 - transport ATPases 20.09.04 - mitochondrial transport 34.01.01.03 - homeostasis of protons 70.16 - mitochondrion	aerobic xylose fermentation aerobic xylose fermentation aerobic respiration

Gene No.	Gene	Protein	Biological Process	Molecular Function	Cellular Component	functional catalog	Pathway
NCU09602	*hsp70-1*	heat shock protein 70-1 (647 aa)	establishment or maintenance of cell polarity response to pH response to heat protein import into mitochondrial matrix response to dsRNA	heat shock protein binding		32.01 - stress response	
NCU05273		Vps52/Sac2 family protein (669 aa)					
NCU05430		ATP synthase beta subunit (520 aa)	ATP synthesis coupled proton transport	hydrogen ion transporting ATP synthase activity, rotational mechanism	soluble fraction mitochondrion mitochondrial outer membrane mitochondrial proton-transporting ATP synthase, catalytic core mitochondrial membrane	02.13.03 - aerobic respiration 02.45.15 - energy generation (e.g. ATP synthase) 16.19.03 - ATP binding 34.01.01.03 - homeostasis of protons 70.16 - mitochondrion	aerobic xylose fermentation aerobic xylose fermentation aerobic respiration
NCU09014		cleavage and polyadenylation specificity factor subunit 5 (265 aa)					
NCU04075		hypothetical protein (599 aa)					
NCU07997		hypothetical protein (342 aa)					
NCU03972	*rpn-7*	proteasome regulatory particle (493 aa)				12.04 - translation 14.13.01.01 - proteasomal degradation (ubiquitin/proteasomal pathway) 16.07 - structural protein binding	
NCU01547	*rpn-8*	26S proteasome regulatory subunit rpn-8 (353 aa)	ubiquitin-dependent protein catabolic process		proteasome regulatory particle, lid subcomplex	14.13 - protein/peptide degradation 70.07 - endoplasmic reticulum 70.10 - nucleus	
NCU06361		cwl1 (330 aa)					
NCU06854		RuvB-like helicase 2 (482 aa)	chromatin remodeling regulation of transcription from RNA polymerase II promoter rRNA processing snoRNA metabolic process	ATPase activity ATP-dependent 5'-3' DNA helicase activity	Swr1 complex nucleus chromatin remodeling complex Ino80 complex	11.02.03 - mRNA synthesis	
NCU00502		ATP synthase subunit 4 (242 aa)					

Gene No.	Gene	Protein	Biological Process	Molecular Function	Cellular Component	functional catalog	Pathway
NCU00489	*crp-10*	cytoplasmic ribosomal protein-10 (263 aa)	translation	structural constituent of ribosome	cytosolic small ribosomal subunit preribosome, small subunit precursor	12.01.01 - ribosomal proteins	
NCU00793		trehalose phosphate synthase (930 aa)	response to light stimulus			01.05 - C-compound and carbohydrate metabolism 02.19 - metabolism of energy reserves (e.g. glycogen, trehalose)	
NCU01113		hypothetical protein (497 aa)					
NCU09700		T-complex protein 1 subunit beta (558 aa)	protein folding cytoskeleton organization	unfolded protein binding	cytoplasm chaperonin-containing T-complex cytoskeleton	14.01 - protein folding and stabilization 70.03 - cytoplasm	
NCU02634		hypothetical protein (394 aa)				98 - CLASSIFICATION NOT YET CLEAR-CUT	
NCU01589	*hsp60*	heat shock protein 60 (575 aa)	protein folding protein import into mitochondrial matrix	single-stranded DNA binding	mitochondrion mitochondrial nucleoid		
NCU04294	*sad-2*	hypothetical protein (1098 aa)	pachytene meiotic prophase I gene silencing reproductive sporulation	cytoplasm perinuclear region of cytoplasm			
NCU00726	*csr-1 / CyP20, cyp*	cyclosporin-resistant-1 (224 aa)	protein folding response to acetate	peptidyl-prolyl cis-trans isomerase activity	mitochondrion mitochondrial matrix cytosol glyoxysome	14.01 - protein folding and stabilization 70.16 - mitochondrion	
NCU00413		60S ribosomal protein L2 (255 aa)	translation	structural constituent of ribosome	cytosolic large ribosomal subunit	12.01.01 - ribosomal proteins 70.03 - cytoplasm	
NCU09068	*nit-2 / amr, pink*	nitrate nonutilizer-2 (1037 aa)	cellular response to nitrogen levels regulation of glycogen metabolic process	protein domain specific binding sequence-specific DNA binding		01.02.07 - regulation of nitrogen, sulfur and selenium metabolism 11.02.03.04.01 - transcription activation 16.03.01 - DNA binding 70.10 - nucleus	
NCU03126		hypothetical protein (315 aa)				11.02.03.04 - transcriptional control 16.03.01 - DNA binding 40.01 - cell growth / morphogenesis 70.10.03 - chromosome	

Gene No.	Gene	Protein	Biological Process	Molecular Function	Cellular Component	functional catalog	Pathway
NCU04190		exocyst complex component Sec8 (1112 aa)					
NCU02533		DNA-directed RNA polymerase I and III polypeptide (379 aa)				11.02.01 - rRNA synthesis 11.02.02 - tRNA synthesis 16.03.01 - DNA binding 70.10 - nucleus	
NCU08761		vacuolar sorting receptor (371 aa)					
NCU08604		hypothetical protein (1519 aa)				20.09.01 - nuclear transport	
NCU02755		PAP2 domain-containing protein (489 aa)				42.10.05 - nuclear membrane	
NCU04245	*tom70 / mom72*	translocase of outer mitochondrial membrane 70 (623 aa)	protein targeting to mitochondrion mitochondrion organization hyphal growth conidium formation	preprotein binding	mitochondrial outer membrane mitochondrial outer membrane translocase complex mitochondrial membrane	14.04 - protein targeting, sorting and translocation 20.03 - transport facilities 20.09.04 - mitochondrial transport 70.16 - mitochondrion	
NCU05485	*ckb-1 / chr,ckb 1*	casein kinase II regulatory beta subunit-1 (334 aa)	protein phosphorylation response to pH temperature compensation of the circadian clock regulation of circadian rhythm	casein kinase activity	nucleus cytoplasm	14.07.03 - modification by phosphorylation, dephosphorylation, autophosphorylation 30.01.05.01 - protein kinase 34.11.11 - rhythm (e.g. circadian, ultradian)	
NCU09712		hypothetical protein (553 aa)					
NCU07697	*tca-4*	isocitrate dehydrogenase subunit 2 (380 aa)	tricarboxylic acid cycle isocitrate metabolic process glutamate biosynthetic process	isocitrate dehydrogenase (NAD+) activity	mitochondrion mitochondrial membrane	01.05 - C-compound and carbohydrate metabolism 02.10 - tricarboxylic-acid pathway (citrate cycle, Krebs cycle, TCA cycle) 70.16 - mitochondrion	TCA cycle variation III (eukaryotic)
NCU04414	*rpt-5*	hypothetical protein (461 aa)	ubiquitin-dependent protein catabolic process	endopeptidase activity ATPase activity	proteasome regulatory particle, base subcomplex		

Gene No.	Gene	Protein	Biological Process	Molecular Function	Cellular Component	functional catalog	Pathway
NCU06419	*mek-1*	MAP kinase kinase (519 aa)	MAPKKK cascade	MAP kinase kinase activity			
			syncytium formation by plasma membrane fusion	structural constituent of cell wall	cell	14.07.03 - modification by phosphorylation, dephosphorylation, autophosphorylation	
			sporocarp development involved in sexual reproduction			30.01.05.01.03 - MAPKKK cascade	
			hyphal growth				
			regulation of melanin biosynthetic process				
			conidium formation				
NCU07012		hypothetical protein (1201 aa)					
NCU02948	*ncw-4 / mig-1*	non-anchored cell wall protein-4 (206 aa)	response to light stimulus	plasma membrane enriched fraction		01.05.11.07.01 - aerobic aromate catabolism	
				cytoplasm			
				fungal-type cell wall			
				membrane raft			
NCU06943		SIK1 (522 aa) - Salt sensing	rRNA modification	nucleus		11.02.01 - rRNA synthesis	
			rRNA processing	box C/D snoRNP complex		11.04.01 - rRNA processing	
				small-subunit processome		70.10 - nucleus	
NCU06367		Yip1 domain-containing protein (313 aa)					
NCU03482		RuvB-like helicase 1 (459 aa)	chromatin remodeling	ATPase activity	Swr1 complex	10.01.09.05 - DNA conformation modification (e.g. chromatin)	
			regulation of transcription from RNA polymerase II promoter	ATP-dependent 3'-5' DNA helicase activity	nucleus	11.02.03.01 - general transcription activities	
				sequence-specific DNA binding	chromatin remodeling complex	70.10 - nucleus	
					Ino80 complex		
NCU07366	*gfa1*	glucosamine-fructose-6-phosphate aminotransferase (701 aa)	cell wall chitin biosynthetic process	glutamine-fructose-6-phosphate transaminase (isomerizing) activity		01.05 - C-compound and carbohydrate metabolism	
			establishment or maintenance of cell polarity			01.01 - amino acid metabolism	isoleucine biosynthesis I (from threonine)
NCU01666	*ilv-4*	acetolactate synthase small subunit (331 aa)	branched chain family amino acid biosynthetic process	acetolactate synthase activity	mitochondrion	70.16 - mitochondrion	acetoin biosynthesis II
			response to acetate	enzyme regulator activity	acetolactate synthase complex		valine biosynthesis
					mitochondrial nucleoid		
NCU09017		hypothetical protein (661 aa)					

Gene No.	Gene	Protein	Biological Process	Molecular Function	Cellular Component	functional catalog	Pathway
NCU00040		eukaryotic translation initiation factor 3 110 kDa subunit (1060 aa)				12.04.01 - translation initiation 70.03 - cytoplasm	
NCU07414		hypothetical protein similar to protein mitochondrial targeting protein Mas5 (415 aa)				14.04 - protein targeting, sorting and translocation 20.01.10 - protein transport 20.09.04 - mitochondrial transport	
NCU06977		hypothetical protein (290 aa)					
NCU01317		60S ribosomal protein L12 (166 aa)	ribosomal large subunit assembly translation	structural constituent of ribosome	cytosolic large ribosomal subunit	12.01 - ribosome biogenesis	
NCU07829		60S ribosomal protein L7 (249 aa)	translation	structural constituent of ribosome	cytosolic large ribosomal subunit		
NCU03703		60S ribosomal protein L17 (187 aa)	translation	structural constituent of ribosome	cytosolic large ribosomal subunit cytoplasm	12.01 - ribosome biogenesis 70.03 - cytoplasm	
NCU03396		nucleolar protein nop-58 (598 aa)	rRNA modification rRNA processing	box C/D snoRNP complex small-subunit processome		11.04.01 - rRNA processing 70.10.07 - nucleolus	
NCU00566		synaptobrevin (117 aa)	endocytosis vesicle-mediated transport		cytoplasm endoplasmic reticulum Golgi apparatus cytoplasmic vesicle membrane cell cortex of cell tip medial cortex		
NCU06232	*leu-1*	leucine-1 (369 aa)	leucine biosynthetic process	3-isopropylmalate dehydrogenase activity	soluble fraction	01.01.11.04.01 - biosynthesis of leucine	leucine biosynthesis
NCU04826		hypothetical protein (1423 aa)				98 - CLASSIFICATION NOT YET CLEAR-CUT	
NCU04185	*prk-1*	protein kinase gsk3 (395 aa)	positive regulation of molecular function, epigenetic	protein serine/threonine kinase activity protein serine/threonine/tyrosine kinase activity	nucleus cytosol	01.05.03 - polysaccharide metabolism	
NCU05007		spindle poison sensitivity protein Scp3 (667 aa)	response to light stimulus				
NCU05650		karyopherin Kap123 (1095 aa)				14.04 - protein targeting, sorting and translocation 20.09.01 - nuclear transport	

Gene No.	Gene	Protein	Biological Process	Molecular Function	Cellular Component	functional catalog	Pathway
NCU04352	*chs-5*	chitin synthase C (1799 aa)				01.05.03 - polysaccharide metabolism 42.01 - cell wall	PWY2T-19
NCU03292	*pmr-1*	calcium-transporting ATPase type 2C member 1 (1026 aa)	hyphal growth regulation of growth rate conidium formation response to calcium ion calcium ion import conidiophore development	calcium-transporting ATPase activity	Golgi apparatus	20.01.01.01 - cation transport (H+, Na+, K+, Ca2+ , NH4+, etc.) 20.03.22 - transport ATPases 34.01.01.01 - homeostasis of metal ions (Na, K, Ca etc.)	
NCU01729		hypothetical protein (790 aa)					
NCU09808		dynamin-1 (802 aa)	mitochondrion inheritance mitochondrial fission mitochondrion organization peroxisome organization hyphal growth protein homooligomerization	GTPase activity identical protein binding protein homodimerization activity	mitochondrion mitochondrial outer membrane	42.16 - mitochondrion 70.16 - mitochondrion	
NCU04718		hypothetical protein (574 aa)					
NCU06644		hypothetical protein (1385 aa)					
NCU09711		hypothetical protein (823 aa)					
NCU06743		hypothetical protein (164 aa)				12.01.01 - ribosomal proteins	
NCU03833	*cnb-1*	calcineurin B-1 (175 aa)	cellular ion homeostasis cellular cell wall organization conidium formation	calcium-dependent protein serine/threonine phosphatase activity calcineurin complex		16.17.01 - calcium binding 30.01.09.03 - Ca2+ mediated signal transduction	
NCU01455		signal recognition particle protein (683 aa)				14.04 - protein targeting, sorting and translocation	
NCU08840		chromatin remodeling complex subunit (752 aa)				42.10.03 - organization of chromosome structure 70.10 - nucleus	
NCU07952		C2H2 type zinc finger domain-containing protein (711 aa)					
NCU06560		hypothetical protein (485 aa)					

Gene No.	Gene	Protein	Biological Process	Molecular Function	Cellular Component	functional catalog	Pathway
NCU04380		acyl-CoA synthetase (707 aa)			mitochondrial outer membrane	01.06 - lipid, fatty acid and isoprenoid metabolism	fatty acid β-oxidation I PWY-5136-1 fatty acid activation PWY-5972 PWY2T-2575 PWY2T-2576
NCU01633		hexose transporter HXT13 (533 aa)					PWY2T-42 cellulose degradation
NCU04100		vacuolar sorting protein 1 (707 aa)	protein targeting to vacuole peroxisome organization vacuolar transport actin cytoskeleton organization hyphal growth protein retention in Golgi apparatus	GTPase activity	membrane fraction cytoplasm mitochondrial outer membrane peroxisome		
NCU06047		40S ribosomal protein S2 (266 aa)	translation regulation of translational fidelity	structural constituent of ribosome	cytosolic small ribosomal subunit small-subunit processome	12.01.01 - ribosomal proteins 70.03 - cytoplasm	
NCU03083		hypothetical protein (459 aa)					
NCU02839		T-complex protein 1 (534 aa)	protein folding cytoskeleton organization	unfolded protein binding	cytoplasm cytoskeleton	14.01 - protein folding and stabilization 70.03 - cytoplasm	
NCU06703	*mid-1*	calcium channel subunit Mid1 (700 aa)	hyphal growth regulation of growth rate				
NCU02207		T-complex protein 1 subunit beta (531 aa)	protein folding cytoskeleton organization	unfolded protein binding	cytoplasm chaperonin-containing T-complex cytoskeleton		
NCU06211	*tca-16*	malate dehydrogenase (331 aa)	tricarboxylic acid cycle aerobic respiration cellular response to glucose starvation	L-malate dehydrogenase activity	mitochondrion mitochondrial matrix glyoxysome	02.10 - tricarboxylic-acid pathway (citrate cycle, Krebs cycle, TCA cycle) 70.16 - mitochondrion	mixed acid fermentation gluconeogenesis I glyoxylate cycle aspartate degradation II TCA cycle variation III (eukaryotic)
NCU01439		D-3-phosphoglycerate dehydrogenase 1 (467 aa)	serine family amino acid biosynthetic process	phosphoglycerate dehydrogenase activity	cytoplasm	01.01.09.01.01 - biosynthesis of glycine 01.01.09.02.01 - biosynthesis of serine 02.45 - energy conversion and regeneration	serine biosynthesis

Gene No.	Gene	Protein	Biological Process	Molecular Function	Cellular Component	functional catalog	Pathway
NCU08597		hypothetical protein (1514 aa)					
NCU07739		YTP1 (521 aa)					
NCU01826		DUF250 domain membrane protein (400 aa)				20.01.03 - C-compound and carbohydrate transport 20.03 - transport facilities	
NCU02669		signal sequence binding protein (1529 aa)				14.04 - protein targeting, sorting and translocation 20.09.07 - vesicular transport (Golgi network, etc.) 20.09.13 - vacuolar/lysosomal transport	
NCU03608		ketol-acid reductoisomerase (403 aa)	mitochondrial genome maintenance branched chain family amino acid biosynthetic process cellular response to glucose starvation	ketol-acid reductoisomerase activity	mitochondrion mitochondrial nucleoid	01.01.11.02.01 - isoleucine biosynthesis I (from threonine) 01.01.11.03.01 - biosynthesis of valine	valine biosynthesis
NCU08940		ubiquinol-cytochrome c reductase complex protein (124 aa)	mitochondrial electron transport, ubiquinol to cytochrome c aerobic respiration respiratory chain complex III assembly	ubiquinol-cytochrome-c reductase activity	mitochondrion mitochondrial respiratory chain complex III	02.11 - electron transport and membrane-associated energy conservation 20.01.15 - electron transport 20.03 - transport facilities 70.16 - mitochondrion	aerobic respiration -- electron donor II aerobic xylose fermentation aerobic xylose fermentation PWY2T-21 aerobic respiration
NCU10042	*emp-7*	enolase (439 aa)	gluconeogenesis glycolysis	phosphopyruvate hydratase activity	phosphopyruvate hydratase complex cytoplasm mitochondrion	01.05 - C-compound and carbohydrate metabolism 01.05.02.07 - sugar, glucoside, polyol and carboxylate catabolism 01.20.15 - metabolism of derivatives of dehydroquinic acid, shikimic acid and chorismic acid 02.01 - glycolysis and gluconeogenesis	gluconeogenesis I glycolysis I glycolysis II xylose fermentation
NCU07922		elongation factor 3 (1057 aa)	translational elongation	translation elongation factor activity ATPase activity	cytosolic ribosome	12.04.01 - translation initiation 70.03 - cytoplasm	
NCU03500		aminotransferase (518 aa)			mitochondrial outer membrane	01.02 - nitrogen, sulfur and selenium metabolism	

Gene No.	Gene	Protein	Biological Process	Molecular Function	Cellular Component	functional catalog	Pathway
NCU00905		N-acylethanolamine amidohydrolase (611 aa)			mitochondrial outer membrane	01.02 - nitrogen, sulfur and selenium metabolism	
NCU02010	*leu-4*	2-isopropylmalate synthase (626 aa)	leucine biosynthetic process	2-isopropylmalate synthase activity	cytoplasm	01.01.11 - metabolism of the pyruvate family (alanine, isoleucine, leucine, valine) and D-alanine	leucine biosynthesis
					mitochondrion	70.03 - cytoplasm	
						70.16 - mitochondrion	
NCU00951		inorganic pyrophosphatase (445 aa)	establishment or maintenance of cell polarity	inorganic diphosphatase activity	mitochondrion	01.04 - phosphate metabolism	
						70.03 - cytoplasm	
NCU03616	*smco-7*	semicolonial-7 (230 aa)	cellular response to nitrogen starvation	GTPase activity		18.02.05 - regulator of G-protein signalling	
			spindle organization			30.01.05.01 - protein kinase	
			establishment or maintenance of cell polarity			40.01.03 - directional cell growth (morphogenesis)	
			fungal-type cell wall biogenesis			42.01 - cell wall	
			ascospore formation			43.01.03 - fungal and other eukaryotic cell type differentiation	
			proteasomal ubiquitin-dependent protein catabolic process			43.01.03.06 - hyphae formation	
						43.01.03.09 - development of asco- basidio- or zygospore	
NCU00634		ribosomal protein L14 (143 aa)				12.01.01 - ribosomal proteins	
						70.03 - cytoplasm	
NCU04859	*nst-4*	Hst3p (1328 aa)				11.02.03.04 - transcriptional control	
NCU00046		leucine Rich Repeat domain-containing protein (857 aa)					
NCU00627		hypothetical protein (570 aa)					
NCU06871	*do / fks*	1,3-beta-glucan synthase component GLS1 (1956 aa)	1,3-beta-D-glucan biosynthetic process	1,3-beta-D-glucan synthase activity	1,3-beta-D-glucan synthase complex	01.05 - C-compound and carbohydrate metabolism	PWY2T-19
						43.01.03.09 - development of asco- basidio- or zygospore	
NCU03509	*pmg / naap / nap-2*	amino acid permease NAAP1 (637 aa)	amino acid transport	amino acid transmembrane transporter activity	fungal-type vacuole lumen		
			gamma-aminobutyric acid transport	L-proline transmembrane transporter activity	endosome		

Gene No.	Gene	Protein	Biological Process	Molecular Function	Cellular Component	functional catalog	Pathway
			polyamine transport	polyamine transmembrane transporter activity	plasma membrane		
			ammonia assimilation cycle		integral to plasma membrane		
					ER to Golgi transport vesicle		
NCU04795		hypothetical protein (714 aa)					
NCU06198		GDP-mannose transporter (393 aa)	protein N-linked glycosylation	nucleotide-sugar transmembrane transporter activity	mitochondrion	20.01.03 - C-compound and carbohydrate transport	
			lipid glycosylation		Golgi apparatus	20.09.07 - vesicular transport (Golgi network, etc.)	
NCU03523	*stk-22*	serine/threonine protein kinase (1247 aa)	hyphal growth			14.07.03 - modification by phosphorylation, dephosphorylation, autophosphorylation	
			conidiophore development			30.01 - cellular signalling	
NCU04823		NADP-dependent alcohol dehydrogenase C (365 aa)	response to light stimulus			01.05 - C-compound and carbohydrate metabolism	
						02.16.01 - alcohol fermentation	
NCU08480	*hssf-2*	HSF-type DNA-binding domain-containing protein (580 aa)	response to heat				
			response to light stimulus				
			conidium formation				
NCU03635		60S ribosomal protein L38 (81 aa)				12.01 - ribosome biogenesis	
NCU07380		eukaryotic translation initiation factor 3 (592 aa)	translational initiation	translation initiation factor activity	nucleus	10.03.05.01 - spindle pole body/centrosome and microtubule cycle	
			spindle assembly	protein binding	cytosol	16.01 - protein binding	
					eukaryotic translation initiation factor 3 complex	70.10 - nucleus	
NCU04087		Aha1 domain-containing protein (327 aa)				14.01 - protein folding and stabilization	
						32.01 - stress response	
NCU05132		hypothetical protein (2904 aa)					
NCU03223		sn-1,2-diacylglycerol cholinephosphotransferase (431 aa)				01.06 - lipid, fatty acid and isoprenoid metabolism	choline biosynthesis III
						20.09 - transport routes	phosphatidylcholine biosynthesis I
						70.07 - endoplasmic reticulum	phosphatidylethanolamine biosynthesis II

Gene No.	Gene	Protein	Biological Process	Molecular Function	Cellular Component	functional catalog	Pathway
NCU05390		mitochondrial phosphate carrier protein (320 aa)	phosphate transport	inorganic phosphate transmembrane transporter activity	mitochondrion	01.04 - phosphate metabolism	
					mitochondrial envelope	20.01.01.07.07 - phosphate transport	
					mitochondrial membrane	20.03 - transport facilities	
						34.01.03.03 - homeostasis of phosphate	
						70.16 - mitochondrion	
NCU02505	*suc*	succinate (1193 aa)	gluconeogenesis	pyruvate carboxylase activity	cytosol	01.05 - C-compound and carbohydrate metabolism	
			NADPH regeneration			01.06.05 - fatty acid metabolism	
			response to heat			01.07 - metabolism of vitamins, cofactors, and prosthetic groups	
			cellular response to glucose starvation			02.01 - glycolysis and gluconeogenesis	
						16.19.03 - ATP binding	
NCU03733		hypothetical protein (338 aa)					
NCU00618		40S ribosomal protein S27 (83 aa)	translation	RNA binding	cytosolic small ribosomal subunit	12.01.01 - ribosomal proteins	
			signal transduction	structural constituent of ribosome		70.03 - cytoplasm	
				zinc ion binding			
NCU08175		hypothetical protein (459 aa)					
NCU04350		chitin synthase 6 (1820 aa)					PWY2T-19
NCU02813		eukaryotic translation initiation factor 3 subunit M (435 aa)					
NCU07567		T-complex protein 1 subunit theta (548 aa)	protein folding	unfolded protein binding	cytoplasm	14.01 - protein folding and stabilization	
			cytoskeleton organization		chaperonin-containing T-complex cytoskeleton		
NCU09866		thyroid hormone receptor interactor 12 (1973 aa)					
NCU07830		cytoplasmic ribosomal protein-2 (151 aa)	translation	structural constituent of ribosome	cytosolic small ribosomal subunit	12.01.01 - ribosomal proteins	
				protein binding			
NCU07982		acetolactate synthase (690 aa)	branched chain family amino acid biosynthetic process	acetolactate synthase activity	mitochondrion	01.01.11.02.01 - biosynthesis of isoleucine	isoleucine biosynthesis I (from threonine)
				flavin adenine dinucleotide binding	acetolactate synthase complex	01.01.11.03.01 - biosynthesis of valine	acetoin biosynthesis II
							valine biosynthesis

Gene No.	Gene	Protein	Biological Process	Molecular Function	Cellular Component	functional catalog	Pathway
NCU04251	*chs-3*	chitin synthase 3 (889 aa)	ascospore formation ascospore wall assembly ascospore wall chitin biosynthetic process	chitin synthase activity	porous cell septum vacuole endoplasmic reticulum spitzenkorper chitosome	42.01 - cell wall	PWY2T-19
NCU03737		elongation factor Tu (438 aa)	translational elongation	translation elongation factor activity GTPase activity	mitochondrion	12.04 - translation 70.16 - mitochondrion	
NCU11181		Ras superfamily GTPase (190 aa)	ER to Golgi vesicle-mediated transport establishment or maintenance of cell polarity	GTPase activity	COPII vesicle coat	16.19.05 - GTP binding 20.09.16 - cellular export and secretion	
NCU07434		short-chain dehydrogenase/reductase SDR (349 aa)				01.06 - lipid, fatty acid and isoprenoid metabolism	
NCU00895		RAB GTPase Ypt5 (221 aa)	regulation of vesicle fusion	GTP binding	nucleus cytosol	14.04 - protein targeting, sorting and translocation 16.19.05 - GTP binding 20.09.13 - vacuolar/lysosomal transport 20.09.18 - cellular import 30.01 - cellular signalling	
NCU00475		40S ribosomal protein S18 (157 aa)	translation	structural constituent of ribosome	cytosolic small ribosomal subunit	12.01.01 - ribosomal proteins	
NCU02954	*lys-7*	homoisocitrate dehydrogenase (358 aa)	lysine biosynthetic process	homoisocitrate dehydrogenase activity	mitochondrion	01.01.11.02.01 - biosynthesis of isoleucine 01.01.11.03.01 - biosynthesis of valine 01.01.11.04.01 - biosynthesis of leucine	lysine biosynthesis IV
NCU06031	*rhd*	mitochondrial peroxiredoxin PRX1 (226 aa)	sporocarp development involved in sexual reproduction cell redox homeostasis		glyoxysome	32.01.01 - oxidative stress response 32.07.07 - oxygen and radical detoxification 70.16 - mitochondrion	
NCU06863		histone H1 (237 aa)			nucleus	10.03.04.03 - chromosome condensation 16.03.01 - DNA binding 70.10.03 - chromosome	

Gene No.	Gene	Protein	Biological Process	Molecular Function	Cellular Component	functional catalog	Pathway
NCU05221	*nuo-21 / nuo-18*	NADH:ubiquinone oxidoreductase 21kD subunit (219 aa)	NADH oxidation	electron carrier activity	mitochondrion	aerobic respiration -- electron donor II	02.13.03 - aerobic respiration
				oxidoreductase activity	mitochondrial respiratory chain complex I	aerobic respiration -- electron donor III	20.01.15 - electron transport
						aerobic xylose fermentation	70.16 - mitochondrion
						aerobic xylose fermentation	
						PWY2T-21	
						aerobic respiration	
NCU10498		60S ribosomal protein L35 (126 aa)			mitochondrial outer membrane	12.01.01 - ribosomal proteins	
NCU06247		hypothetical protein (1354 aa)					
NCU05554	*un-25*	60S ribosomal protein L13 (215 aa)	telomere maintenance	structural constituent of ribosome	cytosolic large ribosomal subunit		
			translation				
NCU08517		hypothetical protein (794 aa)					
NCU04304	*por*	outer mitochondrial membrane protein porin (284 aa)				20.03.01 - channel / pore class transport	
						20.09.04 - mitochondrial transport	
						70.16 - mitochondrion	
NCU06003		mannose-1-phosphate guanyltransferase (365 aa)	cell wall mannoprotein biosynthetic process	mannose-1-phosphate guanylyltransferase activity	cytoplasm	01.05 - C-compound and carbohydrate metabolism	GDP-mannose biosynthesis
			protein glycosylation			42.01 - cell wall	
			GDP-mannose biosynthetic process				
NCU08982		hypothetical protein (463 aa)					
NCU07182		40S ribosomal protein S24 (137 aa)	translation	structural constituent of ribosome	mitochondrion	12.01 - ribosome biogenesis	
					cytosolic small ribosomal subunit		
NCU02435		histone H2B (138 aa)					
NCU01948		ribosomal protein Srp1 (161 aa)	translation	structural constituent of ribosome	cytosolic large ribosomal subunit	12.01.01 - ribosomal proteins	
						70.03 - cytoplasm	
NCU06413		hypothetical protein (762 aa)					
NCU03393	*rap-1*	ribosome-associated protein (291 aa)	ribosomal small subunit assembly	structural constituent of ribosome	cytosolic small ribosomal subunit	12.01 - ribosome biogenesis	
			translation				

Gene No.	Gene	Protein	Biological Process	Molecular Function	Cellular Component	functional catalog	Pathway
NCU09327	*cyt-4*	protein phosphatase (1118 aa)	Group I intron splicing		mitochondrion	01.03.16 - polynucleotide degradation 10.03.01 - mitotic cell cycle and cell cycle control 10.03.04.05 - chromosome segregation/division 11.04.03 - mRNA processing (splicing, 5'-, 3'-end processing) 14.07.03 - modification by phosphorylation, dephosphorylation, autophosphorylation 70.16 - mitochondrion	
NCU09109		60S ribosomal protein L33 (110 aa)	translation	structural constituent of ribosome	cytosolic large ribosomal subunit	12.01.01 - ribosomal proteins 70.03 - cytoplasm	
NCU07914	*pgk*	phosphoglycerate kinase (419 aa)	gluconeogenesis	phosphoglycerate kinase activity	cytoplasm	01.05 - C-compound and carbohydrate metabolism	gluconeogenesis I
			glycolysis		mitochondrion	02.01 - glycolysis and gluconeogenesis	glycolysis I
						70.03 - cytoplasm	glycolysis II xylose fermentation
NCU10836		hypothetical protein (941 aa)					
NCU08471	*tca-9*	succinyl-CoA ligase beta-chain (448 aa)	tricarboxylic acid cycle	succinate-CoA ligase (ADP-forming) activity	mitochondrion	02.10 - tricarboxylic-acid pathway (citrate cycle, Krebs cycle, TCA cycle)	TCA cycle variation III (eukaryotic)
			succinyl-CoA metabolic process				
NCU05891		arid/bright domain-containing protein (1290 aa)					
NCU07698	*sec5*	exocyst complex component Sec5 (1075 aa)	establishment or maintenance of cell polarity				
NCU04003		ERP1 protein (220 aa)				20.09.07.03 - ER to Golgi transport	
NCU11859 (NCU16698)		twinfilin-1 (339 aa)				14.07.03 - modification by phosphorylation, dephosphorylation, autophosphorylation	
NCU02064		hypothetical protein (281 aa)			mitochondrial membrane		
NCU03647		hypothetical protein (1063 aa)					
NCU06435		VPS9 domain-containing protein (779 aa)					

Gene No.	Gene	Protein	Biological Process	Molecular Function	Cellular Component	functional catalog	Pathway
NCU00345		hypothetical protein (1126 aa)					
NCU03124	*cka / prd-3*	casein kinase II subunit alpha (337 aa)	protein phosphorylation temperature compensation of the circadian clock circadian regulation of gene expression regulation of growth rate conidium formation	casein kinase activity			
NCU02193	*cfp / pdc-1*	cellular filament polypeptide (571 aa)	response to acetate	pyruvate decarboxylase activity		02.16.01 - alcohol fermentation 70.03 - cytoplasm	valine degradation II leucine degradation III isoleucine degradation II phenylalanine degradation III pyruvate fermentation to ethanol II pyruvate fermentation to acetate VIII xylose conversion to ethanol xylose fermentation cellulose conversion to ethanol PWY3O-4108-1
NCU02810		eukaryotic translation initiation factor 2 gamma subunit (512 aa)	translational initiation establishment or maintenance of cell polarity	translation initiation factor activity	robosome eukaryotic translation initiation factor 2 complex TERM multi-eIF complex	12.04.01 - translation initiation 16.19.05 - GTP binding 70.03 - cytoplasm	
NCU05804		60S ribosomal protein L19 (193 aa)	translation	structural constituent of ribosome	cytosolic large ribosomal subunit	12.01.01 - ribosomal proteins 70.10 - nucleus	
NCU02778	*gh47-1*	mannosyl-oligosaccharide 1,2-alpha-mannosidase (805 aa)				01.05 - C-compound and carbohydrate metabolism 14.07 - protein modification 70.07 - endoplasmic reticulum	
NCU04463		non-repetitive nucleoporin (1442 aa)					

Gene No.	Gene	Protein	Biological Process	Molecular Function	Cellular Component	functional catalog	Pathway
NCU04457		DUF803 domain membrane protein (799 aa)					
NCU02707		60S ribosomal protein L6 (202 aa)	ribosomal large subunit assembly	structural constituent of ribosome	cytosolic large ribosomal subunit		
			translation	RNA binding			
NCU02762	*cch-1 / smco-1*	calcium channel subunit Cch1 (2219 aa)					
NCU07112		hypothetical protein (459 aa)	cellular cadmium ion homeostasis		mitochondrion	01.02 - nitrogen, sulfur and selenium metabolism	
			regulation of sulfur metabolic process			70.16 - mitochondrion	
			response to cadmium ion				
NCU03150		60S ribosomal protein L24 (157 aa)	translation	RNA binding	cytosolic large ribosomal subunit	12.01 - ribosome biogenesis	
				structural constituent of ribosome		70.03 - cytoplasm	
NCU08277		eukaryotic translation initiation factor 2 alpha subunit (311 aa)	translational initiation	translation initiation factor activity	cytoplasm	12.04.01 - translation initiation	
					ribosome		
					eukaryotic translation initiation factor 2 complex		
					multi-eIF complex		
NCU08389		60S ribosomal protein L20 (175 aa)	translation	structural constituent of ribosome	cytosolic large ribosomal subunit	12.01.01 - ribosomal proteins	
						70.03 - cytoplasm	
NCU00014		hypothetical protein (168 aa)					
NCU01827		60S ribosomal protein L27 (136 aa)	translation	structural constituent of ribosome	cytosolic large ribosomal subunit	12.01 - ribosome biogenesis	
NCU02555	*arp-4*	actin-related protein-4, actin (470 aa)				10.03.01 - mitotic cell cycle and cell cycle control	
						20.09.14 - cytoskeleton-dependent transport	
NCU00567	*arg-6 / orn-2*	arginine-6 (872 aa)	regulation of transcription, DNA-dependent	N-acetyl-gamma-glutamyl-phosphate reductase activity	mitochondrion	01.01.03.05.01 - biosynthesis of arginine	ARGSYNBSUB-PWY-1
			arginine biosynthetic process	acetylglutamate kinase activity	mitochondrial matrix	70.16 - mitochondrion	ornithine biosynthesis
			ornithine biosynthetic process				
			response to light stimulus				
			citrulline biosynthetic process				

Gene No.	Gene	Protein	Biological Process	Molecular Function	Cellular Component	functional catalog	Pathway
NCU05689	*cox-4*	cytochrome c oxidase polypeptide IV (187 aa)	mitochondrial electron transport, cytochrome c to oxygen	cytochrome-c oxidase activity	mitochondrion	02.11 - electron transport and membrane-associated energy conservation	aerobic respiration -- electron donor II
			aerobic respiration	zinc ion binding	mitochondrial respiratory chain complex IV	02.13 - respiration	aerobic xylose fermentation
					mitochondrial membrane	70.16 - mitochondrion	aerobic xylose fermentation PWY2T-21
							aerobic respiration
NCU08909	*gel-3*	beta-1,3-glucanosyltransferase (543 aa)	response to salt stress			43.01.03 - fungal and other eukaryotic cell type differentiation	
			hyphal growth			43.01.03.05 - budding, cell polarity and filament formation	
						70.02 - eukaryotic plasma membrane / membrane attached	
NCU02419		mitochondrial 37S ribosomal protein S17 (166 aa)			mitochondrial ribosome	12.01.01 - ribosomal proteins	
NCU04720	*nit-6*	nitrate nonutilizer-6 (1177 aa)	nitrate assimilation	nitrite reductase [NAD(P)H] activity			PWY-5675-1
							2-nitropropane degradation
NCU02840	*rpt-1*	26S protease regulatory subunit 7 (440 aa)	ubiquitin-dependent protein catabolic process	endopeptidase activity	proteasome regulatory particle, base subcomplex		
			response to dsRNA	ATPase activity			
NCU06327		benzoate 4-monooxygenase cytochrome P450 (530 aa)				32.07.01 - detoxification involving cytochrome P450	
NCU00636		ATP synthase subunit D (174 aa)	protein complex assembly	ATPase activity	mitochondrial proton-transporting ATP synthase, stator stalk	02.13 - respiration	aerobic xylose fermentation
			ATP synthesis coupled proton transport	hydrogen ion transporting ATP synthase activity, rotational mechanism	mitochondrion	02.45.15 - energy generation (e.g. ATP synthase)	aerobic xylose fermentation
					mitochondrial proton-transporting ATP synthase complex	20.03.22 - transport ATPases	aerobic respiration
					mitochondrial membrane	34.01.01.03 - homeostasis of protons	
						70.16 - mitochondrion	

Gene No.	Gene	Protein	Biological Process	Molecular Function	Cellular Component	functional catalog	Pathway
NCU01843		T-complex protein 1 subunit gamma (541 aa)	protein folding cytoskeleton organization	unfolded protein binding	cytoplasm chaperonin-containing T-complex cytoskeleton	14.01 - protein folding and stabilization	
NCU07282		hypothetical protein (965 aa)	response to light stimulus				
NCU07702		hypothetical protein (3310 aa)				20.01.03 - C-compound and carbohydrate transport	
NCU08336	*tca-12*	succinate dehydrogenase flavoprotein subunit (649 aa)	tricarboxylic acid cycle mitochondrial electron transport, succinate to ubiquinone	succinate dehydrogenase (ubiquinone) activity	mitochondrion mitochondrial respiratory chain complex II		aerobic respiration -- electron donor II aerobic respiration -- electron donor III superpathway of glyoxylate cycle TCA cycle variation III (eukaryotic)
NCU00421	*snf-5*	SWI-SNF complex subunit (733 aa)	syncytium formation by plasma membrane fusion			11.02.03.04 - transcriptional control	
NCU02509		60S ribosomal protein L11 (175 aa)					
NCU09450	*rpn-2*	26S proteasome regulatory subunit rpn2 (1189 aa)					
NCU01172		GARP complex component (1158 aa)					
NCU04202	*ndk-1*	nucleoside diphosphate kinase-1 (153 aa)	response to oxidative stress response to blue light phosphorylation hyphal growth protein autophosphorylation	nucleoside diphosphate kinase activity NAD binding			pyrimidine ribonucleotides interconversion PWY-6126-1 salvage pathways of pyrimidine ribonucleotides pyrimidine deoxyribonucleotides de novo biosynthesis
NCU09132	*tba-1*	alpha tubulin (455 aa)	mitotic sister chromatid segregation nuclear migration along microtubule	structural constituent of cytoskeleton	spindle pole body polar microtubule kinetochore microtubule nuclear microtubule cytoplasmic microtubule tubulin complex	10.03.05.01 - spindle pole body/centrosome and microtubule cycle 16.19.05 - GTP binding 42.04.05 - microtubule cytoskeleton 70.04.05 - microtubule cytoskeleton	

Gene No.	Gene	Protein	Biological Process	Molecular Function	Cellular Component	functional catalog	Pathway
NCU08616	*un-18*	unknown-18 (1235 aa)	transcription from RNA polymerase I promoter	DNA-directed RNA polymerase activity	DNA-directed RNA polymerase I complex	11.02.01 - rRNA synthesis	
			regulation of circadian rhythm			16.03.01 - DNA binding	
						34.11.11 - rhythm (e.g. circadian, ultradian)	
						70.10 - nucleus	
NCU07735		Grp1p (355 aa)				16.03.01 - DNA binding	
NCU02687		activator 1 41 kDa subunit (388 aa)					

Table A.4 Supplementary movies in DVD

Movies	Results	Interval (s)	Time	Content
Supplementary movie 1	Fig. 3.6	60	9 h	Germlings growing in Ca^{2+}-free medium. Extracellular Ca^{2+} is required for CAT commitment
Supplementary movie 2	Fig. 3.7 A	60	30 min	CAT fusion between two germlings
Supplementary movie 3	Fig. 3.7 B	60	30 min	CAT chemotropism between two germlings
Supplementary movie 4	Fig. 3.7 C	60	3 h	CAT chemotropism between two germlings was stopped by the removal of extracellular Ca^{2+}. Five µM BAPTA was added at the 30 min time point in Supplementary movie 3.
Supplementary movie 5	Fig. 3.7 D	60	8 h	CAT fusion was stopped by the removal of extracellular Ca^{2+}. Five µM BAPTA was added after two CATs had made contact with each other.
Supplementary movie 6	Fig. 6.3 C	5	1 min	CaM-GFP accumulated at the tip of a germ tube showed a dynamic localization between a pronounced accumulation and small dots associated with the plasma membrane.
Supplementary movie 7	Fig. 6.4 A	5	15 sec	The movement of CaM-GFP was associated with nuclear spindle pole bodies.
Supplementary movie 8	Fig. 6.4 B	1	30 sec	Tracking of CaM-GFP movement in the cytoplasm
Supplementary movie 9	Fig. 6.4 D	1	30 sec	CaM-GFP formed spots and moved in the cytoplasm
Supplementary movie 10	Fig. 6.5	1	3 min	CaM-GFP co-localized with H4-dsRed. The movement of CaM spots in the cytoplasm is associated with nuclei and is probably labelling spindle pore bodies.
Supplementary movie 11	Fig. 6.7	30	30 min	CaM localization during septum formation
Supplementary movie 12	Fig. 6.6 B-C	5	10 min	CaM-GFP localization during CAT chemoattraction
Supplementary movie 13	Fig. 6.6 D	30	20 min	CaM-GFP localization during CAT chemoattraction
Supplementary movie 14	Fig 6.9	60	20 min	CaM-GFP localized in a hyphal branch that has just emerged.
Supplementary movie 15	Fig. 6.11 A	30	30 min	CaM-GFP localization in two CATs during CAT chemotropism.

Supplementary movie 16	Fig. 6.11 B	30	30 min	CaM-GFP localization in two homing CATs. The pronounced accumulation at tips disappeared whilst adding BAPTA. Extracellular Ca^{2+} is associated with the tip-focused CaM in CAT tips undergoing chemotropism.
Supplementary movie 17	Fig. 6.12 B	1	3 min	CaM-GFP localization in the treatment of Latrunculin A. The pronounced accumulation of CaM-GFP at tips is sensitive to Latrunculin A.
Supplementary movie 18	Fig. 6.13	1	3 min	CaM-GFP localization in the △*myo-5* strain lacked the pronounced accumulation at tips.
Supplementary movie 19	Fig. 6.14 C	1	3 min	CaM-GFP localization in the treatment of Benomyl. The movement of CaM-GFP in the cytoplasm is sensitive to Benomyl.
Supplementary movie 20	Fig. 7.4 A	1	10 min	Ca^{2+} traces in whole germlings with germ tubes
Supplementary movie 21	Fig. 7.4 B	1	10 min	Ca^{2+} traces in whole germlings with germ tubes
Supplementary movie 22	Fig. 7.4 C	1	10 min	Ca^{2+} traces in whole germlings with germ tubes
Supplementary movie 23	Fig. 7.4 D	1	10 min	Ca^{2+} traces in whole germlings with germ tubes
Supplementary movie 24	Fig. 7.4 E	1	10 min	Ca^{2+} traces in whole germlings with germ tubes
Supplementary movie 25	Fig. 7.4 F	1	10 min	Ca^{2+} traces in whole germlings with germ tubes
Supplementary movie 26	Fig. 7.4 G	1	10 min	Ca^{2+} traces in whole germlings with germ tubes
Supplementary movie 27	Fig 7.4 H	1	10 min	Ca^{2+} traces in whole germlings with germ tubes
Supplementary movie 28	Fig. 7.4 I	1	10 min	Ca^{2+} traces in whole germlings with germ tubes
Supplementary movie 29	Fig. 7.4 J	1	10 min	Ca^{2+} traces in whole germlings with germ tubes
Supplementary movie 30	Fig. 7.5 A	1	10 min	Ca^{2+} traces of two whole germlings undergoing CAT chemotropism
Supplementary movie 31	Fig. 7.5 B	1	10 min	Ca^{2+} traces of two whole germlings undergoing CAT chemotropism
Supplementary movie 32	Fig. 7.5 C	1	10 min	Ca^{2+} traces of two whole germlings undergoing CAT chemotropism
Supplementary movie 33	Fig. 7.5 D	1	10 min	Ca^{2+} traces of two whole germlings undergoing CAT chemotropism

Supplementary movie 34	Fig. 7.5 E	1	10 min	Ca^{2+} traces of two whole germlings undergoing CAT chemotropism
Supplementary movie 35	Fig. 7.5 F	1	10 min	Ca^{2+} traces of two whole germlings undergoing CAT chemotropism
Supplementary movie 36	Fig. 7.5 G	1	10 min	Ca^{2+} traces of two whole germlings undergoing CAT chemotropism
Supplementary movie 37	Fig. 7.5 H	1	10 min	Ca^{2+} traces of two whole germlings undergoing CAT chemotropism
Supplementary movie 38	Fig. 7.5 I	1	10 min	Ca^{2+} traces of two whole germlings undergoing CAT chemotropism
Supplementary movie 39	Fig. 7.5 J	1	10 min	Ca^{2+} traces of two whole germlings undergoing CAT chemotropism
Supplementary movie 40	Fig. 7.6 A	1	20 min	Ca^{2+} traces within whole germlings with CATs undergoing chemotropism to corresponding CATs exhibiting oscillatory of MAK-2
Supplementary movie 41	Fig. 7.6 B	1	20 min	Ca^{2+} traces within whole germlings with CATs undergoing chemotropism to corresponding CATs exhibiting oscillatory of MAK-2
Supplementary movie 42	Fig. 7.6 C	1	37 min	Ca^{2+} traces within whole germlings with CATs undergoing chemotropism to corresponding CATs exhibiting oscillatory of MAK-2
Supplementary movie 43	Fig. 7.7 A	1	10 min	Ca^{2+} traces of two whole germlings undergoing CAT fusion
Supplementary movie 44	Fig. 7.7 B	1	10 min	Ca^{2+} traces of two whole germlings undergoing CAT fusion
Supplementary movie 45	Fig. 7.7 C	1	10 min	Ca^{2+} traces of two whole germlings undergoing CAT fusion
Supplementary movie 46	Fig. 7.8	1	10 min	$[Ca^{2+}]_c$ increases in germlings are very dynamic and localized, and also occur in the form of $[Ca^{2+}]_c$ waves
Supplementary movie 47	Fig. 7.10 A	1	5 min	Time-lapse imaging of $[Ca^{2+}]_c$ waves in vegetative hyphae
Supplementary movie 48	Fig. 7.10 B	1	5 min	Time-lapse imaging of $[Ca^{2+}]_c$ waves in vegetative hyphae
Supplementary movie 49	Fig. 7.10 C	1	5 min	Time-lapse imaging of $[Ca^{2+}]_c$ waves in vegetative hyphae